

https://dspace.org/

# Solid base catalysis: fine chemical synthesis from alcohols

**Ndou, Azwimangadzi Steven**

**2009-05-28T10:39:54Z**
http://hdl.handle.net/10539/6990

Downloaded from a DSpace repository. https://dspace.org/

# SOLID BASE CATALYSIS: FINE CHEMICAL SYNTHESIS FROM ALCOHOLS

**AZWIMANGADZI STEVEN**

**NDOU**

A thesis submitted to the Faculty of Science in fulfilment of the requirements for the degree of

**Doctor of Philosophy**

University of the Witwatersrand

Johannesburg 2005

## DECLARATION

I declare that this thesis is my own, unaided work. It is being submitted for the degree of Doctor of Philosophy in the University of the Witwatersrand, Johannesburg. It has not been submitted before for any degree or examination in any other university, nor has it been prepared with the assistance of any other body or organisation or person outside the University of the Witwatersrand, Johannesburg.

All sources of information have been specifically acknowledged by means of references.

Signed

…...……..

Azwimangadzi Steven Ndou

……. day of ……..2005

## ABSTRACT


### SOLID BASE CATALYSIS: FINE CHEMICAL SYNTHESIS FROM ALCOHOLS

A study of solid base catalysis was conducted in three main categories, namely condensation reactions of primary alcohols, alkylation reactions of dihydroxybenzene and hydrogenation reactions of phenol.

Ethanol was converted into 1-butanol over alkali earth metal oxides and modified MgO catalysts (1-20 % yield). The MgO catalyst exhibits the highest reaction activity and 1-butanol selectivity amongst the catalysts studied. Reaction of various possible intermediates (acetaldehyde, crotonaldehyde, crotylalcohol, butanal) and ethanol over MgO (1 bar, 450 $^{o}$C) revealed that the dimerisation reaction does not proceed primarily through the aldol condensation reaction. The reaction is proposed to proceed through a mechanism, previously proposed by Yang and Meng, in which a C-H bond in the β-position in ethanol is activated by the basic metal oxide, and condenses with another molecule of ethanol, by dehydration to form 1-butanol.

A self-condensation reaction of propanol was carried out at atmospheric pressure over MgO as catalyst. The reaction gave 2-methylpentanol and propionaldehyde as the major products. The introduction of hydrogen before and during the reaction enhanced the catalyst selectivity to 2-methylpentanol. The effect of possible reaction intermediates on the catalyst selectivity and the mechanism of the reaction were investigated over MgO and indicated the important role of hydrogen transfer in the reaction. The highest selectivity (69 %) was achieved in the presence of hydrogen at 450 $^{o}$C with propanol conversion of 24 %.

Condensation reactions of ethanol with butanol or propanol to higher alcohols were carried out at atmospheric pressure over various solid-base catalysts. The ability of ethanol to be activated at either the $CH_2$ or $CH_3$ units played a significant role in the formation of a wide range of long chain alcohols. The major products observed during the reaction between ethanol and butanol were 2-ethylbutanol, 1-hexanol and to a lesser extent 2-ethyhexanol. The main products in the reaction of ethanol and propanol were 2-methylbutanol, 1-pentanol and butanol. Trace amounts of 2-methylpentanol were also observed.

The vapour phase alkylation of catechol over supported cesium catalysts gave good selectivity to guaiacol formation. The TPD studies of the

catalysts used indicated that the results can be correlated with the presence of weak basic sites on the catalyst.

The gas phase selective hydrogenation of phenol to cyclohexanone was investigated over palladium supported catalysts in order to clarify the influence of the support on products distribution. High selectivities towards cyclohexanone (about 86 %) were observed on palladium supported on high surface area titanium oxide supports. On the basis of the TPD studies, it has been suggested that the basic properties of the support strongly influence the adsorption-desorption of phenol and products, and are therefore responsible for the selectivity towards the reaction products.

## DEDICATION

This thesis is dedicated to my wife Valerie, my son Ofhatutshedza and my parents Mr and Mrs N.D. Ndou. You gave me inspiration and the determination to succeed.

Vha Venda vhe, “I rema nga lunwe mbevhana mulindi wa vhuya wa dala”.

## ACKNOWLEDGMENTS

I would like to express my sincere gratitude to the following people:

My supervisor Prof. N J Coville for his guidance, support and mentorship throughout my PhD studies.

Basil Chassoulas, Barry Fairbrother, Steve Ganon, Ziggy Heis and Richard Mampha for their technical support.

All members of the catalysis group, in particular Mpfunzeni Raphulu, James Tshilongo, Alufelwi Tshavhungwe, Mbangiseni Mabudafhasi and Neville Plint for their constant support and friendship during my studies.

My neglected friends and family, in particular my wife for their moral support and encouragements.

Dr. V. Vishwanathan and The Indian Government for allowing me to conduct part of my research at the Indian Institute of Chemical Technology (IICT), Hyderabad.

The National Research Foundation, Department of Labour, Mellon Foundation, DAAD Scholarship and the University of the Witwatersrand for financial support throughout my studies.

## TABLE OF CONTENTS

**CHAPTER 1**

**INTRODUCTION ..... 1**

**1.1 Scope and Aims of Thesis ..... 3**

1.1.1 Alkylation of 1,2-dihydroxybenzene (catechol)* ..... 5

1.1.2. Condensation of primary alcohols to higher alcohols* ..... 5

1.1.3. Hydrogenation of phenol ..... 6

**1.2 References ..... 7**

**CHAPTER 2**

**LITERATURE REVIEW ..... 10**

**2.1 Introduction ..... 11**

**2.2 Generation of Basic Sites ..... 15**

**2.3 Characterization of Solid Base Catalysts ..... 20**

2.3.1 Indicator Methods ..... 20

2.3.2 Temperature Programmed Desorption (TPD) of Carbon Dioxide ..... 22

2.3.3 Temperature Programmed Desorption of Hydrogen ..... 23

2.3.4 X-ray Photoelectron Spectroscopy (XPS) ..... 26

2.3.5 IR Spectra of Carbon Dioxide ..... 29

**2.4 Types of Solid Base Catalysts .....30**

2.4.1 Single Component Catalysts (Metal Oxides) .....30

2.4.2 Zeolites .....34

2.4.3 Solid Base Catalysts of the Non-Oxide Type .....35

2.4.4 Solid Superbasic Catalysts .....37

**2.5 Application of Solid Base Catalysts .....39**

2.5.1 Alkylation .....39

2.5.2 Aldol Addition and Condensation Reactions .....41

2.5.3 The Tishchenko Reaction .....44

2.5.4 Michael Addition .....48

2.5.5 The Wittig-Horner Reaction and Knoevenagel Condensation .....50

2.5.6 Nitroaldol Condensations .....54

2.5.7 Conjugate Addition of Alcohols .....55

2.5.8 Hydrogenation .....56

2.5.9 Other Reactions .....60

2.5.9.1 Amination .....60

2.5.9.2 Isomerization .....61

2.5.9.3 Dehydration and Dehydrogenation Reactions .....67

2.5.9.4 Nucleophilic Ring Opening Reactions .....68

2.5.9.5 Oxidation Reactions .....70

2.5.9.6 Meerwein-Ponndorf-Verley Reaction .....73

**2.6 Conclusion .....77**

**2.7 References .....79**

**CHAPTER 3**

**EXPERIMENTAL METHODS AND APPARATUS .....90**

**3.1 Introduction to Catalyst Synthesis .....92**

3.1.1 Catalyst Preparation .....95

**3.2 Catalyst Characterization .....97**

3.2.1 BET (Brunauer-Emmett-Teller) .....98

3.2.2 $CO_2$ Temperature Programmed Desorption (TPD) .....100

3.2.3 Scanning Electron Microscopy (SEM) .....105

3.2.4 Transmission Electron Microscopy (TEM) .....109

3.2.5 Thermogravimetric Analysis (TGA) .....111

**3.3 Catalyst Testing System .....113**

**3.4 References .....119**

**CHAPTER 4**

**DIMERISATION OF ETHANOL TO BUTANOL .....118**

**4.1 Introduction .....120**

**4.2 Experimental .....122**

4.2.1 Catalyst preparation ..... 122

4.2.2 Apparatus and procedure ..... 123

**4.3 Results and Discussion ..... 125**

4.3.1 Catalyst screening ..... 125

4.3.2. Effect of temperature and contact time on the reaction ..... 133

4.3.3 Reaction Mechanism ..... 136

**4.4 Conclusions ..... 144**

**4.5 References ..... 145**

**CHAPTER 5**

**SELF CONDENSATION OF PROPANOL ..... 145**

**5.1 Introduction ..... 147**

**5.2 Experimental ..... 149**

5.2.1 Catalyst preparation ..... 149

5.2.2 Apparatus and procedure ..... 150

**5.3 Results and Discussion ..... 151**

5.3.1 Catalyst screening ..... 151

5.3.2 Influence of hydrogen and other reagents on catalyst activity and product selectivity ..... 1642

5.3.3. Study of possible reaction intermediates ..... 1675

5.3.4 Reaction mechanism ..... 169

**5.4 Conclusion .....174**

**5.5 References .....176**

**CHAPTER 6**

**SYNTHESIS OF 2-ETHYLBUTANOL AND 1-HEXANOL .....176**

**6.1 Introduction.....1786**

**6.2 Experimental .....18179**

6.2.1 Catalyst Preparation .....18179

6.2.2 Apparatus and procedure .....1820

**6.3 Results and Discussion.....1842**

6.3.2 Investigation of reaction parameters.....1886

**6.4 Reaction Mechanism.....1953**

6.4.1 The Effect of Reaction Parameters on Linear/Branched

Alcohols Ratio .....2020

**6.5 Conclusions .....2108**

**6.6 References .....2120**

**CHAPTER 7**

**SYNTHESIS OF 2-METHYLBUTANOL AND 1-PENTANOL ..... 212**

**7.1 Introduction.....2142**

**7.2 Experimental .....2175**

**7.3 Results and Discussion .....2175**

**7.4 Reaction Mechanism .....2253**

7.4.1 The Effect of Reaction Parameters on Linear/Branched alcohols Ratio .....2308

**7.5 Conclusions .....2364**

**7.6 References .....2375**

**CHAPTER 8**

**VAPOUR PHASE ALKYLATION OF CATECHOL .....237**

**8.1 Introduction .....2397**

**8.2 Experimental .....238**

8.2.1 Catalyst Preparation .....2408

8.2.2 Apparatus and Procedure .....24139

**8.3 Discussion of Results .....239**

**8.4 Conclusion .....2475**

**8.5 References .....2486**

**CHAPTER 9**

**SELECTIVE HYDROGENATION OF PHENOL.....247**

**9.1 Introduction.....2497**

**9.2 Experimental.....2520**

9.2.1 Catalyst preparation.....2520

9.2.2 Reactor Studies.....2542

**9.3 Results and Discussion.....2553**

9.3.1 Investigation of Reaction Parameters over Titanium Oxide ($TiCl_4$-$TiO_2$) Supported Palladium Catalyst .....2620

9.3.2 Investigation of Reaction Parameters over Titanium Oxide (NaOH-$TiO_2$) Supported Palladium Catalyst.....2675

**9.4 Discussion.....2731**

**9.5 Conclusions.....2764**

**9.6 References.....2775**

**CHAPTER 10**

**SUMMARY OF RESULTS.....278**

## LIST OF FIGURES


| Number | | Page |
|---|---|---|
| **Figure 2.1** | Evolution of $H_2O$ and $CO_2$ from Mg $(OH)_2$ [8,9] | 15 |
| **Figure 2.2** | Variations of activity of MgO for different types of reactions as a function of pre-treatment temperature | 16 |
| **Figure 2.3** | TPD plots for hydrogen adsorbed on MgO at various Pre-treatment temperatures | 24 |
| **Figure 2.4** | Schematic bonding model of zeolite | 26 |
| **Figure 3.1** | TPD profiles of alkali and alkali earth metal oxides supported on MgO | 100 |
| **Figure 3.2** | TPD profiles of MgO catalyst calcined at different temperature for 3 h | 101 |
| **Figure 3.3** | The effect of $Cs_2O$ addition on different acidic supports | 102 |
| **Figure 3.4** | SEM image of MgO catalyst at 10 μm | 104 |
| **Figure 3.5** | SEM image of $TiO_2$ support prepared from hydrolysis of $TiCl_4$ (scale 10 μm) | 105 |
| **Figure 3.6** | SEM image of TiO2 support prepared from thermal hydrolysis with NaOH. | 106 |
| **Figure 3.7** | TEM micrograph of titanium oxide nanofibres from $TiO_2$ sample prepared by hydrolysis of $TiCl_4$. | 108 |

**Figure 3.8** TEM micrograph of a titanium oxide sample obtained from thermal hydrolysis of $TiO_2$ with NaOH. 109

**Figure 3.9** Thermal decomposition curve of MgO used in self condensation of propanol [9]. 110

**Figure 3.10** Schematic representation of catalyst testing apparatus 112

**Figure 3.11** Schematic representation of a larger heating jacket (200 mm) 114

**Figure 3.12** Schematic representation of a small heating jacket (40 mm) 115

**Figure 4.1** TPD profiles of some of the catalysts 128

**Figure 4.2** Influence of temperature on the product distribution over MgO 132

**Figure 4.3** Influence of contact time on ethanol conversion and 1-butanol yield over MgO 133

**Figure 4.4** Influence of time on stream on activity and 1-butanol yield over MgO 134

**Figure 5.1** The effect of temperature on conversion and product distribution 154

**Figure 5.2** The influence of calcination temperature on propanol conversion and catalyst selectivity 155

**Figure 5.3** The effect of calcination temperature on the catalyst basicity (strength and basic site distribution). 157

**Figure 5.4** The effect of contact time on propanol conversion and product selectivity 159

**Figure 5.5** The effect of time on catalyst activity and product selectivity 160

**Figure 5.6** Thermogravimetric analysis (TGA) profile of used MgO 161

**Figure 5.7** The influence of % hydrogen on catalyst activity and product selectivity 163

**Figure 5.8** The influence of pre-treatment time (in hydrogen) on catalyst activity and product selectivity 164

**Figure 6.1** The effect of temperature on catalyst activity and product distribution 187

**Figure 6.2** The effect of butanol to ethanol mole ratio on product distribution 189

**Figure 6.3** The influence of contact time on product distribution 190

**Figure 6.4** The effect of time on stream on catalyst activity and selectivity 192

**Figure 6.5** Thermogram of MgO catalyst used in the reaction of ethanol and butanol 193

**Figure 6.6** The effect of temperature on linear/branched alcohols ratio 202

**Figure 6.7** The effect of butanol/ethanol mole ratio on linear/branched alcohol ratio 203

**Figure 6.8** The effect of contact time on linear/branched alcohol ratio 204

**Figure 6.9** The effect of time-on-stream on linear/branched ratio 206

**Figure 7.1** The effect of temperature on conversion and product distribution 218

**Figure 7.2** The influence of contact time on conversion and product selectivity 220

**Figure 7.3** The effect of time-on-stream on catalyst stability and product selectivity 222

**Figure 7.4** Thermogram of MgO catalyst after the reaction 223

**Figure 7.5** The effect of temperature on the ratio of linear/branched alcohols 229

**Figure 7.6** The influence of contact time on linear/branched ratio of alcohols 231

**Figure 7.7** The effect of time-on-stream on linear/branched ratio of alcohols 233

**Figure 8.1** $CO_2$ TPD profiles of MgO and $Al_2O_3$ 243

**Figure 8.2** $CO_2$ TPD profiles of Cs on $TiO_2$, $SiO_2$ and $Al_2O_3$ 244

**Figure 9.1** TPD profiles of high surface area titanium oxide supports 257

**Figure 9.2** TEM micrograph of high surface area $TiO_2$ (prepared from $TiCl_4$ hydrolysis) 258

**Figure 9.3** TEM micrograph of high surface area $TiO_2$ (prepared from thermal hydrolysis of $TiO_2$ with NaOH) 259

**Figure 9.4** TEM micrograph of $TiO_2$ (Deggusa P25) 259

**Figure 9.5** The influence of temperature on products distribution over $TiCl_4$-$TiO_2$ 261

**Figure 9.6** The effect of $H_2$/Phenol mole ratio on product distribution over $TiCl_4$-$TiO_2$ 262

**Figure 9.7** The influence of contact time on product selectivity over $TiCl_4$-$TiO_2$ 263

**Figure 9.8** The effect of time on stream on catalyst stability over ($TiCl_4$-$TiO_2$) 264

**Figure 9.9** The effect of temperature on product distribution over NaOH-$TiO_2$ 266

**Figure 9.10** The influence of H2/phenol mole ratio on product distribution over NaOH-$TiO_2$ 268

**Figure 9.11** The effect of contact time on catalyst activity and product selectivity over NaOH-$TiO_2$ 269

**Figure 9.12** The effect of time-on-stream on catalyst stability over NaOH-$TiO_2$ 270

## LIST OF REACTION SCHEMES


| Number | | Page |
|---|---|---|
| **Scheme 1.1** | Overview of Thesis | 4 |
| **Scheme 2.1** | Aldol addition of acetone | 41 |
| **Scheme 2.2** | Esterification of benzaldehyde | 44 |
| **Scheme 2.3** | Self condensation of butyraldehyde | 46 |
| **Scheme 2.4** | Hydrogenation of 1,3-Butadiene | 57 |
| **Scheme 2.5** | Amination of 1,3-Butadiene | 60 |
| **Scheme 2.6** | 1-Butene Isomerization | 61 |
| **Scheme 2.7** | Double bond migration of allylamines to enamines | 65 |
| **Scheme 2.8** | Hydrogen transfer from 2-propanol to aldehydes and ketones | 73 |
| **Scheme 2.9** | Meerwein-Ponndorf-Verley reduction of ketones and aldehyde with 2-propanol | 75 |
| **Scheme 2.10** | Meerwein-Ponndorf-Verley reaction of cyclohexanone with 2-propanol | 76 |
| **Scheme 4.1** | Reaction network for the formation of 1-butanol from ethanol | 135 |
| **Scheme 4.2** | Classical condensation reaction of ethanol and acetaldehyde to form 1-butanol | 136 |

**Scheme 4.3** Condensation reaction of ethanol and acetaldehyde to form 1-butanol 137

**Scheme 4.4** Dimerization of ethanol to form 1-butanol. 137

**Scheme 5.1** Aldol condensation of propanol to 2-methylpentanol 166

**Scheme 5.2** Detailed molecular mechanism of the Aldol condensation reaction over MgO [7,8]. 171

**Scheme 6.1** Schematic representation of the 2-ethylbutanol formation mechanism from ethanol and butanol reactions 195

**Scheme 6.2** Schematic representation of the 1-hexanol formation mechanism from ethanol and butanol reactions 197

**Scheme 6.3** Summary of reactions for ethanol / butanol conversion over MgO 199

**Scheme 7.1** Schematic representations of ethanol and propanol reaction mechanism for the formation of 1-pentanol 225

**Scheme 7.2** Reaction network of ethanol and propanol mixture 227

**Scheme 9.1** Two-site model of phenol adsorption and hydrogen dissociation on palladium supported catalysts [5] 273

## LIST OF TABLES


Number Page

**Table 3.1** Surface areas, pore size and pore volume of various catalysts 97

**Table 4.1** Activities of basic oxides and alkali-loaded $Al_2O_3$ in the solid base condensation of ethanol to butanol 125

**Table 4.2** Activities of alkaline earth and transition metals loaded on MgO catalysts in the solid base condensation of ethanol to butanol 127

**Table 4.3** Activities of acid doped magnesium oxide catalysts for the solid base condensation of ethanol to butanol 130

**Table 4.4** The product distribution of the liquid products from the reaction of (i) pure intermediates (100%) and (ii) ethanol/intermediate (1:1) mixtures over MgO 140

**Table 5.1** Liquid product distribution form the self-condensation reaction of propanol over various solid base catalysts 151

**Table 5.2** The liquid product distribution from the reaction of neat reactants and propanol/intermediate (1:1 v/v) mixtures over MgO 168

**Table 5.3** The liquid product distribution from the reaction of propanol and propionaldehyde mixtures in the presence of hydrogen gas (100%) 169

**Table 6.1** The effect of catalyst on the liquid product distribution using 1:2 butanol:ethanol mole ratio 183

**Table 7.1** Product distribution of the reaction between propanol and ethanol over MgO catalyst 216

**Table 8.1** Reaction data for the vapour phase alkylation of catechol over unsupported and supported cesium catalysts 241

**Table 9.1** The effect of titanium oxide preparation methods on product distribution 255

## LIST OF ABBREVIATIONS AND/ ACRONYMS

| Abbreviation and/ acronym | Description |
|---|---|
| ALPON | Aluminophosphate Oxynitride |
| BE | Bonding Energy |
| BET | Brunauer-Emmett-Teller |
| Conv. | Conversion |
| FID | Flame Ionization Detector |
| FT-IR | Fourier Transform Infrared |
| GC | Gas Chromatography |
| GC-MS | Gas Chromatography-Mass Spectroscopy |
| GHSV | Gas Hourly Space Velocity |
| IR | Infrared |
| K | Kelvin |
| MS | Mass Spectrometry |

| Abbreviation and/ Acronym | Description |
|---|---|
| NMR | Nuclear Magnetic Resonance |
| SA | Surface Area |
| SAPO | Siliconaluminaphosphate |
| SEM | Scanning Electron Microscopy |
| T | Temperature |
| TEM | Transmission Electron Microscopy |
| TCD | Thermal Conductivity Detector |
| TGA | Thermogravimetric Analysis |
| TPD | Temperature Programmed Desorption |
| V/V | Volume by Volume |
| WHSV | Weight Hourly Space Velocity |
| XAFS | X-ray Absorption Fine Structure |
| XPS | X-ray Photoelectron Spectroscopy |

| | |
|---|---|
| XRD | X-Ray Diffraction |
| ZSM | Zeolite Socony Mobil |

**Presentations and Publications related to this work.**

**(i) Presentations**

1. CATSA Conference, Durban (SA), 2003

   “The use of Ethanol as a Building Block for Higher Alcohol Synthesis”

   A.S. Ndou and N.J. Coville

2. CATSA Conference, Cape Town (SA), 2002

   “Self-Condensation of Propanol over Solid Base Catalysts”

   A.S. Ndou and N.J. Coville

3. CATSA/SACI Conference, Pilanesberg (North West, SA), 2001

   “Dimerization of Ethanol to Butanol over Solid Base Catalyst”

   A.S. Ndou and N.J. Coville

**(ii) Publications**

1. V. Vishwanathan, S. Ndou, L. Sikhwivhilu, N. Plint, K.V. Rghavan, N.J. Coville, Chem. Commun. (2001) 893.

2. A.S. Ndou, N. Plint, N.J. Coville, Applied Catalysis A: General, 251 (2003) 337.

3. A.S. Ndou, N.J. Coville, Applied Catalysis A: General, 275 (2004) 103.

4. A.S. Ndou, N.J. Coville, The use of ethanol as a building block for higher alcohol synthesis. To be submitted.

5. A.S. Ndou, V. Vishwanathan, N.J. Coville, Selective hydrogenation of phenol over high surface area titanium oxide supported palladium catalysts. To be submitted.

# Chapter 1

## INTRODUCTION

Solid base catalysts have been actively studied for many decades and this interest has gone on unabated in the 21st century. Many reviews have appeared on the topic over the years [1-5]. A variety of organic reactions are catalyzed in a very selective manner by base catalysts. In particular, solid bases offer convenient and environmentally benign routes for organic synthesis. A major objective in the modern chemical industry is to avert the production of noxious and environmentally undesirable effluents including salts and organic solvents [6–8]. Indeed the replacement of liquid acid catalysts with solid acid catalysts has led to more than 100 industrial processes operated that are currently operated in the world [4]. However, to date less success has been achieved with solid base catalysts and only a few processes are in operation using solid base materials [4].

Base catalyzed processes such as aldolisation, alkylation, Knoevenagel, Michael condensations and Wadsworth–Emmons additions are commonly used for the manufacture of fine chemicals. In the industrial practice the amount of base is nearly stoichiometric and the neutralization of the reaction medium, post-reaction, produces large amounts of salts. A better preservation of the environment would require substituting the liquid bases (and organometallics) used in these processes by solid catalysts. Indeed, solid catalysts show many advantages from a technical point of view. They present fewer disposal problems; they allow easier separation and recovery of the products, catalysts and solvent, if any; they are non-corrosive, and they offer environmentally benign and more economical pathways for the synthesis of fine chemicals.

Several solid bases have been proposed for the industrial synthesis of chemicals such as alkali ion-exchanged zeolites [9,10], sepiolites [11], alkaline oxides supported on microporous [12] and mesoporous solids [13], sodium metal clusters in zeolites [14], alkali metals supported on alumina [15,16], alkaline earth solids such as magnesium [17-19] and barium oxide [20], aluminium magnesium mixed oxides derived from hydrotalcites [21–23] and nitrides [24,25]. Alkali ion-exchanged zeolites and sepiolites possess only mild basic strength, while alkali metals and alkaline oxides

loaded on supports are considered as super bases that can catalyze a wide range of reactions [26]. These super bases present interesting catalytic properties for substrates of very low reactivity like olefins, but the large majority of base catalyzed reactions involve functionalized substrates which do not need such high basicity.

In this thesis attempts have been made to use solid base catalysts for a range of chemical reactions.

## 1.1 Scope and Aims of Thesis

Scheme 1.1 below shows an overview of the types of reaction investigated in this thesis. The three main reaction categories studied in this work were alkylation, aldol condensation and hydrogenation. The primary starting chemical class used in the study was the alcohols.

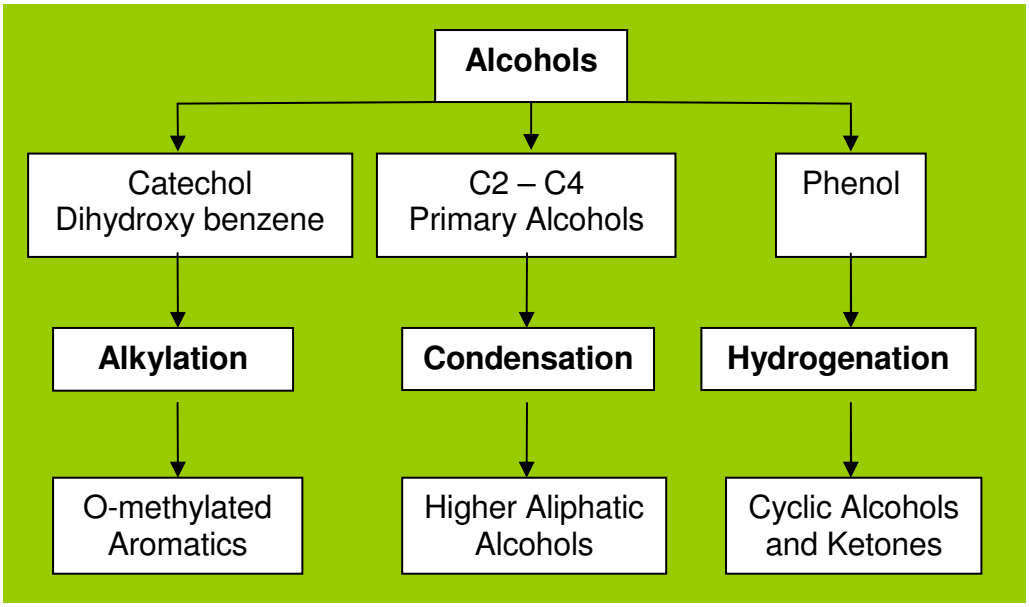


**Scheme 1.1** Overview of Thesis

Although there are three different types of reaction investigated, they are all influenced by the basicity of the catalysts used. The thesis is thus concerned with the use of solid base catalysts in the synthesis of valuable compounds from alcohols and an understanding of the reaction mechanism.

The following is a brief description of the reaction processes within the categories mentioned above:

### 1.1.1 Alkylation of 1,2-dihydroxybenzene (catechol)*

The vapour phase alkylation of catechol was studied over supported cesium catalysts. The reaction gave good selectivity to guaiacol formation. Small amounts of veratrole were also observed during the reaction. The TPD studies indicate that good selectivity towards guaiacol can be correlated with the presence of weak basic sites on the catalyst.

* V. Vishwanathan, S. Ndou, L. Sikhwivhilu, N. Plint, K.V. Rghavan, N.J. Coville, Chem. Commun. (2001) 893.

### 1.1.2. Condensation of primary alcohols to higher alcohols*

In this category, four reactions were investigated. Dimerization of ethanol to butanol was studied over several solid base catalysts. The mechanism of the reaction was studied over magnesium oxide catalyst.

Self condensation of propanol to 2-methylpentanol was also studied over solid base catalysts. Several parameters were investigated and the data obtained was used to propose a mechanism for the reaction.

In the light of the information obtained from the above experiments, mixed alcohols reactions were studied to understand the interaction of two

different alcohols over solid base catalysts. This led to the investigation of ethanol/butanol and ethanol/propanol reactions over solid base catalysts.

* A.S. Ndou, N. Plint, N.J. Coville, Appl. Catal. A: General, 251 (2003) 337.

* A.S. Ndou, N.J. Coville, Appl. Catal. A: General, 275 (2004) 103.

### 1.1.3. Hydrogenation of phenol

Phenol hydrogenation was carried out over palladium supported on high surface area titanates. The reaction focused on the influence of support preparation method on the basicity of the support and the way in which the basicity of the support affects the reaction.

## 1.2 References

[1] F. Figuras, Topics in Catalysis, 29 (2004) 189.

[2] H. Hattori, Appl. Catal. A: General, 222 (2001) 247.

[3] H. Hattori, Chem. Rev. 95 (1995) 537.

[4] K. Tanabe, W.F. Holderich, Appl. Catal. A: General, 181 (1999) 399.

[5] Y. Ono, J. Catal. 216 (2003) 406.

[6] L. Krumenacker, S. Ratton, Actualite Chimique, 29 (1986).

[7] W.F. Holderich, Stud. Surf. Sci. Catal. 75 (1993) 27.

[8] J.M. Thomas, R. Raja, G. Sankar, B.F. Johnson, D.W. Lewis, Chem. Eur. J. 7 (2001) 2973.

[9] A. Corma, V. Fornes, R.M. Martin-Aranda, and H. Garcia, Primo, J. Catal. 59 (1990) 237.

[10] D. Barthomeuf, G. Coudurier, and J.C. Vedrine, Mater, Chem. Phys. 18 (1988) 553.

[11] A. Corma, and R.M. Martin-Aranda, Appl. Catal. A: General, 105 (1993) 271.

[12] J.C. Kim, H.-X. Li, C.-Y. Chen, and M.E. Davis, Micropor. Mater. 2 (1994) 413.

[13] K.R. Kloestra, and H. Van Bekkum, Stud. Surf. Sci. Catal. 105A (1997) 431.

[14] L.R. Martens, P.J. Grobet, and P.A. Jacobs, Nature 315 (1985) 568.

[15] G. Suzukamo, M. Fukao, T. Hibi, K. Tanaka, K, and K. Chikaishi, Acid-Base Catal., Proc. Int. Symp. (1989) 405.

[16] V. Vishwanathan, S. Ndou, L. Sikhwivhilu, N. Plint, K.V. Rghavan, N.J. Coville, Chem. Commun. (2001) 893.

[17] H. Moison, F. Texier-Boullet, and A. Foucaud, Tetrahedron 43 (1987) 537.

[18] A.S. Ndou, N. Plint, N.J. Coville, Appl. Catal. A: General, 251 (2003) 337.

[19] A.S. Ndou, N.J. Coville, Appl. Catal. A: General, 275 (2004) 103.

[20] A. Aguilera, A.R. Alcantara, J.M. Marinas, and J.V. Sinisterra, Can. J. Chem. 65 (1987) 1165.

[21] V. Corma, V. Fornes, R.M. Martin-Aranda, and F. Rey, J. Catal. 134 (1992) 58.

[22] A. Guida, M.H. Lhouty, D. Tichit, F. Figueras, and P. Geneste, Appl. Catal. A: General, 164 (1997) 251.

[23] A. Corma, S. Iborra, S. Miquel, and J. Primo, J. Catal. 173 (1998) 315.

[24] P. Grange, P. Bastians, R. Conanec, R. Marchand, and Y. Laurent, Appl. Catal. A: General, 114 (1994) 191.

[25] M.J. Climent, A. Corma, V. Forne´ s, A. Frau, R. Guil-Lo´ pez, S. Iborra, and J. Primo, J. Catal. 163 (1996) 392.

[26] B.F. Sels, D.E. De Vos, and P.A. Jacobs, Catal. Rev.-Sci. Eng. 43 (2001) 443.

# CHAPTER 2

# Literature Review

## 2.1 Introduction

A variety of organic reactions are catalyzed in a very selective manner by solid base catalysts since solid bases offer a convenient and environmentally benign pathway in organic synthesis. The use of solid base catalysts in organic synthesis has been reviewed by Hattori et al. [1] and most recently by Yoshio Ono [2].

The first study of heterogeneous basic catalysts was reported by Pines et al [3]. In this reaction, sodium metal dispersed on alumina was used as an effective catalyst for the double bond migration of alkenes. Considering the

strong tendency of Na to donate electrons, it seems natural that Na dispersed on alumina acts as a heterogeneous basic catalyst.

Following the report by Pines et al. [3], certain metal oxides with a single component were found to act as heterogeneous basic catalysts in the absence of such alkali metals as Na and K. In the 1970s, Kokes et al. reported that hydrogen molecules were adsorbed on zinc oxide by acid-base interaction to form proton and hydride species on the surface [4,5]. They proved that the heterolytically dissociated hydrogen atoms act as intermediates for alkene hydrogenation. In the same period, Hattori et al. reported that calcium oxide and magnesium oxide exhibited high activities for 1-butene isomerization if the catalysts were pre-treated under proper conditions such as high temperature and high vacuum [6]. The 1-butene isomerization over calcium oxide and magnesium oxide was recognized as a base catalyzed reaction in which the reaction was initiated by abstraction of a proton from 1-butene by the basic site on the catalyst surfaces.

The catalytic activities of basic zeolites were also reported in early 1970s. Yashima et al. reported that side chain alkylation of toluene was catalyzed by alkali ion-exchanged X and Y type zeolites [7]. The reaction is a typical

base-catalyzed reaction, and the activity varied with the type of exchanged alkali cation and with type of zeolite, suggesting that the basic properties can be controlled by selecting the exchanged cation and the type of zeolite.

In addition to the above mentioned catalysts, a number of materials have been reported to act as heterogeneous basic catalysts. Except for non-oxide catalysts, the basic sites are believed to be surface oxygen atoms. Oxygen atoms existing on any materials may act as basic sites because of their ability to interact with protons.

There are four criteria that can be used to recognise certain materials as heterogeneous basic catalysts [1].

(a) Characterization of the surfaces indicates the existence of basic sites: Characterizations of the surfaces by various methods such as colour change of acid-base indicators adsorbed, surface reactions, adsorption of acidic molecules, and spectroscopy (UV, IR, XPS**,** ESR, etc.) indicate that basic sites exist on the surfaces.

(b) A parallel relation between catalytic activity and the amount and/or strength of the basic sites: The catalytic activities correlate well with the amount of basic sites or with the strength of the basic sites measured by various methods. Also, the active sites are poisoned by acidic molecules such as HCl, $H_2O$, and $CO_2$.

(c) Similarities in activity to materials for homogeneous basic catalysts for "base-catalyzed reactions" well-known in homogeneous systems: There are a number of reactions known as base-catalyzed reactions in homogeneous systems. Certain solid materials also catalyze these reactions to give the same products. The reaction mechanisms occurring on the surfaces are suggested to be essentially the same as those occurring in homogeneous basic solutions.

(d) Indications of anionic intermediates participating in the reactions: Mechanistic studies of the reactions, product distributions, and spectroscopic observations of the species adsorbed on certain materials indicate that anionic intermediates are involved in the reactions.

To place this thesis in perspective a brief overview of aspects of base catalysts will be given. This literature review chapter will focus on the generation of basic sites, characterization of basic sites and application of

solid base catalysts. The chapter will also highlight different types of heterogeneous basic catalysts.

## 2.2 Generation of Basic Sites

On exposure to the atmosphere, alkaline earth oxides adsorb carbon dioxide, water, and oxygen to form carbonates, hydroxides, and peroxides. Removal of the adsorbed species from the surfaces is essential to expose the oxide surfaces. Therefore, high temperature pre-treatment is required to obtain the metal oxide surfaces. For a example, Hattori et al. have reported that on evacuation of magnesium hydroxide (a catalyst precursor), water and carbon dioxide begin to evolve at about 700 K (Fig. 2.1) [8,9]. At this temperature, the catalytic activities for different types of reactions increase, and with correct pre-treatment temperature maximum activity can be achieved. The activities even start to decrease after a certain temperature range had been exceeded. Evolution of carbon dioxide, water, and oxygen results in generation of basic sites on the surfaces which act as catalytically active sites for several reaction types.

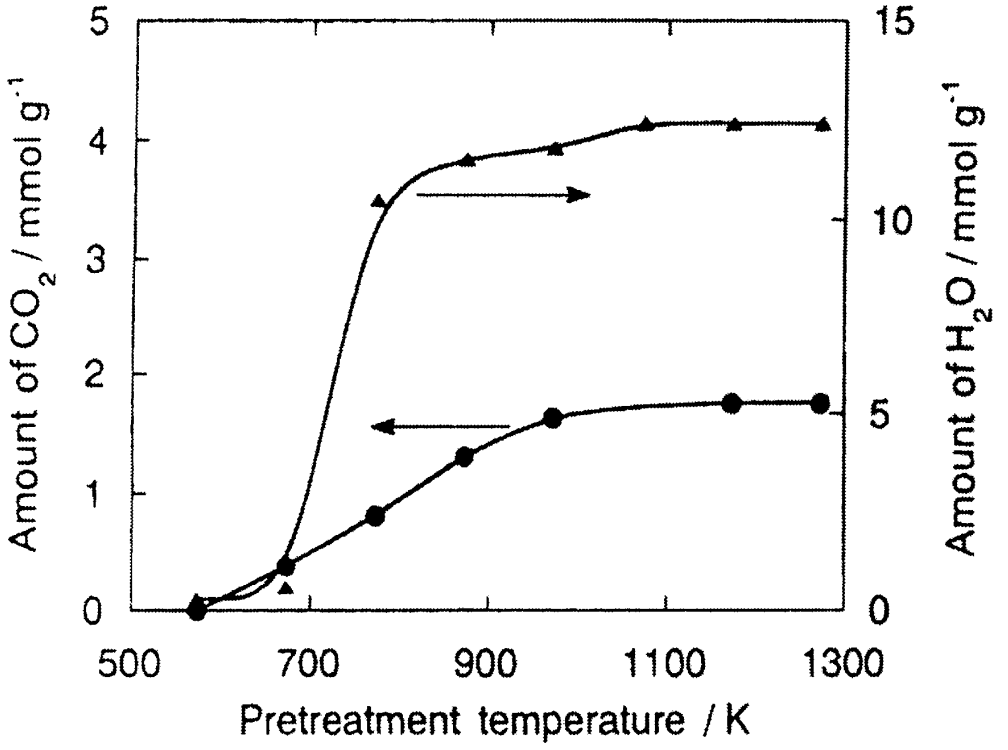


**Figure 2.1 Evolutions of $H_2O$ and $CO_2$ from $Mg(OH)_2$ [8,9].**

The nature of the basic sites generated by removal of molecules covering the surface depends on the severity of the pre-treatment. Changes in the nature of basic sites are reflected in the variations of the catalytic activities as a function of pre-treatment temperature. An example is shown in Fig. 2.2 for the case of MgO [1,9,10]. The temperatures to give the maximum activities vary with the type of reactions. For MgO, the temperatures giving maximum activities are 800 K for 1-butene

isomerization, 973 K for methane–D2 exchange and amination of 1,3-butadiene, and 1300 K for hydrogenation of 1,3-butadiene [9].

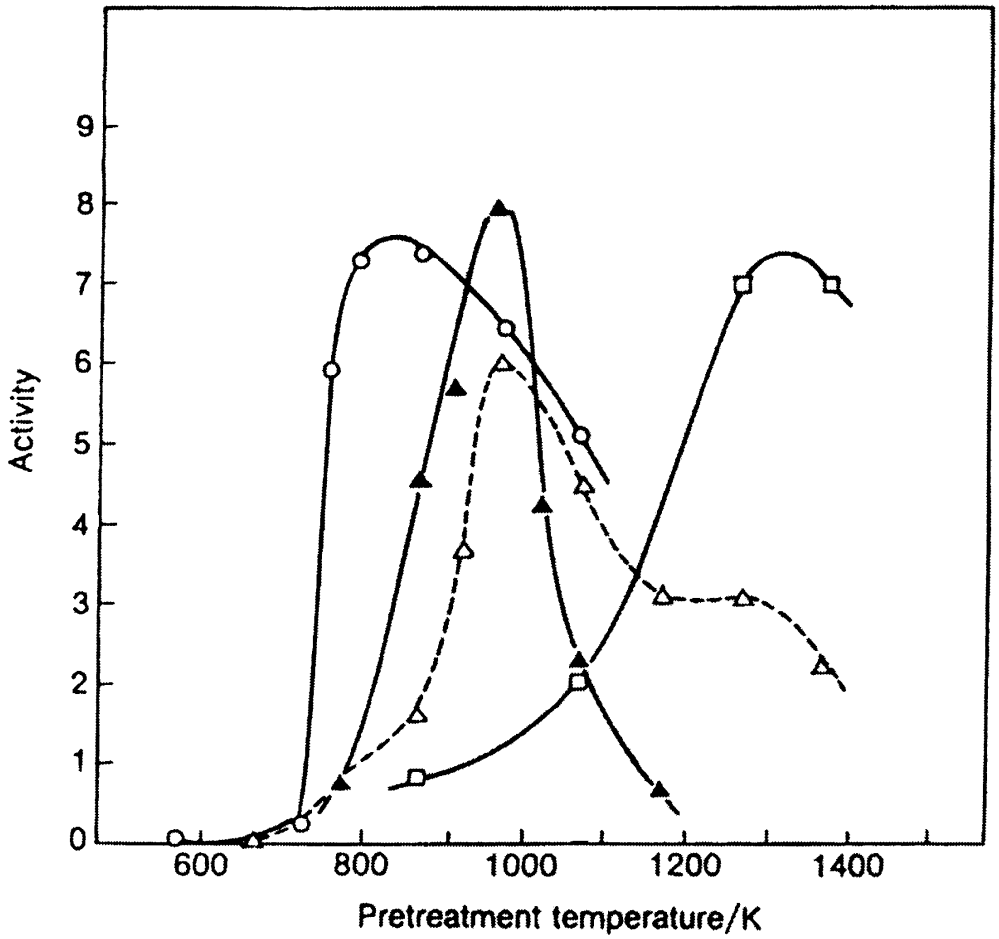


**Figure 2.2** Variations of activity of MgO for different types of reactions as a function of pre-treatment temperature: (o), 1-butene isomerization at 303 K; (▲), $CH_4$–$D_2$ exchange at 673 K; (Δ), amination of 1,3-butadiene with dimethylamine at 273 K, (□), 1,3-butadiene hydrogenation at 273 K [1,9,10].

As the pre-treatment temperature increases, molecules covering the surface are consecutively desorbed according to the strength of interaction with the surface sites. Molecules that are weakly interacting with the surface are desorbed at lower pre-treatment temperatures, and those strongly interacting with the surface are desorbed at higher temperatures. The sites that appear on the surface by pre-treatment at low temperatures are suggested to be different from those appearing at high temperatures. If simple desorption of molecules occurs during pre-treatment, the basic sites that appear at high temperatures should be strong. However, rearrangement of surface and bulk atoms also occurs during pre-treatment, which may change the number and nature of the surface basic sites with increasing the pre-treatment temperature.

According to the proposal by Coluccia and Tench, several Mg–O ion pairs of different coordination numbers exist on the surface of MgO catalyst [11]. Ion pairs of low coordination numbers exist at corners, edges, and high Miller index surfaces. Different basic sites generated by increasing the pre-treatment temperature appear to correspond to the ion pairs of different coordination numbers. Among the ion pairs of different coordination numbers, the most reactive adsorbs carbon dioxide most

strongly. To reveal the most reactive ion pair, the highest pre-treatment temperature is required.

The nature of basic sites varies with the severity of the pre-treatment conditions for most solid base catalysts. The surface sites generated on rare earth oxides, however, behave differently from those of the other solid base catalysts. The sites of rare earth oxides do not seem to vary in nature with pre-treatment temperature. The pre-treatment of $La_2O_3$ at 923 K results in the maximum activity for 1-butene isomerization, 1,3-butadiene hydrogenation, and methane-$D_2$ exchange reactions [12-14]. The surface sites generated by removal of water and carbon dioxide seem to be rather homogeneous since the same surface sites are relevant to all the reactions mentioned above.

It is essential to remove the adsorbed carbon dioxide, water, and, in some cases, oxygen from the surfaces to generate basic sites, though proper pre-treatment temperatures vary with the types of catalysts and reactions.

## 2.3 Characterization of Solid Base Catalysts

The surface properties of the heterogeneous basic catalysts have been studied by various methods. Different characterization methods give different pieces of information about the surface properties. All the properties of basic sites cannot be measured by any single method. Integration of the results obtained by different characterization procedures leads to the understanding of structures, reactivity, strengths, and amounts of the basic sites on the surface. In this section, some of the representative methods for characterization of the surface basic sites are described. The aspects of basic sites disclosed by each characterization method are emphasized.

### 2.3.1 Indicator Methods

Acid-base indicators change their colours according to the strength of the surface sites and $pK_{BH}$ values of the indicators. The strength of the surface sites are expressed by an acidity function ($H_-$) proposed by Paul and Long. The $H_-$ function is defined by the following equation [15,16]:

$$H_- = pK_{BH} + \log [B^-]/[BH]$$

where [BH] and $[B^-]$ are, respectively, the concentration of the indicator BH and its conjugated base, and $pK_{BH}$ is the logarithm of the dissociation constant of BH. The reaction of the indicator BH with the basic site (E) is shown below.

$$BH + E = B^- + EH^+$$

The amount of basic sites of different strengths can be measured by titration with benzoic acid. A sample is suspended in a nonpolar solvent and an indicator is adsorbed on the sample in its conjugated base form. The amount of benzoic acid used is a measure of the amount of basic sites having a basic strength corresponding to the $pK_{BH}$ value of the indicator used. Using this method, Take et al. measured outgassed samples of MgO, CaO, and SrO [17]. The results show that magnesium oxide and CaO possess basic sites stronger than $H_- = 26$.

The indicator method can express the strength of basic sites in a definite scale of *H-,* but this has disadvantages too. Although the colour change is assumed to be the result of an acid-base reaction, an indicator may

change its colour by reactions different from an acid-base reaction. In addition, it requires a long time for benzoic acid to reach adsorption equilibrium when titration is carried out in a solution. In some cases, the surface of heterogeneous basic catalysts may dissolve into a titration solution. If this happens, the number of basic sites would be overestimated. Therefore, special care should be taken with the indicator method.

### 2.3.2 Temperature Programmed Desorption (TPD) of Carbon Dioxide

This method is mostly used to measure the number and strength of basic sites. The strength and amount of basic sites are reflected in the desorption temperature and peak area, respectively, in a TPD plot. However, it is difficult to express the strength in a definite scale and to count the number of sites quantitatively. Relative strengths and relative numbers of basic sites on the different catalysts can be estimated by carrying out the TPD experiments under the same conditions. If the TPD plot gives a sharp peak, the heat of adsorption can be estimated.

Zhang et al. has reported a comparative TPD-$CO_2$ desorption study for alkaline earth oxides under the same conditions [18]. In this study, the strength of basic sites was found to be MgO < CaO < SrO < BaO. The number of basic sites per unit weight that could retain carbon dioxide under the adsorption conditions increased in the order BaO < SrO < MgO < CaO.

Tsuji et al. have also reported an enhancement of basic strength by addition of alkali ions to X-zeolite in excess of the ion exchange capacity demonstrated by TPD plots of carbon dioxide [19]. The peak areas are reported to be larger for the alkali ion-added zeolites than for the ion-exchanged zeolites. In particular, desorption of carbon dioxide still continues at the desorption temperature of 673 K for alkali ion-added zeolites.

### 2.3.3 Temperature Programmed Desorption of Hydrogen

This method gives information about the coordination state of the surface ion pairs when combined with the other methods such as UV absorption

and luminescence spectroscopy. The number of each ion pair can be counted if TPD is accurately measured with a proper calibration method. This method has been applied only to the MgO surface [20,21].

Hydrogen is heterolytically dissociated on the surface of MgO to form $H^+$ and $H^-$, which are adsorbed on the surface of the $O^{2-}$ ion and $Mg^{2+}$ ion, respectively. TPD plots of hydrogen adsorbed on MgO pre-treated at different temperatures are shown in Figure 2.3 [20,21]. Seven desorption peaks appear in the temperature range 200-650 K, and appearance of the peaks varies with the pre-treatment temperature. Appearance of the peaks at different temperatures indicates that several types of ion pairs with different coordination numbers exist on the surface of MgO. The adsorption sites on MgO pre-treated at different temperatures and the coordination numbers of each ion pair have been assigned. The assignment of the surface ion pairs are based on the surface structure model of MgO proposed by Coluccia and Tench [11]. TPD of hydrogen supports the surface model of MgO illustrated.

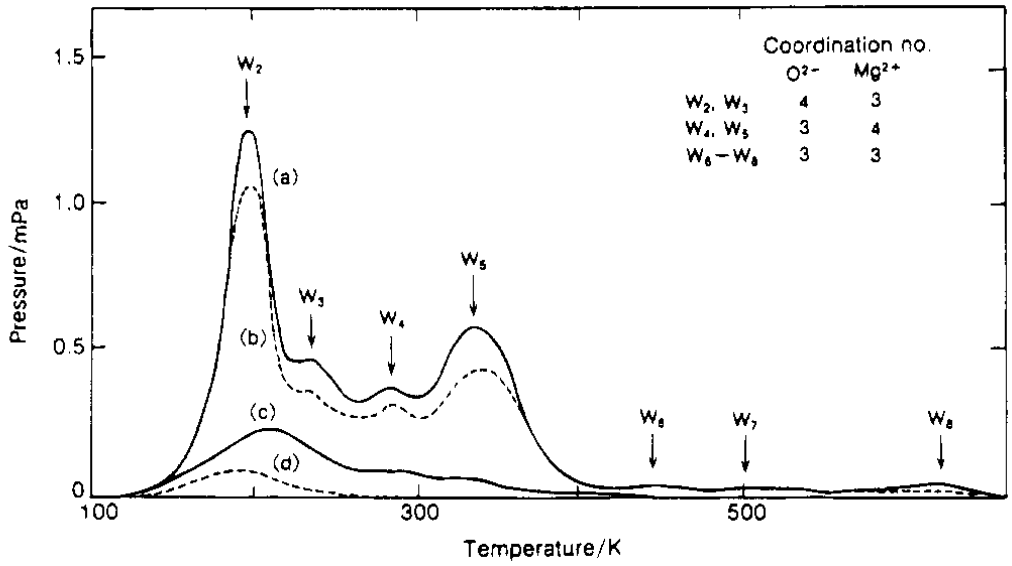


**Figure 2.3** TPD plots for hydrogen adsorbed on MgO at various pre-treatment temperatures: (a) 1123 K, (b) 973 K, (c) 823 K, (d) 673 K [20,21]

Heterolytic dissociation of hydrogen on the MgO surface is also demonstrated by IR spectroscopy. The IR bands for O-H and Mg-H stretching vibration were observed [11].

### 2.3.4 X-ray Photoelectron Spectroscopy (XPS)

The XPS binding energy (BE) for oxygen reflects the basic strength of the oxygen. As the $O_{1s}$ BE decreases, electron pair donation becomes stronger. Okamoto et al. studied the effects of zeolite composition and the type of cation on the BE of the constituent elements for X- and Y-zeolites ion-exchanged with a series of alkali cations as well as H-forms of A, X, Y, and mordenite [22]. The BE values of $O_{1s}$ decreases as the Al content increases.

The effect of an ion-exchanged cation on the $O_{1s}$ BE as a function of the electronegativity of the cation has been reported by Okamoto et al [22]. The $O_{1s}$ BE increases with increasing electronegativity of the cation. The O1s BE of zeolite is directly related to the electron density of the framework oxygen. On the basis of XPS features of zeolites, Okamoto et al. proposed a bonding model of zeolites as shown in Figure 2.4 [22]. Configurations (I) and (II) are in resonance. In configuration (I), extra framework cations form covalent bonds with framework oxygen, while in configuration (II), the cations form fully ionic bonding with the negatively charged zeolite lattice. As the electronegativity of the cation increases

and approaches that of oxygen, the contribution of configuration (I) increases to reduce the net charge on the lattice. This explains the dependences of the $O_{1s}$ BE on the electronegativity of the cation.

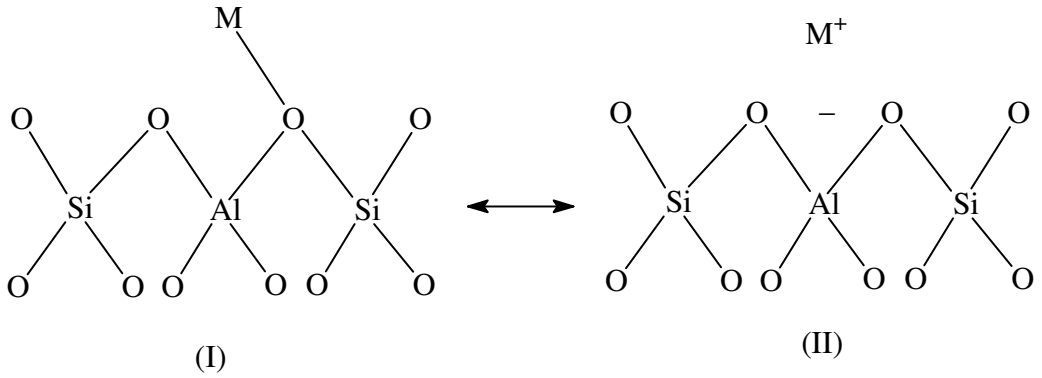


**Figure 2.4** Schematic bonding model of zeolite [22].

Although the relationship between electron density and the basic strength of $O^{2-}$ is not theoretically established, a good correlation between the BE of the $N_{1s}$ band and basicity is well established for a wide variety of organic compounds containing N. It may be acceptable that the BE of the $O_{1s}$ band changes monotonously with the basic strength of $O^{2-}$ when comparison is made within a same series of exchanged cations.

XPS measurement of the probe molecule adsorbed on basic sites gives information about the strength of the basic sites. Huang et al. measured the $N_{1s}$ BE of the pyrrole adsorbed on alkali cation-exchanged X- and Y-zeolites [23]. The $N_{1s}$ envelopes were deconvoluted into three peaks. One of the peaks was assigned to pyrrole adsorbed on the framework oxygen adjacent to the alkali cations other than the sodium cation. The BE of the peak varies with the exchanged cation in such a way that the $N_{1s}$ BE decreases as the basic strength of the zeolite increases as Li < Na < K < Rb < Cs. The deconvolution of XPS $N_{1s}$ peaks into three peaks indicates that the basic strength of the framework oxygen is inhomogeneous in the zeolite cage and that the cation exerts an influence only on the adjacent framework atoms. These results suggest that electrons are localized significantly on $M^+(AlO_2)^-$ units.

In a proposed model for pyrrole chemisorbed on a basic site of alkali cation-exchanged zeolite, the basic strength is reflected in the N-H stretching vibration frequency of pyrrole in the IR spectrum [24]. The $N_{1s}$ BE in XPS correlates linearly with the N-H vibration frequencies of chemisorbed pyrrole. As the exchanged cation changes in the sequence Li, Na, K, Rb, and Cs, both the $N_{1s}$ BE and the frequency of the N-H stretching vibration decrease for X- and Y-zeolites [23].

### 2.3.5 IR Spectra of Carbon Dioxide

This method gives information about the adsorbed state of $CO_2$ on the surface. Carbon dioxide interacts strongly with a basic site and the surface structures including basic sites are estimated from the adsorbed state of $CO_2$ [25].

Carbon dioxide is adsorbed on solid base catalysts in different forms: bidentate carbonate, unidentate carbonate, and bicarbonate. On the MgO surface, the adsorbed form varies with the coverage of the adsorbed carbon dioxide. Bidentate carbonate dominates at low coverage, and unidentate carbonate at high coverage [25]. Evans and Whately reported the adsorption of carbon dioxide on MgO [26]. In addition to unidentate and bidentate carbonates, bicarbonate species were also detected on MgO. For CaO, carbon dioxide is adsorbed in the form of bidentate carbonate regardless of the coverage.

In the adsorption state of unidentate carbonate, only surface oxygen atoms participate, while the metal ion should participate in the adsorption

state of bidentate. In other words, the existence of only a basic site is sufficient for unidentate carbonate formation, but the existence of both a basic site and a metal cation is required for bidentate carbonate.

## 2.4 Types of Solid Base Catalysts

The catalytic properties of solid base catalysts are closely associated with the amount and strength of the basic sites existing on the surface of the solid base. However, the amount and strength of the basic sites are not the only measures available to determine the catalytic properties. It appears that there are also characteristic features commonly observed for a certain type of solid base catalysts. In this section, catalytic features of different types of solid base catalysts are described.

### 2.4.1 Single Component Catalysts (Metal Oxides)

Alkaline earth oxides such as MgO, CaO, SrO, and BaO are most extensively studied [1,9]. They possess strong basic sites. The order of the basic strength is BaO > SrO > CaO > MgO. As described in the earlier

section, the surfaces are covered with $CO_2$ and $H_2O$ before pre-treatment. To be active catalysts, they need pre-treatment at a high temperature to remove adsorbed $CO_2$ and $H_2O$. In addition, the active sites are easily poisoned by even small amounts of impurities like $CO_2$ and $H_2O$ contained in the reactants. To measure the full capabilities of alkaline earth oxides, the reaction system should be kept free of the impurities, which makes the industrial uses of the alkaline earth oxides difficult, especially at low reaction temperatures. At high reaction temperatures, the poisoning effects are reduced, and certain alkaline earth oxides show catalytic activities for the reactions from which poisons like $H_2O$ are liberated.

One of the features of alkaline earth oxides is a high ability to abstract an $H^+$ from an allylic position. This feature is revealed in the double bond migration of olefinic compounds. Butene, for instance, undergoes double bond migration even at 223 K [27].

Rare earth oxides have been studied to a lesser extent as compared to alkaline earth oxides. The reactions for which basic sites of rare earth oxides are relevant are the hydrogenation of olefins, double bond migration of olefins, aldol condensation of ketones, and dehydration of alcohols. The

activity sequences of a series of rare earth oxides have been studied for 1-butene isomerization, 1,3-butadiene hydrogenation, and acetone aldol condensation [28]. The activity sequence was reported to be the same for 1-butene isomerization and 1,3-butadiene hydrogenation, which is different from that of aldol condensation. For the isomerization and the hydrogenation, the oxides of sesquioxide stoichiometry showed activity while the oxides with metal cations of higher oxidation states were entirely inactive. The situation was different in the acetone aldol condensation reaction. The oxides with high oxidation state, $CeO_2$, $Tb_4O_7$, and $Pr_6O_{11}$, showed considerable activity. The oxides with metal cations of oxidation state higher than three possessed weak basic sites sufficient to catalyze the aldol condensation, but not strong enough to catalyze hydrogenation and isomerization [28].

Rare earth oxides show characteristic selectivity in the dehydration of alcohols [29-31]. 2-Alcohols undergo dehydration to form 1-olefins. The formation of thermodynamically unstable 1-olefins contrasts with the formation of stable 2-olefins in the dehydration over acidic catalysts.

Zirconium oxide is a unique solid base catalyst in the sense that two industrial processes have been established that use $ZrO_2$ as a catalyst.

One is reduction of aromatic carboxylic acids with hydrogen to produce aldehydes [32]. The other is dehydration of 1-cyclohexylethanol to vinyl-cylohexane [33]. In addition, the production of diisobutyl ketone from isobutyraldehyde has been preferred industrially for more than 30 years [34].

One of the difficulties associated with most of the heterogeneous basic catalysts used in industries arises from rapid poisoning of the catalyst by $CO_2$ and $H_2O$. This is not the case with $ZrO_2$. Zirconium oxide retains its activity in the presence of water, which is one of the products for the reactions of carboxylic acid and 1-cyclohexylethanol.

The catalytic features of $ZrO_2$ are understood in terms of bifunctional acid-base properties [35-37]. Although the strengths of the basic and acid sites are low, a cooperative effect makes $ZrO_2$ function as an efficient catalyst. Because of weakly acidic and basic sites, the active sites are not poisoned by $CO_2$ and water.

### 2.4.2 Zeolites

The characteristic features of zeolites result from their ion-exchange ability and specific pore structure. The acid-base properties are controlled by selecting the types of ion-exchanged cations and by the Si/Al ratio of the zeolite framework. Wide variation of acid-base properties can be achieved by ion-exchange and ion-addition, while relatively small changes in acid-base properties are achieved by changing the Si/Al ratio.

To prepare basic zeolites, two approaches have been undertaken. One approach is to ion-exchange the zeolite with alkali metal ions, and the other is to impregnate the zeolite pores with fine particles that can act as bases themselves. The former produces relatively weak basic sites, while the latter results in the strong basic sites.

In alkali ion-exchanged zeolites, the type of alkali ions used affects the basic strength of the resulting zeolites. The effect of the alkali ions on the basic strength follows the order: $Cs^+ > Rb^+ > K^+ > Na^+ > Li^+$ [23,24]. The basic sites are framework oxygen. The bonding of the framework oxygen is

rather covalent in nature. This causes the basic sites of ion-exchanged zeolites to be relatively weak as compared to those of alkaline earth oxides.

Besides alkali metal oxides, the fine particles of MgO have been placed in the zeolite cavities [38]. The resulting zeolite also showed strong basic properties, though the basic sites on the fine particles of MgO are not as strong as those of bulk MgO. The ionic nature of the Mg-O bond is reduced for a fine particle of MgO as compared to bulk MgO, and therefore, the basic strength of the $O^{2-}$ ion is reduced. The dependence of the particle size on the strength of basic site was studied for ultra fine MgO particles by Itoh et al [39]. It was also concluded that smaller particles exhibited weaker basicity.

### 2.4.3 Solid Base Catalysts of the Non-Oxide Type

Most solid base catalysts are in the form of oxides. The basic sites are $O^{2-}$ ions with different environments depending on their type. If the basic sites are constituted by elements other than $O^{2-}$, the catalysts are expected to show catalytic properties different than those of the catalysts of the oxide form. Some examples are given below.

Potassium fluoride supported on alumina ($KF/Al_2O_3$) was introduced by Clark [40] and by Ando and Yamawaki [41,42] as a fluorinating reagent and a base catalyst. As a base catalyst, $KF/Al_2O_3$ has been applied to a number of organic reactions. The reactions for which $KF/Al_2O_3$ acts as a catalyst include Michael addition [43-46], Wittig-Honner reactions [47,48], Knoevenagel condensations [47,48], Darzen condensations [47,49] condensation of phenyl acetylene with benzaldehyde [50], alkylations at C, O, N, and S with aldehydes and dimethylsulfate [41,51-53], and disproportionation of alkylsilanes [54].

An example of another catalyst of the non-oxide type, prepared by Baba et al. was a low-valent lanthanide species introduced into zeolite cavities [55,56]. They impregnated K-Y zeolite with Yb and Eu dissolved into liquid ammonia followed by thermal activation.

The chemical states of Yb were studied by TPD, IR, XAFS, and XPS as a function of evacuation temperature. The states of Yb changed from Yb(II, III) amides, to Yb(III) nitride as follows:

$$Yb(NH_2)_3 \longrightarrow YbNH + NH_3 + 1/2N_2 + H_2$$

$$Yb(NH_2)_2 \longrightarrow YbNH + NH_3$$

and

$$2YbNH \longrightarrow 2YbN + H_2$$

It was concluded that the Yb(II) imide species catalyze 1-butene isomerization and the Michael addition and that the Yb(III) nitride species catalyzed ethylene hydrogenation.

### 2.4.4 Solid Super basic Catalysts

To activate a reactant under mild conditions, a catalyst possessing very strong basic sites is desired. There have been some attempts to prepare super basic catalysts.

Suzukamo et al. prepared a super basic catalyst by addition of alkali hydroxides to alumina followed by further addition of alkali metals [57]. Sodium hydroxide was added to a calcined alumina at 583-593 K with stirring under a nitrogen stream. Sodium metal was added after 3 h and the mixture was stirred for another 1 h at the same temperature to give a pale blue solid. The resulting catalyst possessed basic sites stronger than $H_-$ = 37 that catalyzed various reactions such as double bond migrations of 5-vinylbicyclo[2.2.1]lhept-2-ene to 5-ethylidenebicyclo[2.2.1]hept-2-ene at the reaction temperature 243-373 K, 2,3-dimethylbut-l-ene to 2,3-dimethylbut-2-ene at 293 K, safrol to isosafrol at 293 K and side chain alkylations of alkylbenzenes at the reaction temperature of 293-433 K. The former two reactions are initiated by abstraction of an $H^+$ from the tertiary carbon in the molecules to form tertiary carbanions. Because tertiary carbanions are unstable, the abstraction of an $H^+$ from a tertiary carbon requires a strong basic site.

Ushikubo et al. prepared a super basic catalyst by addition of metallic sodium to MgO [58]. Magnesium oxide was pre-treated at a high temperature and mixed with $NaN_3$. The mixture was heated at 623 K to decompose $NaN_3$ to evolve metallic sodium vapour to which MgO was exposed. The resulting catalyst acted as an efficient catalyst for

decomposition of methyl formate to CO and methanol. The activity was much higher than that of MgO. Although the basic strength of Na-added MgO was not compared with that of MgO, the high activity of Na-added MgO for the decomposition of methyl formate appears to be due to the enhancement of basic strength caused by the addition of Na to MgO.

## 2.5 Application of Solid Base Catalysts

In this section, selected examples of solid base-catalyzed reactions are described. Some of the studies were originally undertaken to elucidate the mechanism of the reaction. Other examples reveal the role of solid base catalysts in synthetic organic chemistry.

### 2.5.1 Alkylation

In general, alkylation of alkylaromatics occurs at the ring position over an acidic catalyst, while side chain alkylation takes place over a basic catalyst. Toluene undergoes side chain alkylation with methanol to produce ethylbenzene and styrene over $Cs^+$ ion-exchanged X-zeolite [7].

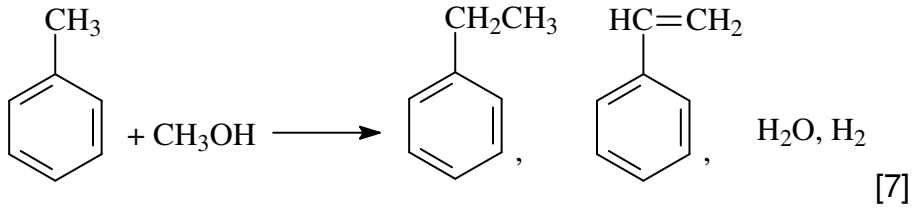


[7]

The first step in this reaction is dehydrogenation of methanol to formaldehyde, which undergoes an aldol type reaction with toluene to form styrene. Ethylbenzene is formed by hydrogenation of styrene. The basic sites in the zeolite catalyst used participate in both the dehydrogenation of methanol and the aldol type reaction.

Alkylation of toluene was studied by computer graphics on the basis of quantum chemical calculation [59,60]. The calculations also suggested that the high activity results from the presence of both acidic and basic sites in a zeolite cavity.

The zeolites having alkali ions in excess of their ion-exchange capacity exhibit higher activities than the simple ion-exchanged zeolites [61]. The high activities are caused by the generation of strong basic sites by addition of alkali ions which are located in the zeolite cavities in the form of alkali oxides.

$K/KOH/Al_2O_3$ is an efficient catalyst for alkylation of isopropylbenzene with olefins such as ethylene and propylene [57]. The reaction occurs at 300 K. In this reaction, alkylation occurs selectively at the side chain. The selective occurrence of the side chain alkylation is due to an anionic mechanism as proposed by Suzukamo et al [57]. The basic sites of $K/KOH/Al_2O_3$ are sufficiently strong to abstract an $H^+$ from isopropylbenzene to form an unstable tertiary anion at a low temperature.

### 2.5.2 Aldol Addition and Condensation Reactions

Aldol addition of acetone to form diacetone alcohol is well known to be catalyzed by $Ba(OH)_2$. Alkaline earth oxides, $La_2O_3$ and $ZrO_2$ are also active for the reaction in the following order: BaO > SrO > CaO > MgO > $La_2O_3$ > $ZrO_2$ [62]. With MgO, addition of a small amount of water increases the activity, indicating that the basic $OH^-$ ions either retained on the surface or formed by dehydration of diacetone alcohol are active sites for the aldol addition of acetone. By the use of tracer experiments in which a mixture containing equal amount of acetone-$d_0$ and $-d_6$ was allowed to react, the slow step was elucidated to be step B in Scheme 2.1 [63].

When the catalysts possessing both acid and base sites are used, the product diacetone alcohol undergoes dehydration to mesityl oxide. If the hydrogenation ability is further added to the catalyst, mesityl oxide is hydrogenated to methyl isobutyl ketone (MIBK).

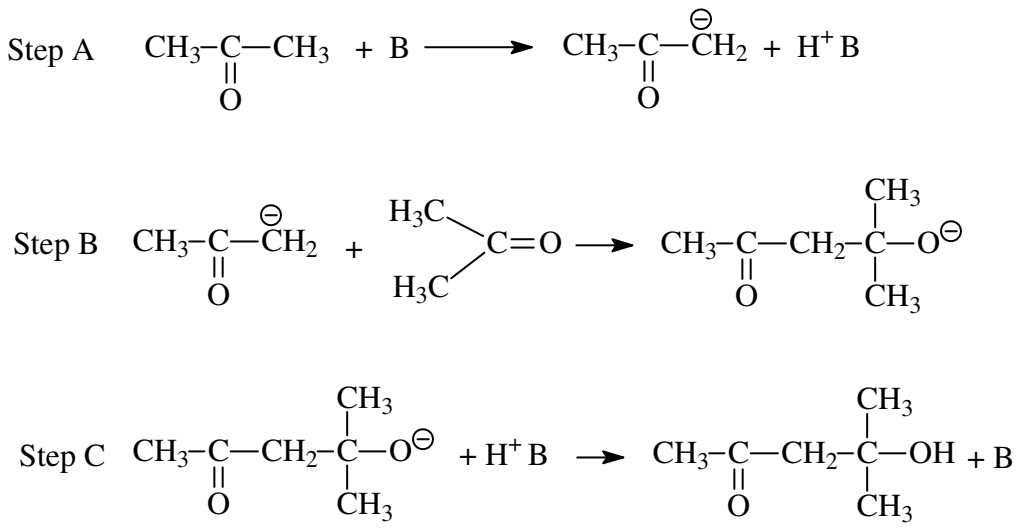


**Scheme 2.1** Aldol addition of acetone [63].

When the aldol condensation of acetone is performed over A-, X-, Y-, or L-zeolites containing alkali metal clusters at 623 K, mesityl oxide and isophorone are produced as the main products [64]. The ratio of the two products is dependent on the types of zeolites used. A-type zeolites favour

the formation of the smaller molecule of mesityl oxide. With X- or Y-zeolite, isophorone is preferentially produced. For the smaller pore sized L-zeolite, the formation of mesityl oxide is about twice as great as that of isophorone [65]. These catalysts possess acidic sites in addition to basic sites. Each product can be selectively obtained by controlling the acid-base properties and the pore size of the zeolite.

Aldol condensation of formaldehyde with methyl propionate to form methyl methacrylate is catalyzed by X- and Y-zeolites having a basic property. The highest conversion was obtained with the zeolite ion-exchanged with K followed by being impregnated with potassium hydroxide [66].

Hydrotalcite ($Mg_6Al_2(OH)_{16}CO_3.4H_2O$) and chrysotile ($Mg_3(OH)_4Si_2O_5$) act as efficient catalysts for the production of methyl vinyl ketone (MVK) through aldol condensation between acetone and formaldehyde at 673 K [67]. Synthetic $Co^{2+}$ ion-exchange chrysotile, $Co_xMg_{3-x}(OH)_4Si_2O_5$, produces methyl vinyl ketone from acetone and methanol. By addition of $Co^{2+}$, dehydrogenation sites are generated. Methanol is dehydrogenated to formaldehyde which undergoes aldol condensation with acetone to produce MVK.

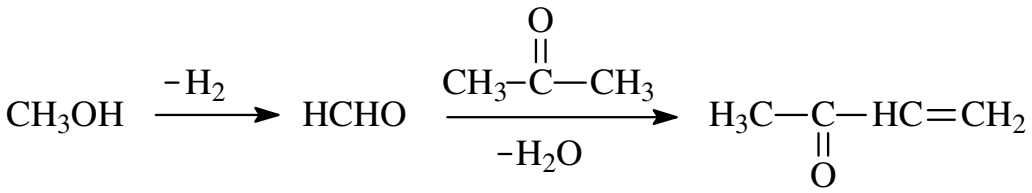

### 2.5.3 The Tishchenko Reaction

The Tishchenko reaction entails the dimerization of aldehydes to form esters. Since the reaction mechanisms are similar to those of the Cannizzaro reaction, the Tischenko reaction is thought to be a base-catalyzed reaction.

Benzaldehyde converts to benzylbenzoate over alkaline earth oxides [68]. This reaction proceeds by a Tishchenko type reaction as shown in Scheme 2.2.

In this reaction, both basic ($O^{2-}$ ion) and acidic sites (metal cation) participate. The slow step is $H^-$ transfer from (III) to (IV). The activities of the alkaline earth oxides were reported to be in the order MgO < CaO <

SrO < BaO, indicating that basic strength is important among alkaline earth oxides.

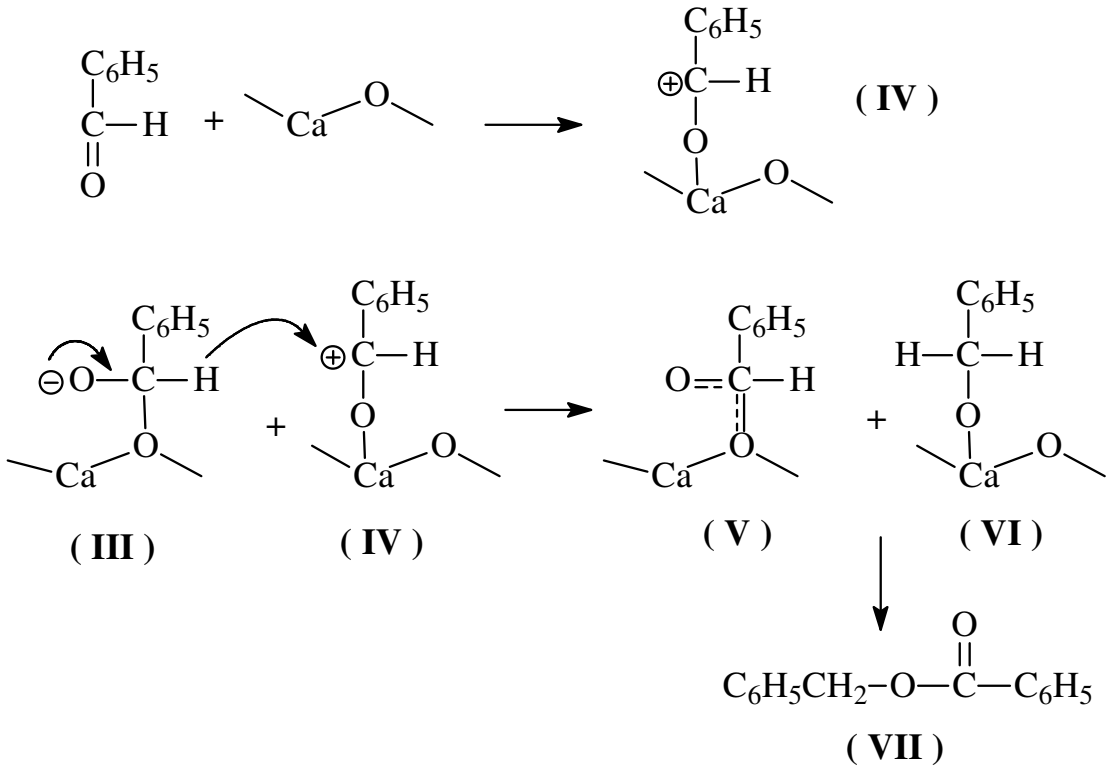


**Scheme 2.2** Esterification of benzaldehyde [68].

For the aldehydes with/without α-hydrogen, such as benzaldehyde and pivalaldehyde, Tishchenko reactions take place selectively to produce corresponding esters.

In the self-condensation of butyraldehyde, the dimers resulting from aldol condensation and the trimers resulting from Tishchenko reaction of the

dimer with butyraldehyde were formed by use of alkaline earth oxides as catalysts, as shown in Scheme 2.3. When alumina modified with alkali ions was used as catalyst, the reaction was selective for the formation of dimer by aldol condensation, and the Tishchenko reaction hardly occurred. For the aldol condensation, the presence of only basic sites is sufficient, but for the Tishchenko reaction, the presence of both basic and acidic sites is required. By modification of alumina with alkali ions, basic sites are generated and the acidic sites are suppressed. Hence, only the aldol condensation takes place. On the other hand, a considerable amount of trimer was formed on alkaline earth oxides. It was suggested that both basic and acidic sites participated in the reaction taking place on alkaline earth oxides.

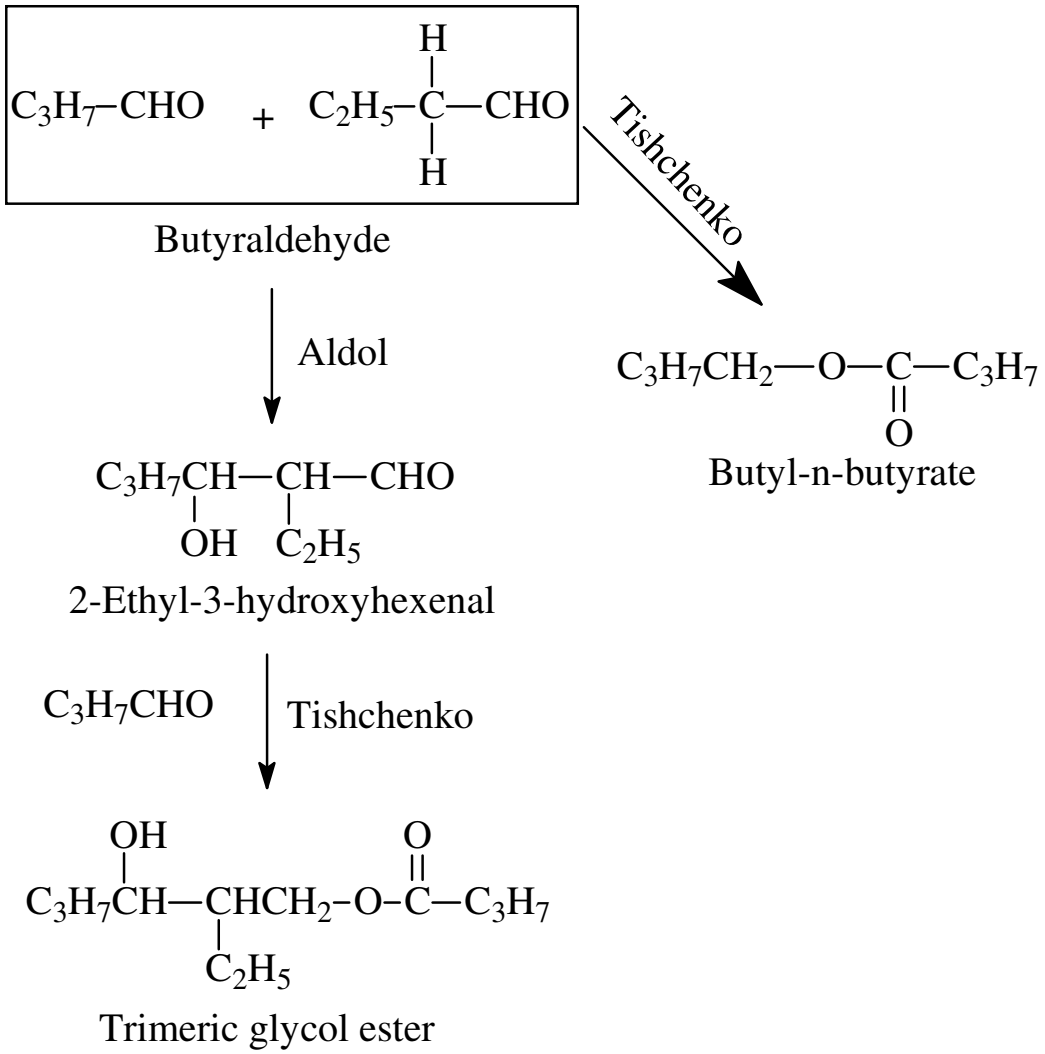


**Scheme 2.3** Self condensation of butyraldehyde [1].

### 2.5.4 Michael Addition

Michael addition is a reaction which involves a nucleophilic addition of a carbanion to α, β-unsaturated carbonyl compound. The reaction is essential for the formation of carbon-carbon bonds. However, only limited types of solid base catalysts have been applied to Michael additions. In solid base catalysis, the basic sites are responsible for forming the carbanion by abstraction of an $H^+$ from the molecule having an α-hydrogen.

Partially dehydrogenated $Ba(OH)_2$ catalyzes Michael addition of chalcones with active methylene compounds such as ethyl malonate, ethyl acetoacetate, acetylacetone, nitromethane, and acetophenone [69].

Potassium fluoride supported on alumina ($KF/Al_2O_3$) and $KOH/Al_2O_3$ are active for the Michael addition of nitromethane with α,β-unsaturated carbonyl compounds, while MgO and CaO showed low activities [70].

Dimerization of methyl crotonate proceeds by self-Michael addition to form methyl diesters of *(Z)*- and (*E*)-2-ethylidene-3-methylglutalic acid (Z-MEG and E-MEG) [71].

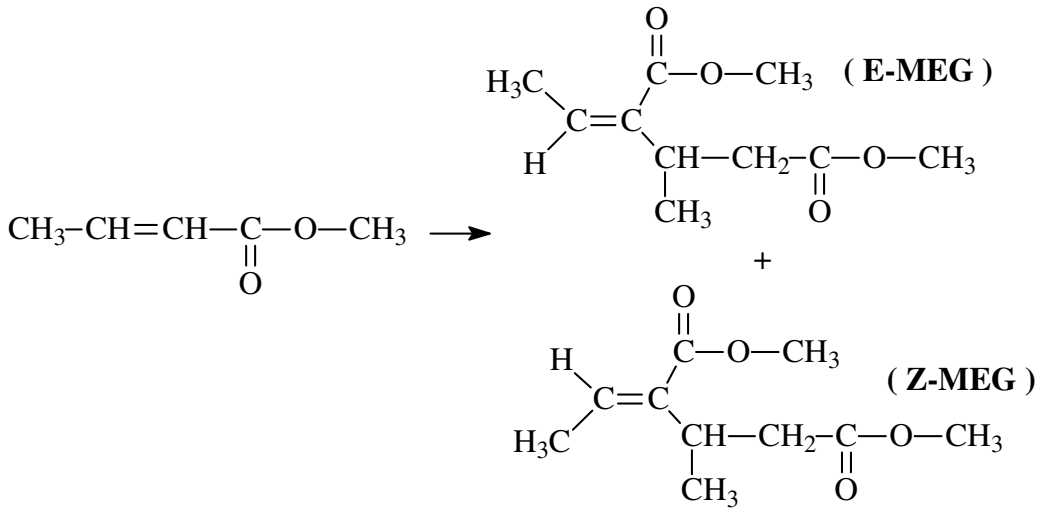


Among the types of basic catalysts used, MgO showed high activity. The reason for high MgO activity is not clear. The other base catalysts such as CaO, $La_2O_3$, $ZrO_2$, $KOH/Al_2O_3$, and $KF/Al_2O_3$ showed negligible activities as compared to MgO. The reaction is initiated by abstraction of allylic H of methyl crotonate by the basic site to form an allyl carbanion. The carbanion attacks a second methyl crotonate at the β-position to form the methyl diester of 3-methyl-2-vinylglutalic acid, which undergoes double bond migration to form the final product.

Mesoporous silica having *N,N*-dimethyl-3-aminopropyl groups prepared by the sol–gel method using a template have shown to be a good catalyst for Michael addition reactions of nitroalkanes to but-3-en-2-one and 2-cyclohaxen-1-one. No leaching of the catalytic component was observed [72].

Reconstructed hydrotalcite having $OH^-$ ions selectively catalyzes Michael additions of methyl vinyl ketone, methyl acrylate, and simple and substituted chalcones by donors such as nitroalkane, malononitrile, diethylmalonate, cyanoacetamide, and thiols [73].

### 2.5.5 The Wittig-Horner Reaction and Knoevenagel Condensation

Knoevenagel condensation is the reaction between a ketone and an active methylene compounds and proceeds over a variety of weakly basic catalysts, such as alkali-ion-exchanged zeolites, alkali-ion-exchanged sepiolite, oxynitrides, and *t*-BuOK supported on xonotlite [74,75].

Reconstructed hydrotalcite is reported to give quantitative yields for a variety of Knoevenagel condensations [76]. Mesoporous silica modified with amino groups was also effective [77–79]. AlPON is effective for the

synthesis of *α*-phenylsulfonylcinnamonitrile by the condensation of phenylsulfonylacetonitrile with benzaldehyde [80].

The two-step synthesis of dicyanomethylene derivative dyes was performed using different solid bases [81]. The first step is the Knoevenagel condensation of acetophenone and malononitrile to give the corresponding *α*-methylbenzylidenemalononitrile (**VIII**). Subsequent condensation of (I) with benzaldehyde gives the 1,1-dicyano-1,3-butadiene dye (**IX**).

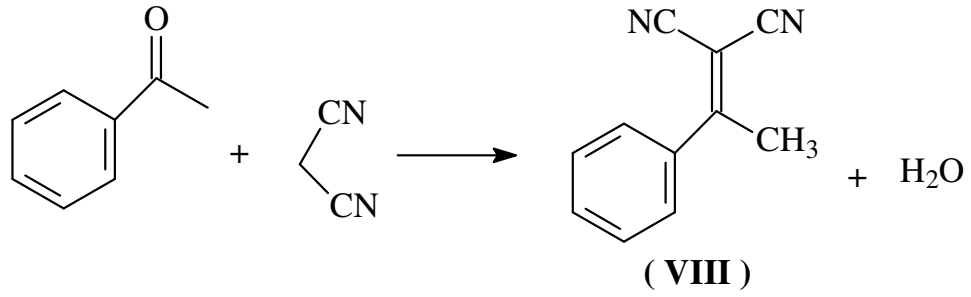


**( VIII )**

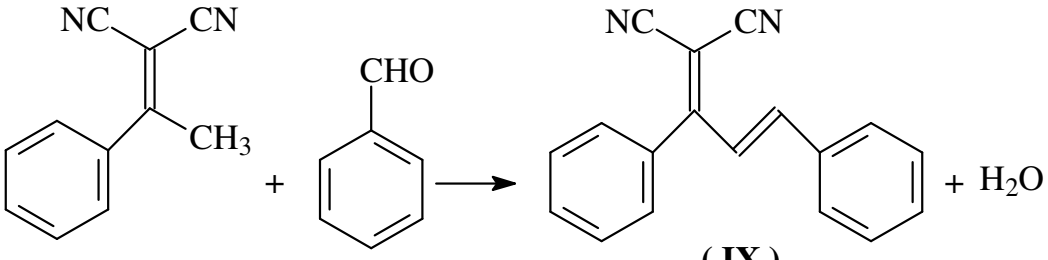


**( IX )**

The first step, the Knoevenagel condensation, was catalyzed by a variety of solid bases such as MgO, calcined hydrotalcites, and AlPONs. Only AlPONs are able to efficiently catalyze the second step. The two-step reaction could also be performed in a “one-pot” system.

The reaction of salicylaldehyde with diethylmalonate in the presence of montmorillonite gave ethyl coumarine-3-carboxylate [82].

Aldehydes react with nitriles over basic catalysts such as MgO, ZnO, and $Ba(OH)_2$ to yield the Wittig-Horner reaction and the Knoevenagel condensation as shown below [83].

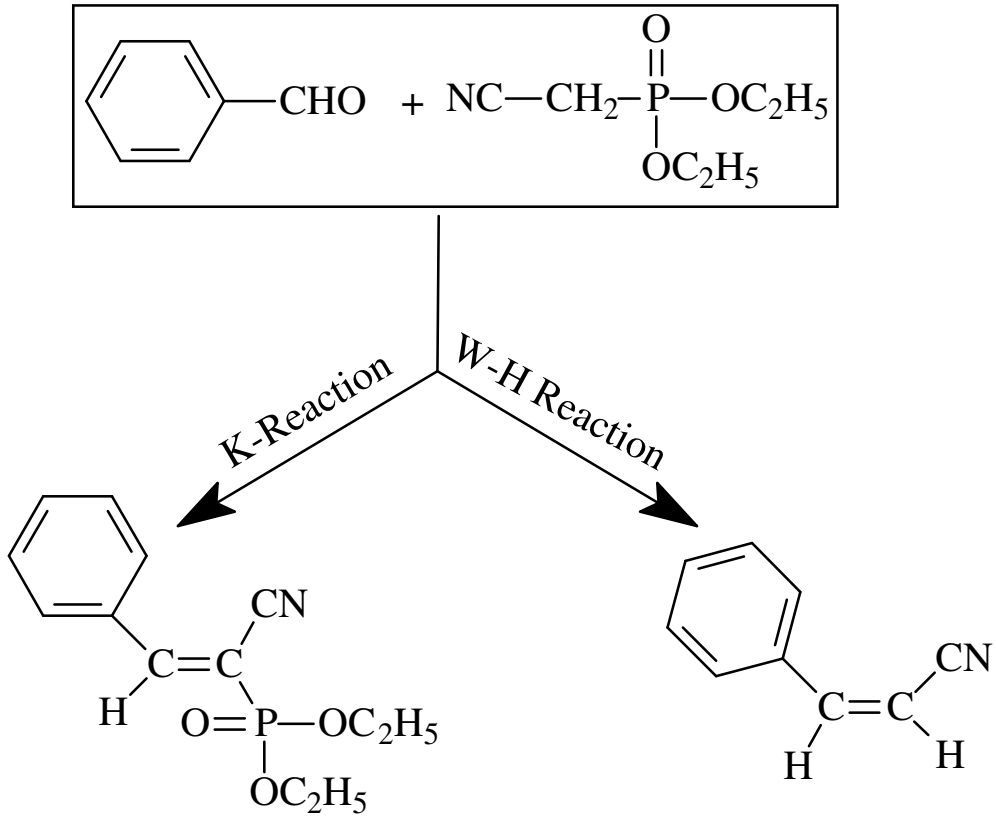


For the Knoevenagel condensation of benzaldehyde with the compounds possessing a methylene group, hydrotalcite and alkali ion-exchange zeolite [84] and alkali ion-exchange sepiolites [85] act as catalysts. For the zeolites and sepiolites, the aldol condensation which would occur as a side reaction is suppressed due to weak basic properties, and Michael addition producing bulky products is also suppressed due to the small space of the cavities where the basic sites are located. The activities of the zeolite are enhanced by replacing framework Si by Ge, which causes a change in the basic properties [86].

### 2.5.6 Nitroaldol Condensations

The nitroaldol condensation of aldehydes with nitroalkanes proceeds in the presence of bases. The reactions often proceed further to give nitroalkenes.

$$R^1CHO + R^2CH_2NO_2 \rightarrow R^1CH(OH)CH(NO_2)R^2$$

$$\rightarrow R^1HC{=}C(NO_2)R^2$$

Mg–Al mixed oxides prepared by calcination of hydrotalcite catalyze the nitroaldol condensation to nitroalcohols. The reaction is diastereoselective. For example, when 3-nitrobenzaldehyde and nitroethane was refluxed in THF, 1-(3-nitrophenyl)-2-nitropropan-1-ol was obtained in a 95% yield with a threolerythro ratio of 12.5 [87].

The nitroaldol reaction of propionaldehyde and nitromethane gives the addition product, 1-nitro-2-hydroxybutane, in the presence of different solid bases at 313 K [9].

Among the solid bases studied, MgO was the most active. The activity was not as strongly dependent on the pre-treatment temperature and was hardly retarded by exposure to air.

The condensation of aromatic aldehydes with nitroalkanes over alkaline ion-exchanged zeolites gives nitroalkenes directly. Consequently, in the reaction of benzaldehyde and chlorobenzene with nitromethane, CsNaX gave the corresponding nitroalkenes in 68 and 80 % yields, respectively, at 413 K [88].

### 2.5.7 Conjugate Addition of Alcohols

Cyanoethylation of alcohols such as methanol, ethanol, and 2-propanol with acrylonitrile occurs at 273 K over alkaline earth oxides and hydroxides, $KF/Al_2O_3$ and $KOH/Al_2O_3$. The reaction was not poisoned by adsorption of carbon dioxide at room temperature [89].

$$ROH + H_2C{=}CHCN \rightarrow ROCH_2CH_2CN$$

Hydrotalcite reconstituted by rehydration after calcination was also found to be also a highly active catalyst for cyanoethylation of alcohols with

acrylonitrile. The catalyst was reusable without a significant loss in activity and was air stable [90].

Conjugate addition of methanol to 3-buten-2-one proceeds to form 4-methoxybutan-2-one over the solid bases such as alkaline earth oxides, strontium hydroxide, barium hydroxide, and $KF/Al_2O_3$, $KOH/Al_2O_3$ at a reaction temperature of 273 K [91]. MgO treated at 673 K gave the highest activity. The catalytic activities of MgO, CaO, and $KF/Al_2O_3$ were not affected by exposure of the catalysts to carbon dioxide or air.

### 2.5.8 Hydrogenation

Kokes and his co-workers studied the interaction of olefins with hydrogen on ZnO, and reported heterolytic cleavage of $H_2$ and C-H bond [4,5]. The negatively charged $\pi$-allyl anions are intermediate for propylene hydrogenation. Participation of heterolytically dissociated $H^+$ and $H^-$ in the hydrogenation is generally applicable in base-catalyzed hydrogenation reaction. The observation that MgO pre-treated at 1273 K exhibited olefin hydrogenation activities was a clear demonstration of heterogeneous base-catalyzed hydrogenation [92]. The hydrogenation occurring on heterogeneous basic catalysts has characteristic features which distinguish

heterogeneous basic catalysts from conventional hydrogenation catalysts such as transition metals and transition metal oxides.

The characteristic features of base-catalyzed hydrogenation reaction are as follows [1].

(1) There is a large difference in the hydrogenation rate between monoenes and conjugated dienes: Conjugated dienes undergo hydrogenation much faster than monoenes. For example, 1,3-butadiene undergoes hydrogenation at 273 K over alkaline earth oxides, while butenes need a reaction temperature above 473 K. The products of diene hydrogenation consist exclusively of monoenes, with no alkanes being formed at 273 K.

(2) There is a predominant occurrence of 1,4-addition of H atoms in contrast to 1,2-addition which is commonly observed for conventional hydrogenation catalysts: In 1,3-butadiene hydrogenation, 2-butenes are preferentially formed over heterogeneous basic catalysts, while 1-butene is the main product over conventional hydrogenation catalysts.

(3) There is retention of the molecular identity of H atoms during reaction: While a hydrogen molecule dissociates on the catalyst surface, two H

atoms used for hydrogenation of one reactant molecule originate from one hydrogen molecule.

Features 1 and 2 are characteristic of hydrogenation in which anionic intermediates are involved [93]. The reaction (Scheme 2.4) of 1,3-butadiene hydrogenation is shown below, where H is replaced by D for clarity. The products contain two D atoms at the terminal C atoms if $D_2$ is used instead of $H_2$.

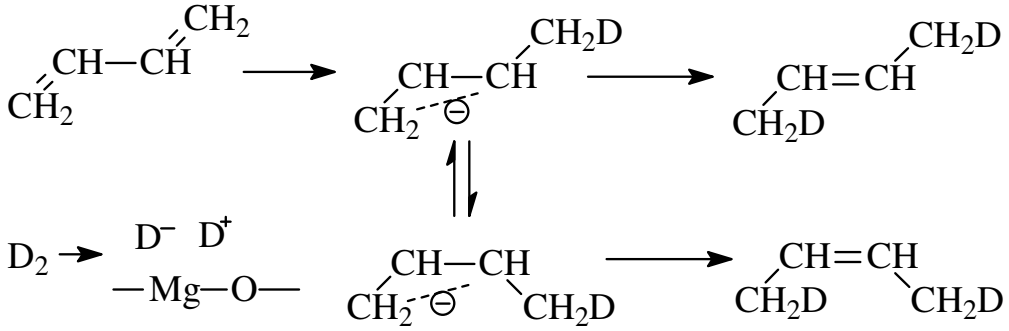


**Scheme 2.4** Hydrogenation of 1,3-Butadiene [93].

A large difference in the reactivity between dienes and monoenes is caused by the difficulty of alkyl anion formation compared to allyl anion formation. Alkyl anions are less stable than allyl anions, hence the

reactions of monoenes with $H^-$ to form alkyl anions require high temperature.

Feature 3 arose from the location of the active sites. Both $D^+$ and $D^-$ on one set of active sites are assumed not to migrate to other sites, and each set of active sites is isolated from the others. This happens when the basic hydrogenation catalysts are metal oxides.

The active sites for hydrogenation on alkaline earth oxides are believed to be metal cation $-O^{2-}$ ion pairs of low coordination. In the surface model structure of MgO, it is possible that the $Mg^{2+}_{3c}$ $-O^{2-}_{3c}$ pairs act as hydrogenation sites [11].

1,3-Butadiene undergoes transfer hydrogenation with 1,3-cyclohexadiene over $La_2O_3$, CaO, $ThO_2$, and $ZrO_2$ [94,95]. The product distributions are similar to those for hydrogenation with $H_2$ except for $ZrO_2$, on which a relatively large amount of 1-butene is formed.

Hydrogenation (or reduction) of aromatic carboxylic acids to corresponding aldehydes using $ZrO_2$ has been industrialized [32,96]. Although the reaction mechanism is not clear at present, the hydrogenation and dehydration abilities, which are associated with the basic properties of

$ZrO_2$, seem to be important for promoting the reaction. The catalytic properties are improved by modification with the metal ions such as $Cr^{3+}$ and $Mn^{4+}$ ions. Crystallization of $ZrO_2$ is suppressed and coke formation is avoided by addition of the metal ions.

$$ArCOOH + H_2 \longrightarrow ArCHO + H_2O$$

### 2.5.9 Other Reactions

#### 2.5.9.1 Amination

Amines undergo an addition reaction with conjugated dienes over heterogeneous basic catalyst [97]. Primary and secondary amines add to conjugated dienes to form unsaturated secondary and tertiary amines, respectively. Amination with monoenes hardly proceeds over basic catalysts. The reaction mechanisms for amination with conjugated dienes are essentially the same as those for the hydrogenation reactions in the sense that heterolytic dissociation of hydrogen ($H_2 << H^+ + H^-$) and amine ($RNH_2 << H^+ + RNH^-$) are involved in the reaction. The sequence in which the anion and $H^+$ successively add to the 1,4 position of conjugated dienes is common to hydrogenation and amination. As an example, the reaction

mechanisms for addition of dimethylamine to 1,3-butadiene is shown in Scheme 2.5. The reaction occurs over CaO at 273 K.

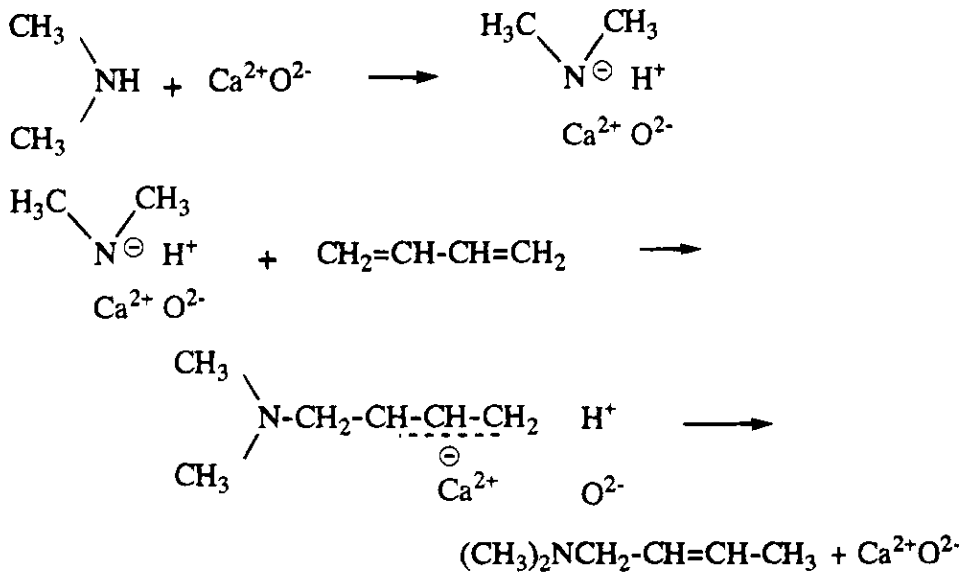

**Scheme 2.5** Amination of 1,3-Butadiene [97].

### 2.5.9.2 Isomerization

1-Butene isomerization to 2-butenes has been extensively studied over many solid base catalysts to elucidate the reaction mechanisms and to characterize the surface basic properties. The reaction proceeds at room temperature or below over most of heterogeneous basic catalysts. Over MgO, for example, the reaction occurs even at 223 K if the catalyst is properly activated.

The reaction mechanisms for 1-butene isomerization are shown in Scheme 2.6 [27]. The reaction is initiated by abstraction of allylic H by basic sites to form cis or trans forms of the allyl anion. In the form of the allyl anion, the cis form is more stable than the trans form. Therefore, *cis*-2-butene is predominantly formed at the initial stage of the reaction. A high cis/trans ratio observed for the base-catalyzed isomerization is in contrast to the value close to unity found for acid-catalyzed isomerization.

The cis to trans ratio in 2-butenes produced could be used to judge whether the reaction is a base catalyzed or acid-catalyzed one. Tsuchiya measured the ratio cis/trans in 1-butene isomerization, and found a high value for $Rb_2O$ [98].

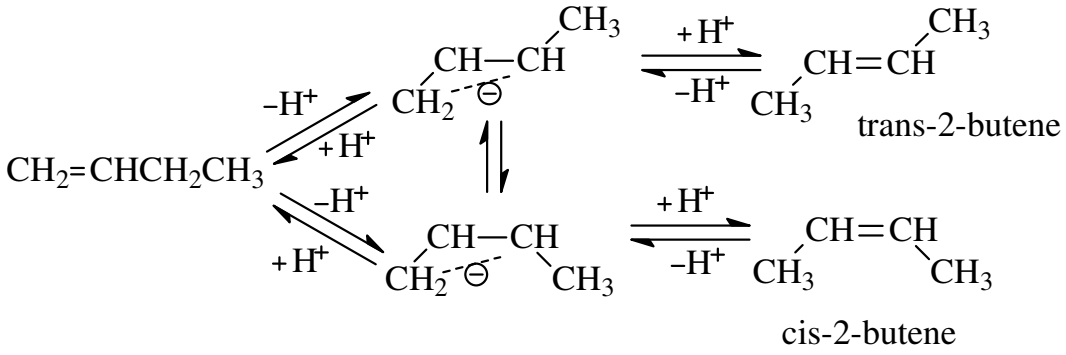


**Scheme 2.6** 1-Butene Isomerization [27].

Simultaneous isomerization of butene-$d_0$ and $-d_8$ is a useful method to determine the reaction mechanism [99]. In the co-isomerization reaction, a mixture containing equal amounts of non-deuteriobutene ($d_0$) and per-deuteriobutene ($d_8$) is allowed to react, and the isotopic distributions in the products and reactant are analyzed. If the reaction proceeds by hydrogen addition-abstraction mechanisms, an intermolecular H (or D) transfer is involved and the products will be composed of $d_0$, $d_1$, $d_7$, and $d_8$ isotopic species. On the other hand, if the reaction proceeds by hydrogen abstraction-addition mechanisms, an intramolecular H (or D) transfer is involved, and then the products will be composed of $d_0$ and $d_8$ isotopic species.

Since an $H^+$ is abstracted first for base-catalyzed isomerization to form allyl anions to which the $H^+$ returns at a different C atom, an intramolecular H (or D) transfer is expected. Therefore, an intramolecular H (or D) transfer and a high cis/trans ratio are characteristic features for 1-butene double bond isomerization over heterogeneous basic catalyst [100,101].

The fundamental studies of 1-butene double bond isomerization over heterogeneous basic catalysts were extended to the double bond migration of olefins having more complex structures such as carene **(X),**

pinene **(XI),** protoilludene **(XIII),** illudadiene **(XIV),** as shown below [57,102,103].

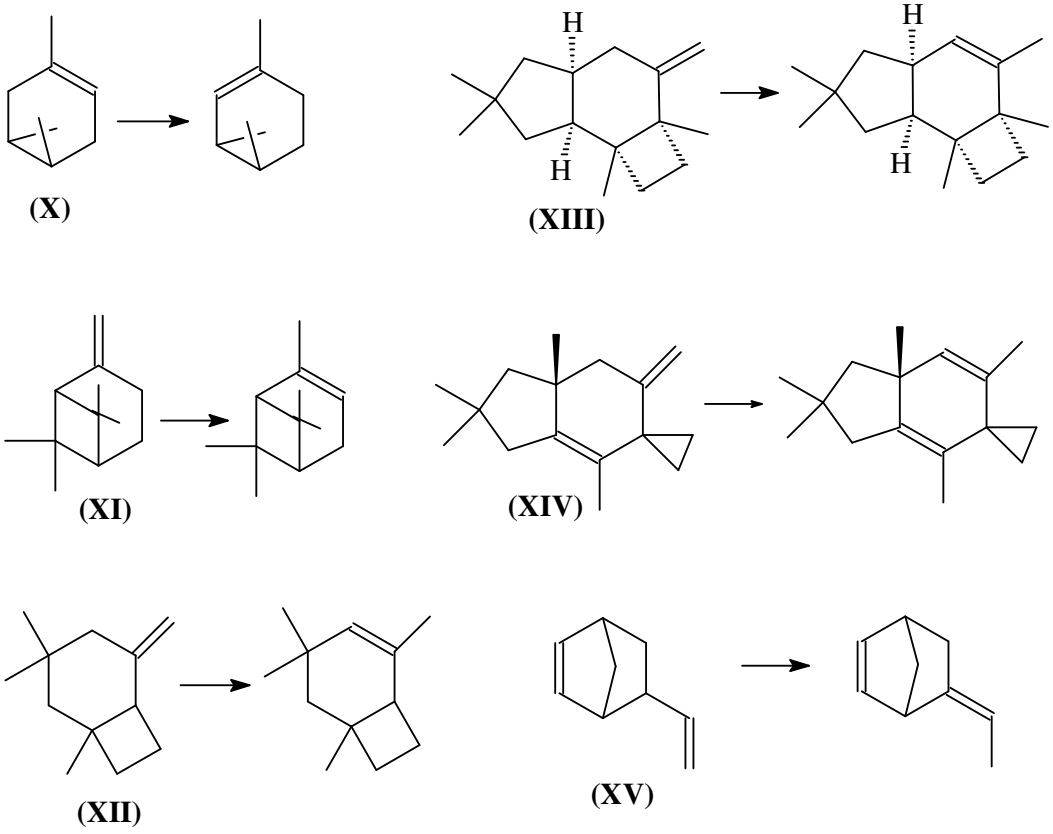


**(X)** **(XIII)**

**(XI)** **(XIV)**

**(XII)** **(XV)**

These olefins contain three-membered and four-membered rings. If acidic catalysts were used, the ring-opening reactions would easily occur, and the selectivity for double bond migration should markedly decrease. A characteristic feature of solid base catalysts is that the double bond migration selectively occurs without C-C bond cleavages over solid base catalysts.

The solid base catalysts are highly active for low temperature double bond migration. This is beneficial for olefins which are unstable at high temperature. Because of this advantage, the heterogeneous basic catalyst, $Na/NaOH/Al_2O_3$, is used on an industrial process for the selective double bond migration of 5-vinylbicyclo[2.2.1]heptene (**XV**) [57,104]. The reaction proceeds at the low temperature of 243 K.

Solid base catalysts have another advantage in double bond migration. For the double bond migration of unsaturated compounds containing heteroatoms such as N and O, solid base catalysts are more efficient than acidic catalysts [105,106]. Acidic catalysts interact strongly with heteroatoms, became poisoned, and show no activity. On the other hand, the active sites of solid base catalysts interact weakly with heteroatoms and, therefore, act as efficient catalysts.

Allylamines undergo double bond migration to enamines over alkaline earth oxides (Scheme 2.7) [105]. In this scheme, 1-N-pyrrolidino-2-propene isomerizes to 1-N-pyrrolidino-1-propene over MgO, CaO, SrO, and BaO at 313 K. The reaction mechanisms are essentially the same as those for 1-butene isomerization. The cis-form of the intermediate of the allyl anion is

more stable than the trans-form, and the products are mostly in the thermodynamically less stable cis-form.

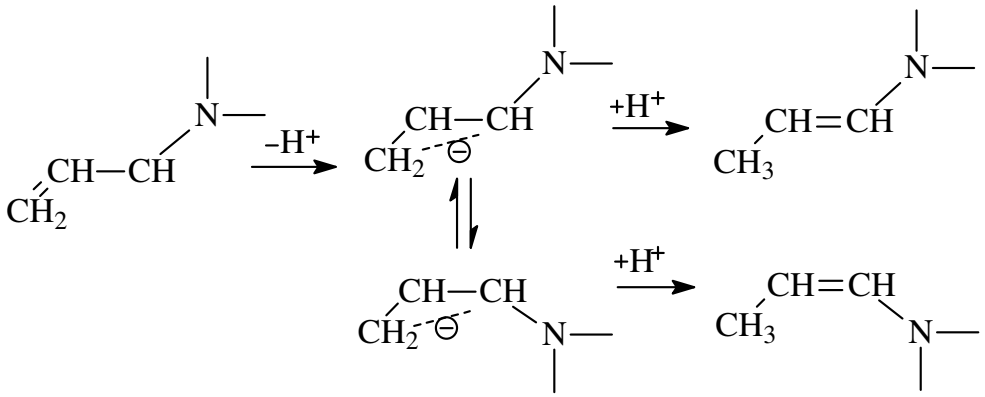

**Scheme 2.7** Double bond migration of allylamines to enamines [105].

The isomerization of alkyn-1-yl alcohol to *α,β*-unsaturated ketones proceeds over solid-base catalysts [106]. Thus, in the reaction of compound (**XVI**) in dioxane with $Cs_2CO_3/Al_2O_3$ for 20 h at 303 K, product (**XVII**) was obtained in a 97% yield.

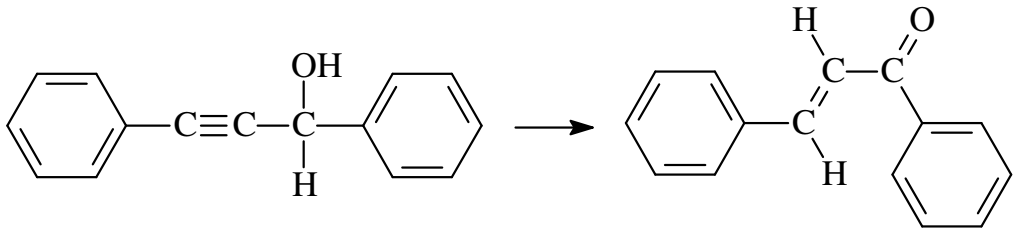

**( XVI )** **( XVII )**

### 2.5.9.3 Dehydration and Dehydrogenation Reactions

In general, alcohols undergo dehydration to olefins and ethers over acidic catalysts and dehydrogenation to aldehydes or ketones over basic catalysts. In some cases, however, solid base catalysts promote dehydration of alcohols in which the mechanisms and product distribution differ from those for acid-catalyzed dehydration. The characteristic features of base-catalyzed dehydration are observed for 2-butanol dehydration. The products consist mainly of 1-butene over the rare earth oxides [29], $ThO_2$ [30,31] and $ZrO_2$ [33]. This is in contrast to the preferential formation of 2-butenes over acidic catalysts. The initial step in the base-catalyzed dehydration is the abstraction of an $H^+$ at C-1 to form an anion.

$ZrO_2$ is used as a catalyst for the industrial dehydration of 1-cyclohexylethanol to vinylcyclohexane [35]. In the dehydration of 2-alcohols to the corresponding 1-olefins over $ZrO_2$, the selectivity of 1-olefins depends on the amount of Si contained in $ZrO_2$ as an impurity. Si contaminants in $ZrO_2$ generate acidic sites. By treatment of $ZrO_2$ with NaOH to eliminate the acidic sites, the by-products of 2-olefins are markedly reduced and the selectivity for 1-olefins is increased.

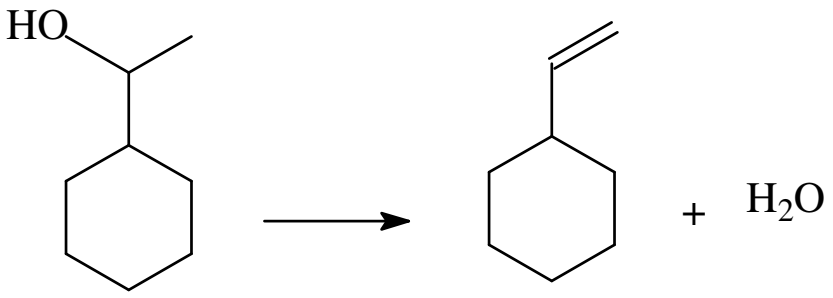


Intramolecular dehydration of monoethanolamine to ethylenimine has also been industrialized by use of the mixed oxide catalyst composed of Si, alkali metal, and P. The catalyst possesses both weakly acidic and basic sites [107]. Because monoethanolamine has two strong functional groups, weak sites are sufficient to interact with the reactant. If either acidic sites or basic sites are strong, the reactant interacts too strongly with the sites and forms undesirable by-products. It is proposed that the acidic and basic sites act cooperatively.

#### 2.5.9.4 Nucleophilic Ring Opening Reactions

Ring opening of glycidol with fatty acids provides a route to monoglycerides, which are important food additives as emulsifiers and antimicrobial agents. Cauvel et al. found that MCM-41 grafted with 3-

aminopropyl and 3-piperidinopropyl groups are active catalysts for the ring opening of glycidol with lauric acid [77]. The selectivity was improved by treating the catalysts with hexamethyldisilazane to block the residual OH groups of the surface. The gas chromatographic and isolated yields of lauric monoglyceride was >95 and 70%, respectively.

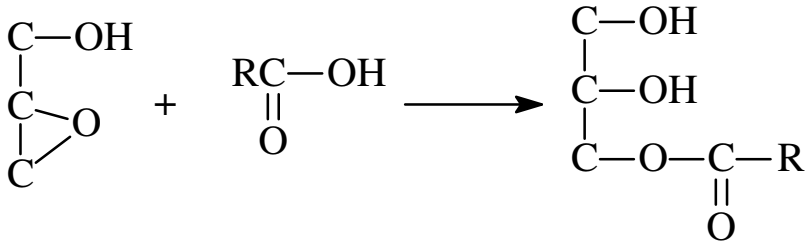

Lin and co-workers also prepared MCM-41 grafted with various amine functions and carried out the ring opening of glycidol with lauric acid [108,109]. The most active form was MCM-41 on which triazabicyclo[4,4,0]dec-5-ene was immobilized.

MgO is an efficient catalyst for the cycloaddition of carbon dioxide under mild conditions. The reaction of carbon dioxide with (*R*)-styrene oxide gives (*R*)-phenylcarbonate in 97% *ee* with retention of stereochemistry [110].

Cycloaddition of carbon dioxide to epoxides proceeds also in the presence of mixed oxide prepared by calcination of hydrotalcite [111].

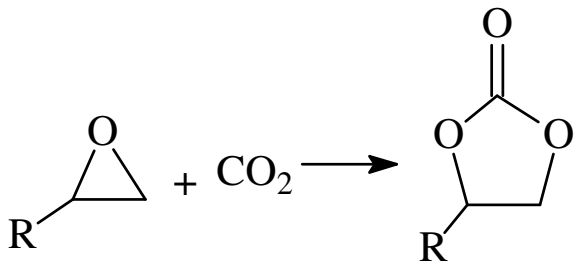

### 2.5.9.5 Oxidation Reactions

The recent development in the use of solid bases in oxidation reactions was reviewed by Fraile et al. [112].

The epoxidation of electron-deficient alkenes is commonly carried out with hydroperoxides in the presence of a base. In this reaction, a proton is abstracted from $H_2O_2$ or ROOH to form $HOO^-$ and $ROO^-$ ions, respectively. These ions act as nucleophiles and epoxidize electron-deficient alkenes such as *α,β*-unsaturated carbonyl compounds [113].

Choudary et al. found that hydrotalcite, where *t*-butoxy ions were introduced by ion exchange, was a much more efficient catalyst than the

mixed oxide prepared by calcination of hydrotalcite for the epoxidation of *α,β*-unsaturated carbonyl compounds such as chalcone [114].

In the case of epoxidation with *t*-butyl hydroperoxide (TBHP), KF/$Al_2O_3$ is used as a base. The method was first reported by Yadav and Kapoor [115,116]. For example, cyclopentenones are oxidized in good, usually quantitative yields without showing any aldol products [116].

In the epoxidation of *α*-isophorone, the use of TBHP in combination with KF/$Al_2O_3$ gave better results over $H_2O_2$ with hydrotalcite [117]. The epoxide was obtained at a 96% yield after reaction for 24 h at 393 K in toluene.

Fraile et al. carried out the epoxidation of two chiral alkenes derived from D-glyceraldehyde, bearing different electron-withdrawing groups [118]. Here again, TBHP–KF/Al2O3 was more efficient and selective than $H_2O_2$ calcined hydrotalcite, leading to a high diastereometric excess (de). Thus, TBHP–KF/$Al_2O_3$ gave 100% conversion of (**XVIII**) and (**XIX**), with high diastereoselectivities, 40% de (**XIX**) and 50% de (**XXII**) and no detectable by-products.

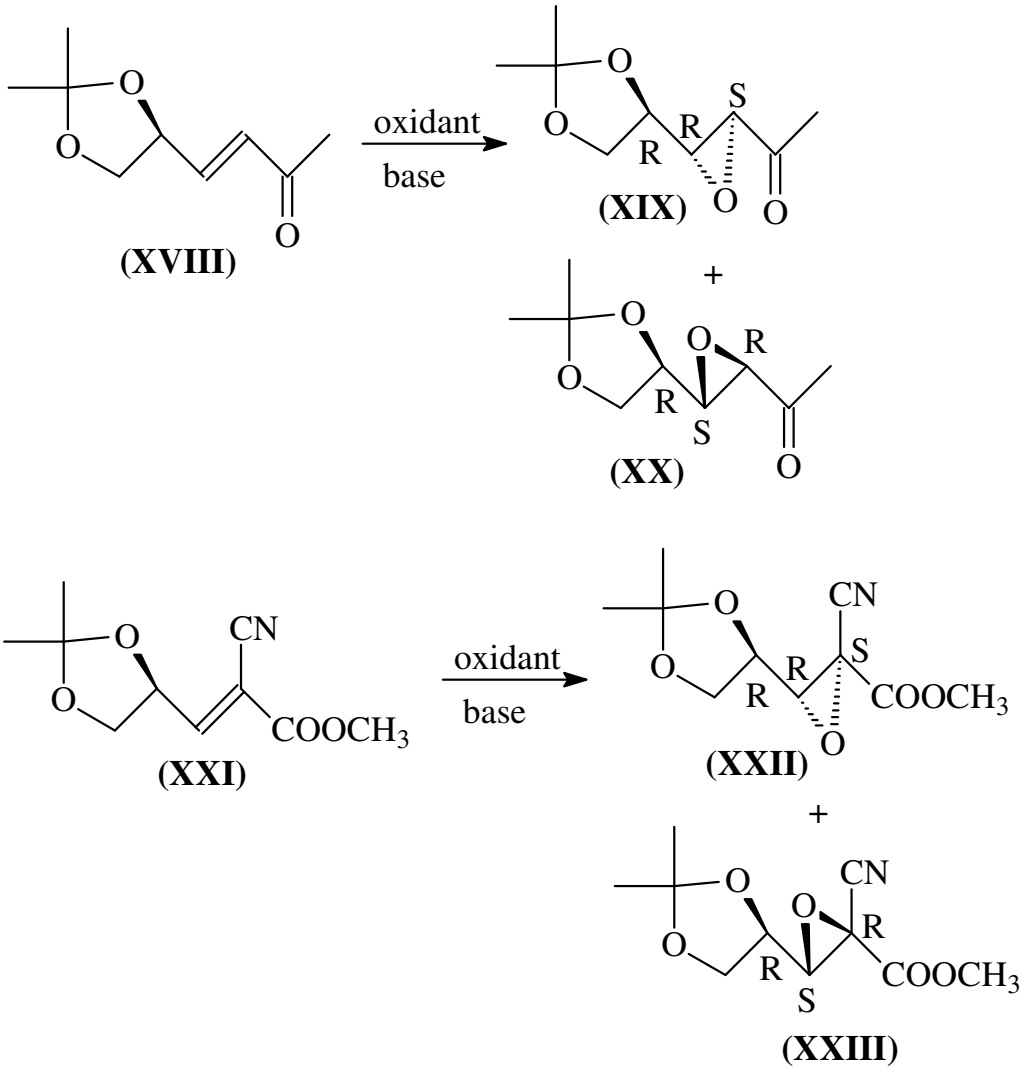


Various alkenes are epoxidized by hydroperoxide in combination with benzonitrile in the presence of as-synthesized hydrotalcite with $CO_3^{2-}$ ions [119,120]. For example, linear and cyclic alkenes such as oct-1-ene and

cyclohexene gave the corresponding epoxides in excellent yields. Norbornene and styrene gave *exo*-norbornene oxide and styrene oxide, respectively, in high yields. Hydrotalcite with *t*-butoxide in the interlayers has much higher activity for the epoxidation of unfunctionalized alkenes such as styrene than as-synthesized hydrotalcite with $CO_3^{2-}$ ions in the presence of benzonitrile [114].

Kaneda and co-workers reported that Baeyer–Villiger oxidation of ketones by molecular oxygen in combination with benzaldehyde was greatly enhanced by adding as-synthesized hydrotalcite [121,122].

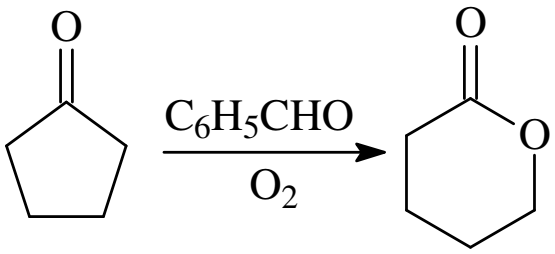


**2.5.9.6 Meerwein-Ponndorf-Verley Reaction**

Meerwein-Ponndorf-Verley reaction is the hydrogenation in which alcohols are used as a source of hydrogen and entail a hydrogen transfer reaction. Aldehydes and ketones react with alcohols to produce corresponding alcohols by Meerwein-Ponndorf-Verley reduction:

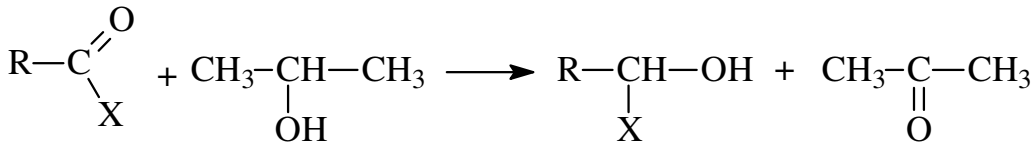

Shibagaki et al. studied Meerwein-Ponndorf-Verley reduction of various kinds of aldehydes and ketones in the temperature range 273-473 K [123]. They found hydrous zirconium oxide as a highly active catalyst for the reactions. 2-Propanol was used as a hydrogen source. On the basis of the isotope effect and kinetic analysis, it was suggested that the slow step is hydride transfer from the adsorbed 2-propanol to the adsorbed carbonyl compound (Scheme 2.8).

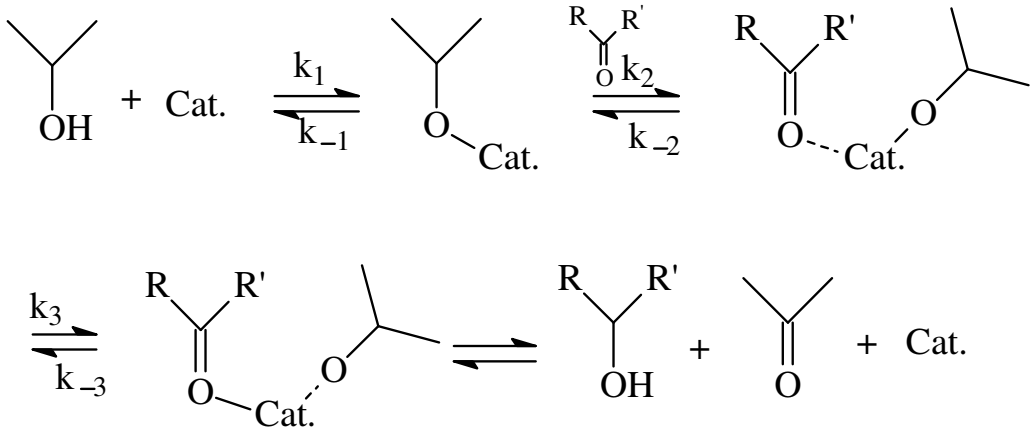

**Scheme 2.8** Hydrogen transfer from 2-propanol to aldehydes and ketones [123].

The reactions of carboxylic acids with alcohols to form esters are also catalyzed by hydrous zirconium oxide at a reaction temperature above 523 K [124]. Similarly, amidation of carboxylic acids or esters with amines or ammonia proceeds over hydrous zirconium oxide in the temperature range 423-473 K [125].

Although hydrous zirconium oxide is proposed to be an effective catalyst for the above reactions, the nature of the active sites has not been elucidated. The reaction mechanisms involving the active sites are not established for the hydrous zirconium oxide catalyzed reactions.

Meerwein-Ponndorf-Verley reduction of ketones or aldehydes with 2-propanol proceeds over X-zeolites ion-exchanged with $Cs^+$ and $Rb^+$ [126]. The mechanism proposed for the zeolites is shown in Scheme 2.9. The reaction is initiated by abstraction of an $H^+$ from 2-propanol by the basic sites of the catalyst. In addition to the basic sites, exchanged cations play a role of stabilizing the ketone by the hydride transferring from adsorbed 2-propanol to the ketone.

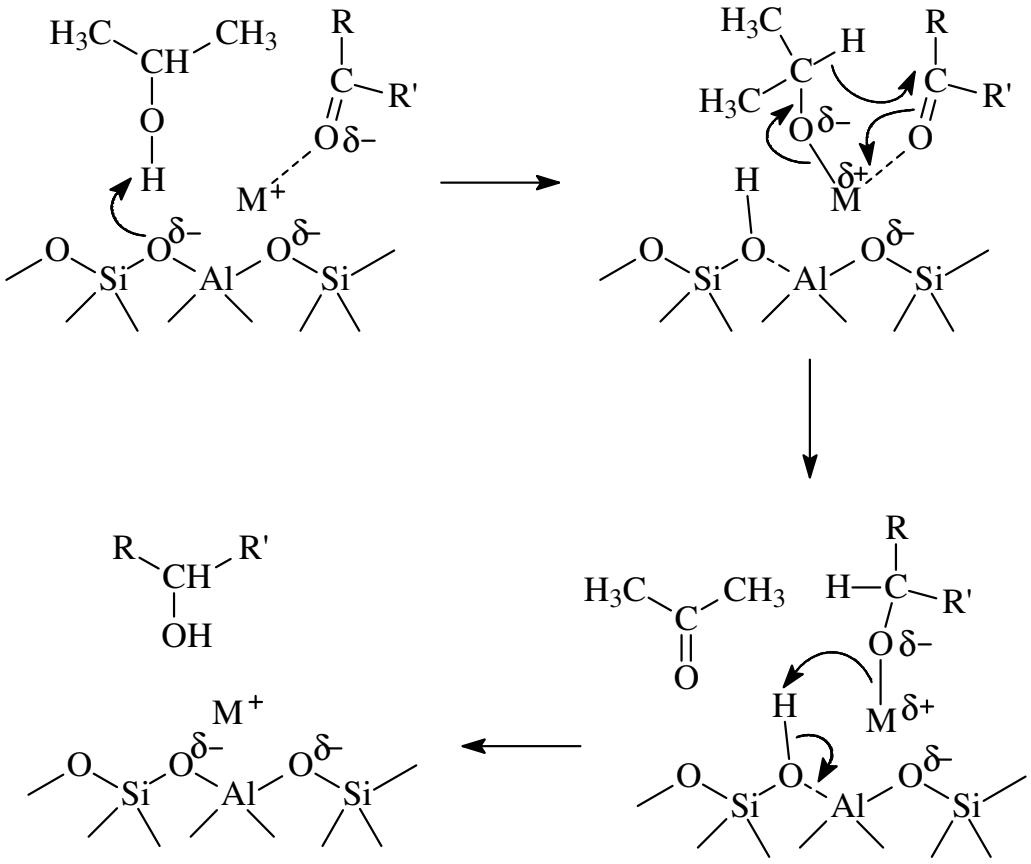

**Scheme 2.9** Meerwein-Ponndorf-Verley reduction of ketones and aldehyde with 2-propanol [126].

Aramendia et al. has studied the Meerwein-Ponndorf-Verley reaction of cyclohexanone with isopropyl alcohol over magnesium oxide based catalysts [127]. During the reaction, the alcohol is oxidized to a ketone and

cyclohexanone is reduced to cyclohexanol as shown in scheme 2.10 below.

A comparison of the catalytic activity for the MgO catalysts tested revealed that the most catalytically active catalysts possessed the largest number of basic sites.

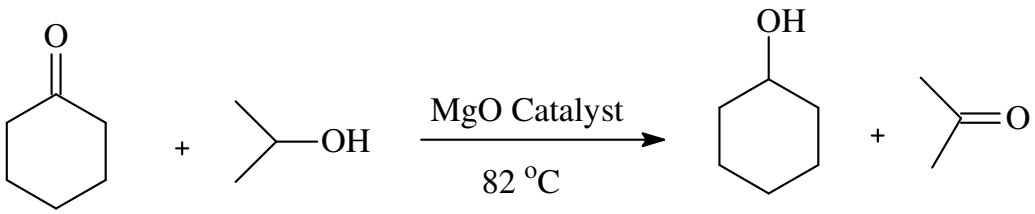


**Scheme 2.10** Meerwein-Ponndorf-Verley reaction of cyclohexanone with 2-propanol [127].

## 2.6 Conclusion

As described above, an increasing number of reactions are catalyzed by basic catalysts. A variety of solid base materials with different base strengths can be synthesized. However, the reactions for which solid base

catalysts have been used are only a fraction of a great number of organic reactions.

There should be many reactions which solid base catalysts can efficiently promote, but have not been used for. One of the reasons for the limited use of solid base catalysts arises from rapid deactivation while being handled under the atmosphere. This however, can be minimised by insitu activation of the catalyst at high temperatures. If this care is taken, solid base catalysts should promote a large number of reactions.

Some of the reactions described in this chapter specifically proceed on solid base catalysts. The catalytic activities of solid base catalysts are not simple copies of those of homogeneous basic catalysts, though it is not clearly understood where the features of solid base catalysts originated. To clarify this point, characterization of the surface active sites together with elucidation of the reaction mechanisms occurring on the surface should be extended.

## 2.7 References

[1] H. Hattori, Chem. Rev. 95 (1995) 537.

[2] Y. Ono, J. catal. 216 (2003) 406.

[3] H. Pines, J. A. Veseley, V. N. Ipatieff, J. Am. Chem. Soc. 77 (1955) 6314.

[4] R. J. Kokes, A. L. Dent, Advan. Catal. 22 (1972) 1.

[5] R. J. Kokes, Proceedings of the 5th International Congress of Catalysis Miami Beach, FL, (1972) 1.

[6] H. Hattori, N. Yoshii, K. Tanabe, Proceedings of the 5th International Congress on Catalysis, Miami Beach, FL, (1972) 233.

[7] T. Yashima, K. Sato, T. Hayasaka, N. Hara, J. Catal. 26 (1972) 303.

[8] H. Hattori, K. Maruyama, K. Tanabe, J. Catal. 44 (1976) 50.

[9] H. Hattori, Appl. Catal. A: General, 222 (2001) 247.

[10] K. Tanabe, M. Misono, Y. Ono, H. Hattori, New Solid Acids and Bases; Kodansha (Tokyo)-Elsevier (1989) 39.

[11] S. Coluccia, A.J. Tench, Proceedings of the 7th International Congress on Catalysis Tokyo, Japan: (1980) 1160.

[12] Y. Fukuda, H. Hattori, K. Tanabe, Bull. Chem. Soc. Japan, 51 (1978) 3151.

[13] Y. Imizu, K. Sato, H. Hattori, J. Catal. 71 (1981) 64.

[14] M. Utiyama, H. Hattori, K. Tanabe, J. Catal. 4 (1978) 237.

[15] L.P. Hammett, Physical Organic Chemistry; McGraw-Hill: New York, (1940) Chapter IX.

[16] M.A. Paul, F.A. Long, Chem. Rev. 57 (1957) 1.

[17] J. Take, N. Kikuchi, Y. Yoneda, J. Catal. 21 (1971) 164.

[18] G. Zhang, H. Hattori, K. Tanabe, Appl. Catal. 36 (1988) 189.

[19] H. Tsuji, F. Yagi, H. Hattori, Chem. Lett. (1991) 1881.

[20] T. Ito, M. Kuramoto, M. Yoshida, T. Tokuda, J. Phys. Chem. 87 (1983) 4411.

[21] T. Ito, T. Murakami, T. Tokuda, J. Chem. Soc. Trans. Faraday, 79 (1983) 913.

[22] Y. Okamoto, M. Ogawa, A. Maezawa, T. Imanaka, J. Catal. 112 (1988) 427.

[23] M. Huang, A. Adnot, S. Kaliaguine, J. Catal. 137 (1992) 322.

[24] D. Barthomeuf, J. Phys. Chem. 55 (1978) 138.

[25] Y. Fukuda, K. Tanabe, Bull. Chem. Soc. Japan, 46 (1973) 1616.

[26] J.V. Evans, T.L. Whateley, Trans. Faraday Soc. 63 (1967) 2769.

[27] H. Hattori, Stud. Surf. Sci. Catal. 78 (1993) 35.

[28] H. Hattori, H. Kumai, K. Tanaka, G. Zhang, K. Tanabe, Proc. 8th National Symposium on Catalysis Sindri, India, (1987) 243.

[29] A.J. Lundeen, R. van Hoozen, J. Org. Chem. 32 (1967) 3386.

[30] T. Tomatsu, H. Yoneda, H. Ohtsuka, Yukagaku, 17 (1968) 236.

[31] K. Thomke, Proceedings of the 6th International Congress on Catalysis London, UK, (1976) 303.

[32] T. Yokoyama, T. Setoyama, N. Fujita, M. Nakajima, T. Maki, K. Fukii, Appl. Catal. A: Gen. 88 (1992) 149.

[33] T. Yamaguchi, H. Sasaki, K. Tanabe, Chem. Lett. (1976) 677.

[34] I. Koga, Yuki Gouseikagaku 33 (1975) 702.

[35] K. Takahashi, T. Hibi, Y. Higashio, M. Araki, Shokubai (Catalyst) 35 (1993) 12.

[36] T. Yamaguchi, Sekiyu Gakkaishi, J. Jpn. Petroleum Inst. 36 (1993) 250.

[37] T. Tanabe, Proceedings of the 8th International Congress on Catalysis, Calgary, Canada, 5 (1988) 85.

[38] H. Tsuji, F. Yagi, H. Hattori, H. Kita, Proceedings of the 10th International Congress on Catalysis, Budapest, Hungary, (1992) 1171.

[39] H. Itoh, S. Utamapanya, J.V. Stark, K.J. Klabunde, Schlup, J. Chem. Mater. 5 (1993) 71.

[40] J.H. Clark, Chem. Rev. 80 (1980) 429.

[41] J. Yamawaki, T. Ando, Chem. Lett. (1979) 45.

[42] T. Ando, J. Yamawaki, Yukigosei Kyokaishi (J. Org. Syn. Inst.), 39 (1981) 14.

[43] J.M. Campelo, M.S. Climent, J.M. Marinas, React. Kinet. Catal. Lett. 47 (1992) 7.

[44] P. Laszlo, P. Peuneteau, Tetrahedron Lett. 22 (1983) 2645.

[45] J.H. Clark, D.G. Cork, M.S. Robertson, Chem. Lett. (1983) 1145.

[46] D. Villemin, J. Chem. Soc. Chem. Commun. (1983) 1092.

[47] D. Villemin, Chem. Ind. (London) (1985) 166.

[48] F. Texier-Bullet, D. Villemin, M. Licard, H. Mison, A. Foucaud, Tetrahedron, 41 (1985) 1259.

[49] J. Yamawaki, T. Kawate, T. Ando, T. Hanafusa, Bull. Chem. Soc. Jpn. 56 (1983) 1885.

[50] D. Villemin, M. Richard, Tetrahedron Lett. 75 (1984) 1059.

[51] J. Yamawaki, T. Ando, T. Hanafusa, Chem. Lett. (1981) 1143.

[52] T. Ando, J. Yamawaki, T. Kawate, S. Sumi, T. Hanafusa, Bull. Chem. Soc. Jpn. 55 (1982) 2504.

[53] A.E. Elisabeth, E.A. Schmittiling, J.S. Sawyer, J. Org. Chem. 58 (1993) 3229.

[54] Y. Nomoto, E. Suzuki, Y. Ono, Acid-Base Catalysis II, Kodansha (Tokyo)-Elsevier (Amsterdam, Oxford, New York, Tokyo) (1994) 447.

[55] T. Baba, G.J. Kim, Y. Ono, J. Chem. Soc. Faraday Trans. 88 (1993) 891.

[56] T. Baba, S. Hikita, R. Koide, Y. Ono, T. Hanada, T. Tanaka, S. Yoshida, J. Chem. Soc. Faraday Trans. 89 (1993) 3177.

[57] G. Suzukamo, M. Fukao, T. Hibi, K. Chikaishi, Acid-Base Catalysis, Kodansha (Tokyo)-VCH (Basel, Cambridge, New York, Weinheim), (1989) 405.

[58] T. Ushikubo, H. Hattori, K. Tanabe, Chem. Lett. (1984) 649.

[59] H. Ito, A. Miyamoto, Y. Murakami, J. Catal. 64 (1980) 284.

[60] A. Miyamoto, S. Iwamoto, K. Agusa, T. Inui, Acid-Base Catalysis, Kodansha (Tokyo)-VCH (Basel, Cambridge, New York, Weinheim), (1989) 497.

[61] P.E. Hathaway, M.E. Davis, J. Catal. 119 (1989) 497.

[62] G. Zhang, H. Hattori, K. Tanabe, Appl. Catal. 36 (1988)189.

[63] G. Zhang, H. Hattori, K. Tanabe, Appl. Catal. 40 (1988) 183.

[64] T. Yashima, H. Suzuki, N. Hara, J. Catal. 33 (1974) 486.

[65] P. Chu, G.W. Kuehl, US Patent, 4,605,787, (1986).

[66] P. T. Weirzchowski, L. W. Zatorski, Catal. Lett. 9 (1991) 411.

[67] E. Suzuki, S. Idemura, Y. Ono, Chem. Lett. (1987) 1843.

[68] K. Tanabe, K. Saito, J. Catal. 35 (1974) 274.

[69] A. Garcia-Raso, J. Garcia-Raso, B. Campaner, R. Mestres, J.V. Sinisterra, Synthesis, (1982) 1037.

[70] H. Kabashima, H. Tsuji, T. Shibuya, H. Hattori, J. Mol. Catal. A: Chem. 155 (2000) 23.

[71] H. Kabashima, H. Tsuji, H. Hattori, Appl. Catal. A: General, 165 (1997) 319.

[72] J.E.G. Mdoe, J.H. Clark, D.J. Macquarrie, Synlett (1998) 625.

[73] B.M. Choudary, M.L. Kantam, C.V. Reddy, K.K. Rao, F. Figueras, J. Mol. Catal. A: Chem. 146 (1999) 279.

[74] Y. Ono, T. Baba, Catal. Today, 38 (1997) 321.

[75] E.J. Doskocil, S. Bordawekar, R.T. Davis, in: Catalysis, Royal Soc. Chem. Cambridge, UK, 15 (2000) 40.

[76] L. Kantam, B.M. Choudary, Ch.V. Reddy, K.K. Rao, F. Figueras, Chem. Commun. (1998) 1033.

[77] D.J. Macquarrie, D.B. Jackson, Chem. Commun. (1997) 1781.

[78] A. Cauval, G. Renard, D. Brunel, J. Org. Chem. 62 (1997) 749.

[79] M. Laspéras, T. Llorett, L. Chaves, I. Rodriguez, A. Cauvel, D. Brunel, Stud. Surf. Sci. Catal. 108 (1997) 75.

[80] M.J. Climent, A. Corma, R. Guil-Lopez, S. Iborra, J. Primo, Catal. Lett. 59 (1999) 33.

[81] M.J. Climent, A. Corma, R. Guil-Lopez, S. Iborra, Catal. Lett. 74 (2001) 161.

[82] F. Bigi, L.C.R. Maggi, G. Sartori, J. Org. Chem. 64 (1999) 1033.

[83] J.V. Sinisterra, Z. Mouloungui, M. Marinas, J. Colloid Interface Sci. 115 (1987) 520.

[84] A. Corma, V. Fornas, R.H. Martin-Aranda, H. Garcia, J. Promo, Appl. Catal. 59 (1990) 237.

[85] A. Corma, R. H. Martin-Aranda, F. Sanchez, J. Catal. 126 (1990) 192.

[86] F. Texier-Boullet, A. Faucand, Tetrahedron Lett. 23 (1982) 4927.

[87] V.J. Bulbulbe, V.H. Deshpande, S. Velu, A. Sudalai, S. Shivasankar, V.T. Sathe, Tetrahedron Lett. 55 (1999) 9325.

[88] R. Ballini, F. Bigi, R. Maggi, G. Sartori, J. Catal. 191 (2000) 348.

[89] K. Kabashima, H. Tsuji, H. Hattori, React. Kinet. Catal. Lett. 59 (1996) 255.

[90] P.S. Kumbhar, J. Sanchez-Valente, F. Figueras, Chem. Commun. (1998) 1091.

[91] H. Kabashima, T. Katou, H. Hattori, Appl. Catal. A: General, 214 (2001) 121.

[92] H. Hattori, Y. Tanaka, K. Tanabe, J. Am. Chem. Soc. 98 (1976) 4652.

[93] Y. Tanaka, Y. Imizu, H. Hattori, K. Tanabe, Proceedings of the 7th International Congress on Catalysis Tokyo, Japan (1980) 1254.

[94] T. Yamaguchi, J.W. Hightower, J. Am. Chem. Soc. 99 (1977) 4201.

[95] H. Shima, T. Yamaguchi, J. Catal. 90 (1984) 160.

[96] T. Yokoyama, T. Setoyama, M. Nakajima, N. Fujita, T. Maki, Acid-Base Catalysis II, Kodansha (Tokyo)-Elsevier (Amsterdam, Oxford, New York, Tokyo), (1994) 47.

[97] Y. Kakuno, H. Hattori, J. Catal. 85 (1984) 509.

[98] S. Tsuchiya, Acid-Base Catalysis Kodansha (Tokyo)-VCH (Basel, Cambridge, New York, Weinheim), (1989) 169.

[99] J.W. Hightower, K.W. Hall, J. Am. Chem. Soc. 89 (1967) 778.

[100] A. Satoh, H. Hattori, J. Catal. 45 (1976) 36.

[101] H. Hattori, M. Itoh, K. Tanabe, J. Catal. 41 (1976) 46.

[102] H. Hattori, K. Tanabe, K. Hayano, H. Shirahama, T. Matsumoto, Chem. Lett. (1979) 133.

[103] K. Shimazu, K. Tanabe, H. Hattori, J. Catal. 45 (1977) 302.

[104] G. Suzukamo, M. Fukao, M. Minobe, Chem. Lett. (1987) 585.

[105] A. Hattori, H. Hattori, K. Tanabe, J. Catal. 65 (1980) 246.

[106] T. Baba, H. Kizuka, H. Handa, Y. Ono, Appl. Catal. A: General, 194/5 (2000) 203.

[107] M. Ueshima, H. Yano, H. Hattori, Sekiyu Gakkaisi (J. Jpn. Petroleum Inst.) 35 (1992) 362.

[108] X. Lin, G.K. Chuah, S. Jaenicke, J. Mol. Catal. A: Chem. 150 (1999) 287.

[109] S. Jaenicke, G.K. Chuah, X.H. Lin, X.C. Hu, Micropor. Mesopor. Mater. 35/6 (2000) 143.

[110] T. Yano, H. Matsui, T. Koike, H. Ishiguro, H. Fujiwara, M. Yoshihara, T. Mashima, Chem. Commun. (1997) 1129.

[111] K. Yamaguchi, K. Ebitani, T. Yoshida, H. Yoshida, K. Kaneda, J. Am. Chem. Soc. 121 (1999) 4526.

[112] J.M. Fraile, J. García, J.S. Mayoral, Catal. Today, 57 (2000) 3.

[113] J.T. Jothi, T. Raja, K. Sreekumar, M.B. Talawar, B.S. Rao, J. Mol. Catal. A: Chem. 157 (2000) 193.

[114] B.M. Choudary, M.L. Kantam, B. Bharathi, C.V. Reddy, Syn. Lett. (1998) 1203.

[115] V.K. Yadav, K.K. Kapoor, Tetrahedron Lett. 35 (1994) 9481.

[116] V.K. Yadav, K.K. Kapoor, Tetrahedron, 52 (1996) 3659.

[117] J.M. Fraile, J.I. Garcia, J.A. Mayoral, F. Figueras, Tetrahedron Lett. 37 (1996) 5995.

[118] J.M. Fraile, J.I. Garcia, D. Marco, J.A. Mayoral, Appl. Catal. A: General, 207 (2001) 239.

[119] S. Ueno, K. Yamagychi, K. Yoshida, K. Ebitani, K. Kaneda, Chem. Commun. (1998) 295.

[120] K. Yamaguchi, T. Mizugaki, K. Ebitani, K. Kaneda, New J. Chem. 23 (1999) 799.

[121] K. Kaneda, S. Ueno, T. Imanaka, J. Chem. Soc. Chem. Commun. (1994) 797.

[122] K. Kaneda, S. Ueno, T. Imanaka, J. Mol. Catal. 102 (1995) 135.

[123] M. Shibagaki, K. Takahashi, H. Matsushita, Bull. Chem. Soc. Jpn. 61 (1988) 3283.

[124] K. Takahashi, M. Shibagaki, H. Matsushita, Bull. Chem. Soc. Jpn. (1989) 2353.

[125] K. Takahashi, M. Shibagaki, H. Kuno, H. Kawakami, H. Matsushita, Bull. Chem. Soc. Jpn. 62 (1989) 1333.

[126] J. Shabtai, R. Lazer, E. Biron, J. Mol. Catal. 27 (1984) 35.

[127] M.A. Aramendia, V. Borau, C. Jimenez, J.M. Marinas, J.R. Ruiz, F.J. Urbano, Appl. Catal. A: Gen. 244 (2003) 207.

# CHAPTER 3

# Experimental Methods and Apparatus

## 3.1 Introduction to Catalyst Synthesis

Catalysts are usually used as a single chemical phase or multi chemical phase [1]. However, fewer single phase catalysts are employed in chemical reactions. The most commonly used single component catalysts include alkali earth oxides, rare earth oxides and other oxides such as alumina and titanium oxide.

On the other hand, a large number of catalysts are known to consist of two or more components. These components can either act as active phase (a phase mainly responsible for the catalytic activity), promoter (a substance that is not by itself catalytically active but allows the active phase to function at its maximum capacity), or support (a substance usually catalytically inactive on which the active phase and promoter are cast).

There are different ways of synthesizing the above mentioned categories of catalysts. Many of the single phase catalysts used in their oxide form are prepared by thermal decomposition of a catalyst precursor (usually hydroxides and nitrates) at elevated temperatures. The most commonly used methods of multi-phase catalyst preparation are precipitation, Impregnation, ion-exchange and adsorption-deposition methods.

Precipitation methods usually involve the addition of two or more different chemical solutions together to form a precipitate. This method was first studied by Marcilly [2]. The precipitate usually contains some of the constituents from the original solutions and can also be used as a support. The active phase and promoter precursors can be incorporated in the solution of the support to form a multi phase catalyst (precipitate). This process is known as copreciptation. The mechanical and catalytic properties of the resultant precipitate are independent of properties of the starting materials.

The impregnation method involves the addition of an aqueous solution containing ions into the solid support, and the excess water is removed by evaporation. When the amount of a solution added to the support does not

exceed the pore volume of the support, the method is termed impregnation to incipient wetness. The average size of the active phase depends on the concentration of the solution used.

Ion-exchange methods are largely applied in the synthesis of supported metal zeolites. In this catalyst preparation method, the protons on the support are exchanged by other cations such as alkali metal ions.

Lastly, the adsorption-deposition method involves the deposition of particles (mostly as hydroxide) on the surface of the support. This method is favourable on basic supports as there is no additional alkali added in the process. Although it is used on acidic supports, an alkali is then added to aid the reaction.

The catalysts used in this thesis were mainly synthesized by the impregnation method. The precipitation and ion-exchange methods were also used to prepare some of the catalysts.

### 3.1.1 Catalyst Preparation

Magnesium oxide catalysts were prepared from commercial MgO (A.R. Hopkin and Williams LTD). The magnesium oxide was suspended in warm water with stirring and then solidified again by evaporation of the water. It was then dried at 120$^{o}$C for 16 h and calcined in air at 500$^{o}$C for 6 h. The calcined material was used in the form of granules (350-850 μm) prepared by pelletising the MgO catalyst powder using a pneumatic press and crushing to the desired size. This catalyst was found to have a BET surface area of 60 $m^2/g$. All reactions were carried out using 0.5 g of catalyst unless otherwise stated.

CaO and BaO were prepared from the thermal decomposition of calcium hydroxide and barium hydroxide respectively at elevated temperature (500$^{o}$C) for 6 h.

Silica (Aerosil 200) with BET surface area of 68 $m^2/g$ and MgO were used as supports for alkali, alkaline earth and transition metal oxides. γ-Alumina (BET surface area 157 $m^2/g$ and pore volume of 0.23 $cm^3/g$) was also used as a support.

Titanium oxide was used as a support for palladium and cesium catalysts. The preparation method of the support is described below unless otherwise stated.

The nanoparticles of titanium oxide were prepared by hydrothermal treatment of commercial titanium dioxide (Deggusa) [3,4]. Commercial $TiO_2$ (Deggusa) was mixed with equal amounts of sodium hydroxide and water. The mixture was stirred at 120 $^oC$ for 24 h in an autoclave. It was then centrifuged for 30 min followed by washing with deionised water. The latter step was repeated until the conductivity of the mixture was less than 50 micro Siemens. It was then dried overnight in an oven at 120 $^oC$. The surface area of this $TiO_2$ was found to be 330 $m^2/g$.

A second titanium dioxide support was prepared by hydrolysis of $TiCl_4$ [5]. Titanium tetrachloride ($TiCl_4$) (Loba Chemie) was digested in hydrochloric acid and then diluted with distilled water to make a 3 M solution of $TiCl_4$ in water. All the additions were made while keeping the reaction vessel in an ice bath. The pH of the solution was found to be less than 2. A solution (8 M) of hydrazine hydrate, $H_6N_2O$ (Ranbaxy) in water was added drop wise to the stirred $TiCl_4$ solution until the final pH was about 8.0. The mixture was kept under high-speed constant stirring on a magnetic stirrer for an

hour at room temperature. The precipitated titanium oxide was filtered and repeatedly washed with hot distilled water until it was free of chlorine ions. The hydrous oxide was dried overnight at 120 $^{o}$C. The surface area of the titanium oxide was found to be 207 $m^2$/g.

MgO, silica, and $\gamma$-alumina supported catalysts were prepared by the impregnation of the support with an appropriate amount of aqueous metal hydroxide/nitrate solutions to incipient wetness. The catalysts were dried at 120 $^{o}$C for 16 hours and calcined in air at 500 $^{o}$C unless otherwise stated.

### 3.2 Catalyst Characterization

The surface properties of the catalysts used in this thesis have been studied by various methods. Different characterization instruments gave different information about the surface properties.

Assimilation of the results obtained from different characterization methods enabled us to understand the nature, strengths, and distribution of basic

sites of the catalysts. In this section, different instruments used in the characterization of the catalysts and the information they provided will be described.

### 3.2.1 BET (Brunauer-Emmett-Teller)

BET measurements were carried out using an ASAP 2010 micrometrics porosimeter. Approximately 0.2 g of the catalyst was degassed at 120 $^{o}$C under dynamic vacuum until a static vacuum was obtained (approximately 6 h for most samples). This was done to remove moisture and adsorbed contaminants before analysis.

Surface areas of different catalysts were determined by the physical adsorption of nitrogen at the nitrogen liquefication temperature using the six point BET method. The surface area, pore size and pore volume of some of the catalysts used in this thesis are shown in Table 3.1 below.

**Table 3.1** surface areas, pore size and pore volume of various catalysts.

| Catalysts | Surface Area ($m^2/g$) | Pore Size (nm) | Pore volume ($cm^3/g$) |
|---|---|---|---|
| $Al_2O_3$ | 157.3 | 5.7 | 0.23 |
| CaO | 19.6 | N/A | N/A |
| MgO | 60.6 | 10.1 | 0.15 |
| $SiO_2$ | 68.7 | 14.7 | 0.25 |
| $TiO_2$ (Deggusa) | 49.5 | 5.9 | 0.07 |
| $TiO_2$ (Thermal hydrolysis) | 339.2 | 3.1 | 0.27 |
| $TiO_2$ (hydrolysis of $TiCl_4$) | 271.1 | 4.2 | 0.28 |
| 10% $Cs/Al_2O_3$ | 146.2 | 5.8 | 0.21 |
| 10% $K/Al_2O_3$ | 167.6 | 5.9 | 0.25 |
| 10% Ba/MgO | 19.7 | 7.1 | 0.04 |
| 10% Ca/MgO | 22.3 | 6.7 | 0.04 |
| 1% Cu/MgO | 71.9 | 7.4 | 0.13 |
| 1% $H_2SO_4$/MgO | 134.1 | 7.0 | 0.24 |
| 10% Na/MgO | 22.9 | 6.6 | 0.04 |
| 10% $Cs/SiO_2$ | 40.3 | 13.5 | 0.27 |
| 10% $Cs/TiO_2$ (Deggusa) | 33.1 | 4.5 | 0.05 |
| 1% $Pd/TiO_2$ (from $TiCl_4$) | 188.3 | 6.4 | 0.30 |

N/A = not available

### 3.2.2 $CO_2$ Temperature Programmed Desorption (TPD)

Temperature programmed desorption of carbon dioxide is generally used to measure the number and strength of basic sites [6,7]. The strength and amount of basic sites are reflected in the desorption temperature and peak area of a TPD plot respectively. However, it is difficult to express the strength in a definite scale and to count the number of sites quantitatively. Relative strengths and relative numbers of basic sites on the different catalysts can be estimated by carrying out the TPD experiments under the same conditions. If the TPD plot gives a sharp peak, the heat of adsorption can also be estimated.

The temperature programmed desorption (TPD) apparatus consists of a U-shaped quartz reactor housed in a temperature controlled heating jacket. The signal is measured by a low temperature dual filament TCD and recorded by a PC equipped with an I/O card.

Approximately 0.3 g of the catalyst sample was placed in the TPD reactor and calcined in air to the desired temperature before analysis. The

sample is then cooled to 100 $^{o}$C (or room temperature depending on the catalyst) in a helium (AFROX) flow of 30 ml/min. Adsorption of $CO_2$ (AFROX) is carried out at 100 $^{o}$C or room temperature for 1h at a flow rate of 30 ml/min in atmospheric pressure. The system was then purged with helium for 45 to 60 minutes to remove any unadsorbed carbon dioxide on the surface of the catalyst.

The carbon dioxide desorption was achieved by increasing the temperature of the TPD reactor at a rate of 10 $^{o}$C/min up to the desired temperature. The desorption signal was captured by a low temperature dual filament TCD and recorded using a PC equipped with an I/O card.

The TPD profiles of MgO, alkali and alkali earth metal ions supported on MgO are shown in Fig 3.1. Considering the peaks below 600 $^{o}$C only (Fig 3.1), MgO, 10% Ba/MgO, 10% Na/MgO and 10% Ca/MgO showed a similar amount and strength of basic sites. These catalysts showed a fair distribution of both weak and strong basic sites. Only a relatively small amount of basic sites was observed on 10% Na/MgO. The TPD plot of 10% K/MgO showed larger amounts of strong basic sites than weak basic sites.

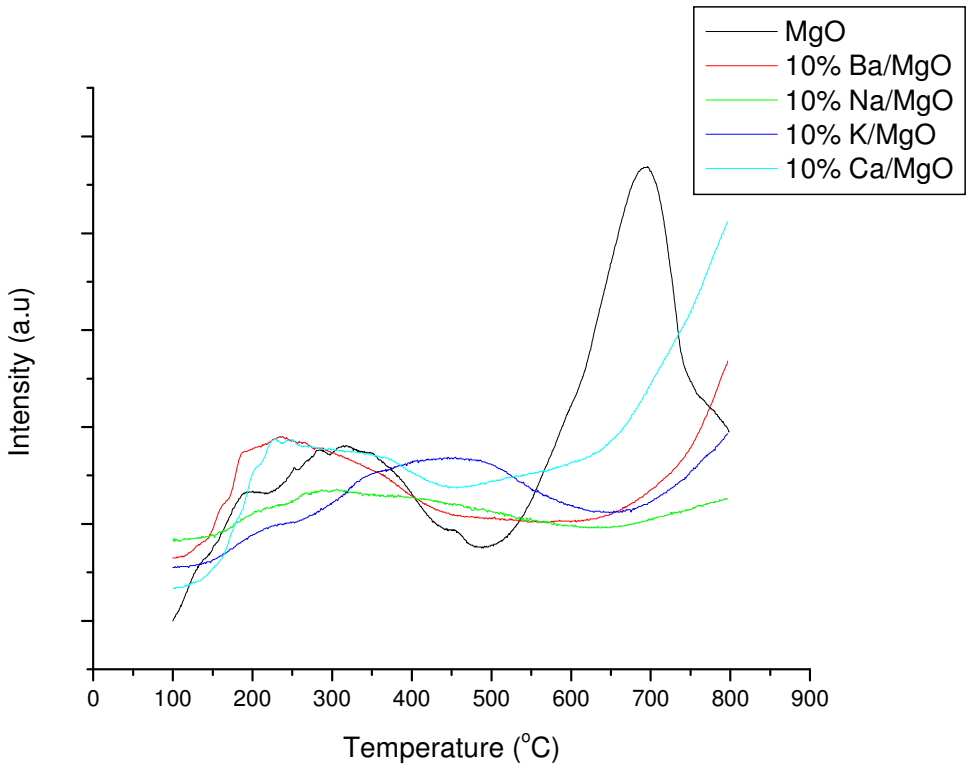


**Figure 3.1** TPD profiles of alkali and alkali earth metal oxides supported on MgO.

The effect of pre-treatment temperature on MgO sample is illustrated in Fig 3.2. There is a slight shift of peaks towards higher temperature as the calcination temperature increases from 500 to 800 °C. This suggests that the basicity of MgO is enhanced by the increase in calcinations

temperature. The small peak observed at 570 °C and 630 °C when the sample was calcined at 800 and 700 °C respectively, emphasizes the existence of strong basic sites at higher calcination temperatures.

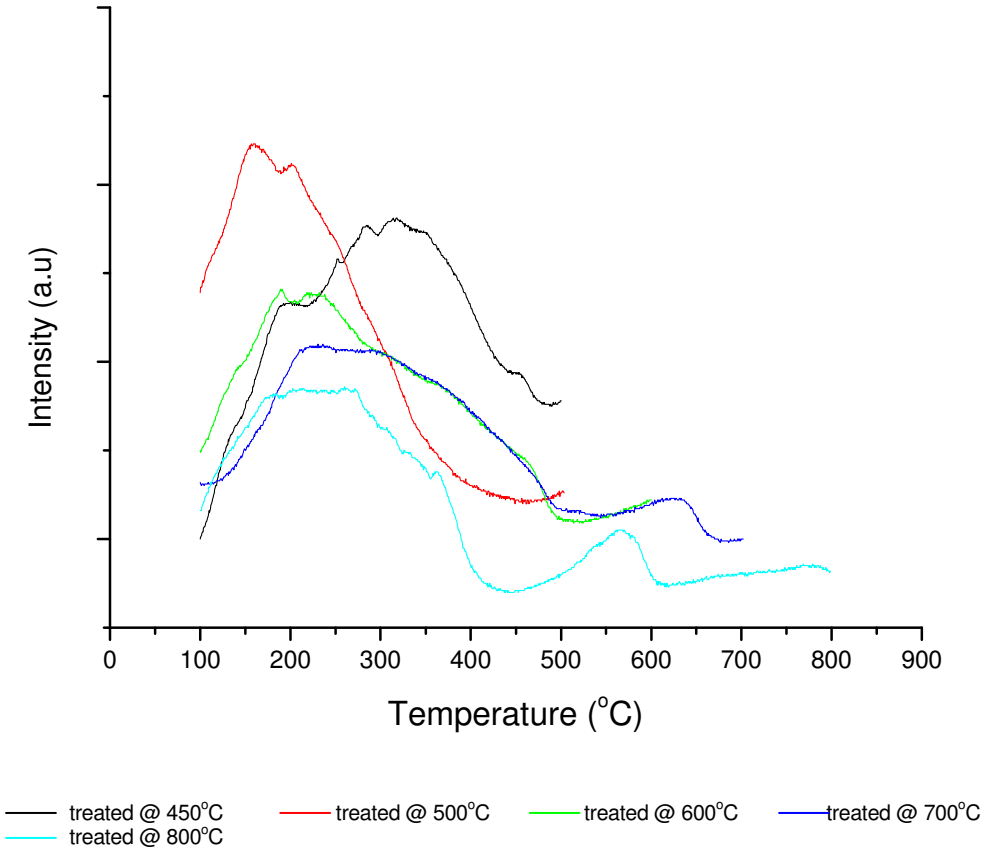


**Figure 3.2** TPD profiles of MgO catalyst calcined at different temperature for 3 h.

TPD profiles of $Cs_2O$ supported catalysts are shown in Fig 3.3. The TPD analysis of $SiO_2$ and $TiO_2$ did not show any indication of basic sites. However, on impregnation of both the $SiO_2$ and $TiO_2$, weak basic sites were observed. Similarly, when cesium was impregnated onto the γ-alumina the amount of weak basic sites was increased.

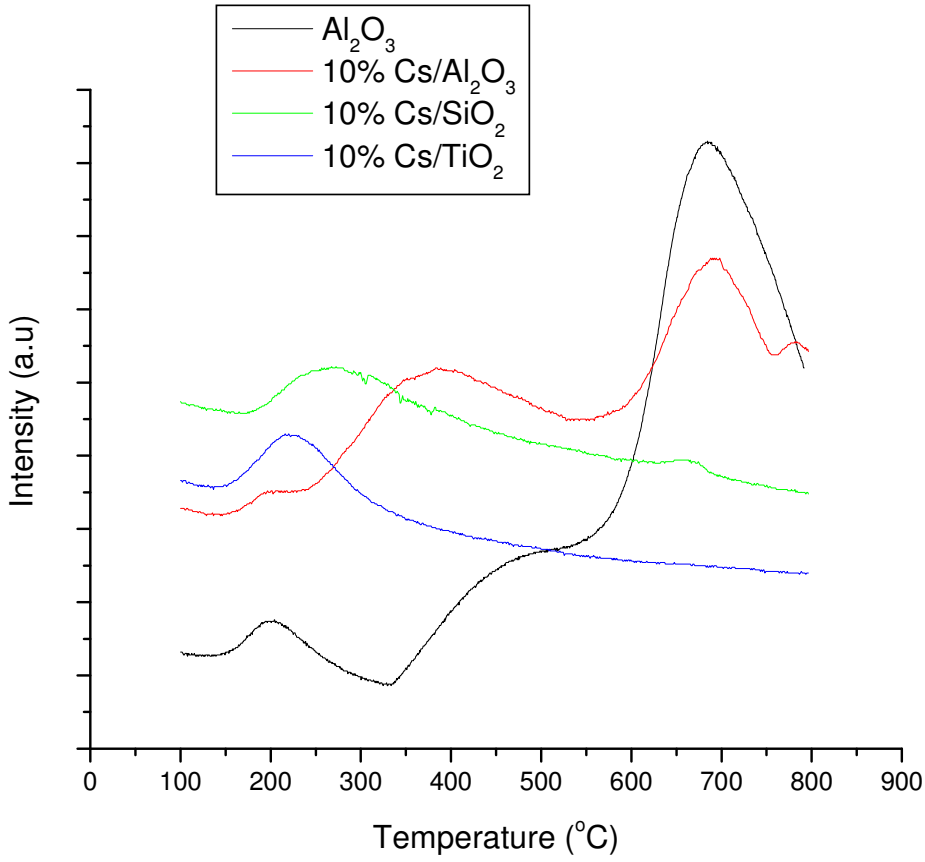


**Figure 3.3** The effect of $Cs_2O$ addition on different acidic supports.

### 3.2.3 Scanning Electron Microscopy (SEM)

Scanning electron microscope is a valuable technique for examining materials under high magnification. Information on topography, texture and surface features such as particle size and shapes of powders or solid particles can be obtained. High magnification and the depth of focus in SEM instruments provide pictures with 3-dimensional quality.

The technique involves scanning of the surface of the sample in a raster pattern with an electron beam. Several types of signals are produced from the surface in this process, including backscattered, secondary, and Auger electrons; and other photons of various energies. Backscattered and secondary electrons serve as the basis of scanning electron microscopy. The signals generated by these electrons are translated into pictures of the sample constituents. The pictures are captured by an on-board digital camera.

The samples were coated with a thin layer of graphite. This is done to prevent any charge build-up on the surface of the sample during analysis,

especially if the sample is a poor electrical conductor. The microscope unit consisted of a Jeol JSM 840 fitted with a LINK AN 1000 X-Ray microanalysis system.

SEM images of MgO and high surface area titanium oxide are shown in Figures 3.4 – 3.6 below.

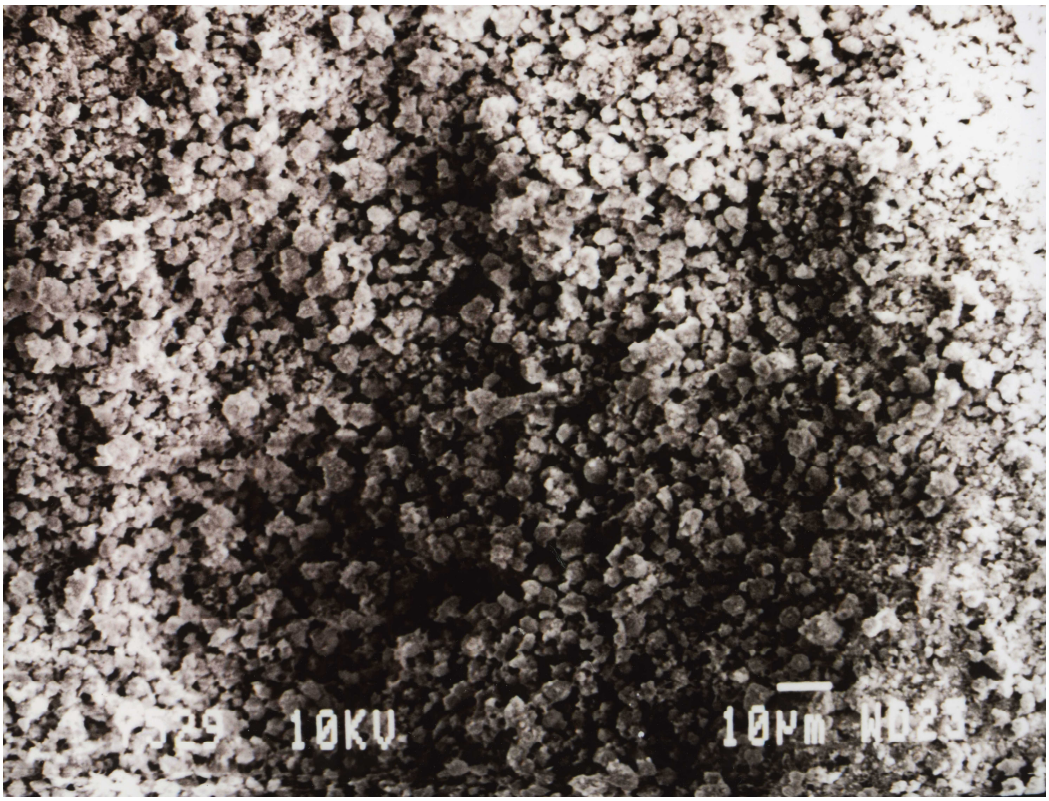


**Figure 3.4** SEM image of MgO catalyst at 10 μm.

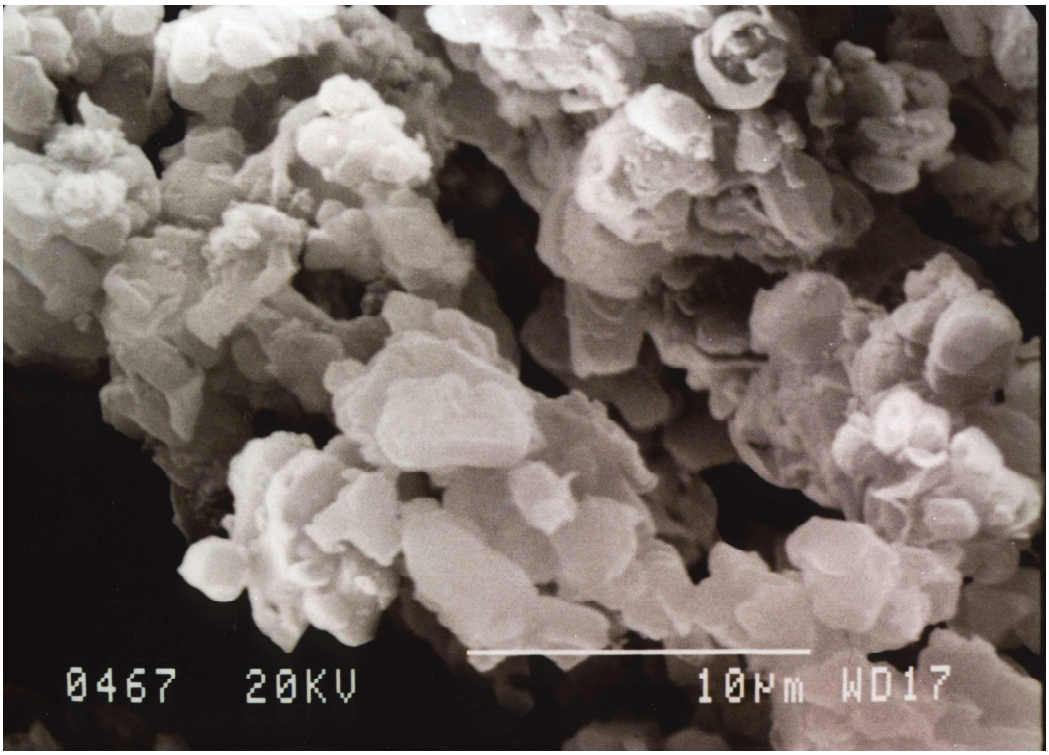


**Figure 3.5** SEM image of $TiO_2$ support prepared from hydrolysis of $TiCl_4$ (scale 10 μm.

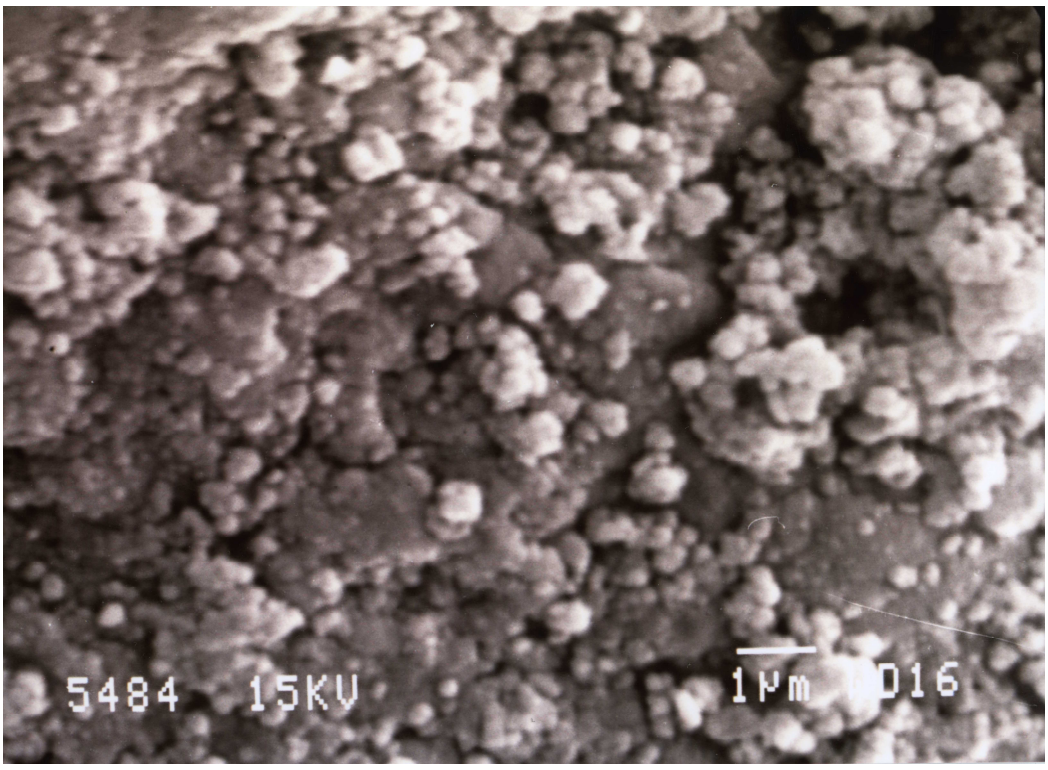


**Figure 3.6** SEM image of TiO2 support prepared from thermal hydrolysis with NaOH.

### 3.2.4 Transmission Electron Microscopy (TEM)

Transmission electron microscope (TEM) was used to determine the presence of nanotubes/fibres in the titanium oxide samples prepared by hydrolysis.

Samples for TEM analysis were prepared by mixing 1 ml of ethanol for every 1 mg of titanium oxide used. The mixture was sonicated for 10 minutes and a few drops of the suspension were placed onto a holy Cu grid coated with a thin film of carbon. Excess liquid was removed by placing the Cu grid on a dry filter paper for about 2 minutes. The Cu grid was then mounted onto the sample holder for analysis.

The type of an instrument used for the analysis is a Jeol JEM 100S transmission electron microscope. The samples were observed under the microscope at an operating voltage of 80 kV and a current of 5.5 μA with a spot size setting in nanometres. Pictures were taken at different magnification.

TEM images of titanium oxide samples are shown in Figures 3.7 and 3.8 below.




**Figure 3.7** TEM micrograph of titanium oxide nanofibres from $TiO_2$ sample prepared by hydrolysis of $TiCl_4$.

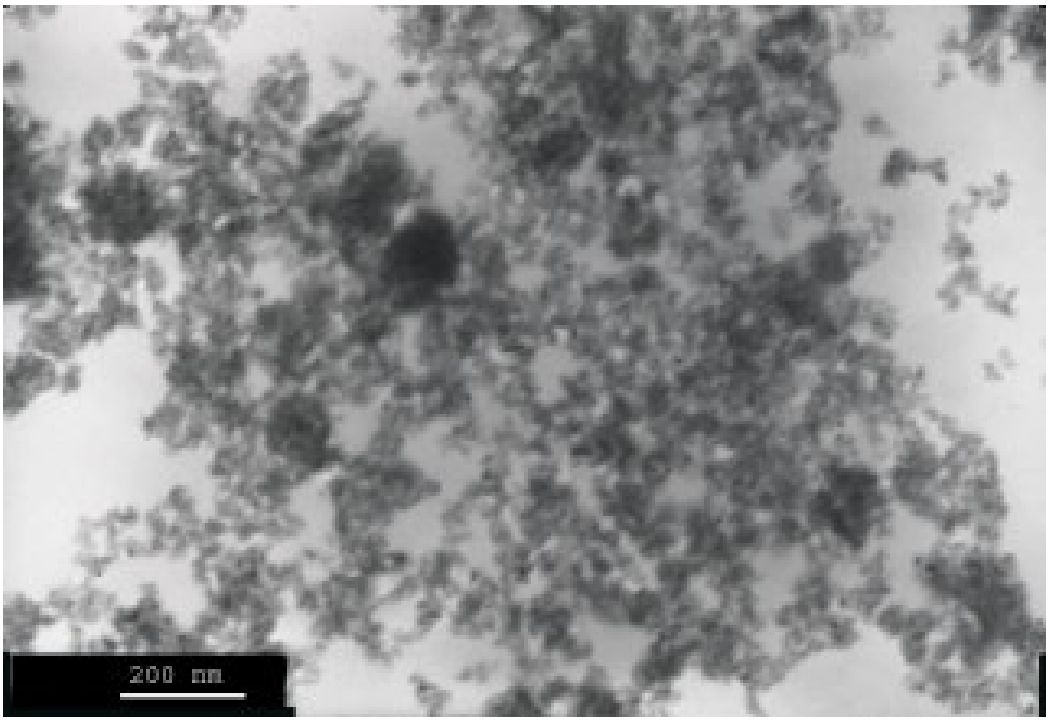


**Figure 3.8** TEM micrograph of titanium oxide sample obtained from thermal hydrolysis of $TiO_2$ with NaOH.

### 3.2.5 Thermogravimetric Analysis (TGA)

In a thermogravimetric analysis the mass of a sample in a controlled atmosphere is recorded continuously as a function of temperature or time as the temperature of the sample is increased [8].

The instrument used for thermogravimetric analysis is a Pyris 1 Perkin Elmer TGA which consists of: (1) a sensitive analytical balance, (2) a furnace, (3) a purge gas system for providing an inert or reactive environment, and (4) a microcomputer for instrument control, data acquisition and display.

A typical thermal decomposition curve of MgO catalyst used in self condensation reaction of propanol [9] is shown in Figure 3.9 below.

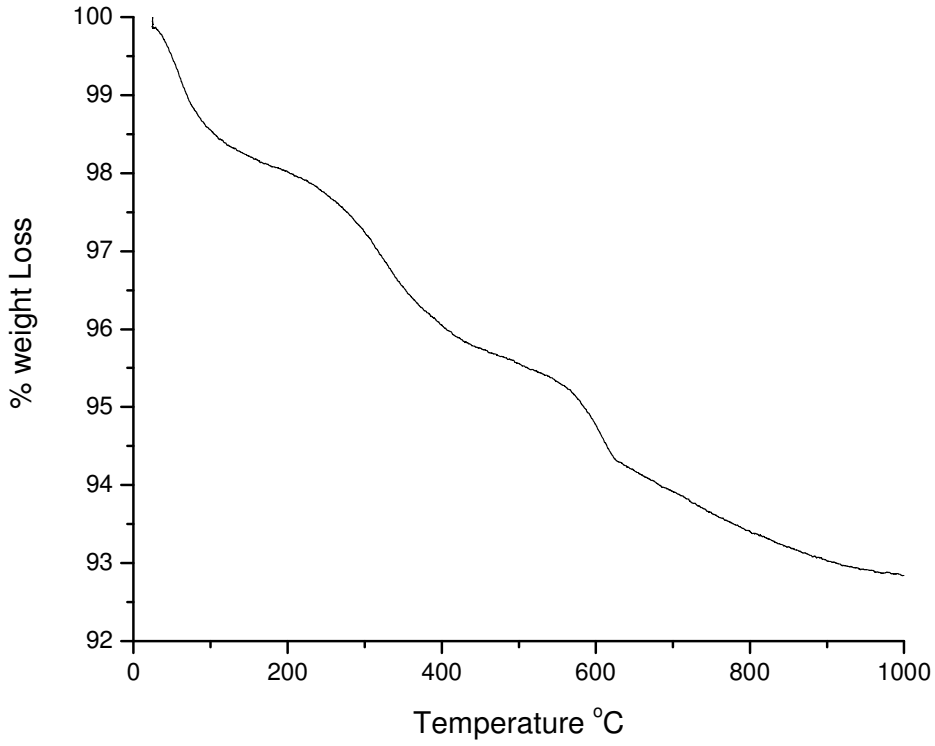


**Figure 3.9** Thermal decomposition curve of MgO used in self condensation of propanol [9].

### 3.3 Catalyst Testing System

The catalyst testing facility consisted of a syringe pump, carrier gas line, heating jacket, temperature controller, glass reactor and gas chromatograph (GC) (Fig 3.10).

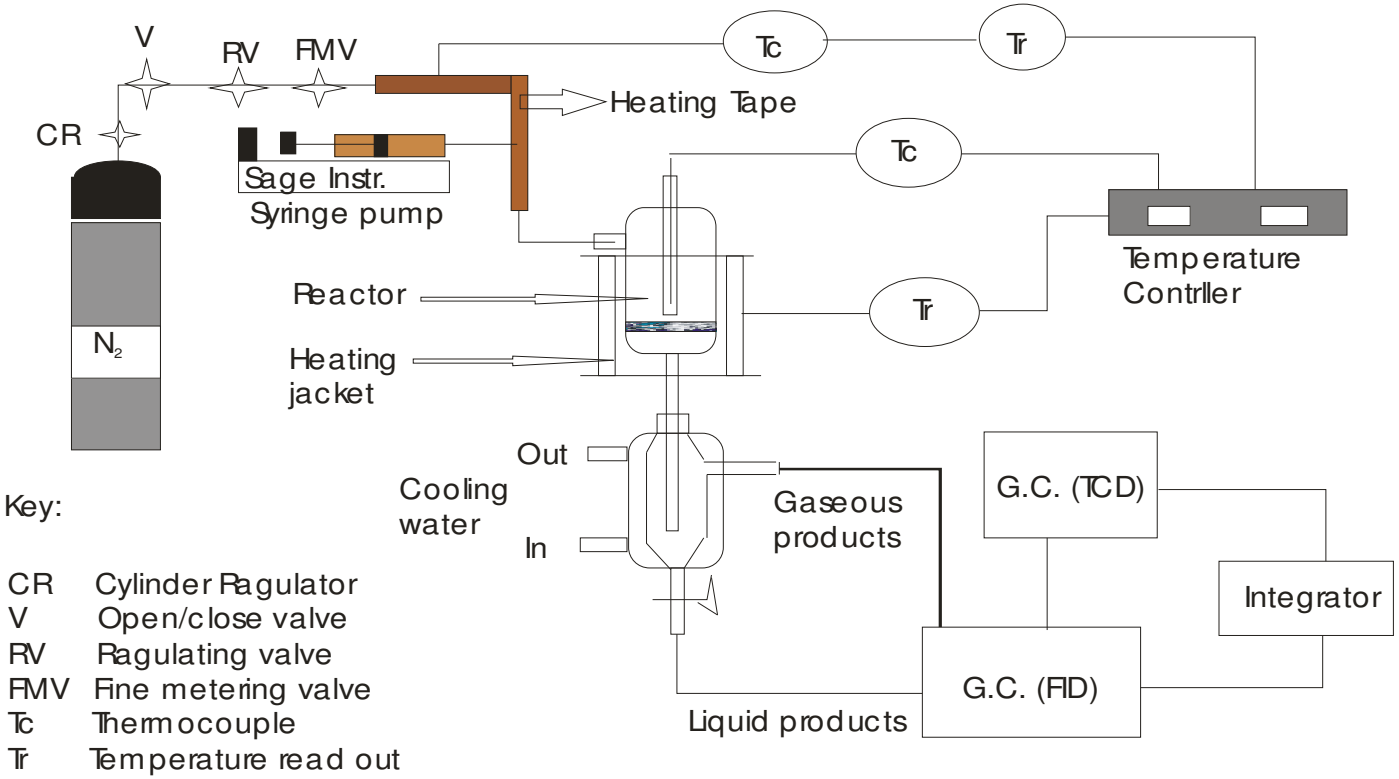


**Figure 3.10** Schematic representation of catalyst testing apparatus.

The starting materials were introduced into the reactor through a heated carrier gas line using 10 and 50 ml Hamilton gas tight syringes. The syringes were mounted onto a Sage model 341B syringe pump.

Two heating jackets were built during this thesis preparation. The two heating jackets were 40 mm and 200 mm in length respectively. The smaller (40 mm) heating jacket consisted of a ceramic tube with a heating wire coiled along its interior wall. Further insulation was provided by the glass fibre wool wrapped around the ceramic tube. The 200 mm heating jacket consisted of a nichrome heating wire coiled around the quartz tube. The heating wire and the quartz tube were inserted into a brass sleeve wrapped in glass fibre wool. This was then inserted into another brass sleeve. The top and the bottom end of the heating jacket were constructed from asbestos and were designed to hold the quartz tube in place. The schematic representations of the two heating jackets are shown in Figures 3.10 and 3.11 below.

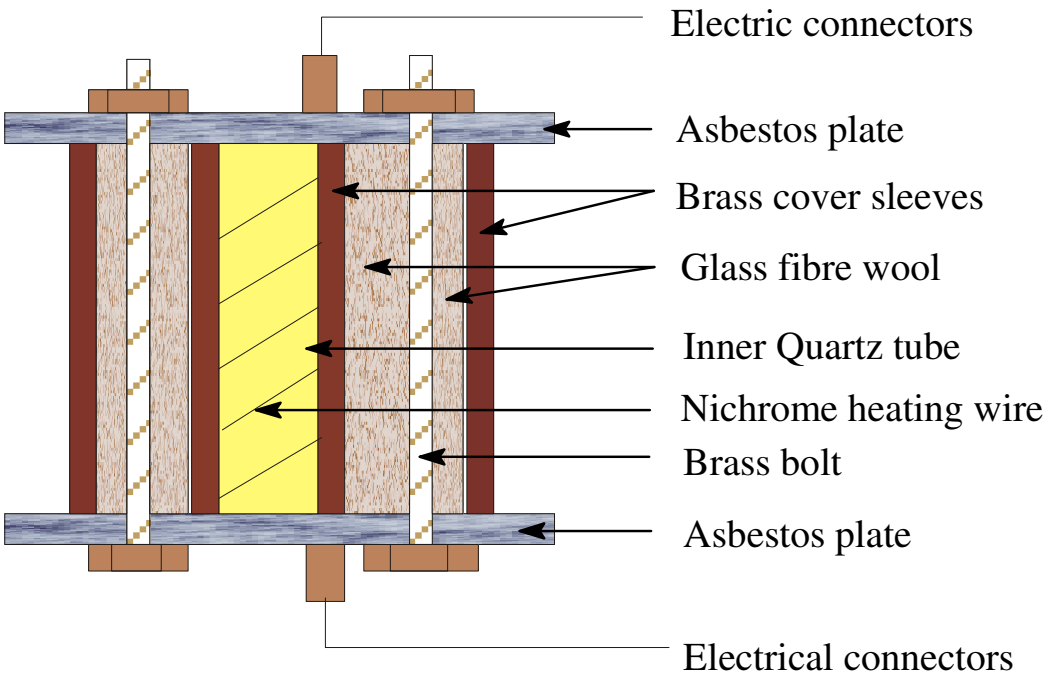


**Figure 3.11** Schematic representation of a larger heating jacket (200 mm).

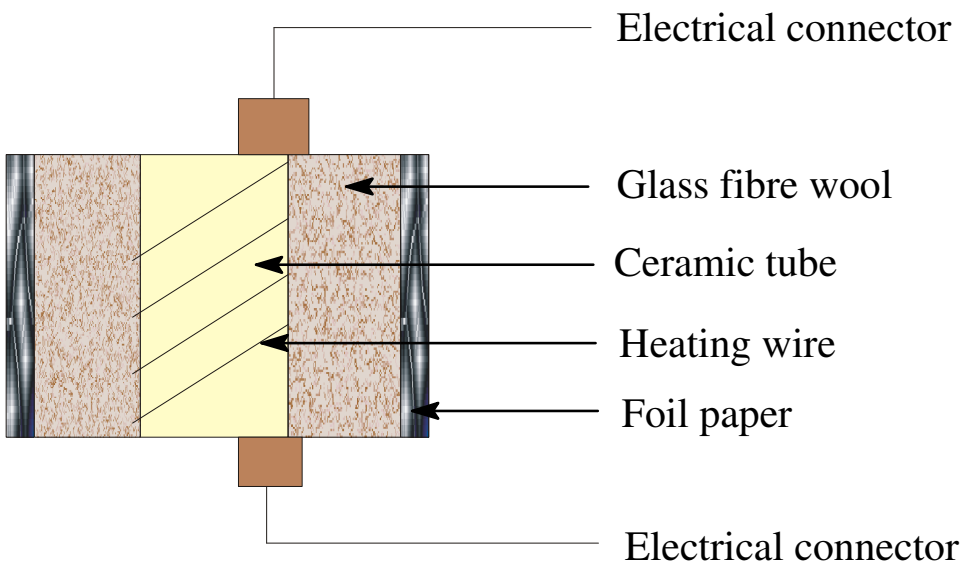


**Figure 3.12** Schematic representation of a small heating jacket (40 mm).

The reaction temperature was monitored by a J-type thermocouple inserted into a well in the reactor and a temperature controller (RKC, PN-4A1C-M). The gas lines were heated by a heating tape supplied by Flexi-heat, and the temperature was monitored by a J-type thermocouple connected to a temperature controller.

Two fixed bed glass reactors were used for catalyst loading in this thesis. The catalyst loading varied from 200 to 500 mg depending on the reaction. The reactors were constructed from pyrex or quartz glass, depending on the reaction parameters to be investigated. One reactor was 40 mm long with an external diameter of 10 mm. The other reactor was 200 mm in length with an external diameter of 14 mm. In both reactors, the catalyst was kept in place by a glass frit.

Liquid products were collected in a water-cooled receiver and analysed in a gas chromatograph (ZB wax, 60 m x 0.32 mm capillary column) equipped with a flame ionization detector (FID). Light gaseous products produced during the reaction were analysed on-line by the gas chromatograph described above. The CO and $CO_2$ given off during the reaction were analysed by another GC equipped with a thermal conductivity detector (TCD). Liquid product identification was achieved by GC-MS (Finnigan TSQ-7000) and $^{13}$C-NMR spectroscopy (Brucker AC 400).

### 3.4 References

[1] G.C Bond, Heterogeneous Catalysis, *Principles and Applications*, 2nd Edn. (1987) 76.

[2] C. Marcilly, Rev. Inst. Fr. Pet. 39 (1984) 189.

[3] T. Kasuga, M. Hiramutsu, A. Hoson, T. Sekino, K. Niihara, Langmuir, 14 (1998) 3160.

[4] T. Kasuga, M. Hiramutsu, A. Hoson, T. Sekino, K. Niihara, Adv. Mater. 11 (1999) 1307.

[5] K.M. Reddy, S.V. Mnorama, A.R. Reddy, Mat. Chem. and Phys. 78 (2002) 239.

[6] H. Hattori, Chem. Rev. 95 (1995) 537.

[7] H. Hattori, Appl. Catal. A Gen. 222 (2001) 247.

[8] D.A. Skoog, F.J. Holler, T.A. Nieman, Principles of Instrumental Analysis, 5th Edn. (1998) 798.

[9] A.S. Ndou, N.J. Coville, Appl. Catal. A: General, 275 (2004) 103.

# CHAPTER 4

## Dimerisation of Ethanol to Butanol over Solid Base Catalysts*

* A.S. Ndou, N. Plint, N.J. Coville, Appl. Catal. A: General, 251 (2003) 337.

### 4.1 Introduction

Chemical conversions over solid acid catalysts have received extensive coverage over the decades [1-4]. An example is the conversion of ethanol into higher value chemicals, a reaction that has received much attention in the literature [5,6]. In comparison to solid acid catalysts less attention has been devoted to solid base catalysts, even though high activities and selectivities are often attained for chemical conversions carried out over liquid bases for many kinds of reactions.

Many homogeneous catalysed base reactions are known and include reactions such as isomerization, addition, alkylation and cyclization [7-10]. Numerous reactions are also known that require a stoichiometric amount of liquid bases [11]. The replacement of liquid bases by solid base catalysts would provide environmental advantages to industrial processes. These include issues relating to decreased reactor corrosion, easier product/catalyst separation and recovery of used catalysts [8].

The use of solid base catalysts for the synthesis of fine chemicals from alcohols has not been extensively studied [8]. Condensation of various primary alcohols to form higher alcohols is however, known [12-16]. An important industrial process that is used to increase the carbon number of alcohols is the Guerbet reaction [17]. In this reaction a primary or secondary alcohol reacts with itself or another alcohol to produce a higher alcohol. This reaction has been developed and various types of heterogeneous catalysts for this reaction have been reported in patents [17,18]. Ueda et al. [19,20] have also reported a catalytic reaction for producing higher alcohols using methanol as a building block. In this reaction, carried out over a solid base metal oxide catalyst, methanol is condensed with other primary or secondary alcohols having a methyl or methylene group at the ß-position.

Surprisingly, the reaction of ethanol to generate 1-butanol, over solid base catalysts has been little reported in the literature. 1-Butanol is a crucial building block for acrylic acid and acrylic esters and is widely used as a solvent [13-15, 21]. It has also found application as an additive to gasoline [21].

Herein we report the synthesis of 1-butanol from ethanol over a base catalyst. A thorough investigation of the reaction using a variety of possible intermediates suggests that the reaction involves a bimolecular condensation reaction [22].

## 4.2 Experimental

### 4.2.1 Catalyst preparation

Magnesium oxide catalysts were prepared from MgO (A.R) (Hopkin and Williams LTD). The magnesium oxide was suspended in warm water with stirring and then solidified again by the evaporation of the water. It was then dried at 120 $^{o}$C for 16 h and finally calcined in air at 500 $^{o}$C for 6 h. This catalyst was found to have a BET surface area of 60 $m^2$/g. CaO and BaO were prepared from the thermal decomposition of cesium hydroxide

and barium hydroxide respectively at elevated temperature (500 $^{o}$C) for 6 h.

Silica (Aerosil 200) with BET surface area of 68 $m^2$/g and MgO (prepared as described above) were used as supports for alkali, alkaline earth and transition metal oxides. $\gamma$-Alumina (BET surface area 157 $m^2$/g and pore volume of 0.23 $cm^3$/g) was also used as a support.

The metal oxide supported catalysts were prepared by an impregnation procedure using an appropriate amount of aqueous metal hydroxide/nitrate solutions (incipient wetness method). The catalysts were dried at 3120 $^{o}$C (16 h) and calcined in air at 500 $^{o}$C.

### 4.2.2 Apparatus and Procedure

The catalytic experiments were carried out in a vertical fixed bed glass reactor (10 mm e.d). All reactions were carried out using 0.5 g of catalyst. The catalysts were used in the form of granules (350-850 $\mu$m) prepared by pelletising the catalyst powder and crushing to the desired size. The reactor was placed inside a temperature controlled heating jacket with a thermocouple placed at the centre of the catalyst bed.

The catalyst was activated in flowing oxygen at 500 $^{o}$C for 1 h prior to flushing with nitrogen gas (10 ml/min). Ethanol was fed from a 10 ml syringe using a syringe pump (Sage instruments, model 341B) through a heated carrier gas (nitrogen) line prior to the reactor. Reactions were conducted under nitrogen flow (10 ml/min). The partial pressure of the ethanol in the feed was kept at 51.77 kPa. The products were collected in a water-cooled receiver after 1 h (unless otherwise stated) and analysed in a gas chromatograph (ZB wax, 60 m x 0.32 mm capillary column; FI Detector). Product identification was achieved by GC-MS (Finnigan TSQ-7000) and $^{13}$C-NMR spectroscopy (Brucker AC 400). The ethanol conversion and products yield were calculated as follows:

% Conversion = (Moles of ethanol reacted / Moles of ethanol introduced) X 100.

% Yield = (Moles of product / Moles of ethanol introduced) X 100

The temperature programmed desorption (TPD) apparatus consists of a U-shaped quartz reactor housed in a temperature controlled heating jacket. The experiments were conducted in atmospheric pressure. The $CO_2$ was adsorbed at 100 $^{o}$C. The signal is measured by a low temperature dual filament TCD and recorded by a PC equipped with an I/O card.

## 4.3 Results and Discussion

### 4.3.1 Catalyst screening

Ethanol was passed over a range of catalysts at 450 $^{o}$C (Table 4.1), and a substantial amount of liquid products were observed. In addition some gaseous light products were formed by thermal decomposition of a part of the ethanol. The selectivities and activities of the different catalysts were evaluated by GC studies. Product compositions were determined by a combination of GC, GC-MS and $^{13}$C NMR spectroscopy. By this means all of the major products were identified.

MgO showed the highest yield of butanol among the catalysts studied (Table 4.1). CaO showed the least activity and produced very little butanol. Barium oxide did not show any butanol formation. Although high *activity* was observed over $\gamma$-alumina, no butanol was formed over this catalyst. Butanal and acetaldehyde, together with substantial amounts of gaseous products, were the major components observed. This is in accord with the acidic nature of this catalyst. The impregnation of alkali metals on $\gamma$-alumina resulted in the formation of a small amount of butanol. Coverage of the $Al_2O_3$ by the metal ions resulted in an increase in the amount of butanol produced relative to $Al_2O_3$ suggesting that the basic sites produced

by the metal ions were required for butanol formation. The ethanol conversion of the $Al_2O_3$ catalysts also showed a general decrease with metal ion coverage.

**Table 4.1** Activities of basic oxides and alkali-loaded $Al_2O_3$ in the solid base condensation of ethanol to butanol.

| Catalyst | Conv. (mol%) | Yield (mol %) | | | | | |
|---|---|---|---|---|---|---|---|
| | | Acetal | Butanal | Crotonal | 2-Butanol | Butanol | Crotanol |
| MgO | 56.14 | 0.65 | 0.78 | 0.50 | 0.14 | 18.39 | 0.31 |
| CaO | 15.16 | 2.83 | 2.15 | 0.32 | 0.07 | 1.16 | 0.06 |
| BaO | 21.19 | 6.56 | 11.37 | - | - | - | - |
| $\Gamma$-$Al_2O_3$ | 82.29 | 5.96 | 19.42 | - | - | - | - |
| 10%Na/$Al_2O_3$ | 35.52 | 0.32 | 2.56 | 0.06 | 0.18 | 0.92 | 0.05 |
| 10% K/$Al_2O_3$ | 54.02 | 1.09 | 0.75 | 0.20 | 0.26 | 3.42 | 0.04 |
| 10%Cs/$Al_2O_3$ | 24.57 | 0.31 | 0.31 | - | - | 0.05 | - |
| 10%Mg/$SiO_2$ | 18.64 | 5.04 | 0.17 | 0.17 | - | 0.38 | 0.05 |

Abbreviations: Acetal = Acetaldehyde; Butanal = Butyraldehyde; Crotonal = Crotonaldehyde; Crotanol = Crotylalcohol.

Attempts were then made to enhance the catalyst selectivity/activity by enhancing the MgO surface area and by addition of metal ions. Dispersion of MgO on a series of metal oxides did not improve the yield of butanol (see an example in Table 4.1, $Mg/SiO_2$). Similarly, addition of the basic metal ions Ca and Ba to MgO also did not enhance the catalyst selectivity (Table 4.2). Thus, even though the basic nature of the MgO was modified by loading calcium and barium on MgO no advantages in terms of catalyst productivity were achieved - little effect on the yield of $C_4$ products was noted and the yield of butanol decreased significantly. Ueda et al. [11,12] have also reported similar findings for the reaction of ethanol and methanol to form 1-propanol, where they found that while the addition of alkali metals increased the basicity of oxygen anions in MgO, condensation rates were decreased.

The addition of a range of transition metals (Zn, Ce, Zr, Pb, Sn) to MgO was also investigated (Table 4.2). These ions were expected to increase the basic nature of the MgO but here again the metal ion addition did not improve the yield of butanol or other $C_4$ compounds. Ueda *et al*. [23] have reported that the surface basicity of MgO was increased by the addition of metal ions when the ionic radius was greater than that of $Mg^{2+}$.

**Table 4.2** Activities of alkaline earth and transition metals loaded on MgO catalysts in the solid base condensation of ethanol to butanol.

| Catalyst | Conversion | Yield (mol %) | | | | | |
|---|---|---|---|---|---|---|---|
| | (mol%) | Acetal | Butanal | Crotonal | 2-Butanol | Butanol | Crotanol |
| 10%Ba/MgO | 34.19 | 15.35 | 0.81 | 0.15 | 0.41 | 7.33 | 0.47 |
| 10%Zn/MgO | 95.61 | 1.11 | 6.93 | 1.79 | 2.91 | 2.95 | 0.03 |
| 10%Ce/MgO | 70.84 | 0.56 | 4.27 | 0.09 | 0.00 | 0.50 | 0.28 |
| 10%Zr/MgO | 52.49 | 6.48 | 5.65 | 0.14 | 0.06 | 0.29 | 0.14 |
| 10%Sn/MgO | 57.21 | 5.62 | 1.56 | 0.85 | 3.95 | 1.27 | 0.05 |
| 10%Cu/MgO | 28.75 | 18.10 | 0.70 | 0.12 | 0.60 | 1.80 | 0.82 |

TPD experiments were performed with $CO_2$ as the probe molecule and the TPD profiles of MgO, Ba/MgO, Na/MgO and K/MgO are shown in Figure 4.1. The experiments were conducted in atmospheric pressure. The $CO_2$ was adsorbed at 100 °C. Only the MgO shows strong basic sites and the reaction data suggests that these sites are required for the condensation reaction.

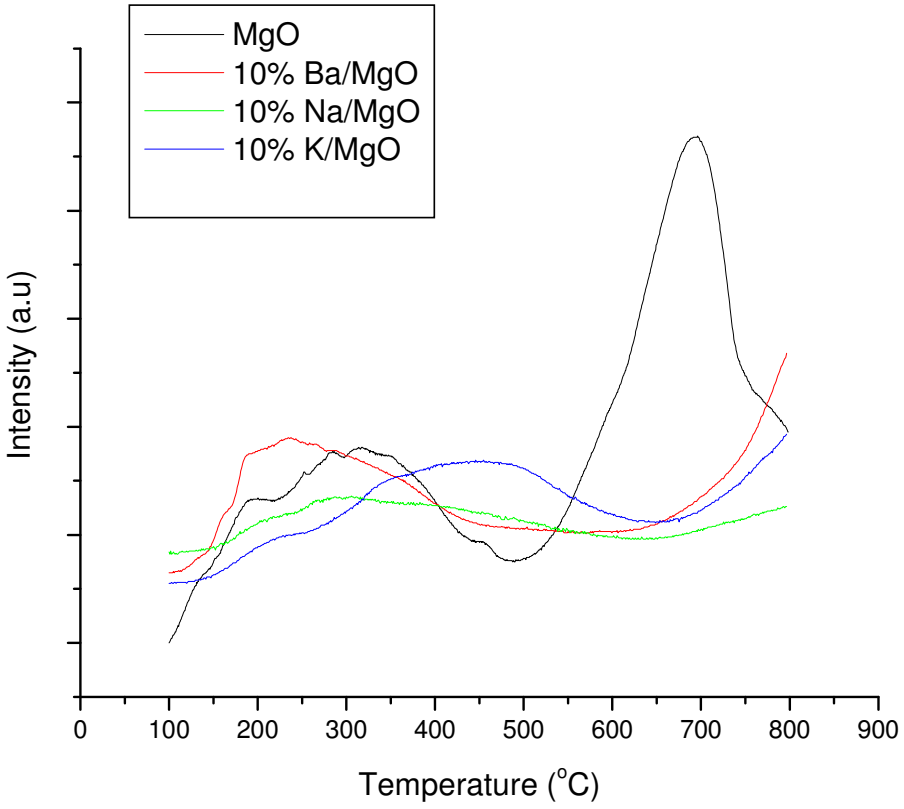


**Figure 4.1** TPD profiles of some of the catalysts.

Attempts were then made to modify the MgO basicity and/or surface area by addition of acids to the MgO (Table 4.3). The impregnation of MgO with HCl solution yielded mostly butyraldehyde (30%) as the major product, while very small amounts of butanol were observed (0.08%).

The phosphoric and acetic acid loaded MgO catalysts showed slightly improved results (butanol yield) when compared to the HCl/MgO catalysts. The addition of 1% $H_2SO_4$ to MgO did not affect the butanol yield significantly. Indeed, the MgO surface area increased (e.g. 1% $H_2SO_4$; surface area = 134 $m^2g^{-1}$) and this compensated for the neutralization of strong basic sites. However, as the sulphuric acid loading on MgO increased, the butanol yield decreased, presumably due to the poisoning of the MgO surface by the large amounts of acid.

**Table 4.3** Activities of acid doped magnesium oxide catalysts for the solid base condensation of ethanol to butanol.

| Catalyst | Conversion (%) | Yield (mol %) | | | | | |
|---|---|---|---|---|---|---|---|
| | | Acetal | Butanal | Crotonal | 2-Butanol | Butanol | Crotanol |
| 10%HCl/MgO | 22.21 | 1.93 | 7.52 | 0.22 | 0.08 | 0.08 | 0.37 |
| 10%$H_2PO_4$/MgO | 42.49 | 12.02 | 1.13 | 0.34 | 0.33 | 8.18 | 0.37 |
| 1% $H_2SO_4$/MgO | 49.17 | 1.65 | 0.78 | 1.06 | 0.17 | 19.26 | 1.09 |
| 5% $H_2SO_4$/MgO | 48.52 | 4.42 | 2.04 | 1.36 | 1.27 | 15.01 | 0.21 |
| 10%$H_2SO_4$/MgO | 50.35 | 3.19 | 1.35 | 0.71 | 0.85 | 8.76 | 0.23 |
| 20%$H_2SO_4$/MgO | 58.81 | 4.16 | 1.08 | 0.48 | 1.04 | 6.83 | 0.08 |

The above study revealed that little advantage was to be gained (activity and/or selectivity) by modification of the MgO with acidic or basic ions. Only a low loading of $H_2SO_4$ to MgO gave comparable results to that of pure MgO. Further studies thus focussed on the unmodified MgO catalyst.

### 4.3.2. Effect of temperature and contact time on the reaction

The effect of reaction temperature on the activity/selectivity of the ethanol dimerisation reaction is shown in Figure 4.2. The data was collected after an hour over a fresh catalyst for each experiment (set of data point). Very little change in the yield of acetal and other $C_4$ products, as the temperature of the reaction increased, is to be noted. However, there is a very sharp increase in butanol yield at a temperature of 450 $^oC$. Further studies were then performed on the catalyst at 450 $^oC$.

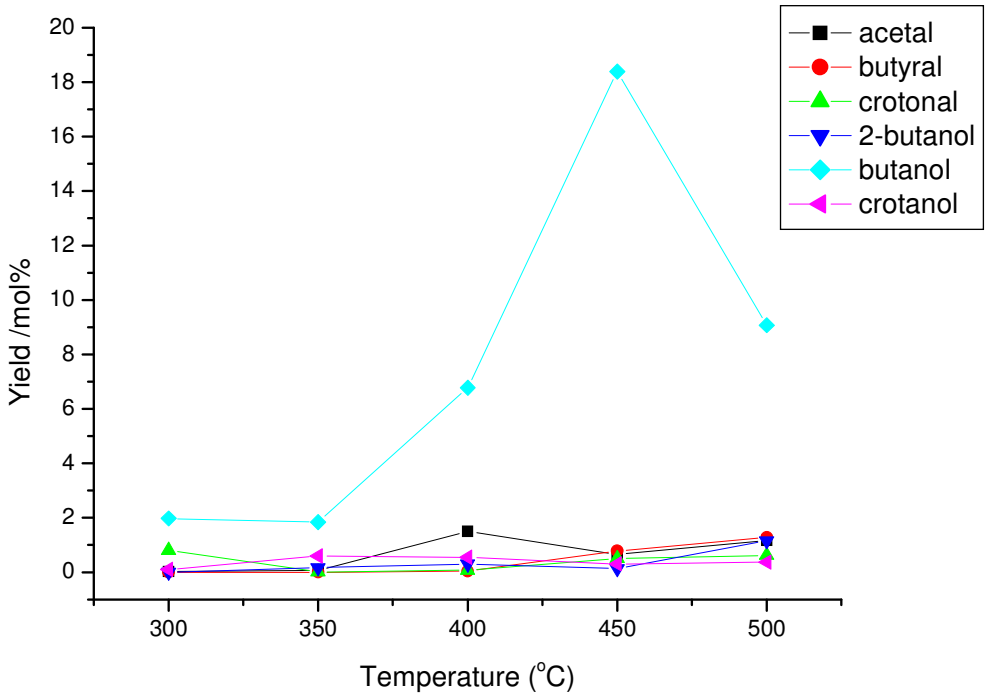


**Figure 4.2** Influence of temperature on the product distribution over MgO.

Figure 4.3 shows the variation of ethanol conversion and 1-butanol yield with WHSV. The experiments were conducted over fresh catalysts for each data point collected. The data was collected over a period of 1 h for each experiment. The conversion of ethanol to products decreased with the increase in WHSV. However, the butanol yield stayed fairly constant with the increase of WHSV, suggesting that it did not decompose over the catalyst via secondary reactions.

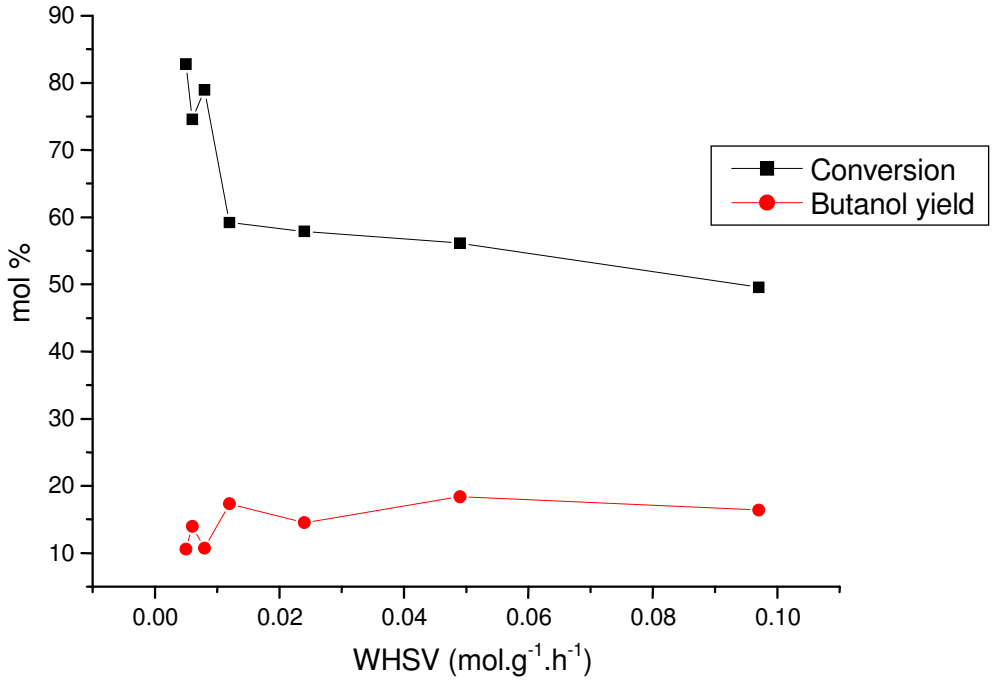


**Figure 4.3** Influence of WHSV on ethanol conversion and 1-butanol yield over MgO.

A decrease in ethanol conversion was also noted to occur with time on stream (Figure 4.4), suggesting that the changes were associated with catalyst decomposition. Again however, the selectivity to butanol was little affected by the change in conversion. The deactivation is assumed to be due to carbon deposition; the catalyst turned black during the reaction. (The catalyst could be reactivated with oxygen at T = 500 $^{o}$C)

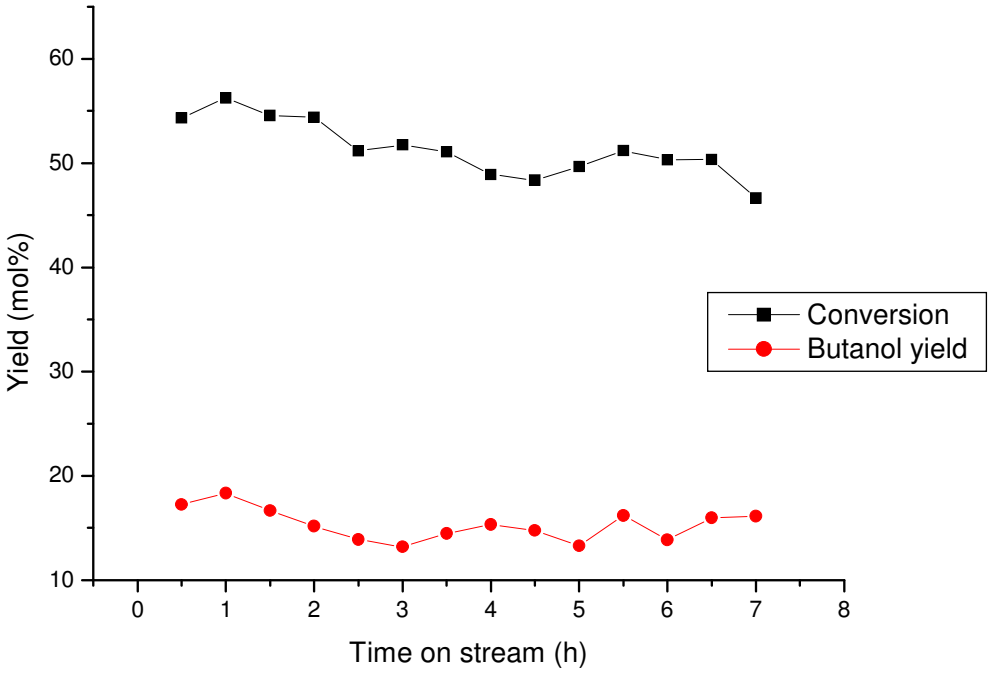


**Figure 4.4** Influence of time on stream on activity and 1-butanol yield over MgO

### 4.3.3 Reaction Mechanism

Dimerisation of ethanol in the presence of $N_2$ or $O_2$ as a carrier gas (preliminary experiments conducted in $O_2$) gave near identical results in terms of butanol (and other products) selectivity and activity. Thus it appears that an oxidizing environment is not necessary for the reaction. An overall reaction scheme has been proposed for the dimerisation of ethanol

to propanol by Iglesia and co-workers [13-16] and this is shown in Scheme 4.1. As can be seen the reaction is proposed to occur via direct and indirect reactions of ethanol molecules.

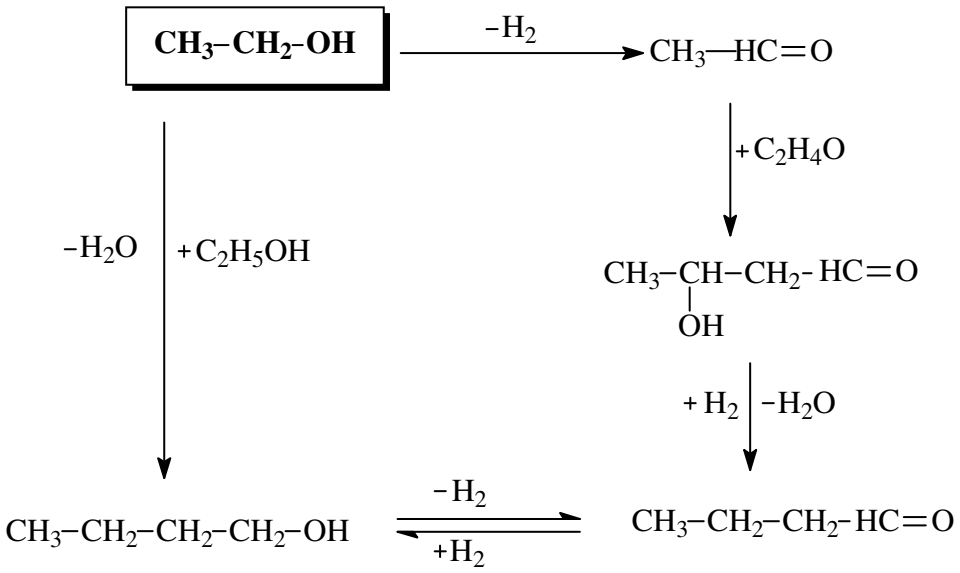


**Scheme 4.1** Reaction network for the formation of 1-butanol from ethanol.

A number of mechanisms for the production of butanol from ethanol can thus be proposed:

i) reaction of ethanol with an alkene via a hydrocarboxylation reaction. This reaction is not considered in this work as no evidence for the presence of ethene was noted (or expected).

ii) oxidation of ethanol to acetaldehyde, followed by aldol condensation of acetaldehyde to form crotonaldehyde and finally hydrogenation to 1-butanol (Scheme 4.2).

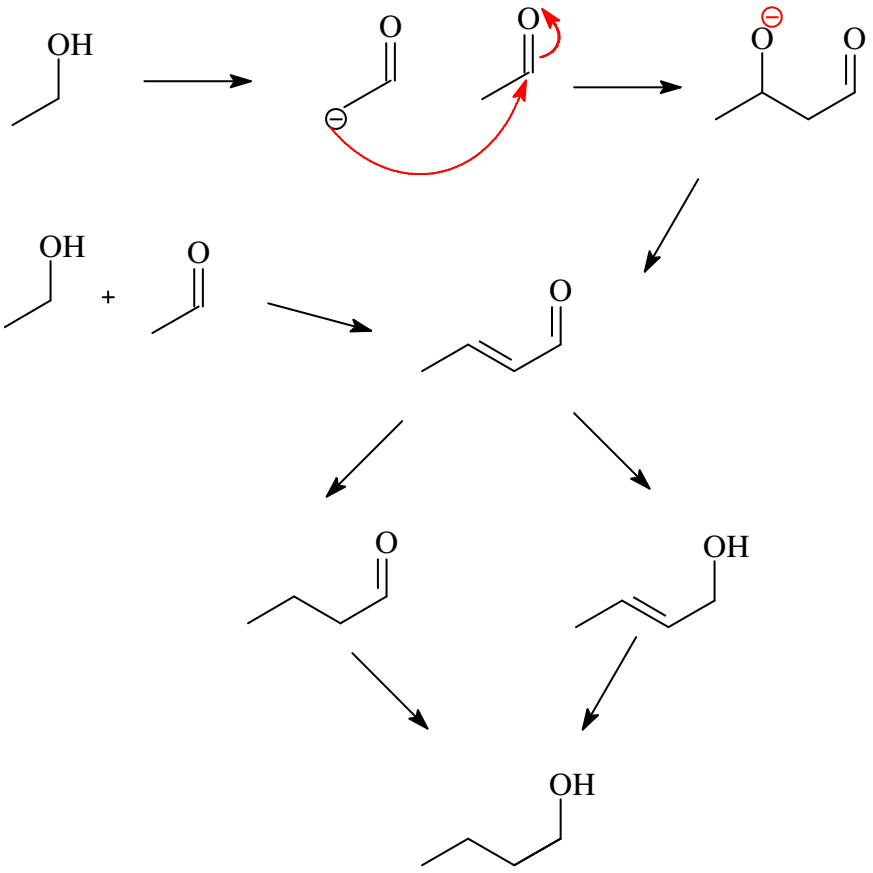


**Scheme 4.2** Classical condensation reaction of ethanol and acetaldehyde to form 1-butanol.

iii) dimerisation of ethanol via H abstraction from a ß C atom (Scheme 4.3 and 4.4) [18]

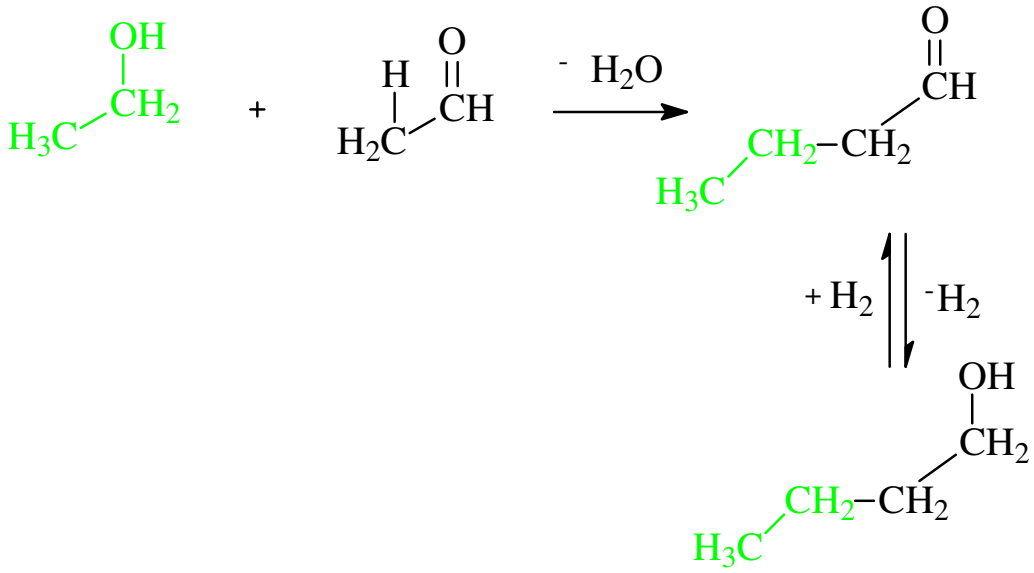


**Scheme 4.3** Condensation reaction of ethanol and acetaldehyde to form 1-butanol.

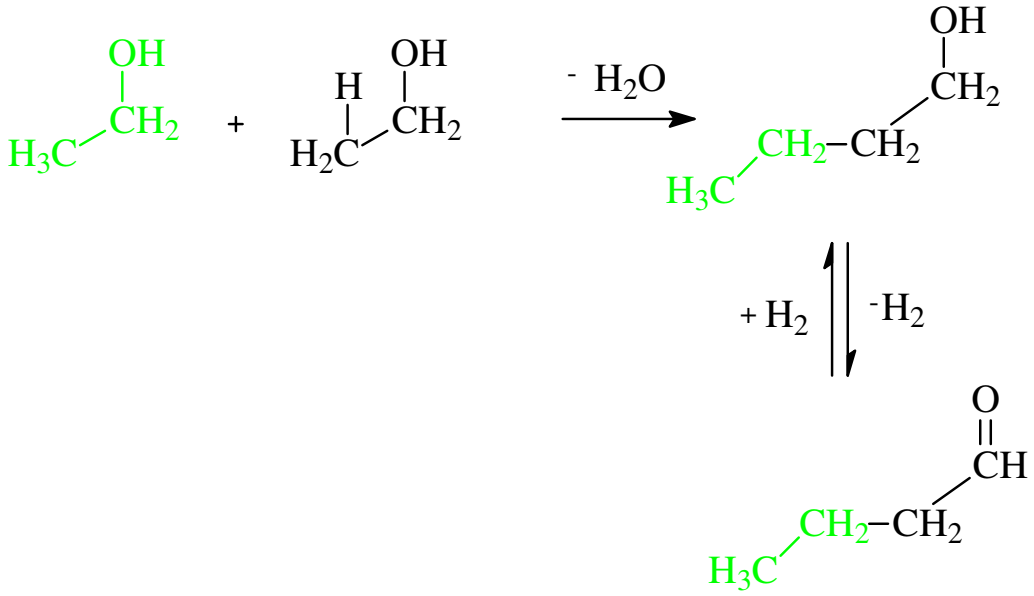


**Scheme 4.4** Dimerization of ethanol to form 1-butanol.

To establish the mechanism over MgO a range of reactions of ethanol with possible reaction intermediates were performed. Reactions were performed using pure reagents or with the reagents mixed with ethanol (1:1 v/v) (Table 4.4).

i) Reaction with pure ethanol provides the base line data as to products formed in the reaction. It is to be noted that very little crotonaldehyde is detected in the reaction.

ii) Passage of pure butanol or butanal over MgO revealed that the two reagents were readily interconverted. Only minor amounts of other $C_4$ products were formed. Very little crotonaldehyde was formed from pure butanol, suggesting no possible reaction reversibility via this route. This data is consistent with the findings of Iglesia and co-workers [13-16].

iii) Passage of acetaldehyde over the MgO did produce some butanol, but also large quantities of crotonaldehyde (19.1%). This suggests that acetaldehyde may not be the major intermediate in the mechanism. (This is consistent with the lack of surface hydrogen fragments).

iv) A mixture of ethanol and acetaldehyde gives the expected decrease in crotonaldehyde yield and increase in butanol yield.

v) Interconversion between crotonalcohol and crotonaldehyde is not significant and crotonaldehyde does not appear to be an intermediate to butanol formation.

vi) Pure crotylalcohol did not produce 2-butanol.

While some of the results are consistent with an expected aldol condensation reaction, the data suggest a limited role for acetaldehyde as an intermediate in the reaction. Further, while the pure reagents give different results from the ethanol/reagent mixtures, the results are predictable and suggest that reactions of key intermediates required from an aldol reaction play little part in the reaction mechanism.

**Table 4.4** The product distribution of the liquid products from the reaction of (i) pure intermediates (100%) and (ii) ethanol/intermediate (1:1) mixtures over MgO.

| Reagents | Yield (mol%) | | | | | |
|---|---|---|---|---|---|---|
| | Acetal | Butanal | Crotonal | 2Butanol | Butanol | Crotanol |
| **Pure reagents** | | | | | | |
| Acetaldehyde | - | 4.7 | 19.1 | 0.7 | 5.8 | 0.4 |
| Butanal | 0.1 | - | 0.1 | - | 15.4 | 0.3 |
| Crotonaldehyde | 0.4 | 9.4 | - | 0.1 | 1.6 | 0.4 |
| Butanol | 0.9 | 13.0 | 0.2 | - | - | 0.1 |
| Crotylalcohol | 1.0 | 0.9 | 4.7 | - | 2.9 | - |
| Ethanol | 0.3 | 2.1 | 0.4 | 0.5 | 18.4 | 0.7 |
| **1/1 mixtures** [a] | | | | | | |
| Acetaldehyde | | 4.1 | 6.4 | - | 10.1 | 3.6 |
| Butanal | 1.1 | - | 1.5 | 1.4 | 40.5 | 3.6 |
| Crotonaldehyde | 0.0 | 1.3 | - | - | 4.7 | 0.6 |
| Crotylalcohol | 3.4 | 2.8 | - | 4.6 | 7.2 | - |
| Butanol | 1.9 | 11.0 | 1.8 | 0.7 | - | 3.0 |

[a] 1/1 mixture of intermediate and ethanol

The data are thus not totally consistent with the mechanism shown in Scheme 4.2. Acetaldehyde, a by-product, does not contribute to the significant growth of the carbon chain. A key issue relates to the role of hydrogen production/use in the reaction cycle.

A mechanism, shown in Schemes 4.3 and 4.4, previously proposed by Yang and Weng [23] for the reaction of ethanol over alkali cation laden zeolites, is consistent with the data shown in Table 4.4. In this mechanism, ethanol undergoes proton abstraction from the ß carbon atom and the nucleophilic centre generated attacks another ethanol molecule, resulting in OH displacement (i.e. dehydration), C-C coupling and hence formation of 1-butanol and water. This mechanism is also alluded to in the mechanism proposed by Iglesia and co-workers for reactions over basic catalysts.

The TPD data are consistent with this proposal – only strong basic sites would achieve this abstraction form an OH activated $CH_3$ group.

Activation of a ∃-H atom is thus the key step in the mechanism. At a molecular level it is suggested that ethanol reacts with surface MgO to generate an ethoxide ion and it is this ion that has an activated ∃-H atom. Further evidence will be required to support this proposal.

## 4.4 Conclusions

Our results suggest that acetaldehyde is not the only major intermediate in the synthesis of butanol from ethanol. It does however, participate in a competing coupling reaction (aldol condensation reaction) resulting in the formation of crotonaldehyde. Further crotonaldehyde is also not an intermediate in the formation of butanol from ethanol.

An alternative coupling reaction proposed by Yang and Weng is possible, (Scheme 4.4), namely- the self-coupling of ethanol. The ethanol/acetaldehyde coupling reaction (Scheme 4.3) is not consistent with the data and thus the self-coupling of ethanol is the mechanism occurring in this reaction.

## 4.5 References

[1] C.R. Patra and R. Kumar, J. Catal., 142 (2002) 216.

[2] D. Das and S. Cheng, Appl. Catal. A: General, 201 (2000) 159.

[3] A.M. Camiloti, S.L. Jahn, N.D. Vlesco, L.F. Moura, D. Cardoso, Appl. Catal. A: General, 182 (1999) 107.

[4] R. Beaumont and D. Barthomeuf, J. Catal., 27 (1972) 45.

[5] R. le van Mao, T.M. Nguyen, G. McLaughlin, Appl. Catal. 48 (1989) 265.

[6] E. Iglesia, D.G. Barton, J.A. Biscardi, M.J.L. Gines and S.L. Soled, Catalysis Today, 38 (1997) 339.

[7] H. Hattori, Stud. Surf. Sci. Catal. 78 (1993) 35.

[8] H. Hattori, Chem. Rev., 95 (1995) 537.

[9] W. O. Haag and H. Pines, J. Am. Chem. Soc., 82 (1960) 387.

[10] S. Bank, J. Org. Chem., 37 (1972) 114.

[11] Y. Ono, T. Baba, Catalysis Today, 38 (1997) 32.

[12] M. Ichikawa, J. Catal., 56 (1979) 127.

[13] J.I. Di Cosimo, C.R. Apesteguia, M.J.L. Gines and E. Iglesia, J. Catal.190 (2000) 261.

[14] M.J.L. Gines and E. Iglesia, J. Catal., 176 (1998) 155.

[15] A.M. Hilmen, M. Xu, M.J.L. Gines and E. Iglesia, Appl. Catal. A: General, 169 (1998) 355.

[16] M. Xu, M.J.L. Gines, A.M. Hilmen, B.L. Stephens and E. Iglesia, J. Catal. 171 (1997) 130.

[17] M.W. Farrar (Monsanto Chemical Co.), US Pat. 2 971 033, (1961).

[18] R.T. Clark (Celanese Corporation), US Pat. 3 972 952, (1976).

[19] W. Ueda, T. Kuwabara, T. Ohshida, Y. Morikawa, J. Chem. Soc. Chem. Commun. (1990) 1558.

[20] W. Ueda, T. Kuwabara, T. Ohshida, Y. Morikawa, Catal. Lett. 12 (1992) 971.

[21] Kirk-Othmer, Encyclopedia of Chemical Technology, 3rd Edition, 4 (1978) 338.

[22] C. Yang and Z. Meng, J. Catal., 142 (1993) 37.

[23] W. Ueda, T. Yokoyama, Y. Moro-oka, T. Ikawa, Chem.Lett. (1985) 1059.

# C H A P T E R 5

## Self Condensation of Propanol over Solid Base Catalysts*

*A.S. Ndou, N.J. Coville, Applied Catalysis A: General, 275 (2004) 103-110

### 5.1 Introduction

Numerous processes have been established to synthesize long chain alcohols, particularly processes that involve CO and methanol as reactants [1]. One of the important industrial processes in which CO plays a key role in alcohol production is the oxo or hydroformylation reaction [2]. Other reported reactions include homologation of lower alcohols to higher ones using carbon monoxide and hydrogen [3], and the metal or metal oxide catalysed direct synthesis of alcohols from syngas [4]. Hilmen et al. [5] also reported the formation of higher alcohols in the synthesis of methanol and isobutanol from $CO/H_2$ mixtures over basic mixed metal oxide catalysts.

Another well known route to higher alcohol synthesis is by the condensation of primary alcohols [3,5-9]. This process is called the

Guerbet reaction and entails the reaction of a primary or secondary alcohol with itself or another alcohol to produce a higher alcohol. Various types of heterogeneous catalysts have been used for this reaction and reported in patents [10,11]. Carlini and his co-workers have reported the synthesis of valuable alcohols (isobutanol and 2-ethyl-1-hexanol) through the Guerbet reaction using both homogeneous and heterogeneous metal catalysts with basic components [12-16]. Ueda et al. [17,18] have also reported in detail on a catalytic reaction carried out over a solid base metal oxide catalyst, in which methanol is condensed with other primary or secondary alcohols having a methyl or methylene group at the β-position.

Higher alcohols are used mainly as ester derivatives in the polymerization industry. They are also used as synthetic lubricants, hydraulic fluids, and brake fluids [19]. A mixture of higher alcohols and methanol can also be used for direct blending with hydrocarbon fuels. This mixture is preferred over pure methanol because of the higher water tolerance, reduced fuel volatility, lower vapour lock tendency, and higher volumetric heating values when compared to the equivalent properties of pure methanol [20].

Herein we report the synthesis of 2-methylpentanol from propanol over MgO as a catalyst.

## 5.2 Experimental

### 5.2.1 Catalyst preparation

Magnesium oxide catalysts were prepared from commercial MgO (A.R. Hopkin and Williams LTD). The magnesium oxide was suspended in warm water with stirring and then solidified again by evaporation of the water. It was then dried at 120 $^{o}$C for 16 h and finally calcined in air at 500 $^{o}$C for 6 h. This catalyst was found to have a BET surface area of 60 $m^2/g$. CaO and BaO were prepared from the thermal decomposition of calcium hydroxide and barium hydroxide respectively at elevated temperature (500 $^{o}$C) for 6 h.

Silica (Aerosil 200) and MgO with BET surface areas of 67 $m^2/g$ and 60 $m^2/g$ respectively were used as supports for alkali, alkaline earth and transition metal oxides. $\gamma$-Alumina (BET surface area 157 $m^2/g$ and pore volume of 0.23 $cm^3/g$) was also used as a support.

The metal oxide supported catalysts were prepared by the incipient wetness procedure using an appropriate amount of aqueous metal hydroxide/nitrate solution. The catalysts were dried at 120 $^{o}$C (16 h) and calcined in air at 500 $^{o}$C for 6 h.

### 5.2.2 Apparatus and procedure

The catalytic experiments were carried out in a vertical fixed bed glass reactor (130 mm long and 10 mm e.d). All reactions were carried out using 0.5 g of catalyst. The catalysts were used in the form of granules (350-850 μm) prepared by pelletising the MgO catalyst powder and crushing to the desired size. The reactor was placed inside a temperature controlled heating jacket with a thermocouple placed at the centre of the catalyst bed. The catalyst was activated in flowing oxygen at 500 $^{o}$C for 1 h prior to flushing with nitrogen gas. Propanol was fed at 1.5 ml/min from a 10 ml syringe using a syringe pump (Sage instruments, model 341B) through a heated carrier gas (nitrogen; flow rate 40 ml/min) line prior to the reactor. The partial pressure of propanol in the feed was kept at 17.12 kPa.

The products were collected in a water-cooled receiver after 1 h (unless otherwise stated) and analysed in a gas chromatograph (ZB wax, 60 m x 0.32 mm capillary column; FID). Light gaseous products including CO and $CO_2$ were produced in the reaction and were analysed on line by gas chromatography. The amount of gaseous products formed during the reaction was small and analysis of these products was subsequently discontinued in later runs. Liquid product identification was achieved by GC-MS (Finnigan TSQ-7000) and $^{13}$C-NMR spectroscopy (Brucker AC

400). The temperature programmed desorption (TPD) apparatus consists of a U-shaped quartz reactor housed in a temperature controlled heating jacket. The signal is measured by a low temperature dual filament TCD and recorded by a PC equipped with an I/O card.

## 5.3 Results and Discussion

### 5.3.1 Catalyst screening

In initial studies propanol was passed over a range of catalysts at 450 $^{o}$C and a substantial amount of liquid products was collected (Table 5.1). In addition some gaseous light products were formed by thermal decomposition of the propanol or reaction intermediates. The selectivities and activities of the different catalysts were evaluated by GC studies. Product compositions were determined by a combination of GC, GC-MS and $^{13}$C NMR spectroscopy. By this means the major liquid products were identified.

Amongst the catalysts screened, MgO showed the highest activity and selectivity towards 2-methylpentanol. Even addition of basic ions (e.g. $Li^{+}$, $Na^{+}$, $K^{+}$, $Ca^{2+}$, $Ba^{2+}$, and $Cs^{2+}$ ; see Supplementary information) did not

enhance the activity/selectivity of the MgO. From the data obtained from the screening reactions, pure MgO was chosen for further extensive investigation.

**Table 5.1** Liquid product distribution form the self-condensation reaction of propanol over various solid base catalysts.

| Catalysts | %Conversion | % SELECTIVITY | | | | | |
|---|---|---|---|---|---|---|---|
| | | Propional-dehyde | Methanol | Ethanol | 2-methyl-pentanal | 2methyl-Pentanol | Others[a] |
| MgO | 27.8 | 16.1 | 7.3 | 3.4 | 2.6 | 50.2 | 20.4 |
| BaO | 9.8 | 35.3 | 9.2 | 6.2 | 1.1 | 11.5 | 37.0 |
| CaO | 4.4 | 21.6 | 8.0 | 7.6 | 1.3 | 8.0 | 53.5 |
| $SiO_2$ | 1.2 | 36.7 | 24.9 | 7.8 | - | 1.4 | 29.2 |
| $ZrO_2$ | 23.3 | 48.5 | 0.7 | 0.8 | 2.1 | 12.0 | 35.9 |
| $\gamma Al_2O_3$ | 0 | 0 | 0 | 0 | 0 | 0 | - |
| 1%$H_2SO_4$/MgO | 26.2 | 33.7 | 3.4 | 1.2 | 2.2 | 38.2 | 21.3 |
| 1%Li/MgO | 5.8 | 2.6 | - | 67.0 | 1.4 | 9.0 | 20.0 |
| 1%Na/MgO | 2.7 | 30.8 | 20.0 | 41.2 | 3.9 | 3.0 | 1.1 |
| 1%K/MgO | 0.6 | 69.2 | - | 28.8 | 1.0 | - | 0.4 |
| 1%Cu/MgO | 27.4 | 12.5 | 6.5 | 3.8 | 2.3 | 44.7 | 32.5 |
| 1%Cu/5%K/ MgO | 14.9 | 19.1 | 7.5 | 17.2 | 1.4 | 13.0 | 41.8 |

| | | | | | | | |
|---|---|---|---|---|---|---|---|
| 5%Cu/MgO | 17.0 | 25.5 | 10.9 | 8.9 | 1.6 | 24.0 | 29.1 |
| 10%Zn/MgO | 62.8 | 11.8 | 17.3 | 22.0 | 8.0 | 2.0 | 38.9 |
| 5%K/MgO | 9.3 | 18.0 | 9.8 | 29.3 | 2.7 | 13.3 | 26.9 |
| 10%K/MgO | 7.3 | 59.1 | 13.3 | 5.7 | 2.1 | 0.9 | 18.9 |
| 10%Na/MgO | 6.2 | 55.8 | 9.7 | 3.5 | 1.3 | 7.1 | 22.6 |
| 10%Cs/MgO | 13.9 | 52.2 | 3.2 | 6.7 | 0.5 | 2.5 | 34.9 |
| 10%Ca/MgO | 17.2 | 54.3 | 6.0 | 5.1 | 0.9 | 20.2 | 13.5 |
| 10%Ba/MgO | 15.3 | 37.5 | 4.1 | 1.0 | 2.2 | 30.1 | 26.1 |
| 10%Cs/$SiO_2$ | 5.8 | 56.4 | 1.1 | 2.8 | 1.7 | 5.1 | 32.9 |
| 10%K/$Al_2O_3$ | 30.5 | 52.8 | 1.1 | 2.2 | 2.6 | 12.3 | 29.0 |
| 50%MgO/$Al_2O_3$ | 33.3 | 46.6 | 1.3 | 2.7 | 1.3 | 10.9 | 37.2 |

[a] Others include, Dipropylether, aldehydes of products and higher molecular weight species.

The effect of reaction temperature on the activity/selectivity of the propanol condensation reaction is shown in Figure 5.1. A fresh catalyst was used for each set of data points in the experiment. Very little change in the selectivity towards propionaldehyde over MgO, as the temperature of the reaction is increased, is to be noted. Although the selectivity towards 2-methylpentanol is very high at lower temperatures it tends to decline as the temperature increases due to the formation of higher mass molecular species (oligomers). The overall conversion at lower temperatures is, however, very small. A reaction temperature of 450 $^{o}$C was selected for further studies of this reaction.

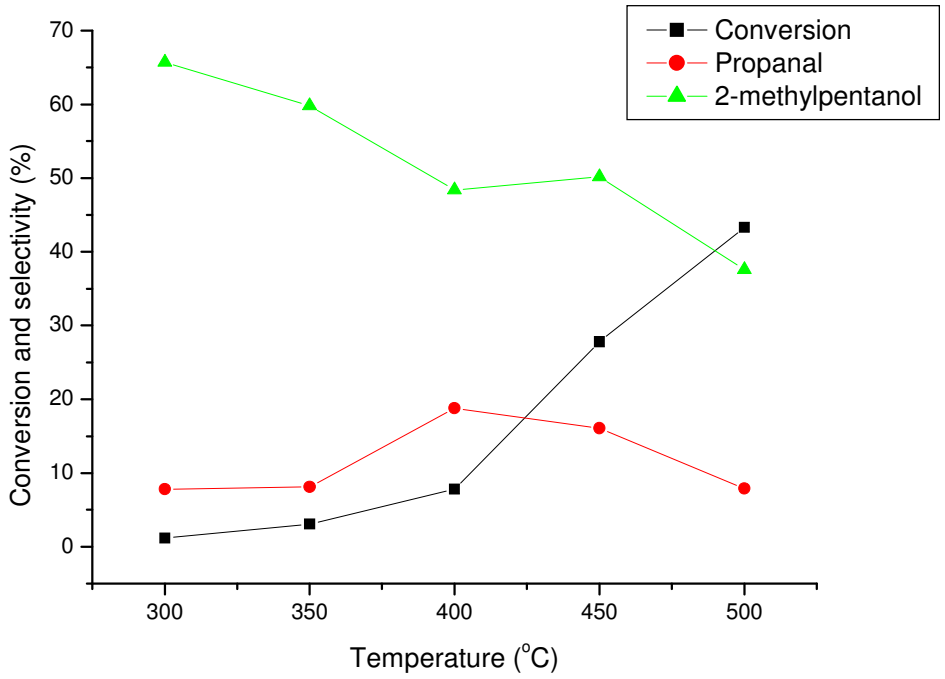


**Figure 5.1** The effect of temperature on conversion and product distribution (calcination temperature 500 °C).

Figure 5.2 shows the variation of propanol conversion and 2-methylpentanol selectivity with MgO calcination temperature. All the reactions were conducted over a fresh catalyst. The conversion of propanol decreased with an increase in calcination temperature. However, the selectivity towards 2-methylpentanol remained fairly constant with the increase of calcination temperature, suggesting that the choice of catalyst

calcination temperature, for further studies, would be determined by conversion issues, with 500 °C being the calcination temperature of choice.

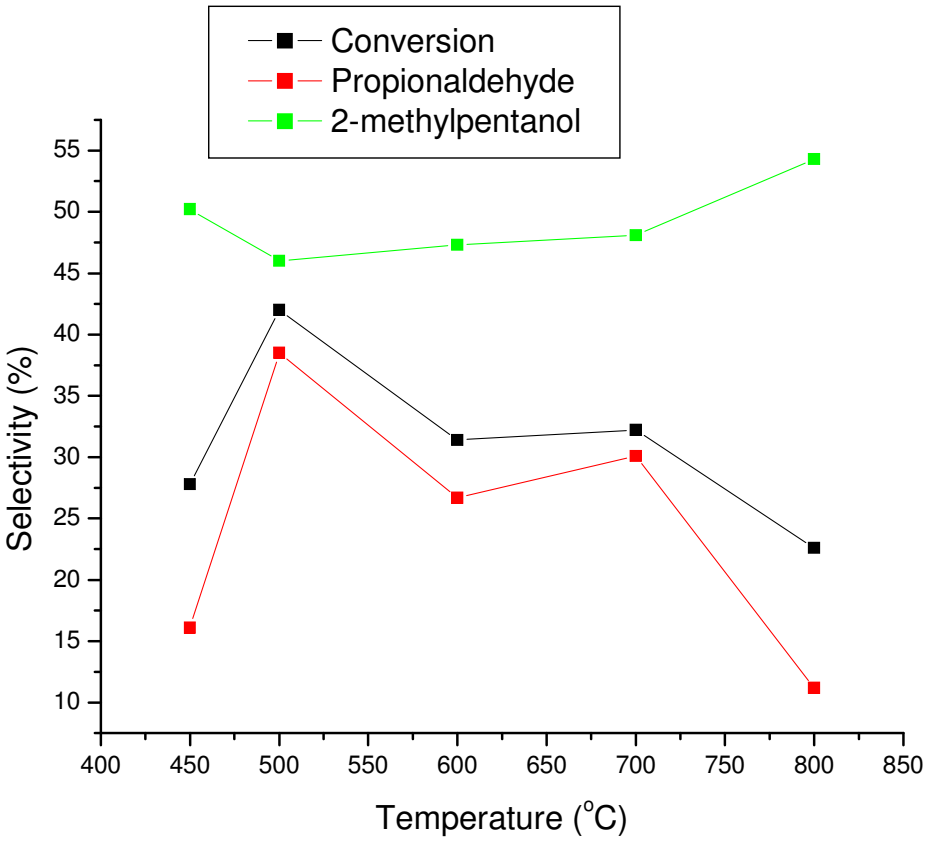


**Figure 5.2** The influence of calcination temperature on propanol conversion and catalyst selectivity (reaction temperature 450 °C).

Further studies were conducted in order to understand the significance of the catalyst calcination temperature and to observe the changes that occur

on the surface of the catalyst. This was partially achieved by temperature programmed desorption (TPD) using $CO_2$ as a probe molecule (Figure 5.3). The experiments were conducted in atmospheric pressure. The $CO_2$ was adsorbed at 100 $^oC$. From the figure it can be seen that the TPD peak in the temperature range 100 to 500 $^oC$ increases as the calcination temperature changes from 450 $^oC$ to 500 $^oC$ and then decreases as the calcination temperature is increased to 800 $^oC$. The peak maxima at ca. 200 $^oC$ (Fig 5.3) correlates with the decrease in the activity of the catalyst as observed in Figure 5.2 above. A lower calcination temperature in the region of 450 $^oC$ to 550 $^oC$ was required for optimum catalytic activity in this reaction.

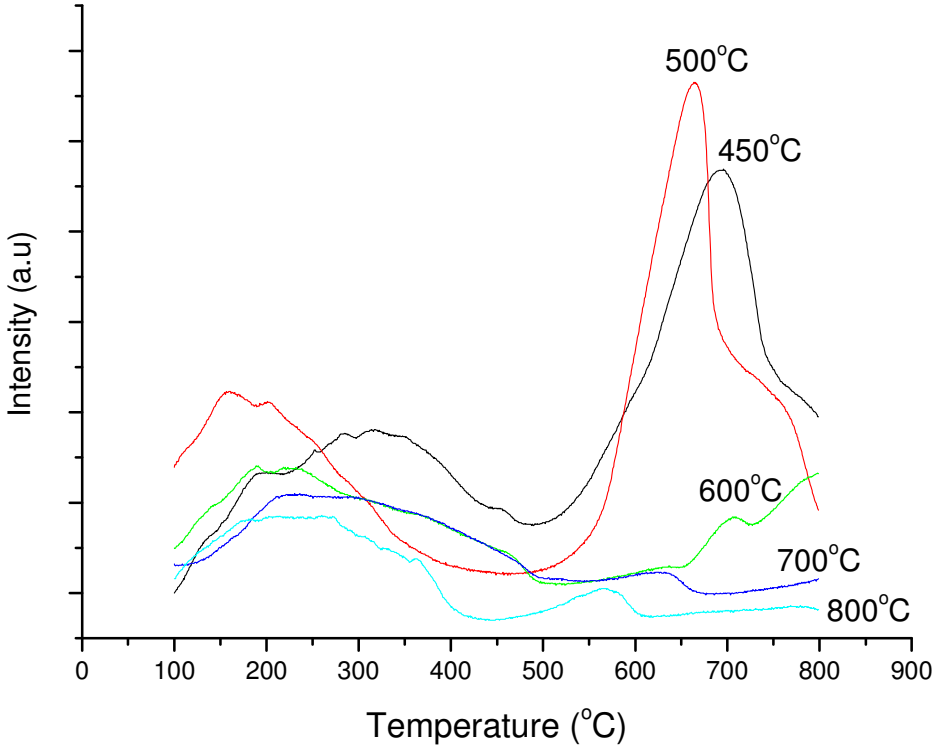


**Figure 5.3** The effect of calcination temperature on the catalyst basicity (strength and basic site distribution).

Figure 5.4 shows the variation of propanol conversion and 2-methylpentanol selectivity with contact time. A fresh catalyst was used for each set of data points presented in this experiment. The data shows an initial increase, followed by a steady decrease in 2-methylpentanol selectivity as the space velocity increases. The selectivity towards propionaldehyde initially increased and then remained near constant as the

space velocity increases. Further, a steady decline in conversion was observed as the space velocity increased.

The above information is consistance with the classical mechanism of higher alcohols formation which postulates the formation of propoinaldehyde as a primary product from which the 2-methylpentanol could be formed.

The data for the propanol reactions can thus be explained as follows. At high space velocities, there is less time for a secondary reaction to occur and hence the slight increase in propionaldehyde yield.

At lower space velocities, there is enough time for further coupling reactions to occur, resulting in lower propionaldehyde yield.

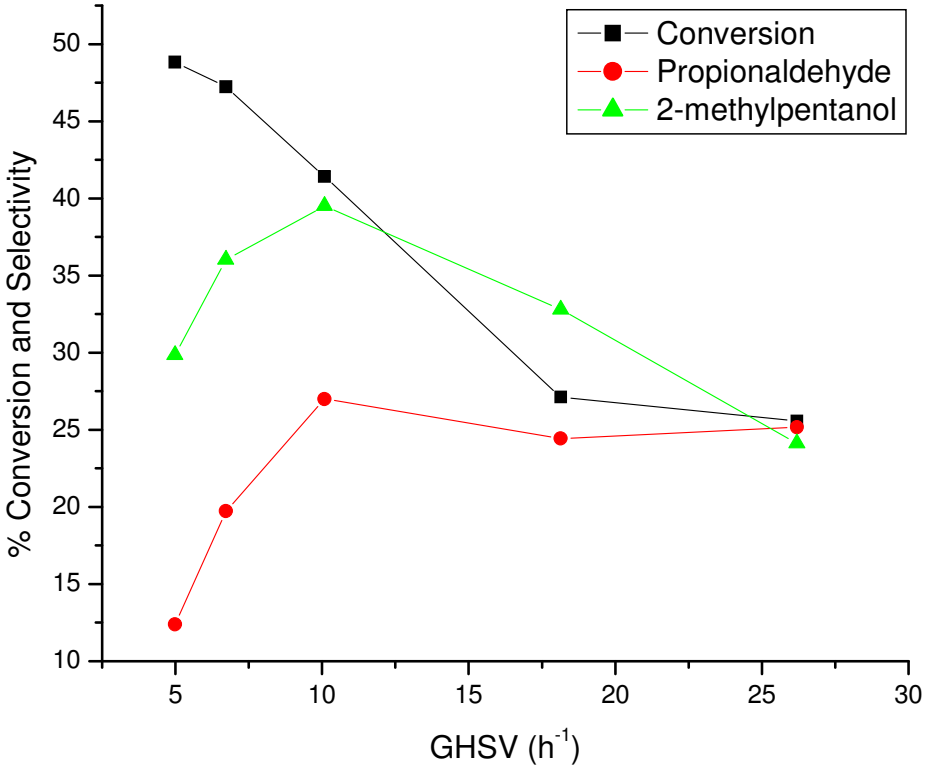


**Figure 5.4** The effect of GHSV on propanol conversion and product yield (reaction temperature 450 °C, calcination at 500 °C for 6 h).

A decrease in propanol conversion with time-on-stream was noted to occur (Figure 5.5). The selectivity towards propionaldehyde initially increased with time-on-stream while the selectivity to 2-methylpentanol initially decreased as time-on-stream increased. In the later stages of the reaction the composition of the two products remained constant with time.

It is be noted that all the catalysts turned black during the reaction and reactivation in oxygen (500 $^{o}$C for 1 h) resulted in a return to the original catalyst colour (white) and at conversion levels observed at the beginning of the reaction. This suggests that the deactivation was due to carbon deposition.

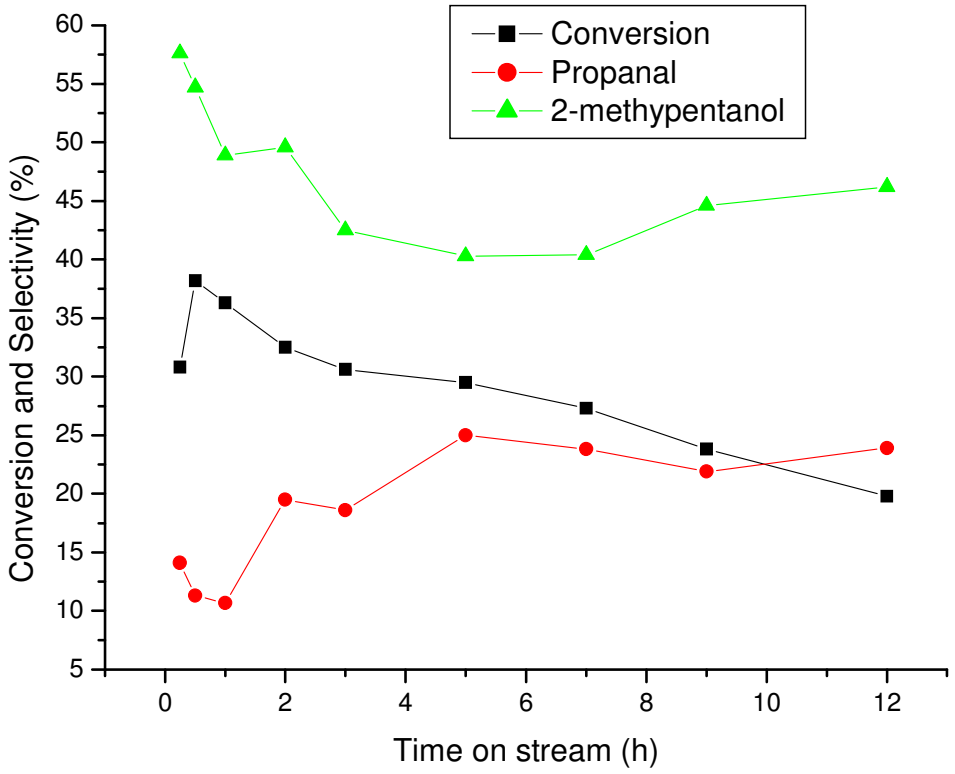


**Figure 5.5** The effect of time on catalyst activity and product selectivity.

The thermogravimetric analysis (TGA) of the catalyst (in air) at the end of a catalysed reaction is shown in Figure 5.6. Below 200 $^{o}$C, mass loss is associated with $H_2O$ removal (~ 2 %) and between 200 $^{o}$C and 400 $^{o}$C, mass loss is associated with easy to remove carbonaceous material (or heavies) (~ 2 %). Mass loss between 400 and 600 $^{o}$C is associated with graphitic carbon removal (~ 2 %) and removal of this material restores both the catalytic activity and catalyst colour.

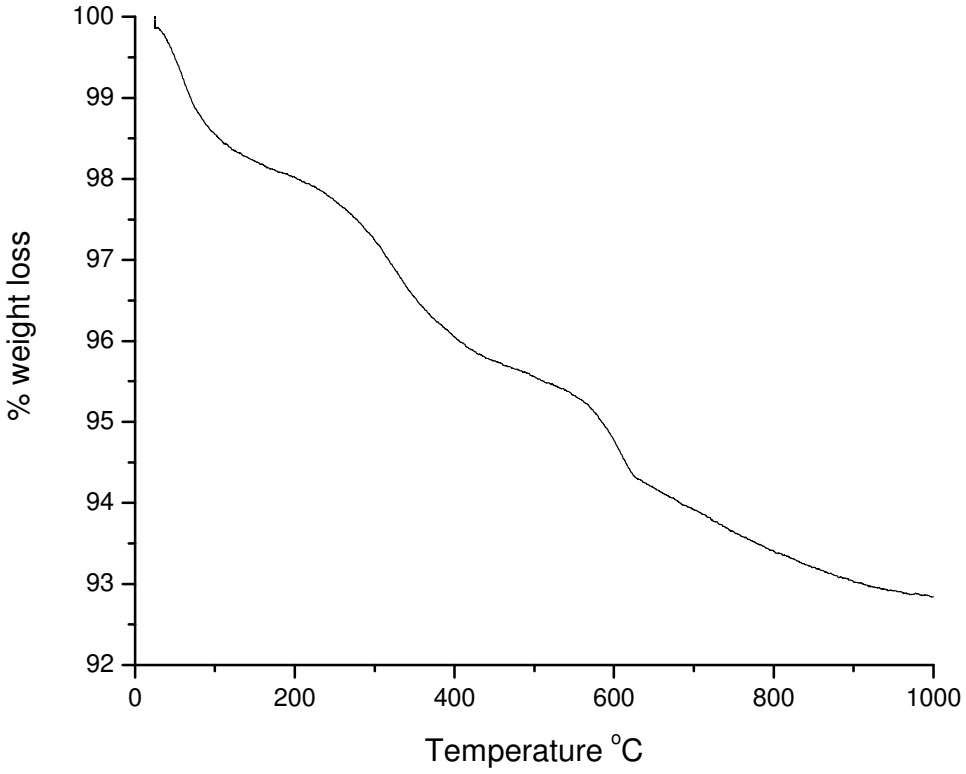


**Figure 5.6** Thermogravimetric analysis (TGA) profile of used MgO.

### 5.3.2 Influence of hydrogen gas on catalyst activity and product selectivity.

The mechanism proposed for the C-C coupling reaction of alcohols requires hydrogen transfer, and consequently, the role of hydrogen in the reaction was also evaluated [8]. This was achieved by varying the amount of hydrogen gas in the carier gas stream.

Figure 5.7 shows the change in conversion and selectivity as the amount of hydrogen gas in the reaction is increased. A fresh catalyst was used for each set of data points collected in this experiment. The propanol conversion shows a small decrease as the hydrogen gas percentage in the carrier gas increases. Although there was an increase in propionaldehyde selectivity as the hydrogen gas percentage increases, the selectivity towards 2-methylpentanol did not show a similar trend.

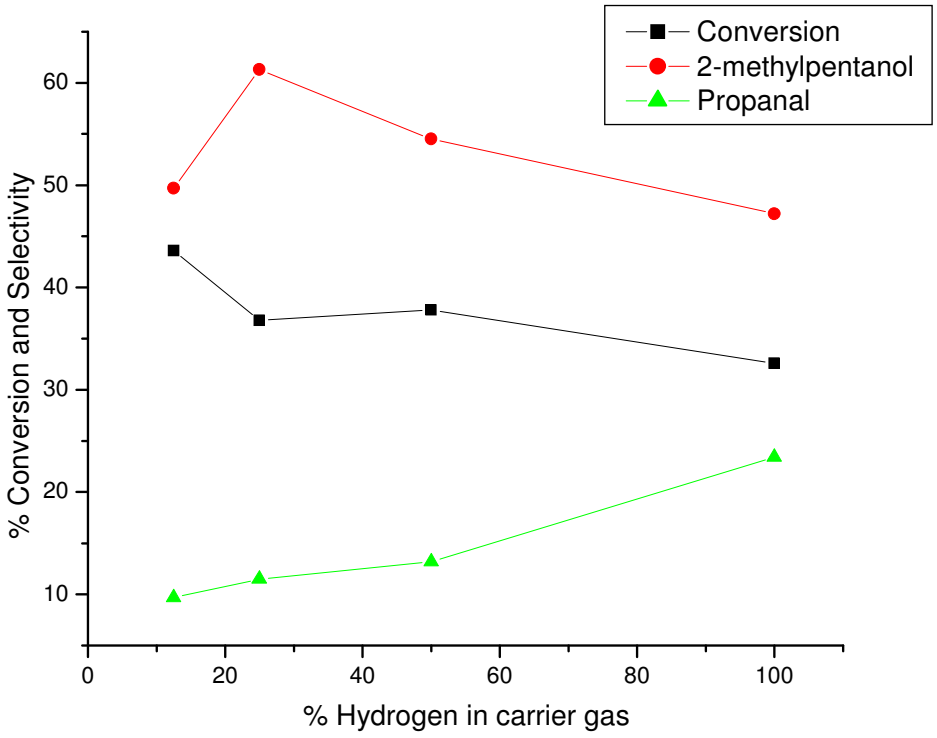


**Figure 5.7** The influence of % hydrogen on catalyst activity and product selectivity (T = 450 $^{o}$C, calcination at 500 $^{o}$C for 6 h).

Hydrogen gas was passed over the catalyst for various time intervals in a pre-treatment step prior to addition of propanol (Figure 5.8). Each pre-treatment step was conducted over a fresh catalyst. 2-methylpentanol selectivity decreased slightly with an increase in hydrogen purging time.

Although hydrogen is required to enhance the selectivity towards 2-methylpentanol both before and during the reaction, only a small amount of hydrogen is required to give an optimum selectivity towards 2-methylpentanol. It can also be noted that the influence of hydrogen pre-treatment on the selectivity towards 2-methylpentanol was very small.

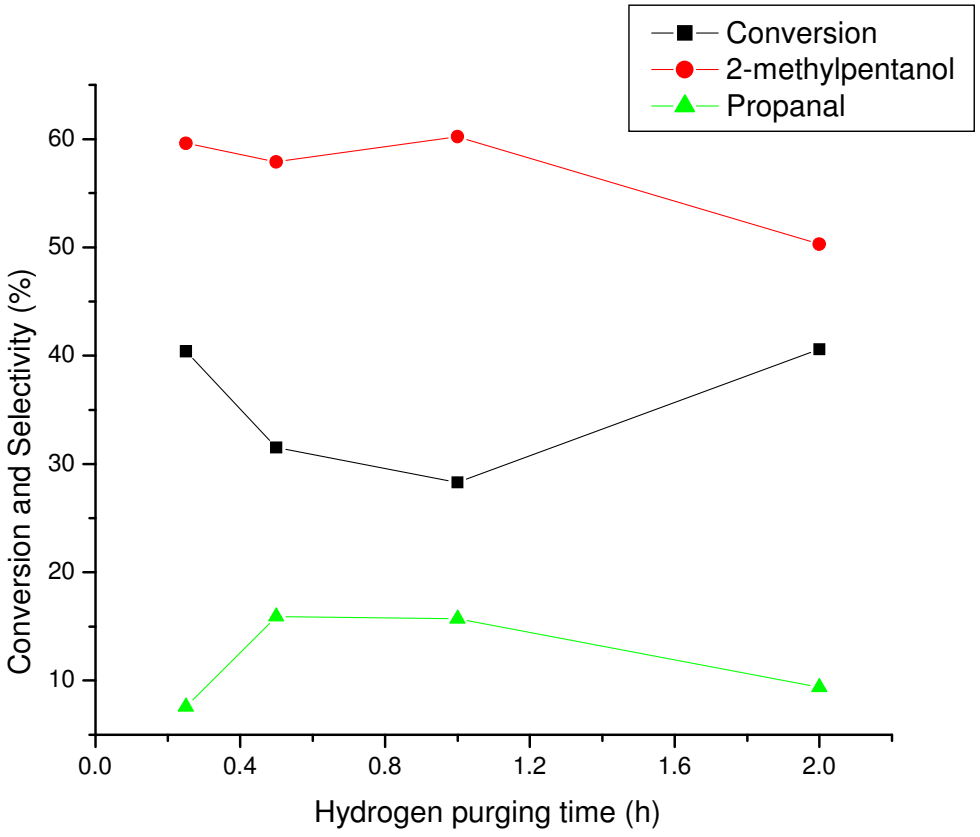


**Figure 5.8** The influence of pre-treatment time (in hydrogen) on catalyst activity and product selectivity (T = 450 $^{o}$C).

### 5.3.3. Study of possible reaction intermediates

To establish the mechanism of the reaction over MgO a range of reactions of propanol with possible reaction intermediates was performed. Reactions were performed using neat reagents or with the reagents mixed with propanol (1:1 v/v) (Table 5.2). The reaction of neat propanol is included in Table 5.2 to give an indication of the product composition under standard conditions. It is to be observed that only small amounts of 2-methylpentanal was detected during the reaction with neat propanol. Further, the introduction of hydrogen gas into the propanol feed resulted in a significant increase in the 2-methylpentanol selectivity, consistent with the mechanism shown in Scheme 5.1 [8] (see discussion below).

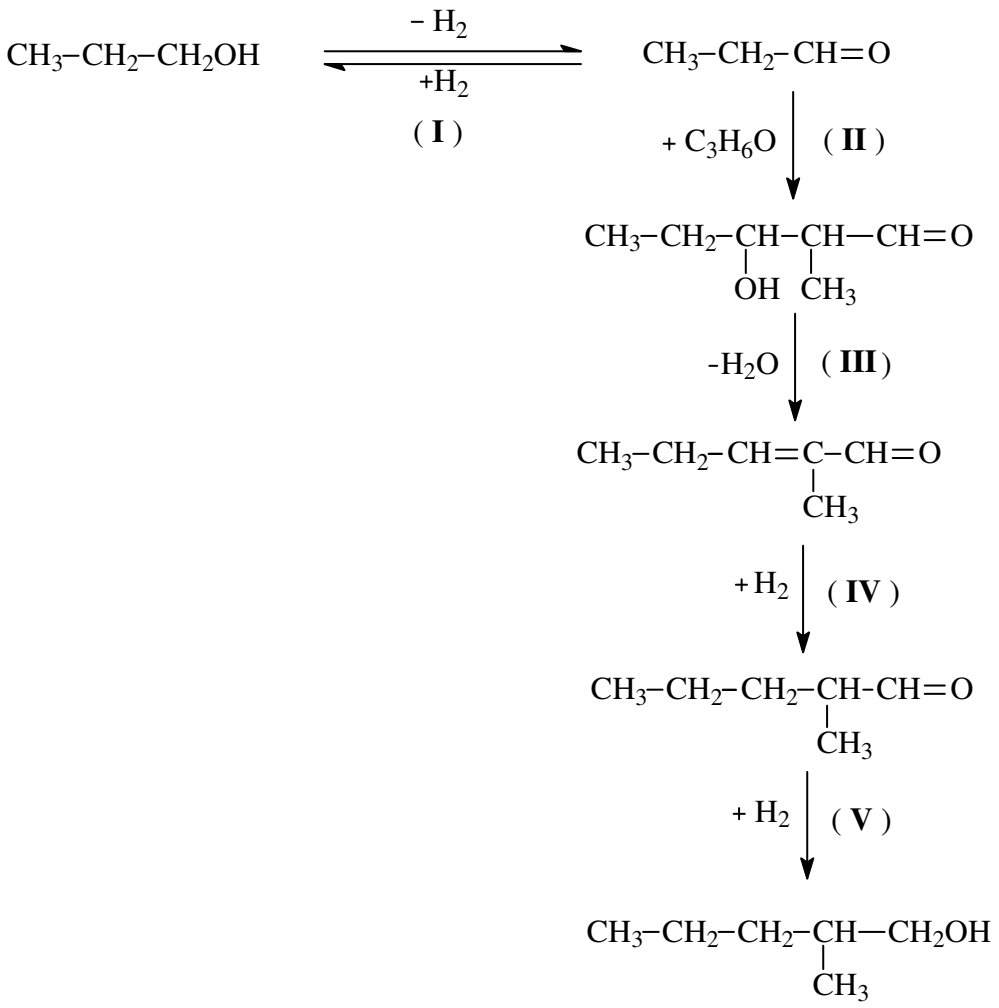


**Scheme 5.1** Aldol condensation of propanol to 2-methylpentanol.

The passage of propionaldehyde over MgO resulted in a high selectivity towards 2-methylpentanal and very little formation of 2-methylpentanol (6.1%). However, the reaction of propionaldehyde in the presence of hydrogen gas gave a high selectivity towards both 2-methylpentanal and 2-methylpentanol (Table 5.2). This shows that the formation of 2-

methylpentanal is preferred over 2-methylpentanol, with propionaldehyde as the feed, even in the presence of hydrogen gas.

It was observed that propionaldehyde was also hydrogenated to propanol (7.4 %, see Table 5.2) during the reaction with $H_2$. This indicated that hydrogenation of both propionaldehyde and 2-methylpentanal to their respective alcohols is possible under the reaction conditions used.

The possibility that the propanol was dehydrated to give propene during the reaction was also considered. However, the addition of propene to propanol over MgO did not affect the 2-methylpentanol selectivity and had no effect on the reaction.

**Table 5.2** The liquid product distribution from the reaction of neat reactants and propanol/intermediate (1:1 v/v) mixtures over MgO.

| Reagents | Conversion (%) | Selectivity (%) | | |
|---|---|---|---|---|
| | | Propio-naldehyde | 2-methyl Pentanal | 2-methyl Pentanol |
| Propanol | 27.8 | 16.1 | 2.1 | 50.2 |
| Propanol + $H_2$ | 24.1 | 9.4 | 1.7 | 69.8 |
| Propionaldehyde | 97.4 | (3.8[a]) | 36.4 | 6.1 |
| Propionaldehyde+$H_2$ | 97.4 | (7.4[a]) | 27.7 | 31.1 |
| Propanol + propene | 30.0 | 12.4 | 2.3 | 51.9 |

[a] propanol selectivity.

The reaction of both propanol and propionaldehyde in the presence of hydrogen gas (100%) was also investigated (Table 5.3). The propanol to propionaldehyde mole ratio was varied in order to understand the influence that each reactant on the product distribution. The selectivity towards 2-methylpentanol increased while that of 2-methylpentanal decreased as the propanol/propionaldehyde mole ratio increased. This result clearly reveals

that propionaldehyde does not supply sufficient hydrogen needed to produce 2-methylpentanol.

**Table 5.3** The liquid product distribution from the reaction of propanol and propionaldehyde mixtures in the presence of hydrogen gas (100%).

| Reagents (mole ratio) Propanol:Propionaldehyde | Conversion. (%) | Selectivity (%) | |
|---|---|---|---|
| | | 2-methyl Pentanal | 2-methyl Pentanol |
| 0: 1 | 97.4 | 27.7 | 31.1 |
| 1: 4 | 72.2 | 27.0 | 31.0 |
| 1: 2 | 53.6 | 20.9 | 23.6 |
| 1: 1 | 34.1 | 15.1 | 17.1 |
| 1.5: 1 | 34.8 | 15.0 | 12.7 |
| 2.3: 1 | 47.8 | 22.3 | 40.2 |
| 4: 1 | 37.5 | 0.5 | 47.3 |
| 1: 0 | 24.1 | 1.7 | 69.8 |

### 5.3.4 Reaction mechanism

The above data allows us to discuss the mechanism of the conversion of propanol to 2-methylpentanol over MgO.

The data obtained in this study are consistent with an aldol condensation reaction as described by others [8,17] and shown in Scheme 5.1. A more detailed description of the reaction is shown in Scheme 5.2 which shows the reaction at the molecular level (after Iglesia and co-workers [7,8]).

The first step in the reaction requires conversion of the propanol to propionaldehyde via loss of hydrogen. Our results indicate that the hydrogen produced is required in later reaction steps. At this stage the propionaldehyde can be rehydrogenated back to propanol (see Table 5.1), but the major reaction is an aldol condensation to generate the C-C coupled product (Scheme 5.1, step II) which rapidly converts to 2-methylpentanal (steps III and IV). Further reaction is determined by the presence of hydrogen. If there is a lack of hydrogen the 2-methylpentanal is removed from the surface, but if sufficient hydrogen is available then 2-methylpentanol is formed (step IV).

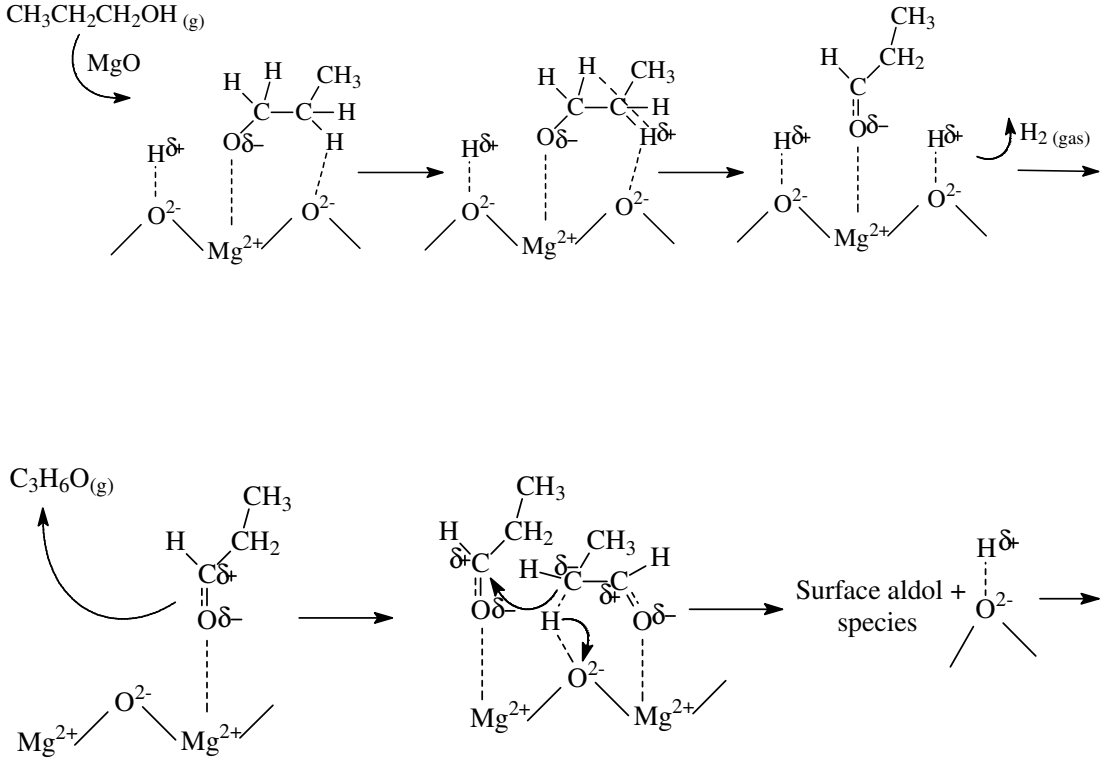


**Scheme 5.2** Detailed molecular mechanism of the Aldol condensation reaction over MgO [7,8].

Addition of hydrogen to propanol resulted in enhanced selectivity to 2-methylpentanol. Surprisingly, while the addition of hydrogen gas to propionaldehyde enhanced conversion to C-C coupled products, less 2-methylpentanol was formed than expected, suggesting that the hydrogen

is best obtained from the propanol. This implies that the surface hydrogen atoms are not as readily formed from gas phase hydrogen.

In studies by Iglesia et.al., [8] the addition of Cu to the catalyst was found to alleviate this constraint. However, we have found that the addition of Cu (1%, 5%; reduction of Cu ions in $H_2$) to MgO resulted in decreased formation of 2-methylpentanol.

The WHSV (Fig. 5.4) also confirms the above mechanism. The increasing yield of propionaldehyde as the space velocity increases, indicate that it is a primary product and that further coupling reactions could be occurring resulting in low yield at low space velocity.

## 5.4 Conclusion

MgO was investigated as a catalyst for the self-condensation of propanol. Good activity and selectivity to 2-methylpropanol were achieved over this catalyst. The impregnation of MgO with either alkali or transition metal oxides did not improve either the activity or the selectivity of MgO. This suggests that MgO has the necessary basic sites required for this reaction.

A study of the reaction has revealed the importance of hydrogen in the reaction. In the absence of a hydrogenating catalyst (e.g. a metal) the reaction still proceeds to generate the hydrogenated product, indicating that MgO also facilitates this role in the catalysed reaction.

The results, in the presence of hydrogen, are consistent with an aldol condensation reaction to give the C-C coupled products.

## 5.5 References

[1] R.A Sheldon, Chemicals from Synthesis Gas (Reidel, Dordrecht, (1983).

[2] Kirk-Othmer, Encyclopedia of Chemical Technology, 3rd Edition, 1 (1978) 716.

[3] M. Ichikawa, J. Catal. 56 (1979) 127.

[4] T. Mizorogi and M. Nakayama, Bull Chem. Soc. Japan, 39 (1964) 236.

[5] A.M. Hilmen, M. Xu, M.J.L. Gines and E. Iglesia, Appl. Catal. A: General, 169 (1998) 355.

[6] J.I. Di Cosimo, C.R. Apesteguia, M.J.L. Gines and E. Iglesia, J. Catal. 190 (2000) 261.

[7] M.J.L. Gines and E. Iglesia, J. Catal. 176 (1998) 155.

[8] M. Xu, M.J.L. Gines, A.M. Hilmen, B.L. Stephens and E. Iglesia, J. Catal. 171 (1997) 130.

[9] M.J. Clement, A. Corma, S. Iborra and A. Velty, J. Mol. Catal. A: Chem. 182 (2002) 327.

[10] M.W. Farrar (Monsanto Chemical Co.), US Pat. 2 971 033, (1961).

[11] R.T. Clark (Celanese Corporation), US Pat. 3 972 952, (1976).

[12] C. Carlini, A. Macinai, A.M.R. Galletti and G. Sbrana, J. Mol. Catal. A: Chem. 212 (2004) 65.

[13] C. Carlini, M Di Girolamo, A. Macinai, M. Marchionna, M. Noviello, A.M.R. Galletti and G. Sbrana, J. Mol. Catal. A: Chem. 204-205 (2003) 721.

[14] C. Carlini, M Di Girolamo, M. Marchionna, M. Noviello, A.M.R. Galletti and G. Sbrana, J. Mol. Catal. A: Chem. 184 (2002) 273.

[15] C. Carlini, M Di Girolamo, A. Macinai, M. Marchionna, M. Noviello, A.M.R. Galletti and G. Sbrana, J. Mol. Catal. A: Chem. 200 (2003) 137.

[16] C. Carlini, A. Macinai, M. Marchionna, M. Noviello, A.M.R. Galletti and G. Sbrana, J. Mol. Catal. A: Chem. 206 (2003) 409.

[17] W. Ueda, T. Kuwabara, T. Ohshida and Y. Morikawa, J. Chem. Soc., Chem. Commun. (1990) 1558.

[18] W. Ueda, T. Kuwabara, T. Ohshida and Y. Morikawa, Catal. Lett. 12 (1992) 971.

[19] Kirk Othmer Encyclopedia of Chemical Technology, 4$^{th}$ Edition, 1 (1991) 865.

[20] P. Forzatti, E. Tronconi, and I. Pasquon, Cat. Rev. Sci. Eng. 33 (1991) 109.

[21] C. R. Narayanan, S. Srinivasan, A. K. Datye, R. Gorte and A. Biaglow, J. Catal. 138 (1992) 659.

[22] R. M. Langer and C. A. Walker, Industrial and Engineering Chemistry, 46 (1954) 1299.

# CHAPTER 6

## Synthesis of 2-ethylbutanol and 1-hexanol from Primary Alcohols over Solid Base Catalyst*

* A.S. Ndou, N.J. Coville, The use of ethanol as a building block for higher alcohol synthesis, To be submitted.

### 6.1 Introduction

2-Ethylbutanol, 1-hexanol and 2-ethylhexanol are part of an important class of compounds that belong to a group of the plasticizer range of alcohols ($C_6$-$C_{11}$). This range of alcohols is utilized primarily in plasticizers, but they also have a wide range of uses in other industrial and consumer products. 2-Ethylbutanol is mainly used as an esterification component to manufacture a wide range of organic compounds used as plasticizers, lubricant additives, hydraulic fluids, diffusion pump oils, heat transfer media, pharmaceuticals, crop protection products and wetting agents [1].

2-Ethylbutanol is also used in penetrating oils, as a cleaning agent for printed circuit boards, and as a metal extracting and separating agent.

The diadipate ester of hexanol is the plasticizer in polyvinylbutyral that is used in automobile safety glass [1]. Hexanol is used in the synthesis of hexylbutyrate, an aroma compound with green notes flavour and widely used in the food industry [2]. 2-Ethylhexanol and hexanol are used as reagents in the polymerization of acrylates, ethylene, and propylene. 2-Ethylhexanol is employed for the synthesis of bis(2-ethylhexyl)phthalate, the most widely applied plasticizer for poly(vinyl chloride) (PVC) [3]. In addition 2-ethylhexanol is utilized as a precursor for the synthesis of the corresponding peroxydicarbonate, a free radical initiator employed in the homopolymerization of vinyl chloride. Furthermore, it is also applied in the preparation of the corresponding trialkyl phosphite, employed as a light stabilizer for plastics as well as for the synthesis of organotin derivatives that are used as PVC heat stabilizers [3].

Large volumes of higher primary alcohols (both plasticizer range and detergent range) are industrially produced through the oxo or hydroformylation reaction. In this process, primary alcohols are produced from mono-olefins in two or more steps. Other reported reactions include homologation of lower alcohols to higher ones using carbon monoxide and

hydrogen [4], and the metal or metal oxide catalysed direct synthesis of alcohols from syngas [5]. Hilmen et al. [6] also reported the formation of higher alcohols in the synthesis of methanol and isobutanol from $CO/H_2$ mixtures over basic mixed metal oxide catalysts. Di Cosimo et al. [7] have reported the synthesis of isobutanol from a mixture of methanol and propanol over a catalyst system with basic properties. The use of alcohol mixtures over a solid base catalyst was also reported by Ueda and his co-workers [8]. They used methanol as a building block for higher alcohol synthesis. The other well known route for higher alcohol synthesis is the Guerbert reaction [9-13].

In recent years, we have been studying the condensation reaction of alcohols over solid base catalysts [14,15]. One of the remarkable features of the ethanol dimerisation reaction was the observation that the data were consistent with activation of the $CH_3$ part of the ethanol molecule. Thus although formation of butanol could arise from an aldol condensation the mechanistic study (Chapter 4) was not fully consistent with this expected proposal. This result thus suggests that addition of other reagents to ethanol could occur via a non-aldo condensation mechanism and should lead to condensation through the $CH_3$ part of the ethanol molecule. Thus reaction of ethanol with $CH_3(CH_2)_nCH_2OH$ could lead to both aldol condensation products (i.e. linear and branched products) as well as

reaction through the $CH_3$ part of the ethanol or acetaldehyde (i.e to give linear products).

Reactions were thus undertaken with ethanol and butanol (as well as propanol) to explore this issue. The study could provide insight into the possible control of the reaction direction (branched/linear products) and hence provide methods to control this ratio.

## 6.2 Experimental

### 6.2.1 Catalyst Preparation

Magnesium oxide catalysts were prepared from MgO (A.R) (Hopkin and Williams LTD). The magnesium oxide was suspended in warm water with stirring and then solidified again by the evaporation of the water. It was then dried at 120 $^oC$ for 16 hours and finally calcined in air at 500 $^oC$ for 6 h. This catalyst was found to have a BET surface area of 60 $m^2/g$. CaO and BaO were prepared from the thermal decomposition of cesium hydroxide and barium hydroxide respectively at elevated temperature (500 $^oC$) for 6 h.

Silica (Aerosil 200) with BET surface area of 68 $m^2/g$ and the MgO synthesized above were used as supports for alkali, alkaline earth and transition metal oxides. $\gamma$-Alumina (BET surface area 157 $m^2/g$ and pore volume of 0.23 $cm^3/g$) was also used as a support.

The metal oxide supported catalysts were prepared by the impregnation of the support with an appropriate amount of aqueous metal hydroxide/nitrate solutions to incipient wetness. The catalysts were dried at 120 $^oC$ for 16 hours and then calcined in air at 500 $^oC$.

### 6.2.2 Apparatus and procedure

The catalytic experiments were carried out in a vertical fixed bed glass reactor (10 mm i.d). All reactions were carried out using 0.5 g of catalyst. The catalysts were used in the form of granules (350-850 μm) prepared by pelletizing the catalyst powder and crushing to the desired size. The reactor was placed inside a temperature controlled heating jacket with a thermocouple placed at the centre of the catalyst bed.

The catalyst was activated in flowing oxygen at 500 $^oC$ for 1 h prior to flushing with nitrogen gas (40 ml/min). A mixture of ethanol and butanol was fed from a 10 ml syringe using a syringe pump (Sage instruments, model 341B) through a heated carrier gas (nitrogen) line prior to the

reactor. The partial pressures of ethanol and butanol in the feed were kept at 12.18 kPa and 6.10 kPa respectively.

Reactions were conducted under nitrogen flow (40 ml/min). The products were collected in a water-cooled receiver after 1h and analyzed in a gas chromatograph (ZB wax, 60 m x 0.32 mm capillary column; FI Detector). Product identification was achieved by GC-MS (Finnigan TSQ-7000) and $^{13}$C-NMR spectroscopy (Brucker AC 400). The temperature programmed desorption (TPD) apparatus consists of a U-shaped quartz reactor housed in a temperature controlled heating jacket. The signal is measured by a low temperature dual filament TCD and recorded by a PC equipped with an I/O card. The conversion of the reactants and selectivity of the catalyst were defined by the equations below.

$$\text{Conversion (butanol)} = \frac{\text{(Amount of reactants in – Amount of reactants out)}}{\text{Amount of reactants in}}$$

Where “in and out” denote the amount of reactants introduced during the reaction and the amount observed after the reaction respectively.

The selectivity of the catalyst towards product “x” is denoted by the following equation:

$$\text{Selectivity (x)} = \frac{\text{Amount of product (x)}}{\text{Total amount of all products in the product stream}}$$

## 6.3 Results and Discussion

A mixture of butanol and ethanol (1:2 mole ratio) was passed over a range of catalysts (Table 6.1). A butanol/ethanol mole ratio of 0.5 was used because it gave good conversion and selectivity towards the desired products (see Fig. 6.2). Numerous products were obtained during the reaction of which the most conspicuous were alcohols, aldehydes and branched (2-ethylbutanol) alcohols (Table 6.1).

**Table 6.1.** The effect of catalyst on the liquid product distribution using a 1:2 butanol:ethanol mole ratio.

| Catalysts | Butanol Conversion (%) | % SELECTIVITY | | | | | |
|---|---|---|---|---|---|---|---|
| | | Acetal | Butyral | 2-Ethyl-butanol | 1-Hexanol | 2-Ethyl-hexanol | Others[a] |
| MgO | 28.9 | 1.8 | 10.5 | 23.7 | 20.6 | 10.6 | 32.8 |
| BaO | 4.0 | 20.9 | 73.8 | 0.0 | 0.0 | 0.0 | 5.3 |
| CaO | 2.7 | 2.8 | 23.7 | 0.0 | 0.0 | 0.0 | 73.5 |
| 1%Cu/MgO | 24.1 | 3.1 | 12.9 | 17.5 | 14.0 | 4.3 | 48.2 |
| 1%Cu/5%K/MgO | 9.2 | 6.5 | 42.6 | 16.9 | 10.5 | 1.4 | 22.1 |
| 1%$H_2SO_4$/MgO | 16.9 | 1.1 | 13.7 | 14.6 | 14.9 | 4.5 | 51.2 |
| 5%K/MgO | 9.3 | 18.4 | 48.6 | 4.8 | 8.9 | 1.9 | 17.4 |
| 5%Cu/MgO | 10.2 | 6.4 | 30.8 | 12.5 | 20.7 | 3.5 | 26.1 |
| 10%Ba/MgO | 5.8 | 7.5 | 32.9 | 24.9 | 28.6 | 3.7 | 2.4 |
| 10%Ca/MgO | 6.2 | 1.9 | 20.8 | 14.2 | 41.8 | 0.0 | 21.3 |
| 10%Cu/MgO | 7.8 | 0.4 | 21.8 | 9.9 | 26.7 | 3.9 | 36.8 |

[a]Others include, ethers of the reactants, aldehydes of the products, and some heavy products.

These products can be formed in the following reactions:

$$2(CH_3CH_2OH) \xrightarrow{\text{catalyst}} CH_3CH_2CH_2CH_2OH + \text{ethers} + \text{aldehydes} \quad (1)$$

$$CH_3CH_2OH + CH_3CH_2CH_2CH_2OH \xrightarrow{\text{catalyst}} C6H13OH + \text{aldehydes} + \text{ethers} \quad (2)$$

$$2(CH_3CH_2CH_2CH_2OH) \xrightarrow{\text{catalyst}} CH_3CH_2CH_2CH_2CH(CH_2CH_3)CH_2OH + \text{aldehydes} + \text{ethers} \quad (3)$$

Amongst the metal oxides tested, MgO gave the highest activity and a good selectivity towards a range of desired products. However, it did not show any good selectivity towards one specific product formed in the reaction of the two major alcohols. The formation of both linear (1-hexanol) and branched (2-methylbutanol) alcohols indicated the ability of ethanol to be activated at both ends (-$CH_3$ and –$CH_2$-). 2-Ethylhexanol was also formed over MgO. The formation of 2-ethylhexanol was due to the self condensation of butanol via a mechanism described in our earlier study of propanol [15]. The substantial amount of 2-ethylhexanol observed over MgO, was exaggerated by the presence of surplus butanol formed in the ethanol dimerisation reaction [7,14]. This resulted in three competing

reactions on the surface of the catalyst and the subsequent low observed conversion.

In an attempt to improve the selectivity of the catalyst, various metal ions were introduced onto the MgO surface (Table 6.1). The impregnation of MgO with $Cu^{2+}$ ions did not improve the selectivity towards alcohols. It is interesting to note that although the activity of the catalyst (Cu/MgO) decreased as the Cu loading increased, the selectivity of 1-hexanol increased with Cu loading while that of 2-ethylbutanol decreased. The dehydrogenation effect of Cu was expected to favour the formation of alcohols. However, the presence of Cu could also facilitate the amalgamation of hydrogen atoms to form hydrogen gas which could easily be lost from the surface [6].

The introduction of a small amount (1% w/w) of sulphuric acid onto the MgO surface increased the surface area of the catalyst from 60 to 195 $m^2/g$ (see experimental). Although the surface area of the catalyst was enhanced, the basicity of the MgO was also compromised. This was evident as indicated by the low activity and selectivity values obtained during the reaction.

Alkali and alkaline earth metals were loaded onto MgO in an attempt to improve the activity and selectivity of the MgO by increasing the basicity of the catalyst. The butanol conversion of these mixed catalysts decreased. However, the selectivity towards alcohols increased (except for 5%K/MgO) with 10%Ca/MgO giving the highest selectivity towards 1-hexanol.

Further reactions were conducted over MgO since it showed good activity and reasonable selectivity towards three alcohols discussed in this reaction.

### 6.3.2 Investigation of reaction parameters

The MgO catalyst was subjected to different reaction temperatures in order to examine the effect that the temperature has on the product distribution (Fig. 6.1). A fresh catalyst was used for set of data points collected during the experiment. The overall conversion of butanol increased with temperature. There is very little change in the selectivity towards 2-ethylhexanol as the reaction temperature increases. Although there is an initial increase in the selectivity towards both 2-ethylbutanol and 1-hexanol as the temperature increases, it tends to decline as the temperature reaches 500 $^{o}$C. A temperature of 450 $^{o}$C was chosen for further study of this reaction.

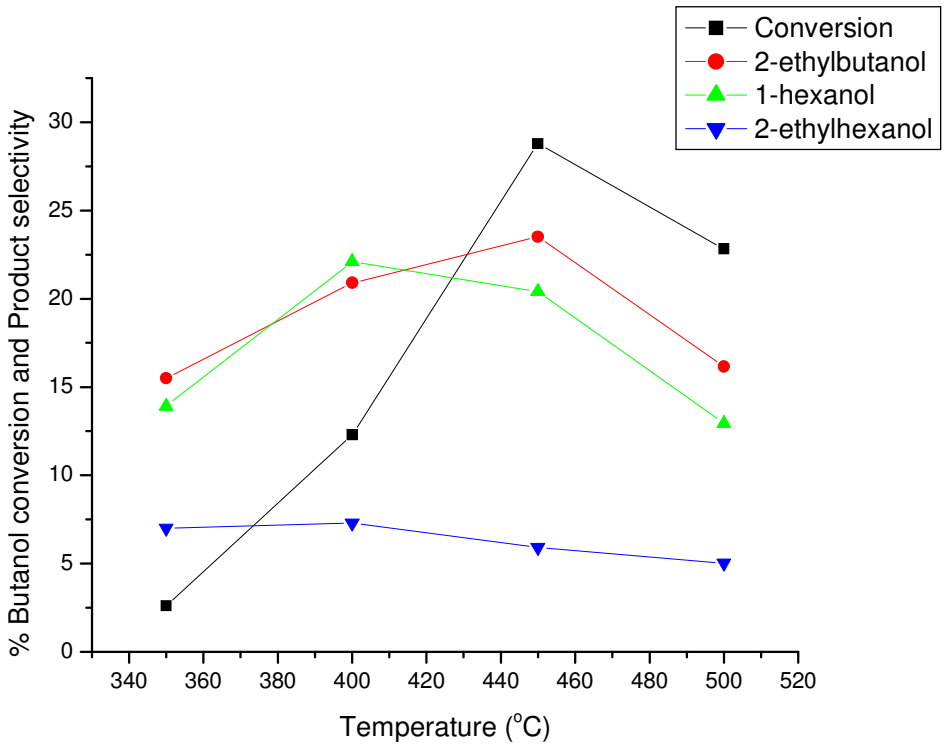


**Figure 6.1** The effect of temperature on catalyst activity and product distribution.

The number of moles of ethanol in the reaction mixture was varied relative to that of butanol (Fig. 6.2). A fresh catalyst was used for each set of experiment shown (Fig. 6.2) below. Although the overall conversion of reactants remained constant when the butanol to ethanol mole ratio was changed from 1:1 to 1:2, there was a significant decline in conversion when the mole ratio was changed from 1:2 to 1:4. A steady decline in

conversion was further observed with subsequent increases in the amount of ethanol. This is due to the dimerisation reaction of ethanol to form butanol [14].

There was a slight increase in the selectivity towards 2-ethylbutanol and 1-hexanol. Although the selectivity towards 2-ethylhexanol is higher at lower moles of ethanol, it tends to decrease as the ethanol moles increase. This suggests that there is an excess amount of butanol on the surface of the catalyst for this side reaction to occur. As the amount of ethanol increases more butanol is required for the formation of 2-ethylbutanol and 1-hexanol, and this yields a low selectivity towards 2-ethylhexanol.

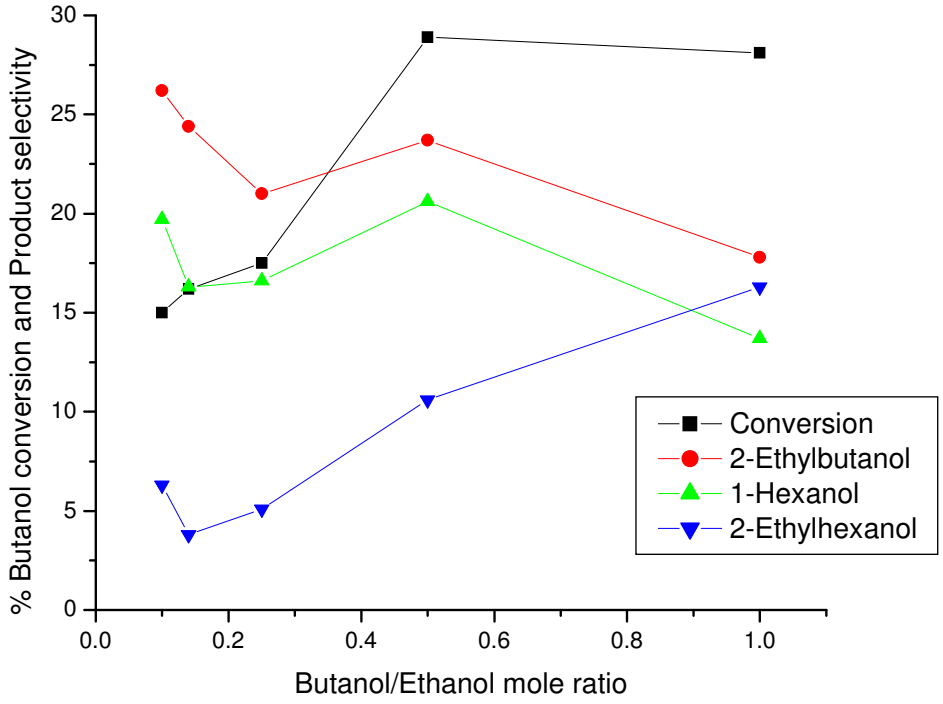


**Figure 6.2** The effect of butanol to ethanol mole ratio on product distribution.

Figure 6.3 shows the variation of product selectivity with space velocity. A fresh catalyst was used for each set of data points collected in this experiment. The selectivity towards acetaldehyde and butyraldehyde increases as the space velocity increases. This confirms the two are primary products in aldol coupling of ethanol and butanol respectively. The data also indicated a moderate decline in selectivity towards 2-ethylbutanol, hexanol and 2-ethylhexanol as the space velocity increased.

This is consistence with the mechanism of aldol coupling reactions of alcohols (Scheme 6.3). However, the change in the selectivity towards 1-hexanol as the space velocity increased was very small.

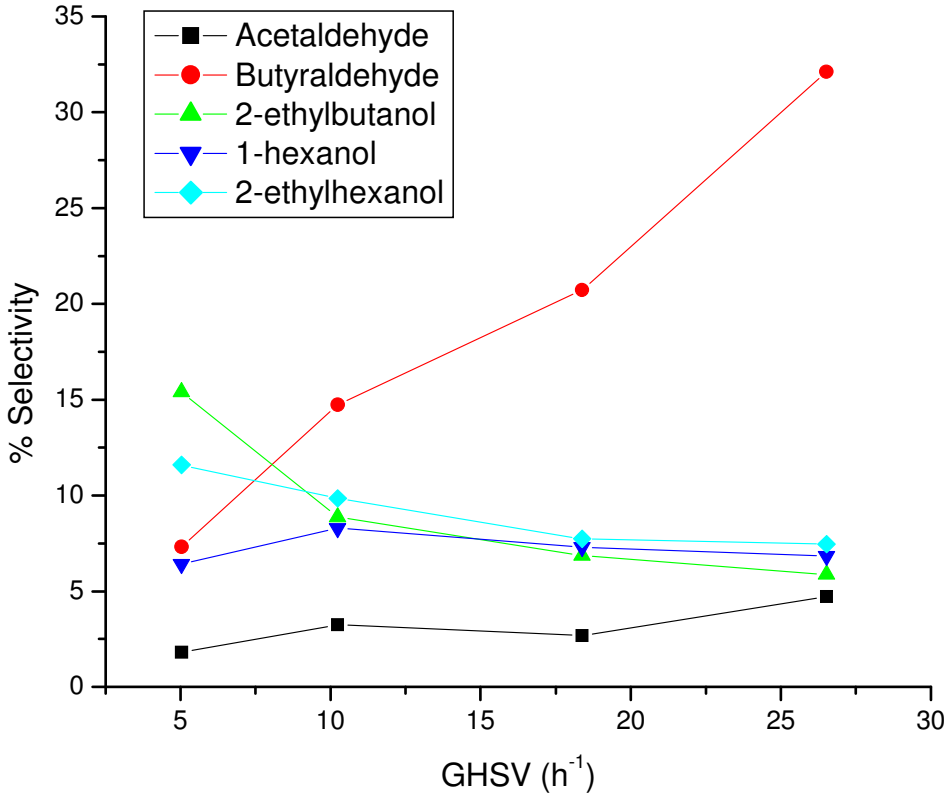


**Figure 6.3** The influence of space velocity (GHSV) on product distribution.

The effect of time on stream on the catalyst activity and selectivity is shown in Fig. 6.4. The catalyst activity initially increased with time for the first two hours and this gradually decreased with time. This is attributed to the

formation of higher molecular species and carbon deposits (see Fig 6.5 below). The formation of butanol from ethanol also contributes to the decline in conversion.

The selectivity towards 2-ethylbutanol slightly decreased as the time on stream was increased. Although the selectivity towards 1-hexanol initially increased with time on stream, there was a slight decrease in selectivity towards the end of the reaction.

It is interesting to note that as the catalyst deactivates with time, and the formation of 1-hexanol becomes more favourable than that of 2-ethylbutanol. Although the selectivity towards 2-ethylhexanol initially increased with time, there was a slight decrease as the reaction time increased. This decline in selectivity could also be attributed to the shift in selectivity towards 1-hexanol and to a certain extent, catalyst deactivation.

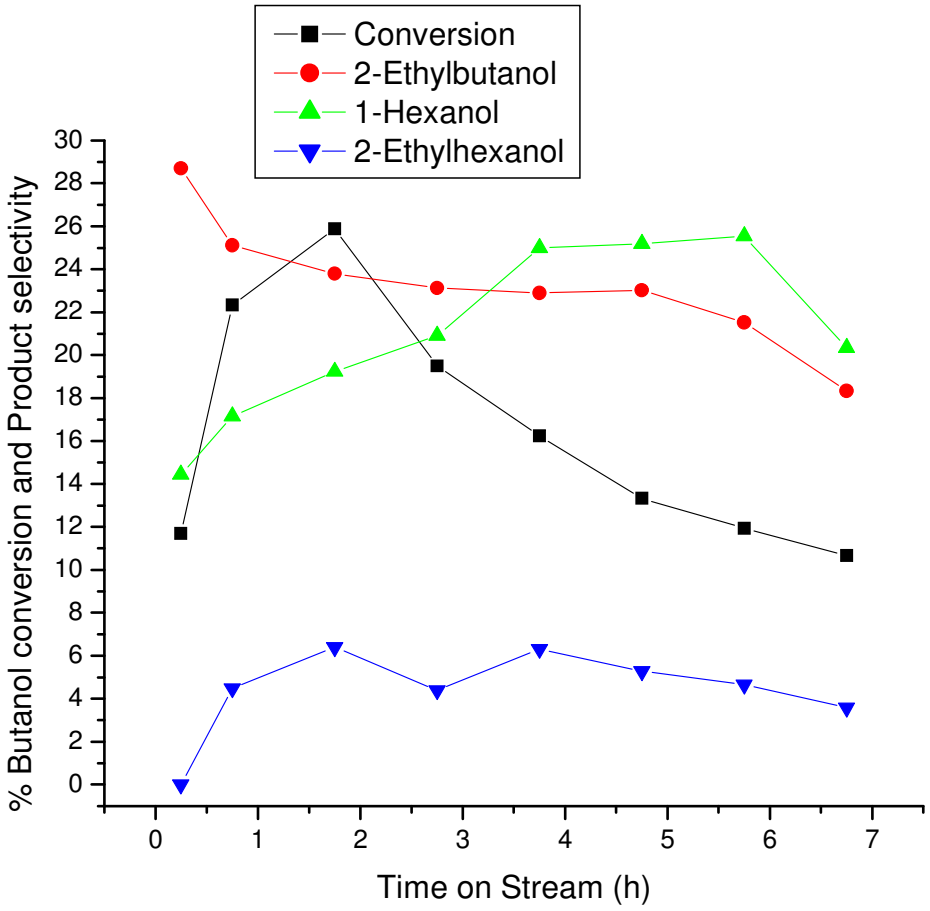


**Figure 6.4** The effect of time on stream on catalyst activity and selectivity.

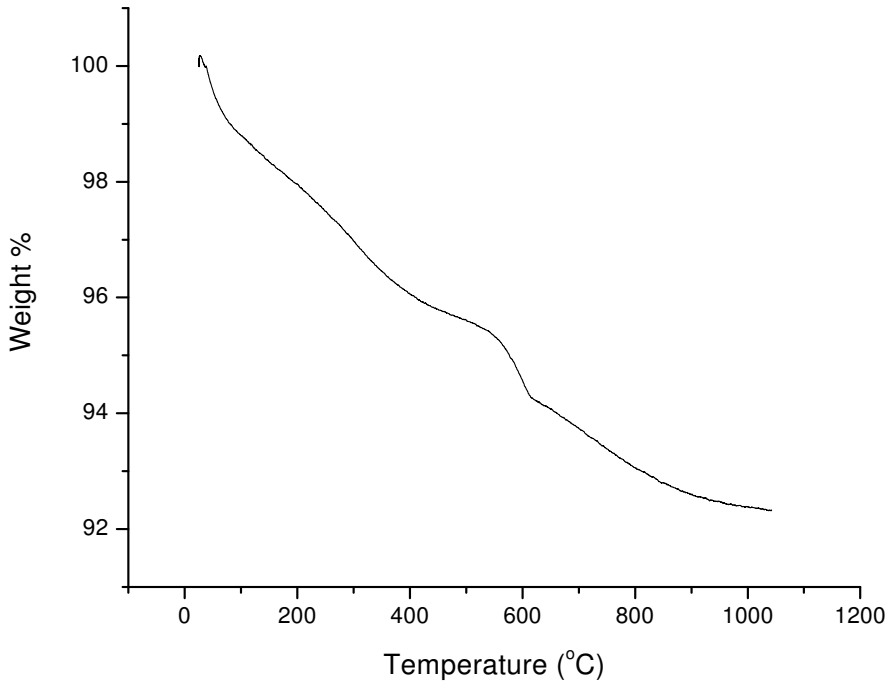


**Figure 6.5** Thermogram of MgO catalyst used in the reaction of ethanol and butanol.

### 6.4 Reaction Mechanism

The above data and previous literature reports [7,14,16,17] allows us to suggest a possible mechanism and reaction network for the formation of 2-ethylbutanol and 1-hexanol (Schemes 6.1 and Scheme 6.2) from butanol and ethanol. These reaction schemes show the detailed formation of 2-

ethylbutanol. In these schemes, ethanol and butanol are converted on an MgO catalyst mainly through dehydrogenation (to respective aldehydes), aldol coupling (of the aldehydes), dehydration (of the resultant coupling product), and hydrogenation (of the unsaturated aldehyde to form 2-ethylbutanol and 2-ethylbutyraldehyde) reactions.

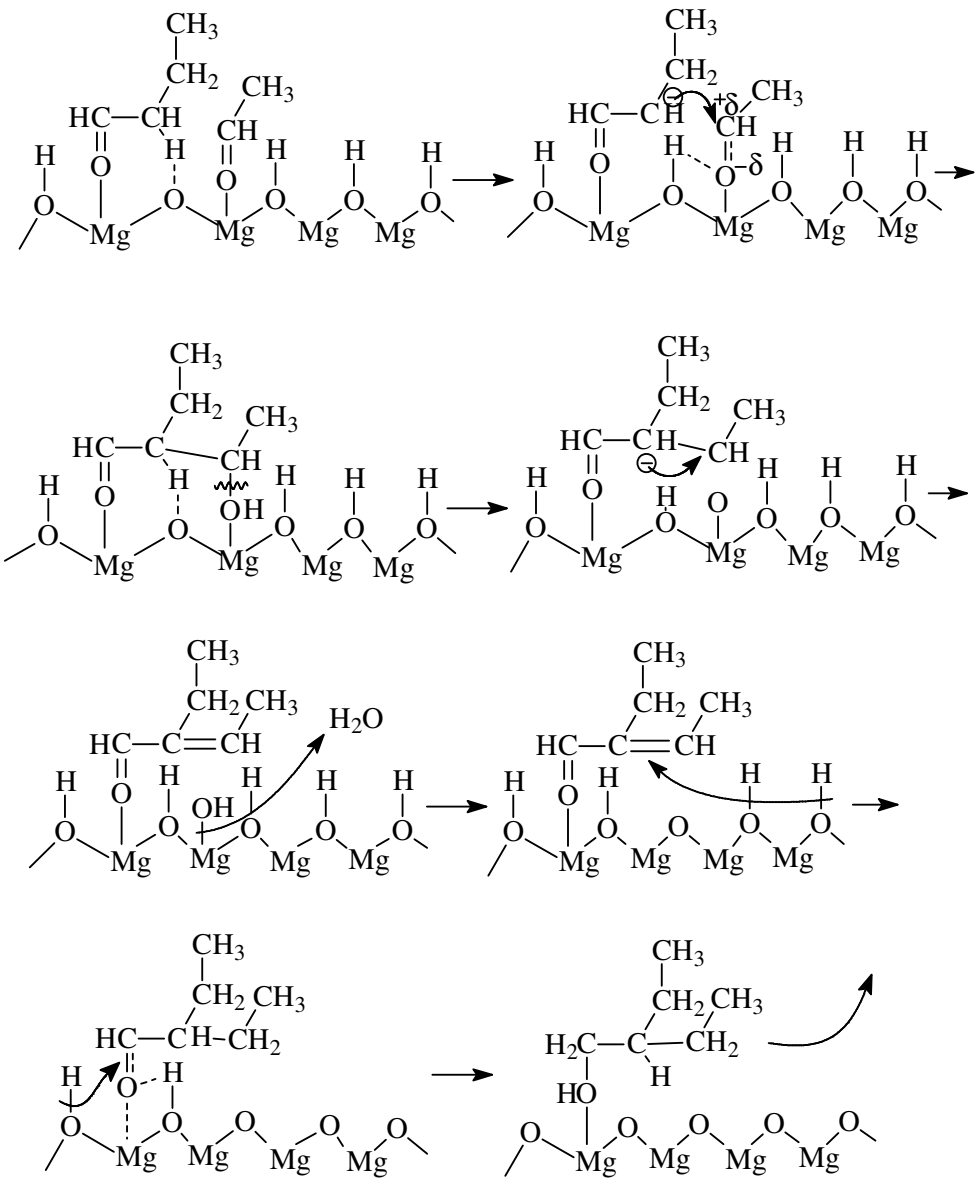

**Scheme 6.1** Schematic representation of the 2-ethylbutanol formation mechanism from ethanol and butanol reactions.

The formation of 1-hexanol could also be illustrated in the same way as shown in scheme 6.1. During the reaction, ethanol and butanol could exchange roles which could see ethanol generating the carbanion on the α-carbon ($CH_3$) and carrying out an attack on butanol (Fig. 6.2). This would lead to the formation of 1-hexanol.

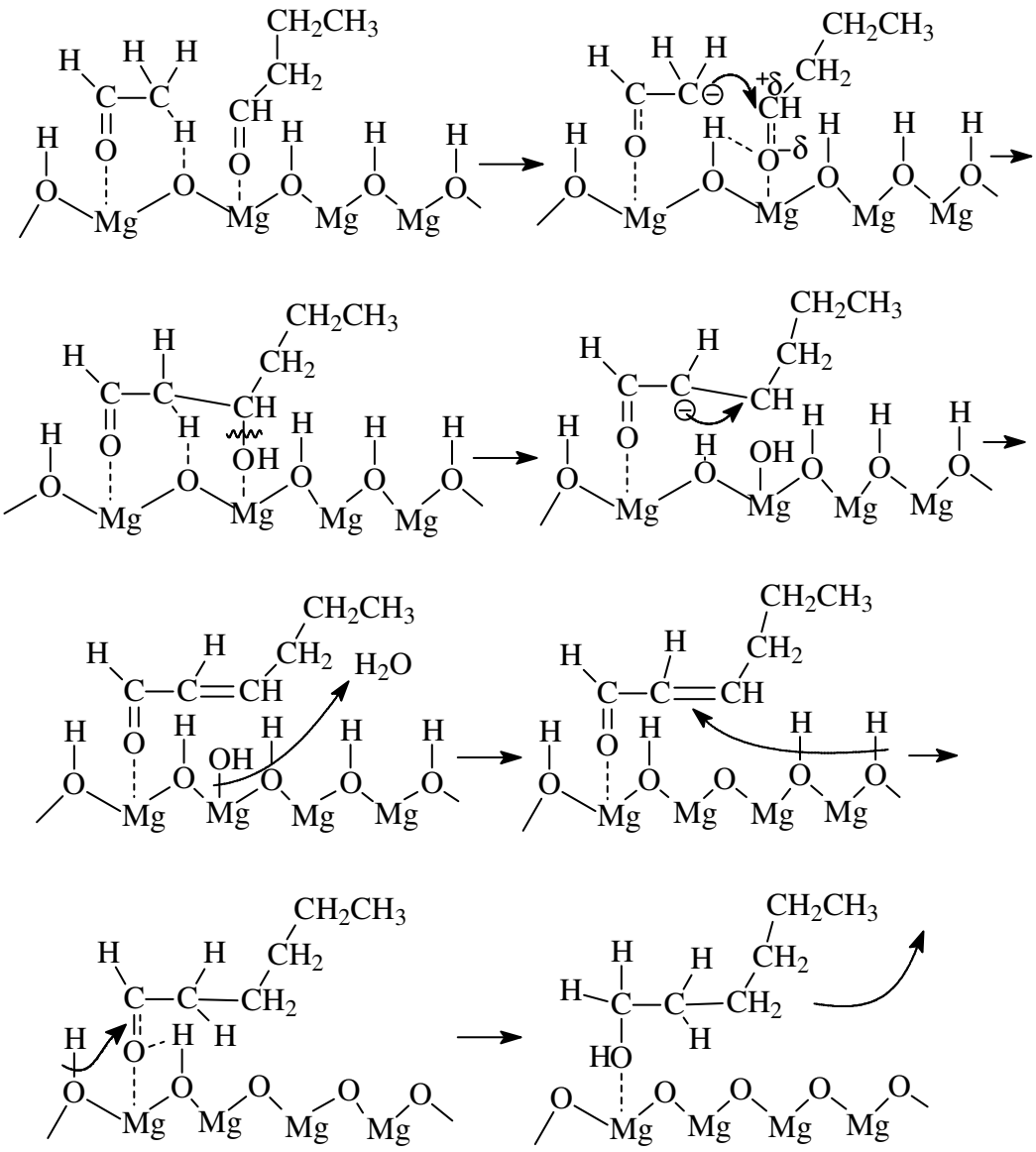

**Scheme 6.2** Schematic representation of the 1-hexanol formation mechanism from ethanol and butanol reactions.

The reaction network for the ethanol and butanol reactions is summarized in scheme 6.3 below. This scheme shows most of the reactions observed on the MgO catalyst. In this scheme, ethanol and butanol are converted (on MgO samples) predominately to higher alcohols. Acetaldehyde and butyraldehyde form via ethanol and butanol dehydrogenation respectively (step XII and V). The aldol intermediates formed from acetaldehyde and butyraldehyde condensation (step IX and XIII) dehydrate to form α,β-unsaturated aldehydes, which rapidly hydrogenates to 2-ethylbutyraldehyde and *n*-hexanal (step X and XIV). The $H_2$ required is formed in the ethanol and butanol dehydrogenation steps. These aldehydes can further be hydrogenated to their respective alcohols (2-ethylbutanol and 1-hexanol).

Acetaldehyde formed from ethanol dehydrogenation can also undergo aldol condensation (step XVI) to form aldol intermediates. These aldol intermediates undergo dehydration and hydrogenation to form *n*-butyraldehyde (step XVII), which can be hydrogenated to butanol (step XVIII). *n*-Butanol can also be formed via direct condensation of ethanol [14,17] (step II). Diethylether and dibutylether are formed in bimolecular dehydration steps (step I and IV). Ethylbutylether is formed in dehydration step (step III). Butyraldehyde can also undergo condensation (step VI) to

form aldol intermediates, which can dehydrate and rapidly hydrogenate to 2-thylhexanal (step VII). 2-Ethylhexanol can be formed by hydrogenation of 2-ethylhexanal.

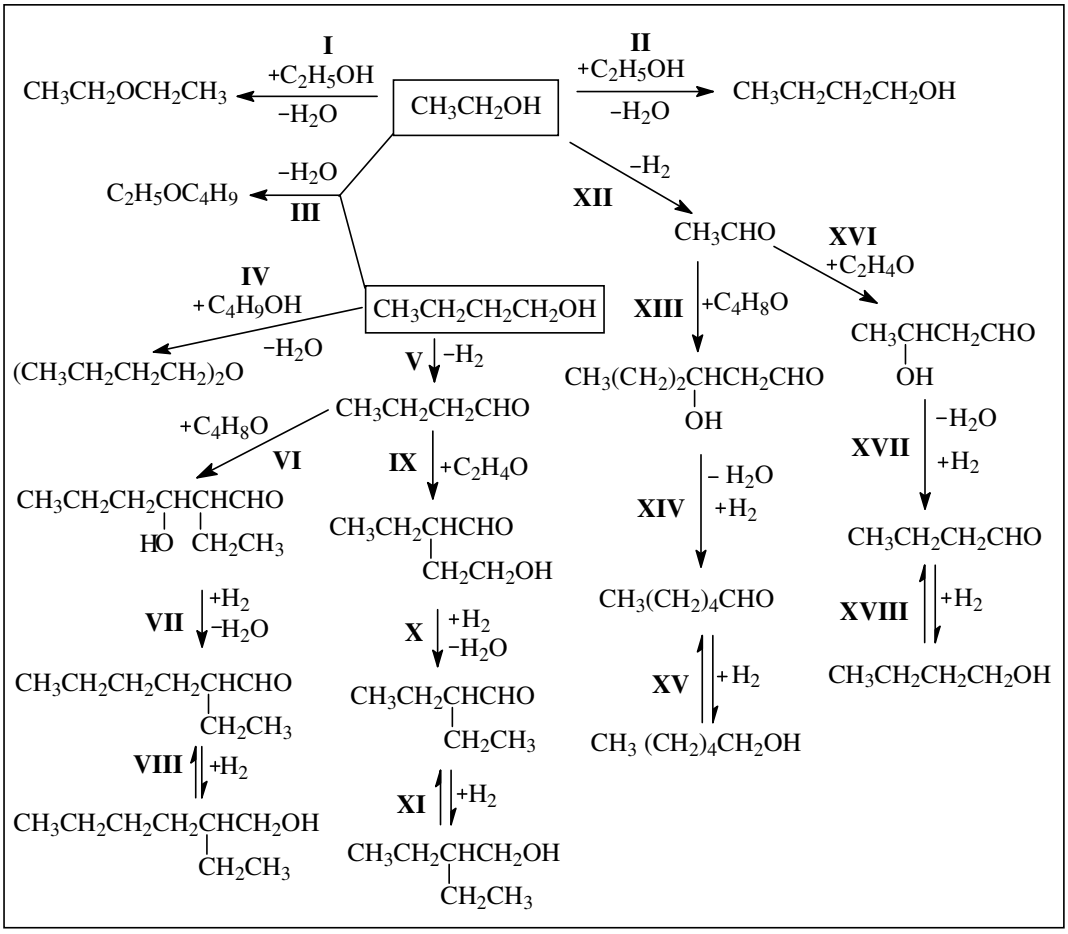


**Scheme 6.3** Summary of reactions for ethanol / butanol conversion over MgO.

### 6.4.1 The Effect of Reaction Parameters on Linear/Branched Alcohols Ratio

As discussed above, both a linear and a branched product are expected to be formed in the reaction. If reaction only occurs via an aldol condensation pathway then the ratio of products will be determined by whether the C2 aldehyde attacks the C4 aldehyde (linear product) or whether the C4 aldehyde attacks the C2 aldehyde (branched product; Scheme 6.1). A further complication arises from the possibility of attack of C4 aldehyde by the CH3 group of the ethanol. This would lead to linear product.

At present there is no method to evaluate the relative reaction rates for the above three processes.

A consideration of the data in Table 6.1 indicates that the linear/branched ratio varies with (i) amount of Cu and (ii) addition of base to MgO. It is noted that the % conversion was not constant but the trends are still apparent. Figure 6.1 clearly demonstrates this finding. Here it is seen that the linear/branched ratio is nearly constant with change in activity.

(i) As the amount of Cu on MgO (1-10 %) increases the linear dimer is favoured. Since there was a significant drop in activity as the Cu loading increased, it is therefore reasonable to suggest that some of the active sites on MgO could have been blocked. This implies that the coverage of some sites by Cu favours the linear dimer.

(ii) The addition of basic ions ($K^+$, $Ba^{2+}$ and $Ca^{2+}$; 10%) to MgO appears to have the same effect as that of Cu. This further demonstrates that the effect of these metals on MgO could be mostly due to a physical process. This implies that the route (aldol) by which the branched dimer is formed could have been blocked. Thus formation of the linear dimer is enhanced but the route to this product (aldol reaction and/or $CH_3$ activation) is less affected by addition of a base or Cu.

The influence of reaction parameters on the MgO catalysed reaction was monitored and is discussed below.

The ratio of linear to branched products as a function of temperature is shown in Figure 6.6. The effect of temperature on the linear/branched ratio is modest. Figure 6.1 also demonstrates this finding.

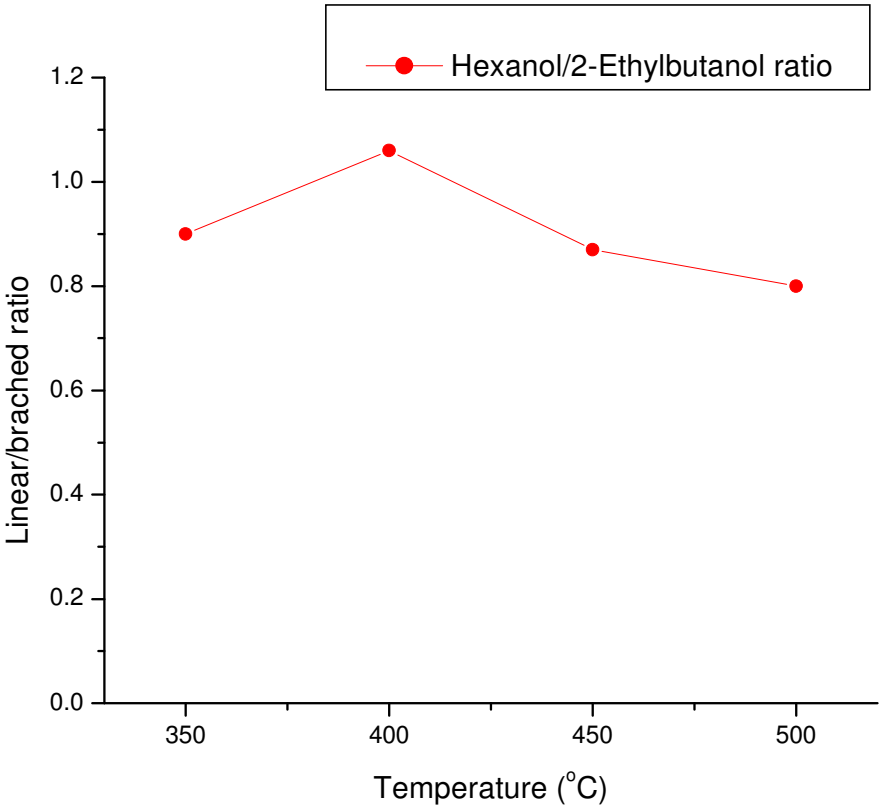


**Figure 6.6** The effect of temperature on linear/branched alcohols ratio.

Figure 6.7 shows the change in linear/branched ratios as the butanol to ethanol mole ratio is varied. Although the amount of a linear alcohol is higher at butanol/ethanol mole ratio of 0.5, respectively, it tends to decrease as the butanol/ethanol mole ratio decreased. The overall change in the products ratio as the butanol/ethanol mole ratio increases is rather

small. The amount of branched alcohol remained higher than that of linear alcohol throughout the ethanol/butanol mole ratio investigated in this reaction.

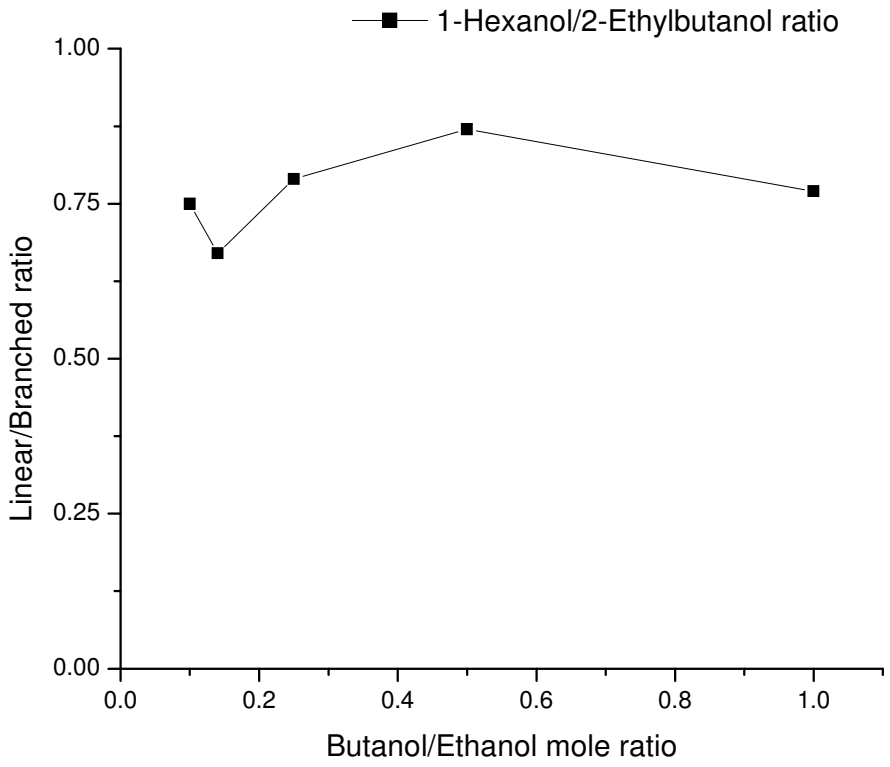


**Figure 6.7** The effect of butanol/ethanol mole ratio on linear/branched alcohols ratio

The effect of contact time on linear/branched alcohols ratio is shown in Figure 6.8. There is a decrease in linear/branched ratio as the contact time increased. At lower contact time, the formation of a linear alcohol is more favoured than the formation of a branched alcohol. At higher contact time, the formation of a branched alcohol is preferred. It also indicates a slow build up of the branched dimer with increasing contact time.

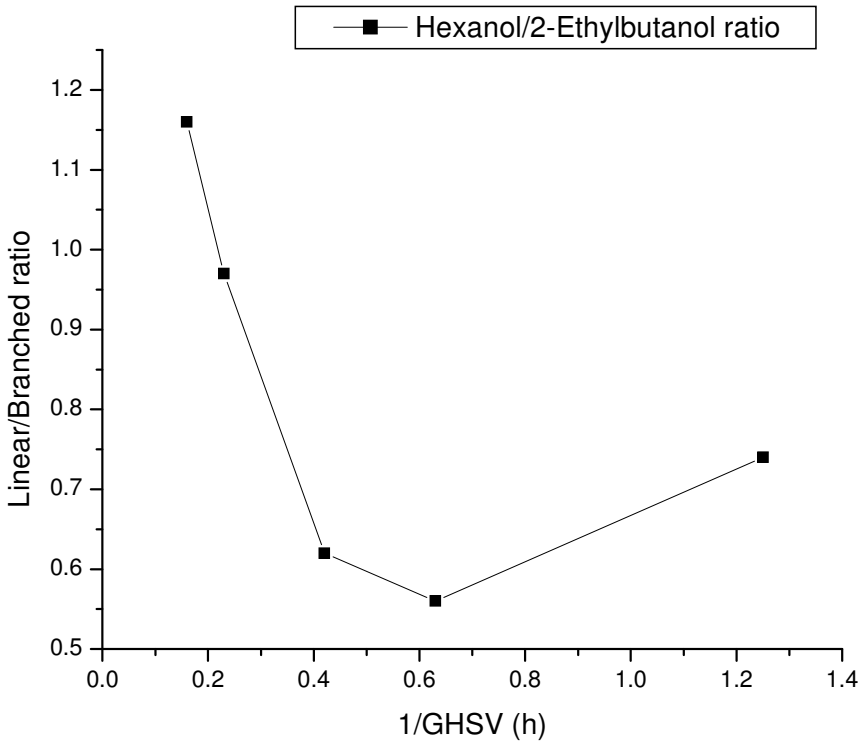


**Figure 6.8** The effect of contact time on linear/branched alcohols ratio.

The change in linear to branched alcohols ratio with time-on-stream is shown in Figure 6.9. Although there is a gradual increase in the formation of a linear alcohol as the reaction time elapsed, the formation of a branched alcohol is preferred in the initial stages (0.25-3 h) of the reaction. As the activity of the catalyst decreases with increasing time-on-stream (Fig 6.4), the formation of the branched dimer also decreases. However, the amount of the linear dimer remained near constant as the activity of the catalyst decreases (Fig 6.4). This indicates that the formation of a branched dimer is more favourable when the MgO catalyst is still fresh.

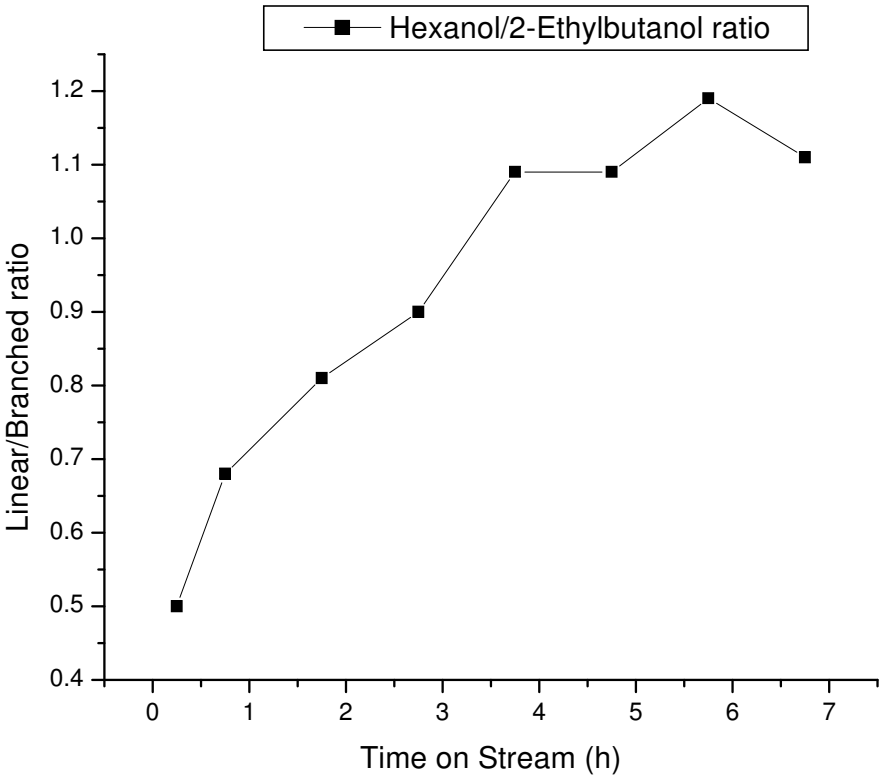


**Figure 6.9** The effect of time-on-stream on linear/branched alcohol ratio.

In attempting to deconvolute the above data it is recognized that assumptions will be needed to be made to allow for an understanding of the data. For example the reaction is a complex one and it is not clear as to the rate determining step(s) in the reaction. However the relative

independence of isomer rate with varying reactant ratios suggests that preferential coverage by either of the alcohols (or aldehydes) is not the key step in the reaction. This to some extent is also indicated by the invariance of the isomer ratio with reaction temperature.

In summary, the preliminary study suggests that it is possible to maximize one isomer (branched, linear) over the other.

i) Branched products are favoured by what appears to be the most active sites. Thus, time on line studies reveal that the branched products are favoured early in the reaction and as the reaction progresses these deactivate first. The data in Fig 6.1 indicate that even though more reactants are formed with time the proportion of branched isomer actually decreases. Also, added ions (Cu, Ca) appear to cover the same sites.

ii) Branched products are favoured by longer reactant/catalyst contact times. Since the reactant ratio does not influence the linear/branched isomer ratio, the data suggest that the issue relates to the stability of the different intermediates. Since the branched isomer is favoured (at high contact times) this suggests that the attack of the C2 species generates more product than attack of the C4 species.

The reason for this is not clear. However, a possibility may relate to the earlier proposal – that attack at C2 can occur at either the $CH_3$ (leads to

linear product) or the -$CH_2$- part of the molecule. In this instance little $CH_3CH_2OH$ is found on the surface (long contact times convert more alcohol to aldehyde) and consequently the attack at the -CH- (actually CHO) unit is favoured. However, little more can be said at this stage.

## 6.5 Conclusions

MgO was investigated as a catalyst for the condensation of ethanol and butanol. Good activity and selectivity towards both 2-ethylbutanol and 1-hexanol was achieved on this catalyst. Attempts to increase the selectivity of the catalyst towards 1-hexanol were largely unsuccessful. Although the impregnation of MgO with calcium ions gave higher selectivity towards 1-hexanol, the overall conversion of reactants was very low. This however could provide the basis for future follow-up studies.

The formation of 2-ethylbutanol occurs via the classical aldol condensation reaction. However, the formation of 1-hexanol occurs via the activation of a methyl group of ethanol. This activation of the methyl group on ethanol can occur via both the aldol condensation mechanism outlined in Scheme 6.2 and an alternative route involving dehydration (see below).

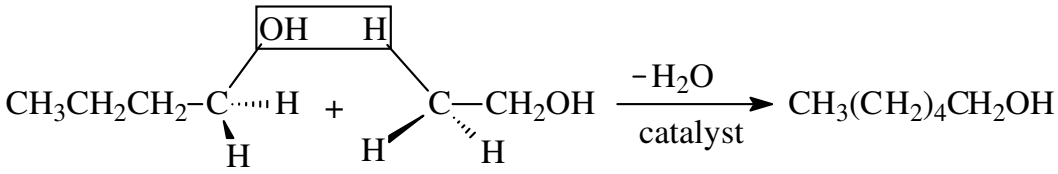


Finally it is to be noted that dimerisation of ethanol does produce one of the reactants, butanol, and this product will modify the actual concentrations of reactants and further complicate the unravelling of the mechanism. The study in the next chapter seeks to remove this variable from the study.

## 6.6 References

[1] R.E. Kirk and D.F. Othmer, Kirk- Othmer Encyclopedia of Chemical Technology, 4th Edition, vol.1 (1991) 865.

[2] C.J. Shieh, S.W. Chang, J.R. Too, Dept. of Food Engineering, Dayeh Univ. Changhua, Taiwan.

[3] D.F. Cadogan, C.J. Howick, in: J.I. Kroschwitz, M. Howe-Grant (Eds.), Kirk- Othmer Encyclopedia of Chemical Technology, vol.19, 4th Edn. Wiley/Interscience, New York, 1991, p. 258.

[4] M. Ichikawa, J. Catal. 56 (1979) 127.

[5] T. Mizorogi and M. Nakayama, Bull Chem. Soc. Japan, 39 (1964) 236.

[6] A.M. Hilmen, M. Xu, M.J.L. Gines and E. Iglesia, Appl. Catal. A: General, 169 (1998) 355.

[7] J.I. Di Cosimo, C.R. Apesteguia, M.J.L. Gines and E. Iglesia, J. Catal., 190 (2000) 261.

[8] W. Ueda, T. Kuwabara, T. Ohshida, Y. Morikawa, J. Chem. Soc., Chem. Commun., (1990) 1558.

[9] M.W. Farrar (Monsanto Chemical Co.), US Pat. 2 971 033, (1961).

[10] R.T. Clark (Celanese Corporation), US Pat. 3 972 952, (1976).

[11] C. Carlini, A. Macinai, A.M.R. Galletti and G. Sbrana, J. Mol. Catal. A: Chem. 212 (2004) 65.

[12] C. Carlini, M Di Girolamo, A. Macinai, M. Marchionna, M. Noviello, A.M.R. Galletti and G. Sbrana, J. Mol. Catal. A: Chem. 204-205 (2003) 721.

[13] C. Carlini, M. Di Girolamo, M. Marchionna, M. Noviello, A.M.R. Galletti and G. Sbrana, J. Mol. Catal. A: Chem. 184 (2002) 273.

[14] A. S. Ndou, N. Plint, N. J. Coville, Appl. Catal. A: General, 251 (2003) 337.

[15] A. S. Ndou, N. J. Coville, Appl. Catal. A: General. 275 (2004) 103.

[16] C. Yang and Z. Meng, J. Catal. 142 (1993) 37.

[17] M. Xu, M. J. L. Gines, A. Hilmen, B. L. Stephens, and E. Iglesia, J. Catal. 171 (1997) 130.

# C H A P T E R 7

## Synthesis of 2-Methylbutanol and 1-Pentanol from Primary Alcohols over Solid Base Catalyst*

* A.S. Ndou, N.J. Coville, The use of ethanol as a building block for higher alcohol synthesis. To be submitted.

*In Chapter 6 it was shown that ethanol had the ability to react with butanol through either the -$CH_3$ or the -$CH_2$- part of the molecule to produce linear and branched products. To further explore this reaction ethanol was reacted with propanol.*

### 7.1 Introduction

The use of lower primary alcohols for the synthesis of fine chemicals and higher primary alcohols has recently received much attention in the

literature [1-6]. These literature reports, many on industrially important alcohols have been reported to form through condensation of lower primary alcohols over catalysts with basic properties. This process is known as the Guerbet reaction and entails the reaction of a primary or secondary alcohol with itself or another alcohol to produce a higher alcohol. Various types of heterogeneous catalysts have been used for this reaction and their use has been reported in patents [7,8]. Ueda et al. [9,10] have also reported in detail on a catalytic reaction carried out over a solid base metal oxide catalyst, in which methanol is condensed with other primary alcohols having a methyl or methylene group at the ß-position to form higher alcohols. Carlini and his co-workers have recently reported the synthesis of valuable alcohols (isobutanol and 2-ethyl-1-hexanol) through the Guerbet reaction using both homogeneous and heterogeneous metal catalysts with basic components [11-15].

In this chapter, the reaction of ethanol and propanol to give 1-pentanol and 2-methylbutanol over a solid base catalyst is reported.

1-Pentanol and 2-methylbutanol are commonly used as a mixture of alcohols known as Pentanol 45. Pentanol 45 is composed of 42 - 52 % 1-pentanol and about 48 - 58 % 2-methylbutanol. It is industrially produced

by hydroformylation of n-butenes and subsequent hydrogenation of the primary $C_5$ aldehydes thus obtained. This process gives Pentanol 45 that is free from secondary and tertiary alcohols. Pentanol 45 is used in a wide range of industries. Like many other alcohols, Pentanol 45 is used as solvent for oils and fats, natural and synthetic resins and waxes, and paraffin waxes. Because of its limited miscibility with water, Pentanol 45 can be used as a versatile extractant for the removal of uranium, neptunium, platinum and zinc salts. It has also been recommended for the extractive purification of lactic acid or acrolein [16]. Esters of Pentanol 45 are used in combination with aliphatic dicarboxylic acids as intermediates for the manufacture of synthetic oil additives.

In the dimerisation reaction between ethanol and butanol, the impact of the butanol produced by the ethanol could have influenced the reactant ratios of the mixed dimer. It was thus decided to investigate the reaction between propanol and ethanol. The dimerisation capability of ethanol is much greater than that of propanol, and this will need to be factored into any discussion.

## 7.2 Experimental

(Same as in Chapter 6)

## 7.3 Results and Discussion

The reaction between propanol and ethanol was conducted over a magnesium oxide catalyst. The major products collected from the reaction included amongst others 2-methylbutanol, 1-pentanol, butanol and 2-methylpentanol. The ethanol/propanol mole ratio was kept at 1 for all the experiments conducted in this chapter. The ethanol and propanol partial pressures were both kept at 9.4 kPa.

The products distribution for the ethanol and propanol reaction at 450 $^{o}$C is shown in Table 7.1 below. The catalyst showed high selectivities towards the mixed dimers pentanol and 2-methylbutanol. However, also noted are the products butanol (from the ethanol dimerisation reaction) and 2-methylpentanol (synthesized either from the self condensation of propanol).

Amongst the aforementioned products, butanol was found in the highest amount. This shows suggested that the dimerization of ethanol was more favourable than the condensation with propanol. This is brought about by the difference in reactivity between the two alcohols. Propanol has an unreactive terminal methyl group that can cause a steric hindrance and limit attack at the methylene group and therefore could lower the reactivity. On the other hand, both the terminal methyl and the methylene groups on ethanol can participate in the reaction. The selectivity towards 2-methylpentanol, a product of self-condensation of propanol was very low.

**Table 7.1** Product distribution of the reaction between propanol and ethanol over MgO catalyst.

| %Conv. | % SELECTIVITY | | | | | |
|---|---|---|---|---|---|---|
| | Acetal | Butanol | 2-methyl butanol | Pentanol | 2-methyl pentanol | Others[a] |
| 21.6 | 14.8 | 30.1 | 16.3 | 21.5 | 1.5 | 15.8 |

[a] Others include, ethers of the reactants, aldehydes of the products and heavy compounds formed by oligomerization.

The effect of temperature on reaction conversion and product selectivity is shown in Figure 7.1 below. A fresh catalyst was used for each set of data points collected in this experiment. To note:

i) As the reaction temperature increased, there was an increase in the reactant conversion. However, the selectivity towards butanol, 2-methylbutanol and pentanol decreased with an increase in temperature. At temperatures above 450 $^{o}$C, secondary reactions which lead to the formation of high molecular weight species occur (Fig. 7.2).

ii) The butanol/pentanol ratio remains fairly constant, following a similar trend with temperature. Thus attack of $CH_3CHO$ by either a C2 or C3 entity is not affected by temperature.

iii) Overall the selectivity towards butanol, 2-methylbutanol and pentanol decreased with an increase in temperature.

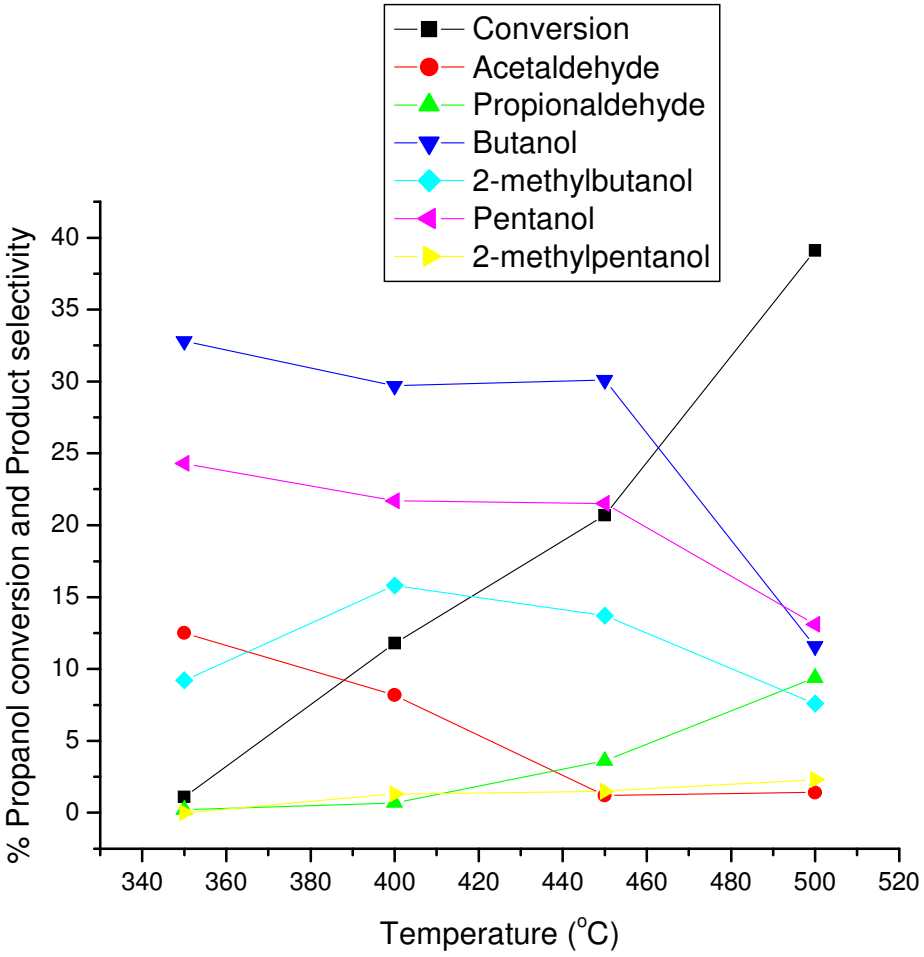


**Figure 7.1** The effect of temperature on conversion and product distribution.

The influence of space velocity on conversion and product selectivity is shown in Figure 7.2 below. A fresh catalyst was for each data points shown in this experiment.

The selectivity towards 2-methylbutanol, pentanol and 2-methylpentanol showed a modest decrease with an increase in space velocity. This indicates that the above mentioned products are being formed through secondary surface reactions since they are favoured by high contact time. However, the selectivity towards acetaldehyde and propionaldehyde increased as the space velocity increased. This indicates that acetaldehyde and propionaldehyde are primary products since they are favoured by short contact time. The selectivity towards butanol showed a slight increase as the space velocity increased. This behaviour could be explained by the findings in chapter 4, which suggest the presence of an alternative route to butanol formation.

The above information suggests that acetaldehyde and propionaldehyde are being converted into butanol, 2-methylbutanol, 2-methylpentanol and 1-pentanol at high contact time.

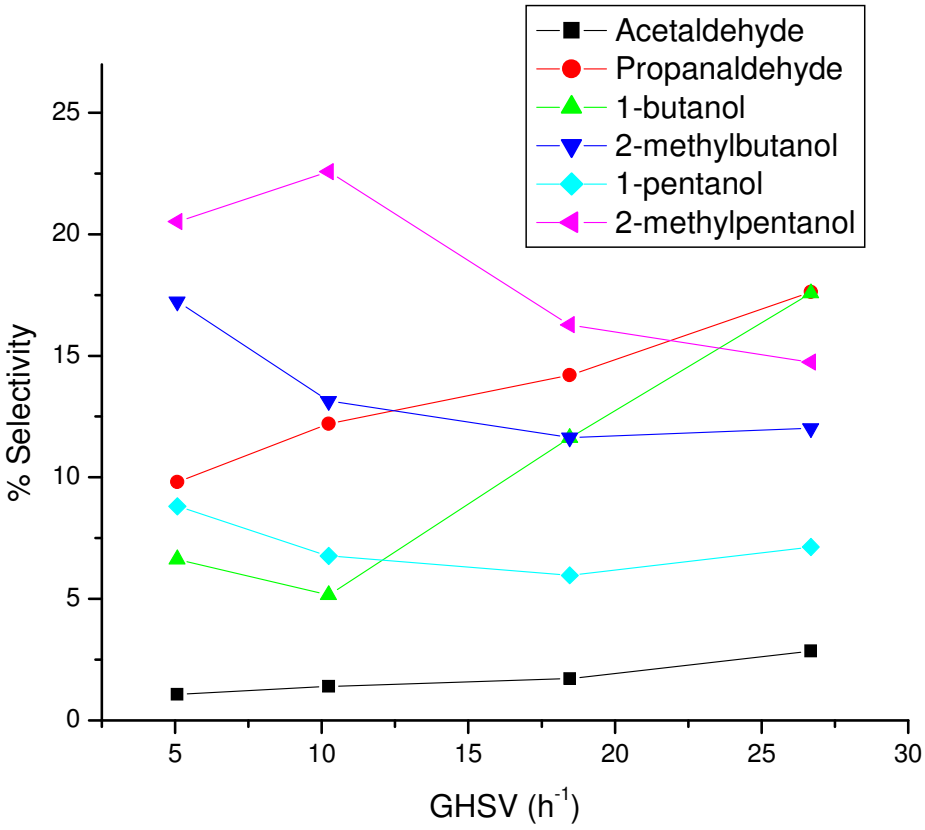


**Figure 7.2** The influence of space velocity (GHSV) on conversion and product selectivity.

The overall conversion of the reaction decreased from about 25% to 18% over 8 h with time on stream (Fig. 7.3). The catalyst also turned grey at the end of the reaction. This suggests that the catalyst deactivated with time due to the accumulation of carbon and high molecular weight species. This was also confirmed by the thermogram of MgO catalyst after the reaction

(Figure 7.4 below). There is a slight decline in weight percentage of the catalyst from 100 to 300 $^{o}$C which can be correlated to the desorption of higher molecular weight species. The remaining weight loss is due to the desorption of carbonaceous material.

There was an initial decline in the selectivity towards butanol and propionaldehyde while the selectivity towards 2-methylbutanol and pentanol remained constant.

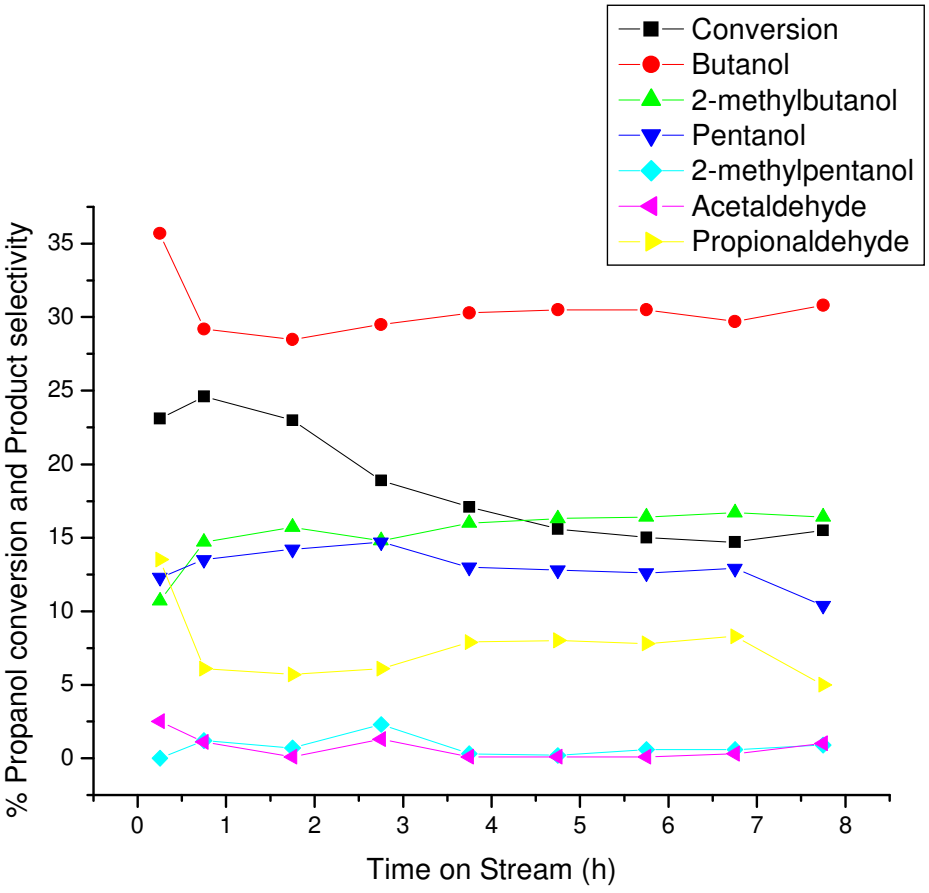


**Figure 7.3** The effect of time-on-stream on catalyst stability and product selectivity.

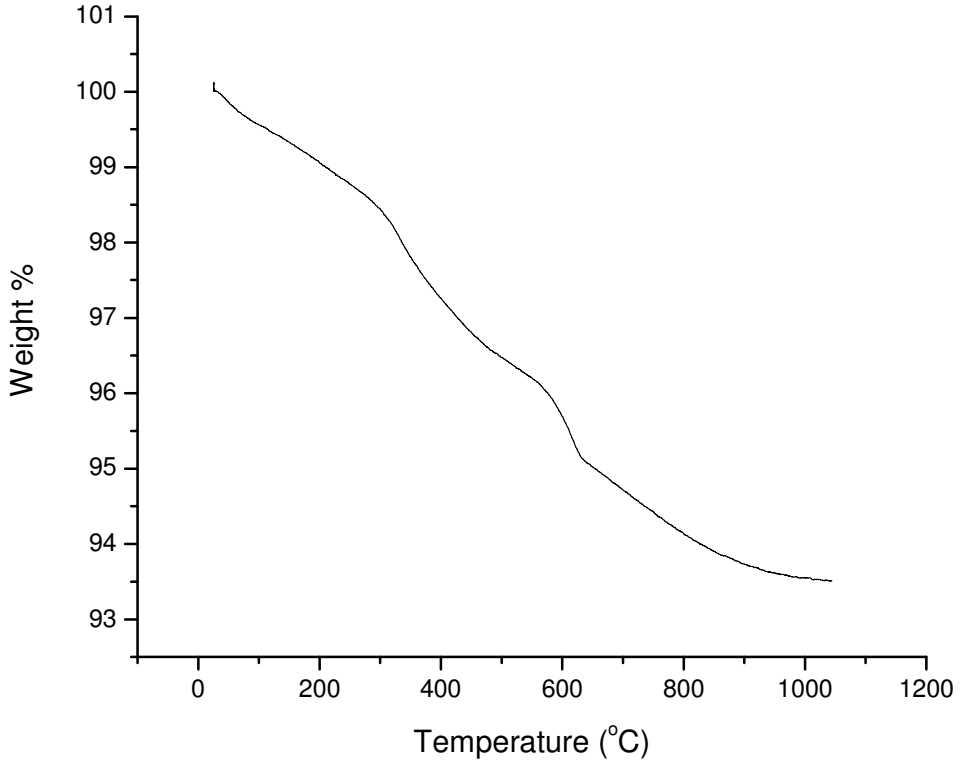


**Figure 7.4** Thermogram of MgO catalyst after the reaction.

## 7.4 Reaction Mechanism

The reaction mechanism for the formation of pentanol is outlined in Scheme 7.1 below. The ethanol to propanol mole ratio used is 1:1. The reaction seems to occur through a mechanism similar to the one discussed

in the previous chapter (Chapter 6), for the formation of hexanol and 2-ethylbutanol from a mixture of ethanol and butanol.

In Scheme 7.1, ethanol and propanol are converted to pentanol through dehydrogenation (to aldehydes), aldol coupling (of aldehydes), dehydration, and hydrogenation reactions over MgO catalyst. Similarly, 2-methylbutanol can also be formed in the same way as illustrated in Scheme 7.1. The formation of butanol and 2-methylpentanol occurs through dimerization (and aldol coupling) and self condensation of ethanol and propanol respectively.

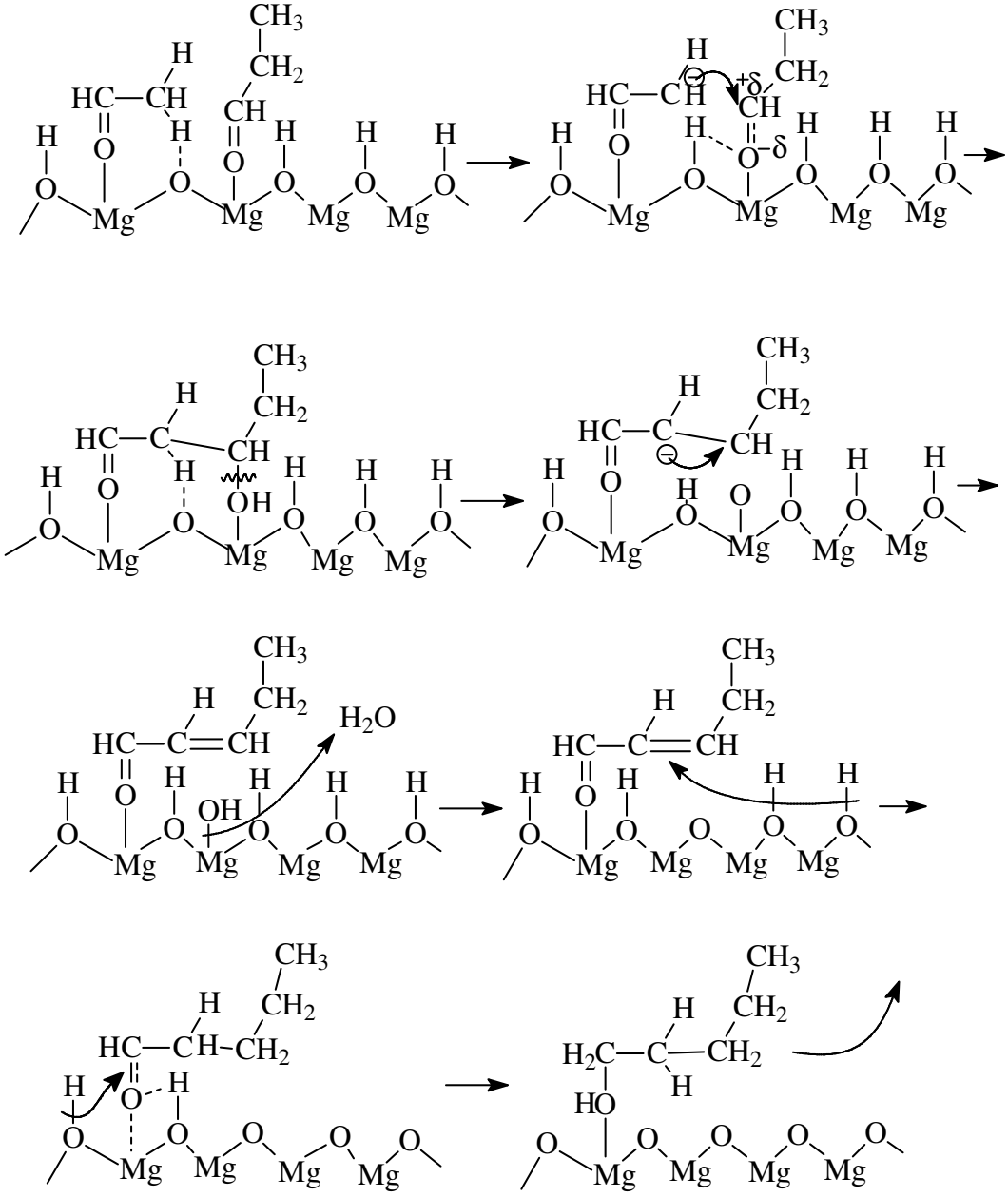

**Scheme 7.1** Schematic representation of ethanol and propanol reaction mechanism for the formation of 1-pentanol.

The detailed reaction network of ethanol and propanol outlining the possible reaction pathways observed over MgO is shown in Scheme 7.2 below. This reaction scheme summarises most of the products observed in the reaction between ethanol and propanol. Acetaldehyde and propionaldehyde form via ethanol and propanol dehydrogenation respectively (steps XII and V). The formation of Butanol and 2-methylpentanol occur via self-condensation of ethanol and propanol respectively (steps II, XVI - XVIII, and VI - VIII).

The formation of the 2-methylbutanol and pentanol from the reaction between ethanol and propanol occurs through dehydrogenation (to their corresponding aldehydes, steps V and XII), aldol condensation of the aldehydes to aldol species (steps IX and XIII), dehydration and hydrogenation of the aldol species (steps X and XIV), and hydrogenation of the resultant aldehydes to their corresponding alcohols (steps XI and XV).

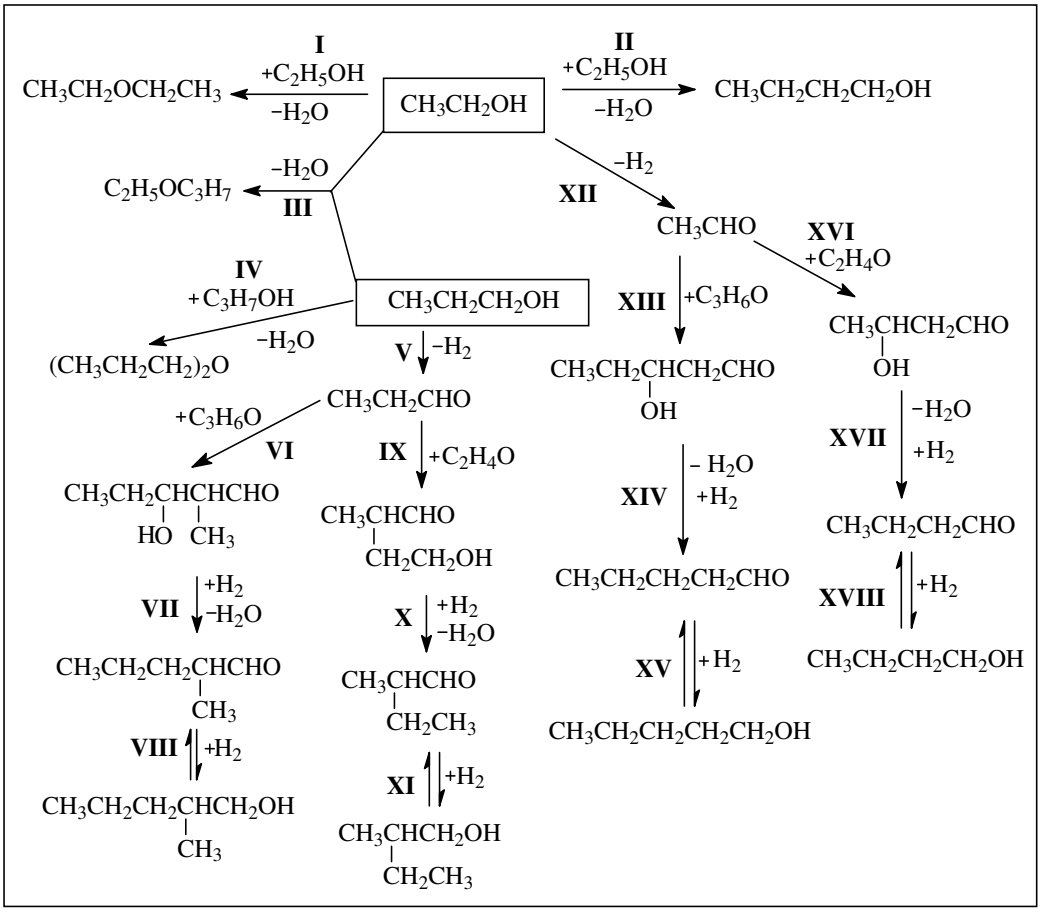


**Scheme 7.2** Reaction network of ethanol and propanol mixture.

### 7.4.1 The Effect of Reaction Parameters on Linear/Branched alcohols Ratio

The ratio of linear to branched alcohols was calculated and plotted against reaction parameters to determine conditions under which the formation of either linear or branched alcohols is favoured.

Figure 7.5 shows the change in ratio of linear/branched alcohols as the reaction temperature is increased. At a lower temperature (about 350 $^{o}$C), the ratio of linear/branched is higher which indicates that the formation of a linear alcohol is more favourable at this temperature. Although there was a decline in the amount of a linear alcohol as the temperature increased, the overall formation of a linear alcohol remained higher than that of a branched alcohol during this study.

The amount of butanol formed was higher compared to that of 2-methylpentanol. This shows that ethanol forms dimers easily. But here butanol formation does not interfere with the analysis as it does in Chapter 6.

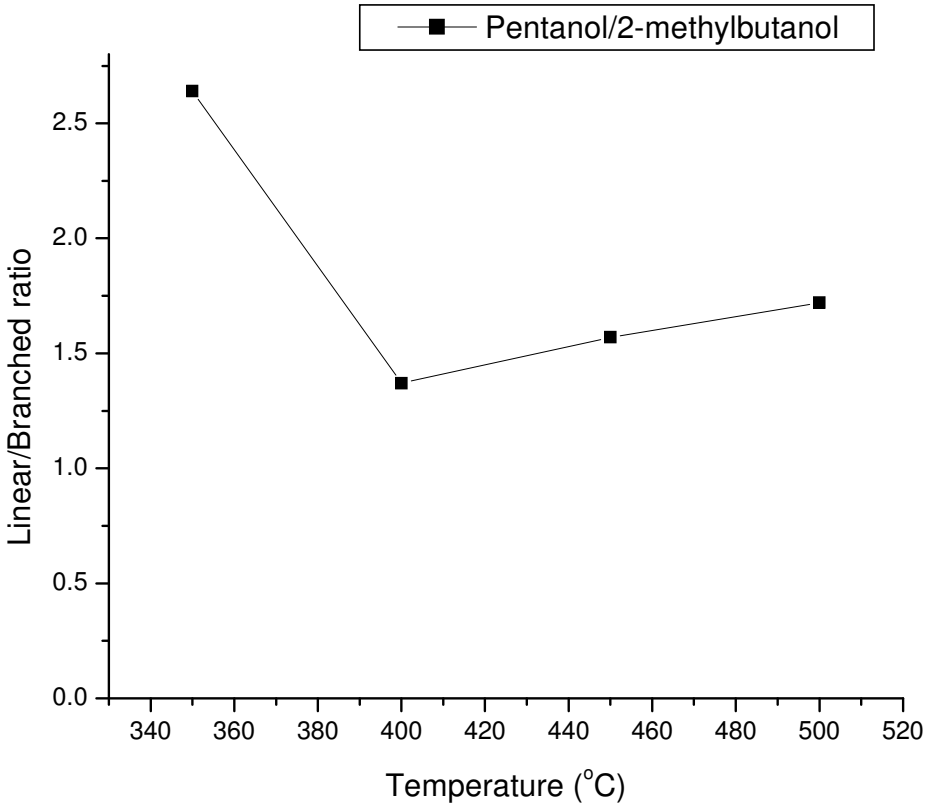


**Figure 7.5** The effect of temperature on the ratio of linear/branched alcohols.

The linear/branched ratio of alcohols is shown in Figure 7.6 as a function of contact time. Contrary to what has been observed for ethanol and butanol reaction, the linear/branched ratio of alcohols in ethanol and propanol reaction increased as the contact time increased.

At lower contact time, the formation of a branched alcohol is favoured over the formation of a linear alcohol. At higher contact time, the formation of a linear alcohol is preferred over that of a branched alcohol. This suggests that the dehydrogenation of ethanol to acetaldehyde and the abstraction of a proton from the β-position of propanol specie occur more rapidly than the abstraction of a proton from the methyl group of ethanol/acetaldehyde. This could relate to a steric effect. Propanol is less bulky than butanol; therefore the $CH_2$ on propanol molecule is more accessible than that of butanol.

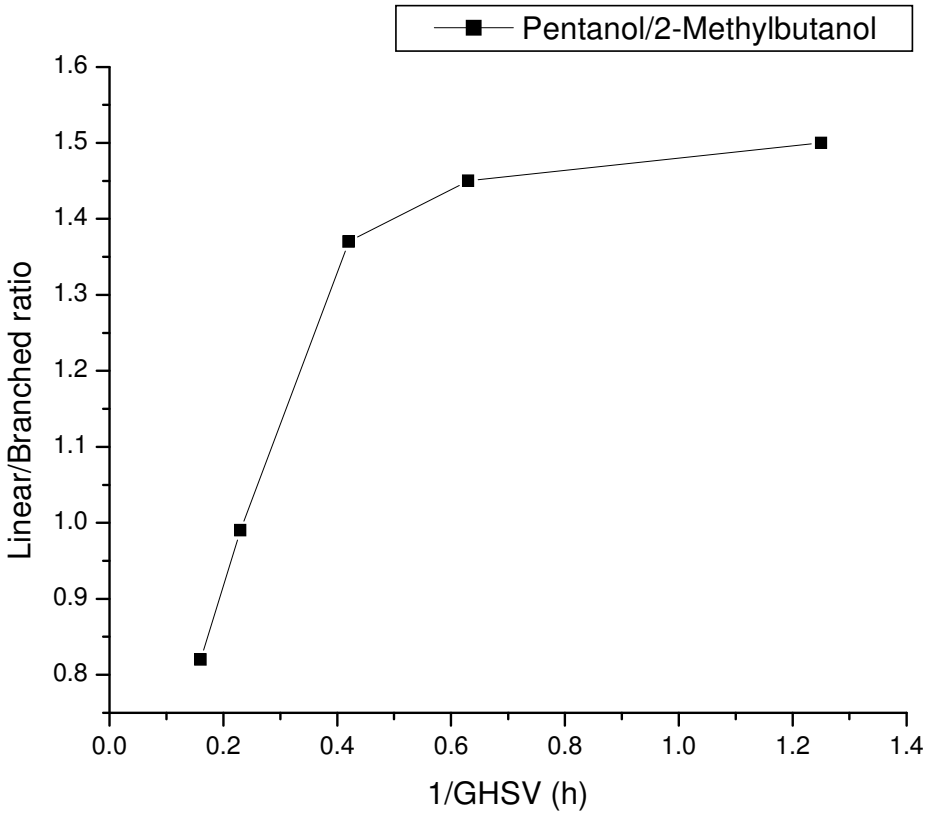


**Figure 7.6** The influence of contact time on linear/branched ratio of alcohols.

Figure 7.7 below shows the effect of time-on-stream on linear/branched ratio of alcohols. The ratio of linear/branched alcohols decreased as the reaction time elapsed. Initially, the formation of a linear alcohol is preferred

over that of a branched alcohol and as the reaction progressed the formation of a branched alcohol increased. This is contrary to what has been observed for ethanol/butanol reaction (Chapter 6, Fig 6.9). The decrease in ratio does parallel that of the reaction activity. Thus it appears that as active sites are removed, formation of the linear complex is disfavoured. The dimerisation of ethanol seems to be strongly competing for the sites responsible for the formation of the linear dimer (pentanol).

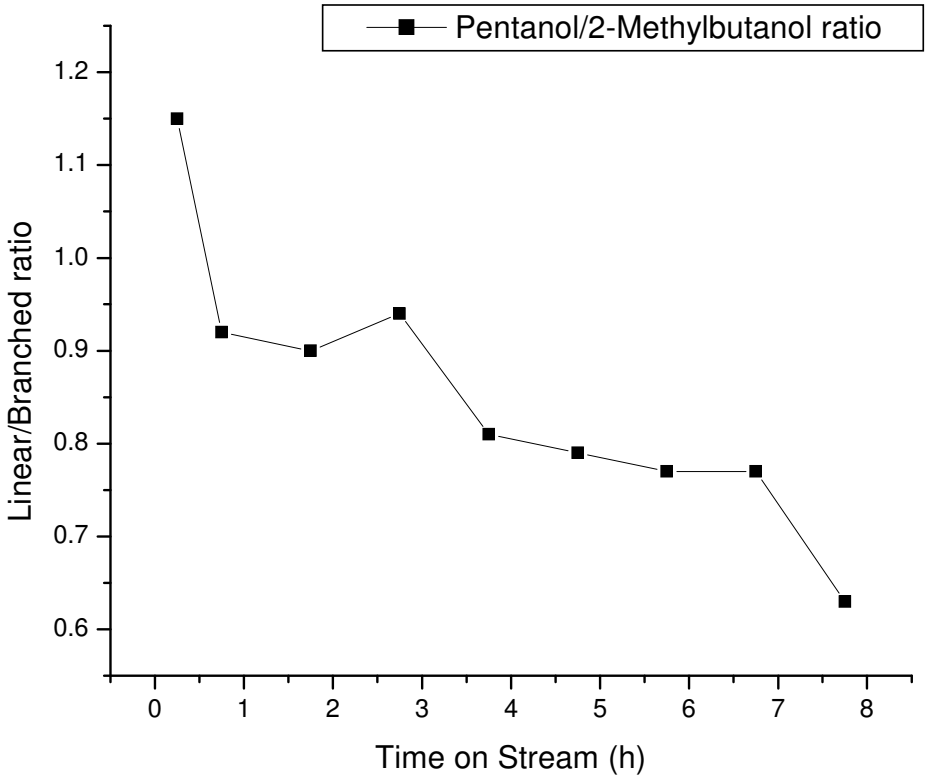


**Figure 7.7** The effect of time-on-stream on linear/branched ratio of alcohols.

## 7.5 Conclusions

MgO has proved to be an effective catalyst for the condensation of primary alcohols to form higher alcohols. In the instances where ethanol and propanol were used as building materials for higher alcohol synthesis, both branched and linear alcohols were observed over magnesium oxide catalyst.

The ethanol and propanol reaction seems to occur via a mechanism similar to the one described for ethanol and butanol (Chapter 6). In this mechanism, the formation of either linear or branched alcohol is dependent upon the position at which the ethanol is activated.

The formation of 1-pentanol is favoured by higher contact time while that of 2-methylbutanol is favoured by lower contact time.

## 7.6 References

[1] M. Ichikawa, J. Catal. 56 (1979) 127.

[2] A.M. Hilmen, M. Xu, M.J.L. Gines and E. Iglesia, Appl. Catal. A: General, 169 (1998) 355.

[3] J.I. Di Cosimo, C.R. Apesteguia, M.J.L. Gines and E. Iglesia, J. Catal. 190 (2000) 261.

[4] M.J.L. Gines and E. Iglesia, J. Catal. 176 (1998) 155.

[5] M. Xu, M.J.L. Gines, A.M. Hilmen, B.L. Stephens and E. Iglesia, J. Catal. 171 (1997) 130.

[6] M.J. Clement, A. Corma, S. Iborra and A. Velty, J. Mol. Catal. A: Chem. 182 (2002) 327.

[7] M.W. Farrar (Monsanto Chemical Co.), US Pat. 2 971 033, (1961).

[8] R.T. Clark (Celanese Corporation), US Pat. 3 972 952, (1976).

[9] W. Ueda, T. Kuwabara, T. Ohshida and Y. Morikawa, J. Chem. Soc. Chem. Commun. (1990) 1558.

[10] W. Ueda, T. Kuwabara, T. Ohshida and Y. Morikawa, Catal. Lett. 12 (1992) 971.

[11] C. Carlini, A. Macinai, A.M.R. Galletti and G. Sbrana, J. Mol. Catal. A: Chem. 212 (2004) 65.

[12] C. Carlini, M Di Girolamo, A. Macinai, M. Marchionna, M. Noviello, A.M.R. Galletti and G. Sbrana, J. Mol. Catal. A: Chem. 204-205 (2003) 721.

[13] C. Carlini, M Di Girolamo, M. Marchionna, M. Noviello, A.M.R. Galletti and G. Sbrana, J. Mol. Catal. A: Chem. 184 (2002) 273.

[14] C. Carlini, M Di Girolamo, A. Macinai, M. Marchionna, M. Noviello, A.M.R. Galletti and G. Sbrana, J. Mol. Catal. A: Chem. 200 (2003) 137.

[15] C. Carlini, A. Macinai, M. Marchionna, M. Noviello, A.M.R. Galletti and G. Sbrana, J. Mol. Catal. A: Chem. 206 (2003) 409.

[16] Kirk-Othmer, Encyclopedia of Chemical Technology, 4$^{th}$ Edn. vol.2 (1992) 709.

# CHAPTER 8

## Vapour Phase Alkylation of Catechol over Solid Base Catalysts*

* V. Vishwanathan, S. Ndou, L. Sikhwivhilu, N. Plint, K.V. Rghavan, N.J. Coville, Chem. Commun. (2001) 893.

### 8.1 Introduction

Vapour phase alkylation of catechol is commercially important for the production of oxy-alkylated products, namely guaiacol and veratrole. These are synthetic intermediates used in the production of flavourings, fragrances and pharmaceuticals [1]. Studies on phenol alkylation have shown that product selectivity depends on the acid–base property of the catalyst surface [2]. The addition of metal ions to alumina is known to generate new active sites which are basic in nature [3]. Available literature on the vapour phase alkylation of catechol over solid base catalysts, though limited, suggests that the basic sites are primarily responsible for

the formation of C-/O-alkylated products [4,5]. This is further supported by the report that $CO_2$ adsorption over the basic sites leads to catalyst deactivation [6,7].

However, there is no evidence to suggest that the weak sites over the base catalysts are primarily important for the formation of mono oxy-methylated products, in particular guaiacol. Here, for the first time, such a correlation is proposed, i.e. that a correlation exists between the weak base sites on a catalyst surface and selectivity to guaiacol.

## 8.2 Experimental

### 8.2.1 Catalyst Preparation

The supported cesium catalysts were prepared by impregnating $Al_2O_3$, $SiO_2$ and $TiO_2$, all of commercial origin, with an appropriate amount of an aqueous solution of cesium hydroxide (10 % Cs by mass). The resulting solids were dried and calcined in air at 400 $^oC$ for 4 h. Temperature programmed desorption (TPD) was performed using $CO_2$ gas at a heating rate of 10 $^oC$/min in the temperature range 100–700 $^oC$.

### 8.2.2 Apparatus and Procedure

The vapour phase alkylation of catechol with methanol was carried out in a vertical flow-type reactor at 350 $^{o}$C at atmospheric pressure (*ca.* 650 mm Hg). Before the start of the experiment, the catalyst (*ca*. 2 g) was activated in the reactor at 400 $^{o}$C for 1 h in nitrogen and then the solid was cooled to the reaction temperature. A pre-mixed catechol–methanol (1:3 w/w ratio) mixture was fed from the top of the reactor at a fixed rate of 5.1 ml/min (methanol-free catechol flow rate 0.95 mol/h) by means of a Sage syringe pump. The partial pressure of catechol was kept at 89.15 kPa during the reaction. After 1 h the liquid products were analyzed by GC (FID) using a DB-1 capillary column. The reaction conversion was determined with respect to the amount of catechol reacted. The reaction products were further confirmed by GC–MS (VG-11-250 data system) and $^{13}$C NMR (Brucker AC-400) spectroscopy.

## 8.3 Discussion of Results

The reaction data for the vapour phase alkylation of catechol over unsupported and supported catalysts are shown in Table 8.1. The acidic oxides ($Al_2O_3$, $SiO_2$ and $TiO_2$) do not show much guaiacol formation.

However, the basic oxide MgO shows a selectivity of 65 % for guaiacol. This suggests that the basic sites on the catalyst surface are involved in the formation of guaiacol.

It is interesting to note that cesium oxide alone shows a low activity and selectivity towards guaiacol formation. However, impregnation of cesium on to the acidic oxides ($Al_2O_3$, $SiO_2$ and $TiO_2$), increased the selectivity for guaiacol significantly. Both alumina and cesium-modified alumina show the highest reaction activity as compared to the other unsupported and supported oxides. This suggests that the stronger and larger number of acidic sites on the catalyst surface promotes more ring alkylation than side (O-) alkylation.

In the case of both alumina and cesium-modified alumina a significant amount of polyalkylated products is also formed. The formation of phenol and to a lesser extent diphenylether indicates that both dehydration and ring alkylation are the two competitive reactions operating over the acidic sites. This is supported by the fact that both $TiO_2$ and $Cs–TiO_2$ show a significant amount of dehydrated products as compared with $Al_2O_3$ and $Cs–Al_2O_3$ catalysts.

**Table 8.1** Reaction data for the vapour phase alkylation of catechol over unsupported and supported cesium catalysts.

| Catalyst | Activity | Selectivity (%) | | | |
|---|---|---|---|---|---|
| | $Molh^{-1}g^{-1}$ | Guaiacol 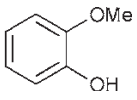 | Veratrole 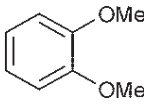 | C-alkylated products[a] | Others[b] |
| $TiO_2$ | 0.718 | 10 | 2 | 36 | 42 |
| $Al_2O_3$ | 2.341 | 18 | 3 | 73 | 6 |
| $SiO_2$ | 0.133 | 20 | 43 | 33 | 4 |
| MgO | 0.106 | 65 | 15 | 15 | 5 |
| $Cs_2O$ | 0.053 | 16 | 17 | 6 | 57 |
| $10\%Cs_2O/TiO_2$ | 0.426 | 37 | 12 | 10 | 41 |
| $10\%Cs_2O/TiO_2$ | 1.409 | 58 | 1 | 28 | 13 |
| $10\%Cs_2O/TiO_2$ | 0.505 | 75 | 16 | 4 | 5 |

a 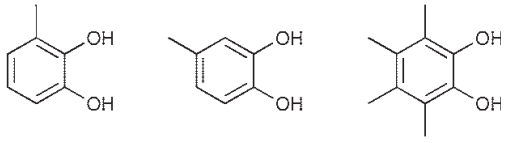

b 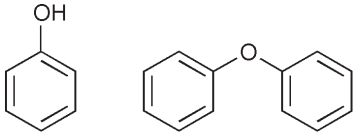

The distribution of basic sites over unsupported and supported catalysts is shown in Fig 8.1 and 8.2. The TPD experiments were conducted in atmospheric pressure. The $CO_2$ was adsorbed at 100 $^oC$. The TPD profiles of $CO_2$ over $Al_2O_3$ and MgO (Fig 8.1) show that although $Al_2O_3$ is more acidic than MgO it also has a larger number of strong basic sites (685 $^oC$) with respect to MgO (715 $^oC$). The stronger basic sites on MgO at 715 $^oC$ indicate that, apart from $O^{2-}$ basic sites of MgO, the adjacent $Mg^{2+}$ sites may also participate in $CO_2$ adsorption [8]. On the other hand, MgO has a greater number of weaker basic sites (320 $^oC$) than $Al_2O_3$.

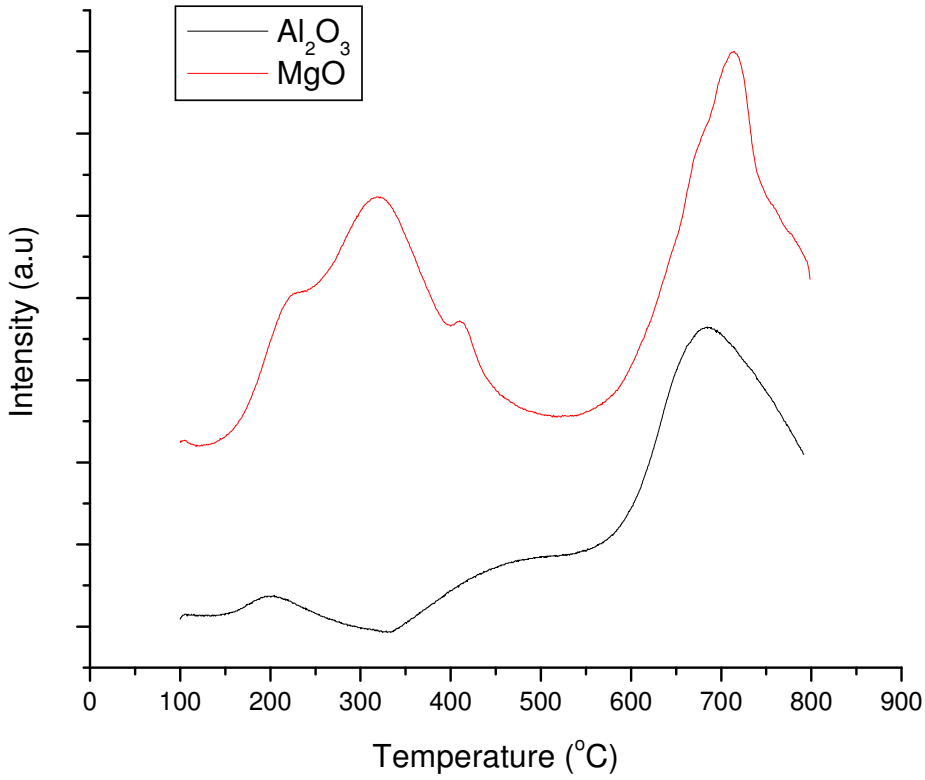


**Figure 8.1** $CO_2$ TPD profiles of MgO and $Al_2O_3$.

The fact that more guaiacol is formed on MgO rather than $Al_2O_3$ indicates that weaker basic sites may be primarily involved for the higher selectivity of guaiacol. Fig 8.2 clearly demonstrates this finding.

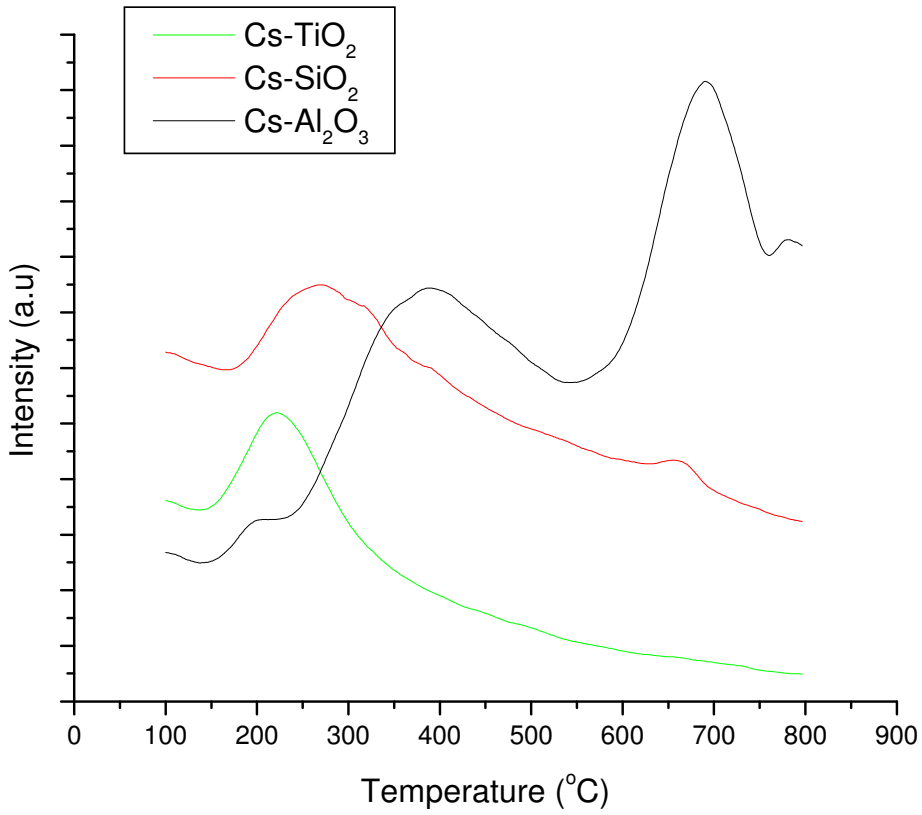


**Figure 8.2** $CO_2$ TPD profiles of Cs on $TiO_2$, $SiO_2$ and $Al_2O_3$.

Here it is seen that addition of cesium to acidic supports transforms stronger base sites into weak sites, thus enhancing the selectivity for guaiacol. The higher selectivity for guaiacol at weaker basic sites over Cs–$SiO_2$ (75 %) as compared with Cs–$Al_2O_3$ (58 %) further supports the assumption that the formation of guaiacol is related to the strength and the number of the weak basic sites. However, in the case of Cs–$TiO_2$, the lower selectivity for guaiacol (37 %) may suggest the possibility of an

interaction between the promoter and titanium oxide, leading to compound formation.

## 8.4 Conclusion

In conclusion, it is evident from the foregoing results that the transformation of stronger basic sites to weaker ones upon addition of $Cs_2O$ results in higher selectivity for guaiacol.

## 8.5 References

[1] G. Dorothea, in Phenol derivatives, Ullman Encyclopedia of Industrial Chemistry, ed. E. Barbara, H. Stephen and S. Gail, VCH Verlagsgerellschaft, Weinhein, A19 (1991) 354.

[2] K. Tanabe and T. Nishizaki, Proceedings of the 6th Congress on Catalysis, London, 2 (1977) 863.

[3] K. Jurczyk and W. Kania, Appl. Catal. 56 (1989) 203.

[4] S. Porchek, L. K. Minsker, R. Doeper and A. Renken, Chem. Eng. Sci. 51 (1996) 2933.

[5] S. Porchek, R. Doeper and A. Renken, Chem. Eng. Technol. 17 (1994) 108.

[6] Y. Fu, T. Baba and Y. Ono, Appl. Catal. A: General, 166 (1998) 419.

[7] Y. Fu, T. Baba and Y. Ono, Appl. Catal. A: General, 166 (1998) 425.

[8] H. Hattori, Chem. Rev. 95 (1995) 545.

# Chapter 9

## Selective Hydrogenation of Phenol over Novel Modified Titanium oxide supported Palladium catalysts*

* A.S. Ndou, V. Vishwanathan, N.J. Coville, Hydrogenation of phenol over novel titanium oxide supported palladium catalysts. To be submitted.

### 9.1 Introduction

Hydrogenation of phenol to cyclohexanone is an important industrial reaction for the production of caprolactam for the synthesis of nylon 6 and adipic acid for nylon 66 [1]. Phenol, on the other hand, is an established environmental toxin [2] and arises from a variety of industrial sources associated with petrochemicals and polymer manufacture [3]. A catalytic hydrogen treatment of phenol wastes to generate reusable raw material is certainly preferable to the standard destructive route by incineration [4].

Industrially, cyclohexanone is produced either by the oxidation of cyclohexane or by the hydrogenation of phenol [1]. The former route requires high temperatures and pressures and generates undesirable by-products that lower the product yield and complicates the recovery/separation steps. In the latter route, phenol is hydrogenated to cyclohexanone either in a single step or in a two-step process via cyclohexanol. The one-step process avoids the endothermic dehydrogenation of cyclohexanol and is therefore considered to be attractive in terms of capital cost and energy savings. The one-step selective hydrogenation of phenol to cyclohexanone is generally carried out over Pd supported on $Al_2O_3$ or MgO-based catalysts [5,6].

It is generally accepted that the role of the support is to adsorb phenol molecules near the Pd particles; the Pd adsorbs $H_2$ molecules and supplies hydrogen atoms to the aromatic ring by a spill-over mechanism [5,7]. Depending on the acid–base properties of the support, the mode of adsorption of phenol varies and this mode directs the product selectivity to either cyclohexanone or cyclohexanol. So far, the reaction has been studied mostly over MgO and $Al_2O_3$ supports [4–8], and over Ni supported on $SiO_2$ or zeolites [9]. Recently, other supports have been used for Pd catalysts in phenol hydrogenation reactions [10,11].

In this study, we have focused on the use of nano-titania materials as novel supports for Pd metal in the phenol hydrogenation reaction. The use of structured materials (nanotubes/nanofibres) to transform the catalytic performance of supported metal is lately attracting the interest of the catalysis community.

Since the discovery of titanium oxide nanotubes by Hoyer [12], several reports on different synthesis methods to prepare these materials have emerged [13-17]. Titanium oxide is a material of interest for its many applications in, for example, photo catalysis and solar energy transfer [18]. Titanium oxide with a large surface area will provide a highly active photo-catalytic material [19] and is also expected to be utilized as a material for highly efficient solar cells [20,21]. It has also been reported that titanium oxide nanotubes can be used as hydrogen sensors [22,23] or in the dye-sensitised solar cell [24,25].

## 9.2 Experimental

### 9.2.1 Catalyst preparation

The nanoparticles of titanium oxide were prepared by hydrothermal treatment of commercial titanium dioxide (Deggusa) with sodium hydroxide [26]. Commercial $TiO_2$ (Deggusa) was mixed with equal amounts of sodium hydroxide and water. The mixture was stirred at 120 $^oC$ for 24 h in an autoclave. It was then centrifuged for 30 min followed by washing with deionised water. The latter step was repeated until the conductivity of the mixture was less than 50 micro Siemens. It was then dried overnight in an oven at 120 $^oC$. The surface area of this $TiO_2$ was found to be 330 $m^2/g$. This $TiO_2$ support will be referred to as NaOH-$TiO_2$.

A second titanium oxide support was prepared by hydrolysis of $TiCl_4$ with hydrazine hydrate [27]. $TiCl_4$ (Loba Chemie) was digested in hydrochloric acid and then diluted with distilled water to make a 3 M solution of $TiCl_4$ in water. All the additions were made while keeping the reaction vessel in an ice bath. The pH of the solution was found to be less than 2. A solution (8 M) of hydrazine hydrate, $H_6N_2O$ (Ranbaxy) in water was added drop-wise

to the stirred $TiCl_4$ solution until the final pH was about 8.0. The mixture was kept under high-speed constant stirring on a magnetic stirrer for one hour at room temperature. The precipitated titanium oxide was filtered and repeatedly washed with hot distilled water until it was free of chloride ions. The hydrous oxide was dried overnight at 120 $^oC$. The surface area of the titanium dioxide was found to be 207 $m^2/g$. This support will be referred to as $TiCl_4$-$TiO_2$.

A third titanium oxide support was prepared by mixing commercial $TiO_2$ (Deggusa) with distilled water. This was dried overnight at 120 $^oC$. The resulting surface area was found to be 49.5 $m^2/g$.

The palladium-loaded catalysts were prepared by impregnating each of the above mentioned supports with an appropriate amount of palladium acetate to give a one percent palladium loading (w/w). The catalysts were dried in air for 16 h and calcined at 300 $^oC$ for 4 h.

### 9.2.2 Reactor Studies

The catalytic experiments were carried out in a vertical fixed bed glass reactor (300 mm long and 15 mm i.d). All reactions were carried out using 0.2 g of catalyst. The catalysts were used in the form of granules (100-350 μm) prepared by crushing the titanium oxide support to the desired size. The reactor was placed inside a temperature controlled heating jacket with a thermocouple placed at the centre of the catalyst bed.

The catalyst was reduced in flowing hydrogen (flow rate 22 ml/min) at 300 $^{o}$C for 1 h. A mixture of phenol and ethanol (1:1 wt/wt ratio) was fed at 2.5 ml/h from a 50 ml syringe using a syringe pump (Sage instruments, model 341B) through a hydrogen gas line (hydrogen flow rate 22 ml/min) into the reactor. The partial pressures of phenol and hydrogen in the feed were kept at 12.88 kPa and 62.16 kPa respectively. The reaction temperature was kept at 165 $^{o}$C, unless otherwise stated. The products were collected in a water-cooled receiver after 1h and analysed in a gas chromatograph (ZB wax, 60 m x 0.32 mm capillary column; FID). Liquid product identification was achieved by GC-MS (Finnigan TSQ-7000) and $^{13}$C-NMR spectroscopy (Brucker AC 400). The temperature programmed desorption (TPD) apparatus used in the analysis of the catalysts, consists of a U-shaped quartz reactor housed in a temperature controlled heating jacket.

The signal is measured by a low temperature dual filament TCD and recorded by a PC equipped with an I/O card. The TPD experiments were conducted in atmospheric pressure. The $CO_2$ was adsorbed at 100 $^oC$.

## 9.3 Results and Discussion

A mixture of phenol and ethanol (mole ratio 1:1) was passed over titanium oxide in the presence of hydrogen during preliminary tests. Neither cyclohexanone nor cyclohexanol were detected during this reaction. Ethanol was used as a solvent in this reaction because it gives good phenol solubility.

Hydrogenation of phenol over palladium supported catalysts led to the formation of cyclohexanone and cyclohexanol, amongst other products, as shown below.

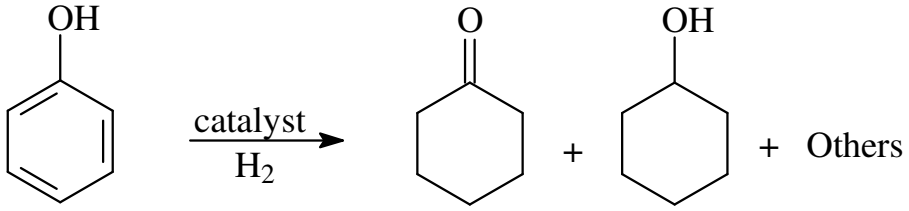

The selectivity towards either of the major products is dependent on the catalyst system used. Product yields from the reaction of phenol over palladium supported on titanium oxide catalysts are shown in Table 9.1 below. Although palladium supported on normal titanium dioxide (Deggusa P25) showed high activity (conv. 22 %) compared to the other two catalysts, the selectivity towards cyclohexanone was very low (29 %). Apart from cyclohexanone and cyclohexanol, other products such as benzene, cyclohexane, diphenylether and dicyclohexylether were also observed. These are common hydrodehydroxylation and condensation products associated with reaction over palladium supported on acidic carriers [5,28].

The other two catalysts showed very good (about 86 %) selectivity towards cyclohexanone. Only small amounts of dicyclohexylether and diphenylether were observed from both catalysts. The high surface area titanium oxide supports present an opportunity for high palladium metal dispersion. This could lead to effective interaction between the palladium metal and the reactant and hence good selectivity towards the hydrogenation products.

**Table 9.1** The effect of titanium oxide preparation methods on products distribution (T= 165 $^{o}$C, reduction T= 300 $^{o}$C, WHSV= 3800 $h^{-1}$, $H_2$/phenol= 4.5).

| Catalysts | S.A($m^2$/g)[a] | % Conv. | Selectivity (%) | | |
|---|---|---|---|---|---|
| | | | C-hexanone | C-hexanol | Others[b] |
| 1%Pd/$TiO_2$[c] | 70 | 22.7 | 28.9 | 12.9 | 58.2 |
| 1%Pd/$TiO_2$[d] | 332 | 11.3 | 86.8 | 3.1 | 10.1 |
| 1%Pd/$TiO_2$[e] | 271 | 12.2 | 86.5 | 8.2 | 5.3 |

[a] is the surface area of the support only;

[b] Others includes benzene, cyclohexane and dicyclohexylether.

[c] is the commercial titanium dioxide (Deggusa P25);

[d] is the titanium oxide prepared from thermal hydrolysis of titanium dioxide sodium hydroxide under mild conditions (NaOH-$TiO_2$);

[e] is prepared from hydrolysis of titanium tetrachloride with hydrazine hydrate at room temperature ($TiCl_4$-$TiO_2$.

Further characterization was conducted to determine features related to the acidity/basicity of the catalysts. The commercial titanium dioxide (Deggusa P25) did not show any $CO_2$ desorption peak (Fig 9.1). The $CO_2$ TPD profiles (Fig. 9.1) of the other two catalysts showed the presence of

weak basic sites (about 100 $^{o}$C). Claus et al. has shown that hydrogenation of phenol in the presence of a basic support gave only cyclohexanone and cyclohexanol as products [29]. The selectivity towards cyclohexanone was reported to be in excess of 95 %. The influence of basic sites on the cyclohexanone selectivity was also investigated by Scire et al. [30]. He found that while the addition of calcium as a promoter for $Pd/Al_2O_3$ catalysts increased the selectivity towards cyclohexanone, it also increased the basicity of the catalyst. This suggests that the basicity of the support is essential for high selectivity towards cyclohexanone. The titanium oxides thus prepared by the hydrolysis method offer high surface area for high metal dispersion and controlled basicity.

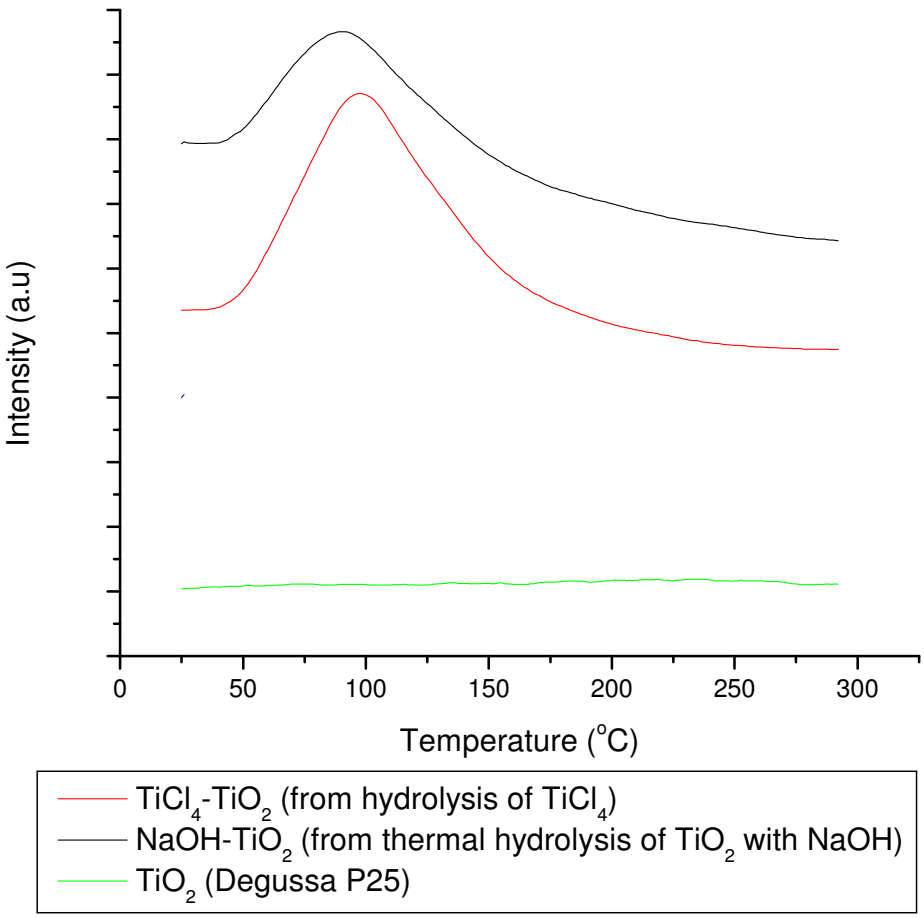


**Figure 9.1** TPD profiles of high surface area titanium oxide supports.

The TEM images of titanium oxide supports are shown in Figure 9.2, 9.3 and 9.4 below. The TEM micrograph for $TCl_4$-$TiO_2$ shown in Fig 9.2 indicates the presence of nanofibres in the material. The other two samples (Fig 9.3 and 9.4) show no presence of nanotubes/fibres. Although

the NaOH-$TiO_2$ has high surface area, under the microscope it looked similar to the normal titanium dioxide (Deggusa P25).




**Figure 9.2** TEM micrograph of high surface area $TiCl_4$-$TiO_2$.

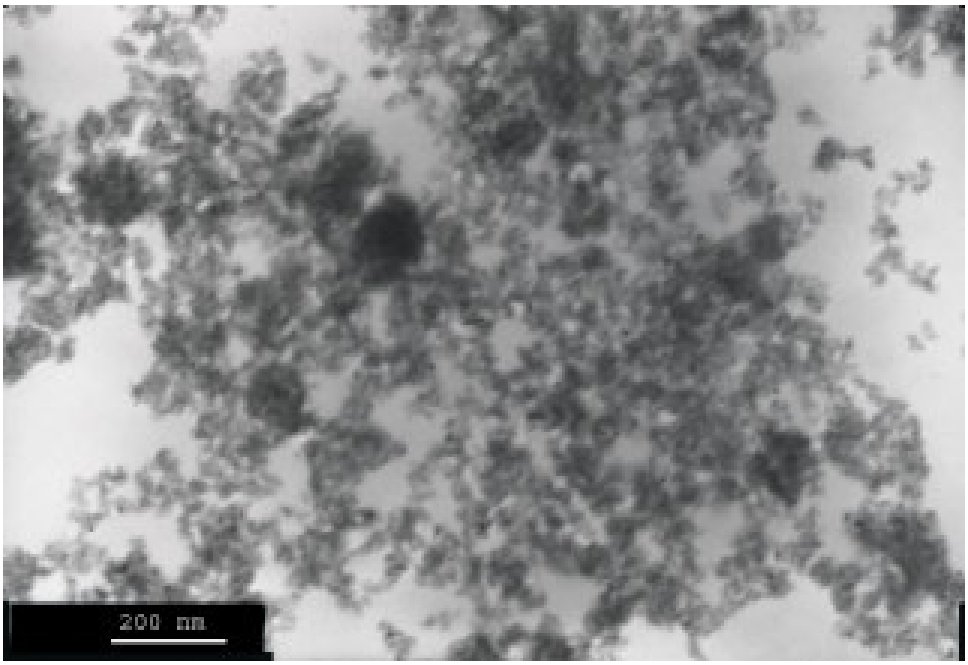


**Figure 9.3** TEM micrograph of high surface area NaOH-$TiO_2$.

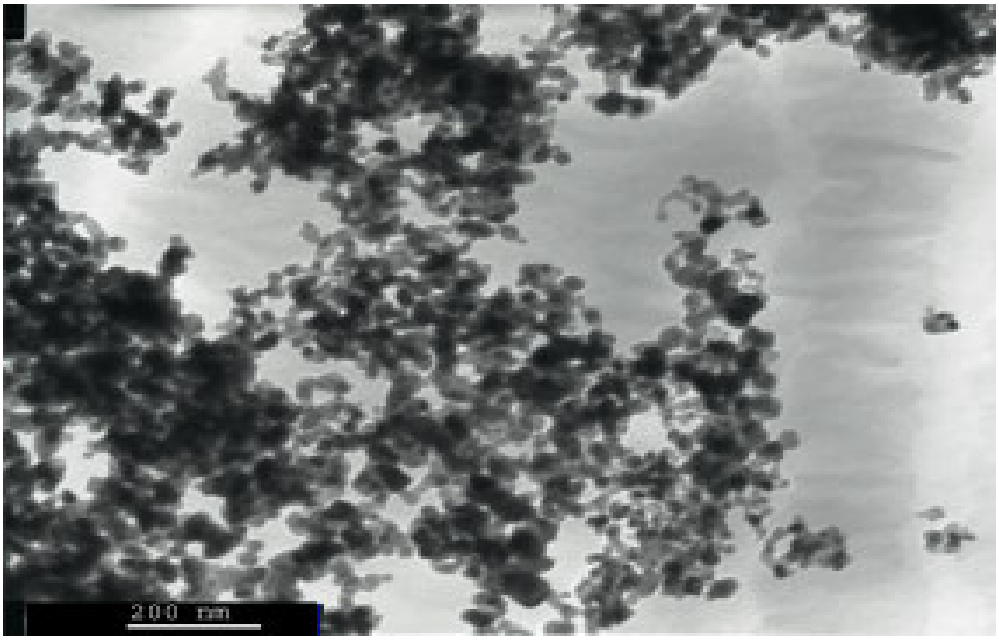


**Figure 9.4** TEM micrograph of normal titanium dioxide (Deggusa P25).

The two modified titanium oxide supported catalysts (1% Pd/$TiCl_4$-$TiO_2$ and 1% Pd/NaOH-$TiO_2$) showed similar activity and basicity. Further studies were conducted on the palladium catalyst supported on these two titanium oxide modified supports.

### 9.3.1 Investigation of Reaction Parameters over Titanium Oxide ($TiCl_4$-$TiO_2$) Supported Palladium Catalyst

The effect of reaction temperature on phenol conversion and product selectivity is shown in Fig 9.5 below. A fresh catalyst was used for each data point collected during the experiment. The catalyst showed an increase in phenol conversion as the reaction temperature increased. However, the selectivity towards cyclohexanone slowly decreases with reaction temperature from 140 to 180 $^oC$ and further decreases rapidly as the temperature approaches 220 $^oC$. At higher temperatures, the reaction favours the hydrodehydroxylation and condensation products such as dicyclohexylether, diphenylether and benzene.

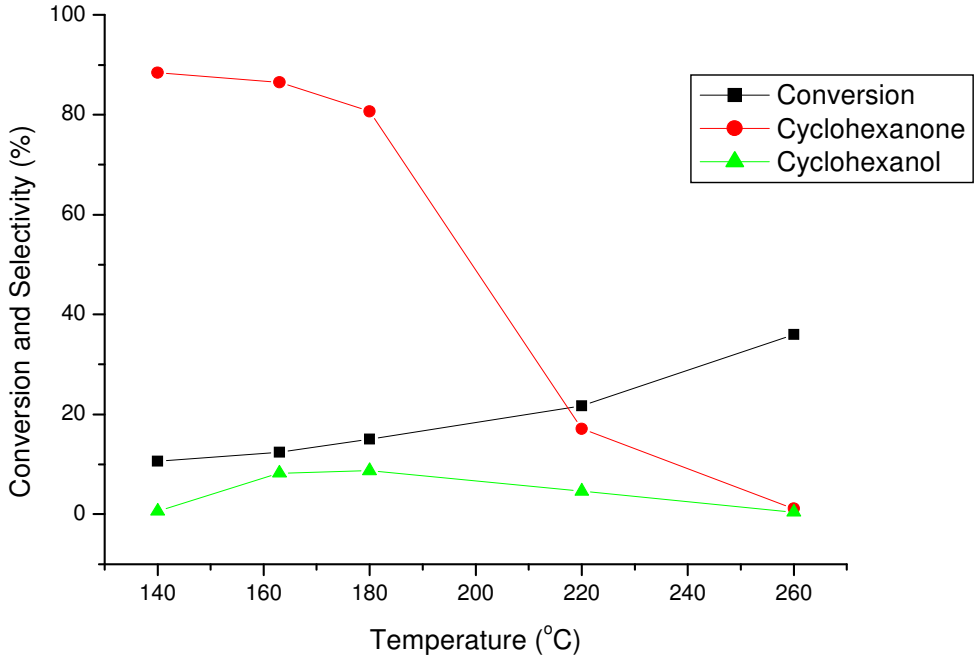


**Figure 9.5** The influence of temperature on products distribution over $TiCl_4$-$TiO_2$. (reduction T= 300 °C, GHSV= 3800 $h^{-1}$, $H_2$/phenol= 4.5).

The hydrogen/phenol mole ratio was varied and the changes recorded are shown in Figure 9.6 below. A fresh catalyst was used for each mole ratio investigated. The reaction conversion remained constant as the amount of hydrogen was increased. However, changes in the selectivity towards cyclohexanone were observed. When the amount of hydrogen was increased, the cyclohexanone selectivity initially increased to a maximum and then declined as the hydrogen/phenol mole ratio was further increased. There was also a slight increase in the cyclohexanol selectivity

as the hydrogen/phenol mole ratio reaches 5.4. This suggests that at high hydrogen/phenol ratio, there is greater probability for complete hydrogenation to occur.

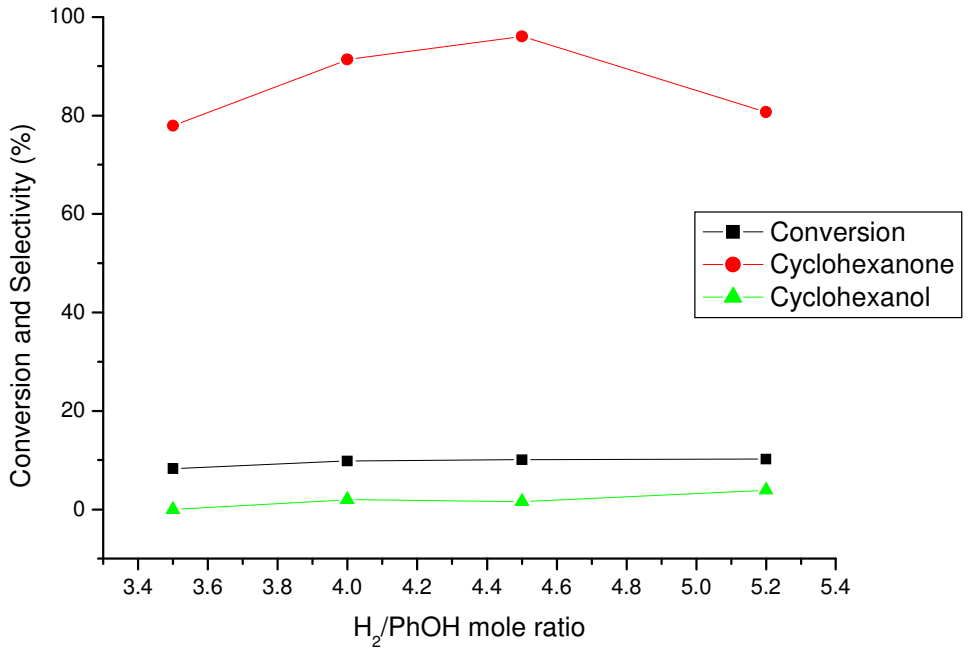


**Figure 9.6** The effect of $H_2$/Phenol mole ratio on product distribution over $TiCl_4$-$TiO_2$. (T= 165 $^oC$, reduction T= 300 $^oC$, GHSV= 3800 $h^{-1}$).

The effect of contact time on the phenol conversion and product selectivity is shown in Figure 9.7 below. A fresh catalyst was used for each data points collected in this experiment. There is a slight increase in phenol conversion as the contact time increases. However, the selectivity towards cyclohexanone decreased as the contact time increased. High

contact time does not only enhance the conversion of reactants to products, but also allows for secondary reactions to occur on the products formed. Hence, a decline in cyclohexanone selectivity and a slight increase in cyclohexanol as the contact time increases.

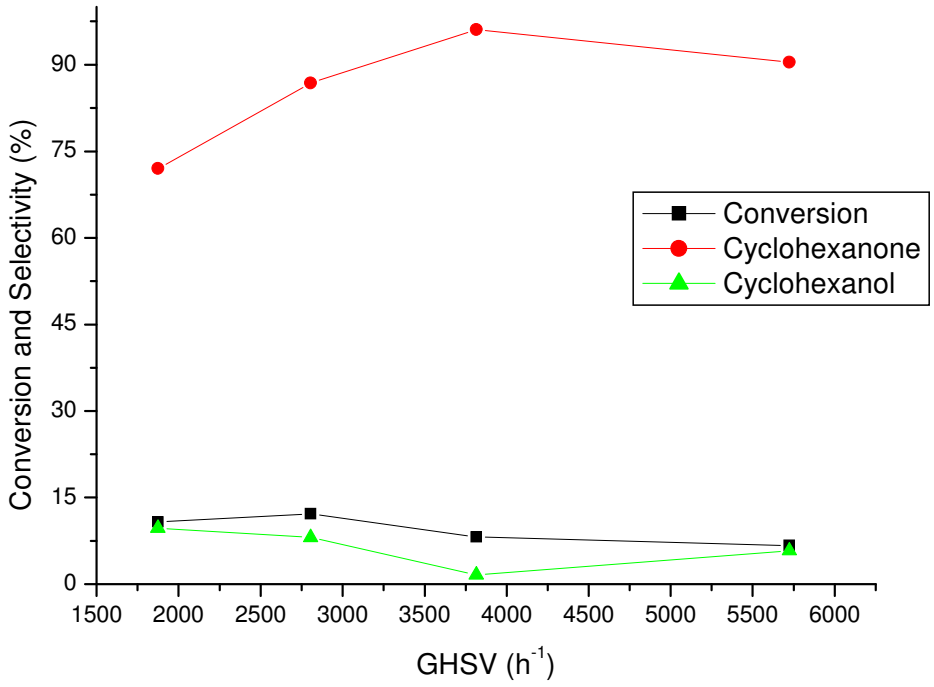


**Figure 9.7** The influence of GHSV on product selectivity over $TiCl_4$-$TiO_2$. (T= 165 °C, reduction T= 300 °C, $H_2$/phenol= 4.5).

The effect of time-on-stream on phenol conversion and product selectivity is shown in Figure 9.8 below. There was a slight decline in the conversion of phenol as the reaction progressed. This suggests that catalyst

deactivation was not severe during the period specified in Figure 9.8. Selectivity towards cyclohexanone initially increased and thereafter remained constant. However, there was a slight decline in the selectivity towards cyclohexanol as the time on stream increased.

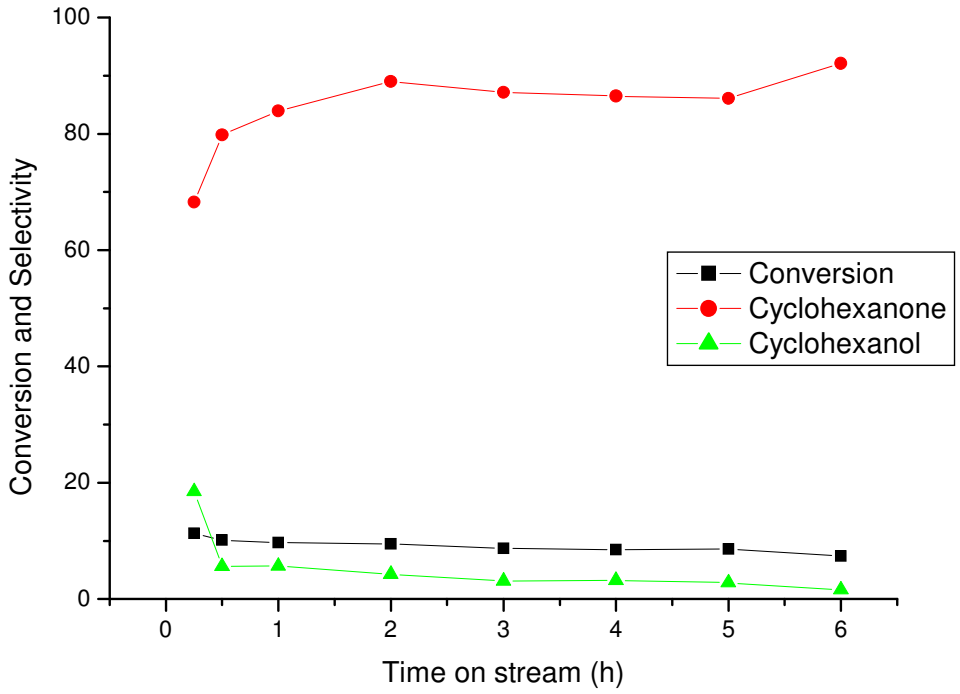


**Figure 9.8** The effect of time on stream on catalyst stability over $TiCl_4$-$TiO_2$. (T= 165 $^oC$, reduction T= 300 $^oC$, GHSV= 3800 $h^{-1}$, $H_2$/phenol= 4.5).

### 9.3.2 Investigation of Reaction Parameters over Titanium Oxide ($NaOH\text{-}TiO_2$) Supported Palladium Catalyst

The influence of temperature on the reaction activity and product distribution is shown in Figure 9.9 below. A fresh catalyst was used for each of the data points collected in this experiment. The selectivity towards cyclohexanone was highly affected by temperature above 240 $^oC$. There was a rapid decline in selectivity towards cyclohexanone above this temperature. The effect of temperature on product selectivity is less severe on this catalyst than it is on $TiCl_4\text{-}TiO_2$ supported catalyst (Fig 9.5 above).

There was a slight increase in percentage conversion as the reaction temperature increased. This was also observed for the $TiCl_4\text{-}TiO_2$ supported catalyst. In both catalysts, the higher temperature and catalyst activity were accompanied by formation of larger amounts of benzene, diphenylether and dicyclohexylether. This catalytic behaviour can be correlated to the basic sites on both catalysts. Figure 9.1 clearly demonstrated this finding. The TPD profiles of the modified titanium oxide supported catalysts indicates that at higher temperatures (above 200 $^oC$), the relative amount of basic sites present on these catalysts is very low.

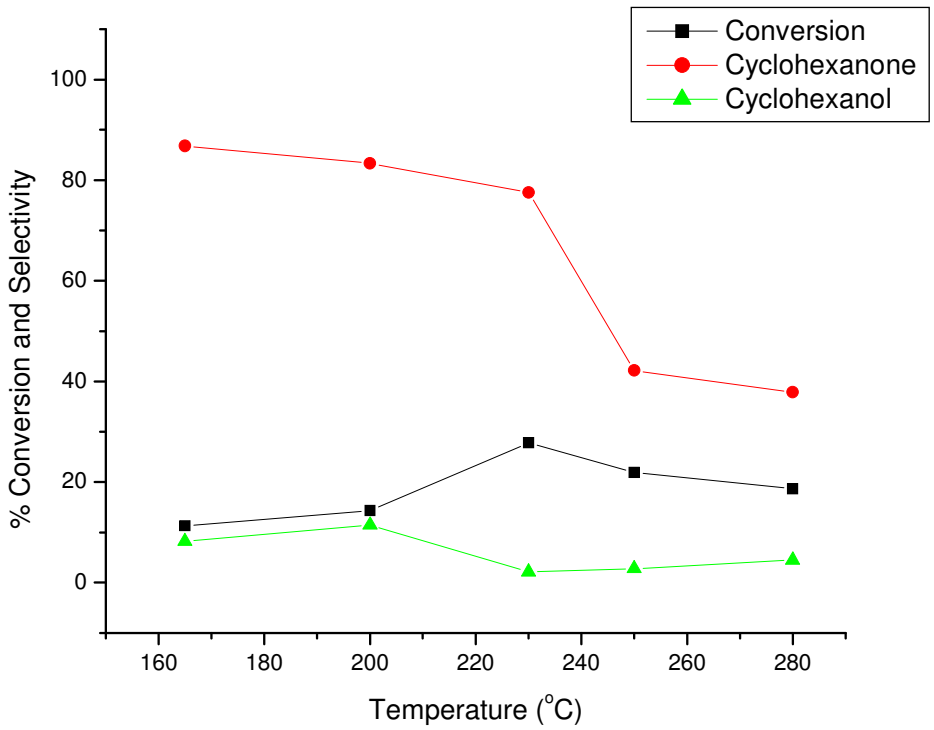


**Figure 9.9** The effect of temperature on product distribution over NaOH-$TiO_2$.

The effect of hydrogen/phenol mole ratio on catalyst conversion and product distribution is shown below (Fig 9.10). A fresh catalyst was used for each of the mole ratio experiments conducted. The selectivity towards cyclohexanone decreased as the $H_2$/phenol mole ratio increased. It can be noted that the relative amount of cyclohexanol also increased as the

$H_2$/phenol mole ratio increased. This suggests that complete hydrogenation of phenol to cyclohexanol is favoured as the amount of hydrogen in the reaction stream is increased.

There was a slight increase in phenol conversion as the $H_2$/phenol mole ratio increased. However, this behaviour was not observed for the $TiCl_4$-$TiO_2$ supported catalyst as both the phenol conversion and cyclohexanol selectivity remained near constant as the $H_2$/phenol mole ratio increased.

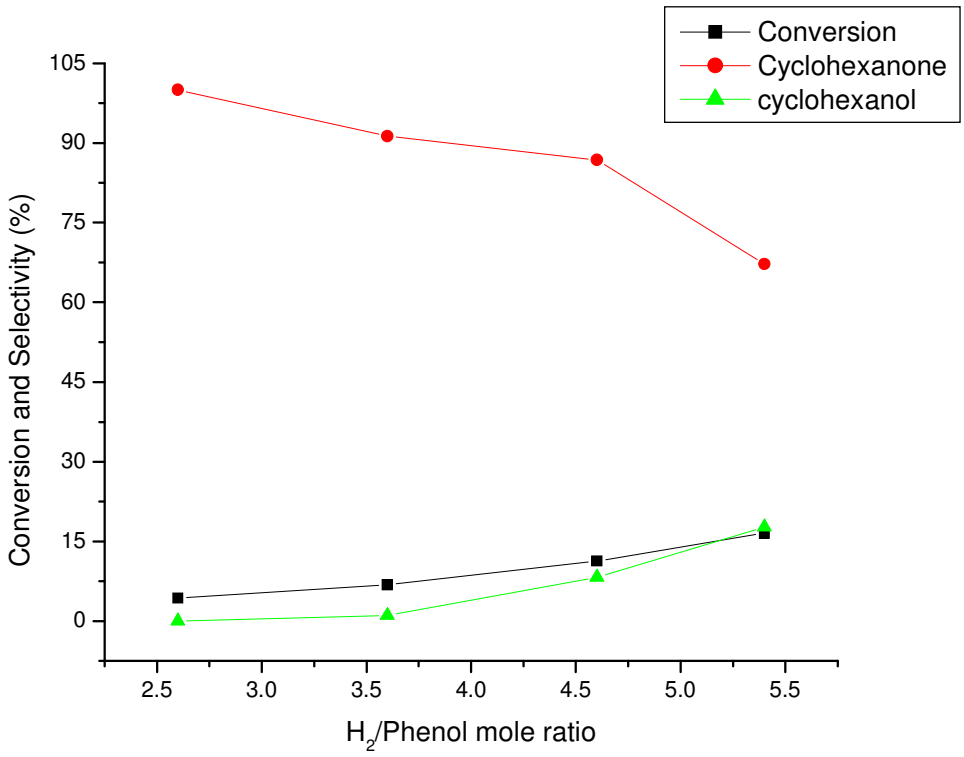


**Figure 9.10** The influence of $H_2$/phenol mole ration on product distribution over NaOH-$TiO_2$.

The effect of contact time on conversion and product distribution for NaOH-$TiO_2$ supported catalyst is shown in Figure 9.11 below. A fresh catalyst was used for each set of data points collected in this experiment. The catalyst showed a similar trend observed for $TiCl_4$-$TiO_2$ catalyst. The selectivity towards cyclohexanone increased as the contact time decreased. There was a slight increase in conversion and cyclohexanol

selectivity as the contact time increased. This slight increase in selectivity towards cyclohexanol could indicate further hydrogenation of surface cyclohexanone.

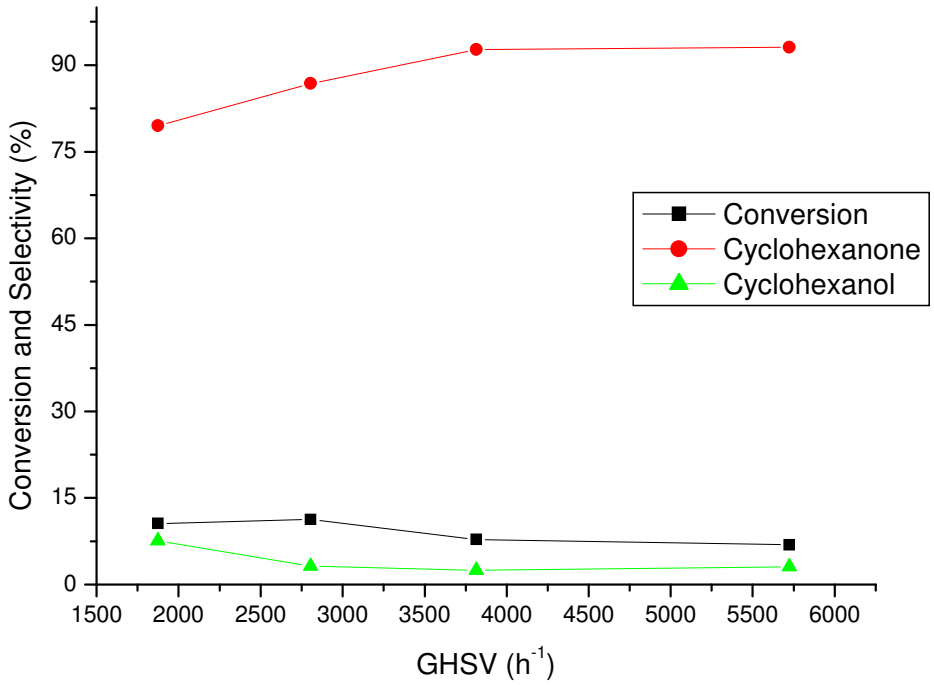


**Figure 9.11** The effect of GHSV on catalyst activity and product selectivity over NaOH-$TiO_2$.

The study of time-on-stream indicated a slight decline in the activity of the catalyst as the reaction progressed. Contrary to what was observed for the

$TiCl_4$-$TiO_2$ supported catalyst, the selectivity towards cyclohexanone in NaOH-$TiO_2$ remained near constant as the time-on-stream increased. Although there was a slight increase in cyclohexanol selectivity, the overall amount of cyclohexanol generated in this study was very low. It is interesting to note that both catalysts showed slow deactivation and the deactivation had no significant effect on the cyclohexanone selectivity.

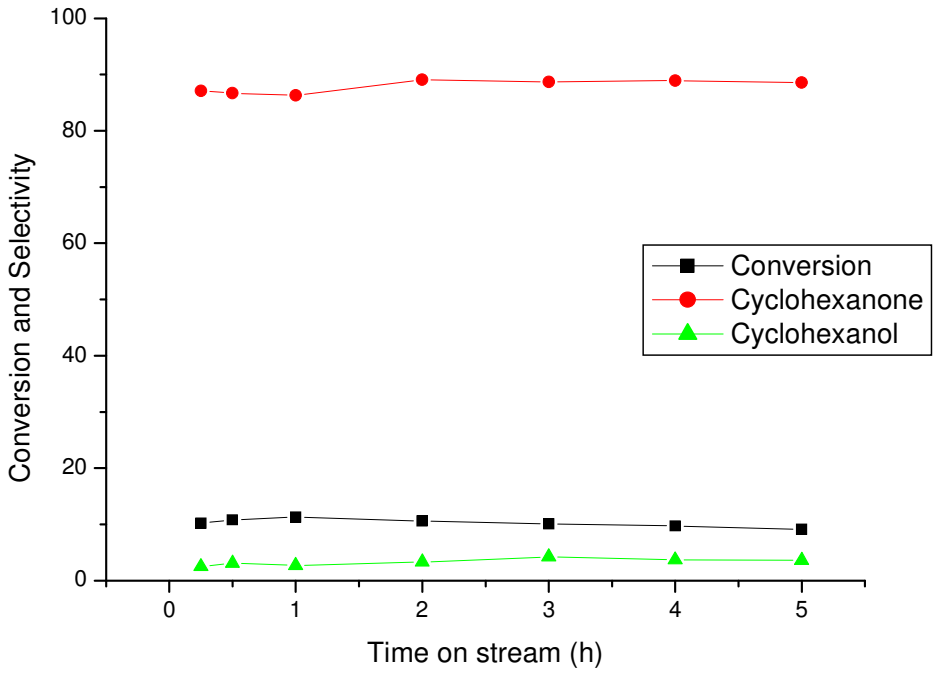


**Figure 9.12** The effect of time-on-stream on catalyst stability over NaOH-$TiO_2$.

## 9.4 Discussion

The data collected in this study indicates the influence of basicity of the support on product selectivity. The presence of basic sites on the support favoured the selectivity towards cyclohexanone. The amount of cyclohexanol produced during the reaction was very low and varied with the reaction parameters.

At higher contact time (Fig 9.7 and 9.11), the reaction favoured the formation of cyclohexanone over that of cyclohexanol. This, as shown in Figures 9.7 and 9.11 indicates that the cyclohexanone formed on the surface could be undergoing further hydrogenation to cyclohexanone. The $H_2$/phenol mole ratio also played an important role in the ratio of products. Figure 9.10 clearly demonstrate this finding. As the amount of hydrogen per given mole of phenol increased, the amount of cyclohexanol increased and that of cyclohexanone decreased.

The higher cyclohexanone selectivity can be attributed to the basicity of the catalysts. This is demonstrated in Figures 9.1, 9.5 and 9.9, which indicated that the selectivity of cyclohexanone decreased for reactions carried out at temperatures above 200 $^{o}$C. In the NaOH-TiO2 catalyst, the basicity is introduced by the addition of NaOH. Although a small amount of dilute

nitric acid is added during washing to remove some of the $Na^+$ ions, the pH of the support remained high (about 10). The pH of the support can be regulated during washing. The same applies for $TiCl_4$-$TiO_2$ where the pH is regulated during the addition of hydrazine hydrate.

Numerous authors have proposed explanations for the influence of the catalyst support (acidity/basicity) on the reaction. Chen et al. [7] have also reported that basic (calcined hydrotalcite) and neutral ($SiO_2$) supports favoured the formation of cyclohexanone. Tanabe and Nishizaki [31] have suggested that a phenol molecule is adsorbed on acidic silica-alumina with an aromatic ring co-planar to the surface while reaction with the basic MgO surface generates a species that is non-planar to the basic MgO surface. Similarly, Neri et al. [5] reported that the co-planar species that show strong interaction between the benzene ring and support are preferentially hydrogenated to cyclohexanol while the non-planar species favour the formation of cyclohexanone. These possibilities are shown in scheme 9.1.

The above proposals could explain the findings noted in this study. In the catalysed reaction, both the co-planar and the non-planar species can be formed on the titanium oxide supported catalysts depending on the amount and strength of both acidic and basic sites on the catalysts (Scheme 9.1).

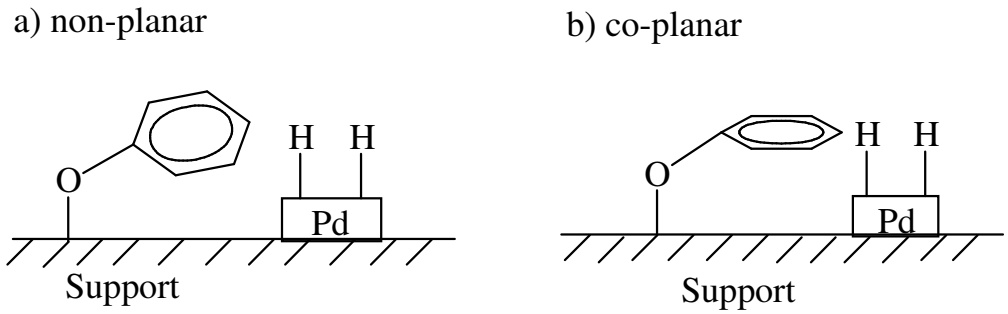


**Scheme 9.1** Two-site model of phenol adsorption and hydrogen dissociation on palladium supported catalysts [5].

Although the both catalysts exhibited high selectivity towards cyclohexanone, the activity remained low for both catalysts. The lower activity can be attributed to a number of factors, including; Pd metal-support interaction, the effect of $Na^+$ ions in the NaOH-$TiO_2$ catalyst, the presence of electron deficient Pd sites on the catalyst and to a lesser extent the amount of Pd loaded on the support. Work is underway to investigate among others, the above mentioned parameters affecting the catalyst activity.

## 9.5 Conclusions

The data collected in this reaction indicate that the presence of basic sites on the support is responsible for the higher selectivity towards cyclohexanone. The high surface area of the modified titanium oxide support offered high surface area for metal dispersion. The catalyst showed very little indication of deactivation.

The TEM micrograph also showed the presence of nanofibres in the titanium oxide support prepared from hydrolysis of titanium tetrachloride with hydrazine hydrate ($TiCl_4$-$TiO_2$).

## 9.6 References

[1] I. Dodgson, K. Griffen, G. Barberis, F. Pignatoro, G. Tauszik, Chem. Ind. (1989) 830.

[2] E.Y. Bezuglaya, A.B. Shchutskaya, I.V Smirnova, Atmos. Environ. 27 (1993) 773.

[3] S.K. Ong, A.R. Bowers, J. Environ. Eng. 16 (1990) 1013.

[4] D.R. van der Vaart, E.G. Marchand, A. Bagely-Pride, Crit. Rev. Environ. Sci. Tech. 24 (1994) 303.

[5] G. Neri, A.M. Visco, A. Donato, C. Milone, M. Malentacchi, G. Guibitosa, Appl. Catal. A: General, 110 (1994) 49.

[6] N. Mahata, K.V. Raghavan, V. Vishwanathan, C. Park, M.A. Kean, Phys. Chem. Phys. 3 (2001) 2712.

[7] Y.Z. Chen, C.W. Liaw, L.I. Lee, Appl. Catal. A: General, 177 (1999) 1.

[8] S. Narayanan, K. Krishna, Catal. Today 49 (1999) 57.

[9] E. Shin, M.A. Keane, Ind. Eng. Chem. Res. 39 (2000) 883.

[10] C. Park and M.A. Kean, J. Col. and Interf. Sci. 266 (2003) 183.

[11] S. Velu, M.P. Kapoor, S. Inagaki, K. Suzuki, Appl. Catal. A: General, 245 (2003) 317.

[12] P. Hoyer, Langmuir, 12 (1996) 1411.

[13] H. Imai, Y. Takei, K. Shimidzu, M. Matsuda, H. Hirahima, J. Mater. Chem. 9 (1999) 2971.

[14] M. Zhang, Y. Bando, K. Wada, J. Mater. Sci. Lett. 20 (2001) 167.

[15] S. Kobayashi, K. Hanabusa, N. Hamasaki, M. Kimura, H. Shirai, Chem. Mater. 12 (2000) 1523.

[16] J.H. Jung, H. Kobayashi, K.J.C. van Bommel, S. Shinkai, T. Shimizu, Chem. Mater. 14 (2002) 1445.

[17] R.A. Caruso, J.H. Schattka, A. Greiner, Adv. Mater. 13 (2001) 1577.

[18] M.K. Hoffmann, S.T. Martin, W. Choi, D.W. Bahnemann, Chem. Rev. 95 (1995) 69.

[19] J.C. Yu, J.G. Zhao, Appl. Catal. B: Environ. 36 (2002) 31.

[20] M. Adachi, Y. Murata, M. Harada, S. Yoshikawa, Chem. Lett. 8 (2000) 942.

[21] Z.B. Zhang, C.C. Wang, R. Zakaria, J.Y. Ying, J. Phys. Chem. B, 102 (1998) 10871.

[22] O.K. Varghese, D. Gong, M. Paulose, K.G. Ong, C.A. Grimes, Sensors and Actuators B, 93 (2003) 338.

[23] C.A. Grimes, K.G. Ong, O.K. Varghese, X. Yang, M. Paulose, E.C. Dickey, C. Ruan, M.V. Pishko, J.W. Kendig, A. Mason, J. Sensors, 3 (2003) 69.

[24] S. Uchida, R. Chiba, M. Tomiha, N. Masaki, M. Shirai, Stud. Surf. Sci. Catal. 146 (2003) 791.

[25] M. Adachi, Y. Murata, I. Okada, S. Yoshikawa, J. Electrochem. Soc. 150 (2003) G488.

[26] T. Kasuga, M. Hiramutsu, A. Hoson, T. Sekino, K. Niihara, Langmuir, 14 (1998) 3160.

[27] K.M. Reddy, S.V. Manorama, A.R. Reddy, Mat. chem. phys. 78 (2002) 239.

[28] A.K. Talukdar, K.G. Bhattacharyya, S. Sivasanker, Appl. Catal. A: General, 96 (1993) 229.

[29] P. Claus, H. Berndt, C. Mohr, J. Radnik, E.J. Shin, M. A. Keane, J. Catal. 192 (2000) 88.

[30] S. Scirè, C. Crisafulli, R. Maggiore, S. Minicò, S. Galvagno, Appl. Surf. Sci. 136 (1998) 311.

[31] K. Tanabe, T. Nishizaki, Proceedings of the Sixth International Congress on Catalysis, Chem. Soc. Letchworth, (1977) 863.

# Chapter 10

## Summary of Results

In the study of dimerization of ethanol (Chapter 4), our results suggest that acetaldehyde is not a major intermediate in the synthesis of butanol from ethanol. It does participate in a competing coupling reaction (aldol condensation reaction) resulting in the formation of crotonaldehyde. Further crotonaldehyde is also not an intermediate in the formation of butanol from ethanol.

An alternative coupling reaction proposed by Yang and Weng is possible, (Scheme 3.4), namely- the self-coupling of ethanol. The ethanol/acetaldehyde coupling reaction (Scheme 5.3) is not consistent with the data and thus the self-coupling of ethanol is the mechanism occurring in this reaction.

In Chapter 5, MgO was investigated as a catalyst for the self-condensation of propanol. Good activity and selectivity to 2-methylpropanol were achieved over this catalyst. The impregnation of MgO with either alkali or transition metal oxides did not improve either the activity or the selectivity of MgO. This suggests that MgO has the necessary basic sites required for this reaction.

A study of the reaction has revealed the importance of hydrogen in the reaction. In the absence of a hydrogenating catalyst (e.g. a metal) the reaction still proceeds to generate the hydrogenated product, indicating that MgO also facilitates this role in the catalysed reaction.

The results, in the presence of hydrogen, are consistent with an aldol condensation reaction to give the C-C coupled products.

Condensation reactions of ethanol with butanol and with propanol were investigated in over MgO in Chapters 6 and 7 respectively.

In the reaction of ethanol and butanol, good activity and selectivity towards 2-ethylbutanol and 1-hexanol was achieved on this catalyst. Attempts to increase the selectivity of the catalyst towards 1-hexanol were largely unsuccessful. Although the impregnation of MgO with basic

ions gave higher selectivity towards 1-hexanol, the overall conversion of reactants was very low. The addition of Cu to MgO (1-10 %) had the same effect as that of basic ions. It was then concluded that the effect of these metal ions on MgO was physical. This implied that the increase in selectivity towards a linear dimmer was due to the coverage of some MgO active sites. This further implied that the route (aldol) by which the branched dimer was formed could have been blocked. Thus formation of the linear dimer was enhanced but the route to this product (aldol reaction and/or $CH_3$ activation) is less affected by addition of a base or Cu.

The formation of 2-ethylbutanol occurs via the classical aldol condensation reaction. However, the formation of 1-hexanol occurs via the activation of a methyl group of ethanol. This activation of the methyl group on ethanol can occur via both the aldol condensation mechanism outlined in Scheme 6.2 and an alternative route involving dehydration.

It was noted that dimerisation of ethanol produced one of the reactants, butanol, and this product would modify the actual concentrations of reactants and further complicated the unravelling of the mechanism.

In the reaction of ethanol and propanol over MgO, 2-methylbutanol, 1-pentanol and 1-butanol were formed in large amount. The products

formation seems to follow the same mechanism as that of ethanol and butanol described above.

MgO has proven to be an effective catalyst for the condensation of primary alcohols to form higher alcohols. In the instances where ethanol was used as a building material for higher alcohol synthesis, both branched and linear alcohols were observed over magnesium oxide catalyst.

The selective vapour phase alkylation reaction of catechol to form guaiacol was conducted over cesium oxide supported catalysts (Chapter 8). The TPD studies showed that upon the addition of $Cs_2O$ on the acidic supports, weak basic sites were generated on the catalysts. The formation of basic sites was further correlated to the higher selectivity for guaiacol observed in this reaction.

The hydrogenation reaction of phenol was carried out over palladium supported catalysts (Chapter 9). High surface area titanium oxide was used as a support for the palladium metal. The reaction showed that the presence of basic sites on the support favoured the catalyst selectivity towards cyclohexanone. The high surface area of the modified titanium

oxide also offered a good opportunity for high metal dispersion on the support. The catalyst showed very little indication of deactivation.

The TEM micrograph also showed the presence of nanofibres in the titanium oxide support prepared from hydrolysis of titanium tetrachloride with hydrazine hydrate.

## ADENDUM

Errors have been identified in the already published results during the preparation of this thesis. However, these errors have been rectified in this thesis. The corrections are as follows:

The x-axis scale label in Figure 3 of the **Dimerization of ethanol to butanol** paper [Ndou et.al. Appl. Catal. A: General, 251 (2003) 337] has been changed to WHSV instead of 1/whsv and the discussion that emanated from this figure has been modified accordingly.

Figure 4 in **Self-condensation of propanol over solid base catalysts** [Ndou et.al. appl. Catal. A: General, 275 (2004) 103] has been replaced by the figure shown below, and the discussion that emanated from the previous figure has been modified accordingly.

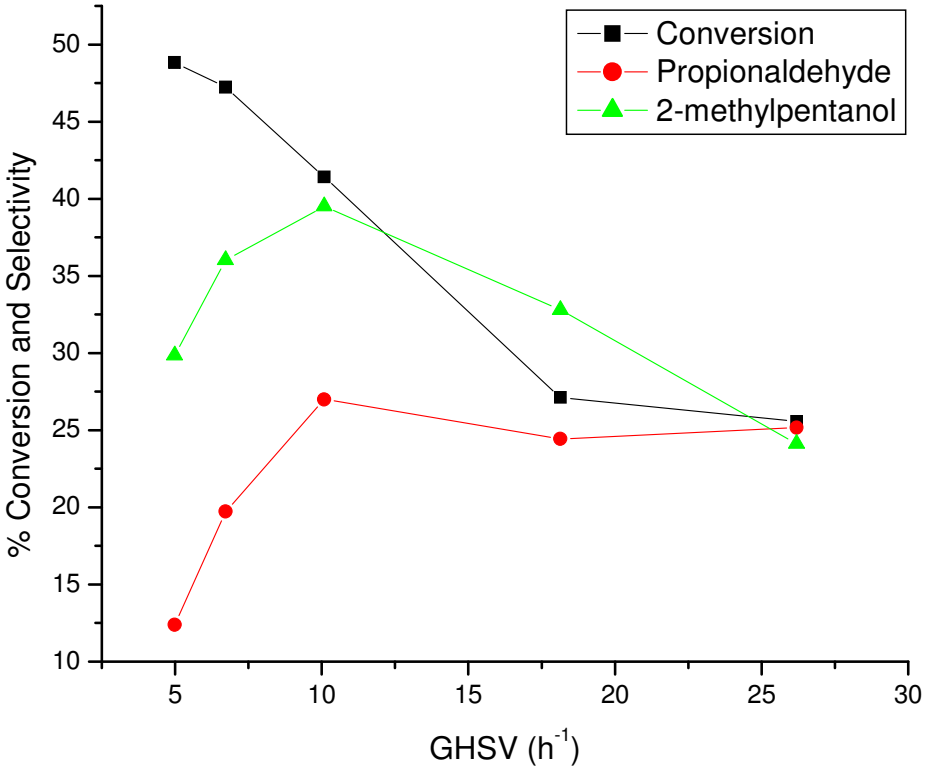


Figure 4 The effect of space velocity on product distribution.